SENSORY NEURON INSULIN SIGNALING AND ITS ROLE IN DIABETIC NEUROPATHY

SENSORY NEURON INSULIN SIGNALING AND ITS ROLE IN DIABETIC NEUROPATHY

By

Caleb W. Grote

Submitted to the graduate degree program in Anatomy and Cell Biology and the Graduate Faculty of the University of Kansas in partial fulfillment of the requirements for the degree of Doctor of Philosophy.

_____
Chairperson Douglas E. Wright, Ph.D.

_____
Lisa Stehno-Bittel, P.T., Ph.D.

_____
Hiroshi Nishimune, Ph.D.

_____
Paige C. Geiger, Ph.D.

_____
William H. Kinsey, Ph.D.

Date Defended: March 29th, 2013

The Dissertation Committee for Caleb W. Grote certifies that
this is the approved version of the following dissertation:

SENSORY NEURON INSULIN SIGNALING AND ITS ROLE IN DIABETIC NEUROPATHY

_____

Chairperson Douglas E. Wright, Ph.D.

Date approved: April 8th, 2013

Abstract

Diabetes is a global concern; approximately 366 million people are currently diagnosed worldwide. Complications of diabetes are numerous and can cause damage to almost every organ system in the body. Neuropathy is the most common complication associated with diabetes and severely impacts patients' quality of life. Diabetic neuropathy (DN) most commonly present as a distal symmetric polyneuropathy with a dichotomous presentation of either peripheral insensitivity or chronic pain. Eventually, patients can develop injury unawareness and foot ulcers, often resulting in amputation. Clearly establishing the mechanisms of diabetes-induced nerve damage will drive the development of more targeted and appropriate treatments. The pathogenesis of DN is multifactorial and the majority of research currently focuses on the toxic pathways induced by hyperglycemia. Interestingly though, insulin has been recently characterized to have direct effects on sensory neurons and is now believed to be a neurotrophic factor that is required for proper development, growth, and maintenance of the nervous system. Here, we tested the hypothesis that reduced sensory neuron insulin signaling contributes to DN pathogenesis via disrupted neurotrophic support. Results demonstrate that PI3K-Akt pathway activation in sensory neurons is insulin dose dependent and that insulin supplementation increases neurite outgrowth, establishing that sensory neurons are insulin responsive. These responses are blunted in type 2 diabetic mice, indicating that sensory neurons demonstrate signs of insulin resistance similar to muscle, liver, and adipose. However, sensory neuron insulin receptor knockout (SNIRKO) mice that maintain euglycemia do not display signs of DN. Suggesting that a disruptions solely in sensory neuron insulin signaling does not cause DN. Surprisingly though, SNIRKO mice are hyperinsulinemic and pancreatic islets from SNIRKO mice display increased insulin content, suggesting a possible feedback mechanism between sensory neuron insulin signaling and insulin production. These results are consistent with a recently described novel pathway of pancreatic beta cell regulation via sensory neuron neuropeptides. In conclusion, while sensory neurons are insulin responsive, reductions in sensory neuron insulin signaling without hyperglycemia does not cause signs of DN and it is most likely the combination of reduced

insulin support and glucose neurotoxicity. Furthermore, the generation of SNIRKO mice has outlined a possible feedback mechanism through which sensory neurons modulate insulin production that could possible aid in establishing new therapeutic avenues for the treatment of diabetes.

Dedication

This dissertation is dedicated to my loving wife, Stephanie Grote, and my amazing daughter, Aubrey Rose Grote. Their love and encouragement are the driving force behind all of my successes. The years that I have known them are the best of my life, and could only be surpassed in joy by the future years with them.

Acknowledgements

An extensive number of people were instrumental in helping me complete this dissertation. Some directly involved by teaching me scientific techniques and data interpretation and others indirectly involved by providing support and encouragement. At times this process was filled with triumphantly successful highs and unbearably stressful lows. Perhaps the most important thing I learned in my PhD training was that the most useful resource is the people around me that kept me grounded during highs and picked me up during lows. To all those involved in pushing me to success, thank you.

First I want to thank my mom, Rose Grote, and my dad, Stan Grote, for their constant support and unwavering love. They taught me the power of a strong work ethic and how to take pride in my work, which has carried me over seemingly insurmountable obstacles. Thank you.

A special thank you to my mentor Dr. Douglas E. Wright. Thanks for everything. I learned an incalculable amount from you, ranging from scientific theory to how to care for my lawn. If I were able to time travel (working on it for my next PhD), I would make all the same choices and mistakes that led me to your lab all over again. Thank you.

Thank you to my friends in the Wright lab, Dr. Natalie Wilson, Anna Groover, Brianne Guilford, Natalie Katz, and Janelle Ryals. Despite all odds you made coming to lab enjoyable, a miraculous feat in itself in a field where failure and disappointment is the norm. My memories from the time with you are fond and will never be forgotten. Thank you and don’t ever change.

Thank you to my dissertation committee of Dr. Lisa Stehno-Bittel, Dr. Hiroshi Nishimune, Dr. Paige C. Geiger, and Dr. William H. Kinsey. You always had an open-door policy with me and were critical when warranted and helpful when needed. Your guidance made several of my scientific endeavors successful.

Thank you to my scientific collaborators for their gracious gifts of knowledge and resources. Dr. Lesya Novikova for her help analyzing pancreas morphology, Dr. Natalie Wilson for assessing SNIRKO mouse mechanical sensitivity, Brianne Guilford for assessing SNIRKO mouse beamwalk, Natalie Katz for assessing SNIRKO mouse thermal sensitivity, Dr. Fan Wang for the Advillin$^{cre/+}$ breeding mice, Dr. John Stanford for always letting me use the sonicator, and Dr. Greg Vanden Heuvel for the tomato mice.

Thank you to the KUMC MD/PhD Program, including: Dr. Joseph Bast (happily retired), Dr. Tim Fields, Dr. Brenda Rongish, Janice Fletcher and students. Everyone in the program provided a sense of stability, support, and community that served as a foundation to help me pursue my academic goals. Thank you.

Thank you to the researchers, labs, and staff on the 2nd floor of HLSIC. There is not a single lab on the floor that I did not go into inquiring about an antibody, protocol, or assay and everyone was always helpful. It is an environment like that which makes research possible. A special thanks to Dr. Julie Christianson for advice on science and life, Dr. Mark Chertoff for help with statistical analysis, and Dr. Ken McCarson for help with pharmacological analysis. Additionally, I would like to thank the staff members of the IDDRC including Michelle Winter, Tina Fowler, and Phil Shafer.

I would not be writing this without Dr. Jill Morris. Dr. Morris took the time out of her busy schedule to help me establish several protocols and techniques early in my PhD training. I am truly grateful for her help. Thank you.

Thank you to Stanton Fernald for the images in this dissertation.

I also want to thank the entire Anatomy and Cell Biology Department and specifically Dr. Dale Abrahamson, Dr. Peggy Petroff, and staff members Kelly-Ann Buszek and Kathleen Bishop for their help in directing through the PhD process. Thank you.

Table of Contents

List of Figures

Chapter 1: Introduction to Dissertation

Chapter 2: In vivo Peripheral Nervous System Insulin Signaling

Figures

Tables

Chapter 3: Insulin Receptor Substrate 2 Expression and Involvement in Neuronal Insulin Resistance in Diabetic Neuropathy

Figures

Chapter 4: *In vivo* Peripheral Nervous System Insulin Resistance

Figures

Tables

Chapter 5: Sensory Neuron Insulin Receptor Knockout Mice

Figures

Tables

Chapter 1: Introduction to Dissertation

1.1 Sensory Neurons of the Peripheral Nervous System

The peripheral nervous system (PNS) is composed of the neuronal cell bodies and peripheral nerves outside the central nervous system (brain and spinal cord). Sensory neurons of the PNS are housed in ganglia. Sensory neurons that innervate the face are located in the trigeminal ganglia and the majority of sensory neurons that innervate the remaining parts of the body are located in the dorsal root ganglia (DRG). The DRG sensory neurons are uniquely susceptible to damage from various insults and these neurons will be the main focus of this dissertation.

Development: DRG sensory neurons along with the glia cells of the PNS are derived from migrating neural crests cells [1]. Neural crest cells delaminate from the roof plate of the neural tube and undergo an epithelial to mesenchymal transition. The induction of neural crest delamination involves a complex signaling network involving Wnt, BMPs, and FGF signaling factors, as well as Sox9, FoxD3, and Snail transcription factors, resulting in changes in cell adhesion and cytoskeletal rearrangement via modifications of cadherins and RhoB, respectively [2]. Neural crest migration begins shortly after neural tube closure (~E9.0 in mice and ~E26 in humans). Beyond the cells of the PNS, neural crest cells also give rise to the craniofacial cartilage and bone, melanocytes, cardiac progenitors, adrenal medulla cells, and odontoblasts.

Sensory neurons are dependent on neurotrophic factors for survival and differentiation during development [3]. A neurotrophic factor is defined as a soluble protein that promotes growth, survival, differentiation, and plasticity of neurons [4]. The best characterized neurotrophic factors are those of the neurotrophin family, including nerve growth factor (NGF), brain-derived growth factor (BDNF), neurotrophin-3 (NT3), and neurotrophin-4 (NT4). Neurotrophins signal through tyrosine kinase receptors trkA (NGF), trkB (BDNF and NT4), and trkC (NT3) [3] as well as p75 [5]. Additional neurotrophic factors include the family of glial derived neurotrophic factors (GDNF), as well as insulin-like growth

factor (IGF) and fibroblast growth factor (FGF). According to the neurotrophic hypothesis established by Victor Hamburger and Rita Levi Montalcini, during development, tissues secrete neurotrophic factors guiding targeted innervation and then promote survival of properly innervated neurons by inhibiting programmed cell death [5-7] . Mouse models of selective neurotrophin knockout or neurotrophin receptor knockout clearly demonstrate that sensory neuron development is dependent on neurotrophic factors and that certain subpopulations require certain neurotrophic factors. Mice lacking NGF display a 70-80% reduction in sensory neurons and a reduction in both thermal and mechanical sensitivity [8]. Mice with a BDNF knockout show approximately a 30% reduction in sensory neurons and have several behavioral deficits included decreased Meissner corpuscle mechanoreceptors [1, 9] . Mice with a null mutation in NT3 have approximately a 60% reduction in sensory neurons and display deficits in posturing and movements [10]. Furthermore, a loss-of-function mutation in the gene encoding trkA in humans results in congenital insensitivity to pain with anhydrosis (CIPA). CIPA is characterized by a loss of NGF dependent fibers resulting in pain insensitivity, anhydrosis, and mental retardation [11].

Due to the profound effect that these proteins have on neuron support, many are currently being investigated as treatments for neurodegenerative diseases including: amyotrophic lateral sclerosis (ALS), Huntington's disease, Alzheimer's disease, Parkinson's disease, and several peripheral neuropathies [4, 12]. In fact, decreased neurotrophic support is considered one of the major mechanisms involved in the pathophysiology of diabetic neuropathy (DN) [13-16]. This process is of such significance that several clinical trials have been performed to test the efficacy of neurotrophic factor treatment on DN. Results have been mixed thus far. Of note, many of the neurotrophic factors activate the same intracellular signaling pathways as insulin, including the PI3K-Akt pathway through insulin receptor substrate [13-15, 17-20].

Organization and Function: Sensory neurons are the only neurons to have a pseudounipolar morphology, with distal axonal projections both into the periphery as well as into the spinal cord of the CNS. DRG pairs are located laterally of the spinal cord in the intervertebral foramen. Within the DRG are

the cell bodies of sensory neurons. Each cell body is surrounded by a layer of satellite glia cells. The peripheral nerves are myelinated by Schwann cells. The DRG consists of a heterogeneous population of sensory neurons that can be subdivided by neuronal size, neurotrophic support, and sensory modalities.

A-alpha and A-beta neurons are large sensory neurons of the DRG. These neurons have large myelinated axons (A-alpha 13-20µm, A-beta 6-12µM) , with fast conduction rates (A-alpha 80-100 m/s, A-beta 35-75 m/s), and express neurofilament-H. Large A-alpha sensory neurons transmit afferent information about reflexes and proprioception and are dependent on NT3 for development and function [10]. The distal projections of A-alpha fibers terminate in sensory structures such as the muscle spindle and Golgi tendon organs. A-beta fibers transmit afferent information about vibration and touch via their distal projections to special mechanoreceptors such as Meissner's and Pacinian corpuscles (vibration) and Merkel cells and Ruffini endings for pressure. A-beta fibers are dependent on several different neurotrophic factors including NGF, NT3, BDNF, and members of the GDNF family [21, 22]. The central projection of large sensory neurons either synapse with interneurons in lamina III and IV of the spinal cord dorsal horn, dive into the ventral horn to synapse with motor neurons or travel cranially in the dorsal column-medial lemniscus (DC-ML) pathway and synapse with second order neurons in either the gracile nucleus (leg) or cuneate nucleus (arm) in the medulla [12].

A-delta and c-fibers are small sensory neurons. A-delta fibers are thinly myelinated with an axon diameter of approximately 1-5 µm and a conduction velocity of approximately 5-30 m/s. C-fibers are unmyelinated with an axon diameter of approximately 0.2-1.5 µm and conduction velocities of approximately 0.2-2.0 m/s. Small sensory neurons can be identified histologically by the expression of peripherin. Small fibers transmit information about pain (nociceptors) and temperature (thermoreceptors) [8]. The distal projections of small sensory neurons innervate tissues throughout the body, ranging from the epidermis of the distal limbs to the internal organs [23]. The axons of small sensory neurons usually terminate as free nerve endings. The central projections of small sensory neurons synapse with secondary neurons in the dorsal horn of the spinal cord at laminas I, II, and V. The secondary neuron then decussates at the anterior white commissure and travels cranially in the anterolateral system (ALS) pathway.

C-fibers can be further subdivided into peptidergic and non-peptidergic classes. Interestingly, during development nerve growth factor (NGF) is required for the survival of almost all sensory and sympathetic neurons; however, during adulthood only about 40% of sensory neurons express trkA, the NGF receptor [24]. It has been demonstrated that a subset of nociceptive neurons downregulates the trkA receptor and upregulates the receptor for GDNF, Ret [25]. Similar to developing sensory neurons, peptidergic fibers express trkA whereas non-peptidergic fibers express Ret. Peptidergic neurons are histologically identified by their expression of neuropeptides such as substance P and calcitonin-gene related peptide (CGRP). Non-peptidergic neurons can be readily identified by the specific binding of isolectin B4 (ILB4). These different classes of C-fibers have been shown to have distinct peripheral projections [26], have different central projects [27] and appear to be differential effected in disease states [28].

Nociceptive small sensory neurons express unique receptors for noxious stimuli relating to thermal, mechanical, or chemical insults [29, 30]. The most well characterized of these receptors is the transient receptor potential vanilloid receptor 1 (TRPV1). TRPV1 was cloned in 1997 [31] and is a ligand gated non-selective cation channel. When activated, TRPV1 opens and allows positively charged ions (Na^+ and Ca^{2+}) to enter the neurons causing depolarization. TRPV1 is activated in response to exogenous stimuli such as heat (>43°C) and capsaicin, or endogenous stimuli such as acidic pH levels and inflammatory mediators [32]. Accordingly, TRPV1-null mice show deficits in response to capsaicin, acidic pH, and thermal sensitization [33]. Interestingly, it has been demonstrated that insulin may modify TRPV1 sensitivity and membrane expression [34, 35] and alterations in TRPV1 have been reported in DN [36, 37]. Furthermore, fibers that express TRPV1 were recently shown to innervate the pancreatic islets of Langerhans and to be involved in the autoimmune destruction of the pancreatic beta cells in non-obese diabetic (NOD) mice [38].

Beyond the well-known and extensively studied afferent function of sensory neurons, they also have important efferent functions. Many of the efferent functions of sensory neurons are mediated through the release of neuropeptides such as substance P and CGRP [39-41]. Substance P and CGRP are

important regulators of neurogenic inflammation through interactions with endothelial and smooth muscle cells of the vasculature to promote vasodilation and vascular permeability, as well as interactions with several immune cells to promote chemotaxis and activation [42]. Neurogenic inflammation is an important physiological process for immune regulation and wound healing, however it is also implicated in the pathology of several diseases, particular chronic neuropathic pain [43]. Recently, along with TRPV1, substance P has been associated with pancreatic beta cell function modulation and autoimmunity in type 1 diabetic NOD mice [38]. The interaction of sensory neuron insulin signaling, TRPV1, neuropeptides, and diabetes pathogenesis will be further discussed in chapter 5.

Injury and Disease: Disease and lesions in the PNS can be characterized by the deficit location (focal, multifocal, or diffuse), the systems involved (muscle, sensory, autonomic or mixed), and the pattern of involvement (distal or proximal or both).

Focal neuropathies include entrapment neuropathies, such as carpal tunnel syndrome, ischemia induced neuropathy resulting from vasculitis, and traumatic injuries [44]. Focal neuropathies resulting from traumatic injury of peripheral nerves can be divided into 3 classes, neuropraxic, axonotemic, and neurotemetic [45]. Neuropraxia is an acute demyelination, normally resulting from a crush injury where the axon and connective tissue of the nerve remain intact. Neuropraxia takes 1-8 weeks to heal depending on the severity.

Axonotemetic injury is characterized by damage to the axon and surrounding myelin, but the connective tissue (endoneurium, perineurium, and epineurium) remains intact. In this case, recovery is length dependent and the nerve can regenerate at a rate of about 1 mm/day. In contrast to the CNS, the PNS has a high capacity for regeneration. Regeneration involves a complex interplay between the neuronal cell body, axons, Schwann cells, and immune cells and is briefly outlined below. After injury, the distal axon begins to degenerate and the cellular debris is phagocytized by Schwann cells and macrophages [46]. Schwann cells proliferate and form endoneurial tubes termed bands of Bungner, which provides the scaffolding for regeneration and helps guide growing axons [47]. These Schwann cells along

with other surrounding cells secrete high levels of neurotrophic factors, including NGF, that promote the survival and growth of injured neurons [48-50]. The neuronal cell bodies and proximal axons switch from a “transmitting mode” to a “growth mode” and upregulate production of growth associated proteins, such as GAP-43, and cytoskeletal proteins such as actin and tubulin [50]. Through these changes, axons generate dynamic growth cones that grow through the endoneurial tubes in response to environmental guidance cues to reinnervate target tissues [45, 47, 50].

Neurotemetic injury is a complete severing of the peripheral nerve, with complete disruption of all supporting elements. A completely severed peripheral nerve fiber cannot recover properly and will eventually result in Wallerian degeneration of the neuron without surgical intervention.

Diffuse neuropathy can result from several different pathogenic mechanisms, including immune-mediated (Guillain-Barre syndrome), hereditary (Charcot-Marie-Tooth), cancer (Schwannomas) and paraneoplastic (lymphomas and leukemias), metabolic, toxins, or infections. As mentioned earlier, DRG neurons are uniquely susceptible to injury, most likely resulting from the reduced blood brain barrier at the DRG [51], and the length of the axon. As such, systemic alterations can results in diffuse sensory neuropathies. Cancer chemotherapeutic agents that target microtubules are particularly damaging to DRG neurons including taxanes (paclitaxel and docetaxel), vinca alkaloids (vincristine), and platinum-based compounds (cisplatinum and oxaliplatin). In fact, peripheral neuropathy is the limiting factor for treatment with these chemotherapeutic agents [52]. Beyond chemotherapy, changes in systemic nutrient levels (B12 deficiency [53]),exposure to toxic metals (cadmium [54] and methyl mercury [55]), and infections (leprosy, HIV, and varicella zoster [56]) can cause peripheral neuropathies. However, in 1994, diabetes mellitus overtook leprosy as the number one cause of peripheral neuropathy worldwide [57].

1.2 Diabetes mellitus

Diabetes mellitus is a complex metabolic disorder characterized by hyperglycemia, polyuria, polydipsia, and unintentional weight loss. These symptoms are a result of either a decreased production or function of insulin. Almost every organ system is affected by diabetes, causing a broad range of

symptoms and complications. After several years, even with strict glycemic control, severe complications can start to develop, including retinopathy, nephropathy, blood vessel damage, foot ulcers, decreased immune function, and neuropathy [58].

Epidemiology: Diabetes is increasing at an alarming rate, with 366 million patients currently diagnosed worldwide, and projections indicating that approximately 552 million will be diagnosed by 2030 [59]. In the United States (US), approximately 18.8 million people are diagnosed, and this number is expected to almost double by 2030 [60, 61], with type 1 accounting for 5-10% [58] of cases and type 2 accounting for 90-95% [58]. The increase in diabetes cases is predominantly due to the increasing number of type 2 cases in association with the obesity epidemic. Furthermore, it is estimated that 79 million people in the US have prediabetes. According to the Center for Disease Control (CDC), in 2007 231,404 deaths were attributed to diabetes, making it the 7^{th} leading cause of death in the US [60]. Diabetes is also the leading cause of kidney failure, peripheral neuropathy, blindness, and non-traumatic amputations in the US [60]. In addition, patients with diabetes have a 2-4 fold higher risk for heart disease and stroke [60]. The estimated cost of diagnosed diabetes in the US was $174 billion in 2007 [60].

Diagnosis: Symptoms of diabetes include increased thirst, increased urination, unintentional weight loss, fatigue, blurred vision, increased hunger, and non-healing wounds. Diabetes is diagnosed using tests to assess blood glucose levels, including fasting glucose, an oral glucose tolerance test, and hemoglobin A1C (HbA1C) (glycosylated hemoglobin) levels. Patients are diagnosed with diabetes with an 8 hour fasting blood glucose level above 126 mg/dl, whereas patients with levels between 100 mg/dl and 125 mg/dl are considered glucose intolerance and prediabetic [62]. Blood glucose of 99 mg/dl or below is considered normal. Additionally, diabetes can also be diagnosed if blood glucose levels remain elevated above 200 mg/dl 2 hours after a 75g oral glucose tolerance test or if HbA1C are above 6.5 [62]. Mouse models of diabetes differ slightly and the diagnosis of diabetes is not as well established and is

strain dependent. However, it is fairly accepted that a blood glucose level over 250 mg/dl is considered diabetic in mice.

Type 1 diabetes: Type 1 diabetes results from the destruction of insulin producing pancreatic beta cells. Patients are normally diagnosed in early childhood, and are dependent on insulin supplementation for survival [58]. If blood glucose levels are not managed properly with exogenous insulin, patients can develop diabetic ketoacidosis, resulting in coma and possibly death.

The destruction of beta cells is driven by autoimmune attack. Autoreactive T-cells appear to the major driver of beta cell destruction in type 1 diabetes, however involvement of both autoreactive B-cells and the innate immune system has been demonstrated [63]. The inciting event causing loss of self-tolerance is not well understood. One of the current leading hypotheses is molecular mimicry after a viral infection [64]. A current model of type 1 diabetes starts with an environmental insult (possibly a virus) in genetically susceptible individuals that causes immune recognition of islet specific antigens. Infiltrating inflammatory cells attack beta cells causing additional release of islet specific antigens and potentiation of the autoimmune attack. Ultimately, beta cells are destroyed, insulin production is ceased, and hyperglycemia ensues [63, 64]. Several autoantigen targets of Type 1 diabetes have been identified, including insulin, glutamate decarboxylase, carboxypeptidase H, and tyrosine phosphatase-like proteins insulinonma antigen-2 and 2β [65]. The best characterized genetic markers of diabetes susceptibility are varying HLA alleles [63].

Type 1 mouse models: Several mouse models of diabetes have been generated. Two of the most commonly used models of type 1 diabetes are induced beta cell death via streptozotocin (STZ) and the non-obese diabetic (NOD) mouse which spontaneously develops diabetes due to autoimmune destruction of beta cells. STZ is an alkylating agent that induces cell death via DNA damage. STZ is specifically taken up by glut2, thus giving it beta cell specificity due to the high level of glut2 on beta cells [66]. In response to STZ, mice develop significantly elevated glucose levels, polydipsia, and failure to maintain

weight. Several mouse strains have been used with STZ. With respect to neuropathy, our lab has demonstrated that C57Bl/6 mice develop mechanical hypoalgesia with little change in thermal sensitivity [67]. A/J mice, on the other hand, develop mechanical hyperalgesia with little change in thermal sensitivity in response to diabetes [68]. However, varying results of DN presentation in mice have been reported.

NOD mice were first described in 1980 and arose from a spontaneous mutation that resulted in insulitis and diabetes [69]. About 60-80% of NOD female mice develop diabetes by 12-14 weeks of age, whereas only 20-30% of males develop diabetes at the same age [70]. NOD mice are characterized by severe islet of Langerhans immune infiltration by autoreactive T-cells, resulting in beta cell destruction. NOD mice also demonstrate a propensity to other autoimmune diseases such as Sjogren-like sialitis/lacrimitis and systemic lupus erythematosus–like disease [70]. Recent evidence has indicated that NOD mice express a hypofunctional mutant TRPV1 on sensory neurons which may drive beta cell stress and autoimmune attack [38]. With respect to neuropathy, NOD mice demonstrate diabetic autonomic neuropathy [71], immune mediated peripheral neuropathy [72], and a reduced capsaicin response [38].

Type 2 diabetes: Type 2 diabetes results from a relative insulin deficiency due to peripheral insulin resistance, in that, muscle, adipose, and liver tissues no longer respond appropriately to insulin. Thus, glucose uptake is blunted and gluconeogenesis continues without regulation, resulting in elevated blood glucose levels. Insulin resistance is closely associated with obesity. The currently most accepted mechanism of insulin resistance is associated with increased circulating levels of free fatty acids and adipose secretions of adipokines (i.e. the proinflammatory mediator TNF-α) that inhibit insulin signaling [73, 74] (cellular mechanisms of insulin resistance will be discussed in detail in Chapters 3 and 4). Increased pancreatic-insulin production can compensate for some time, however eventually insulin production becomes insufficient due to beta cell dysfunction, resulting in hyperglycemia. While insulin resistance is an integral part of type 2 diabetes pathogenesis, it is ultimately the beta cell dysfunction that results in hyperglycemia [74]. Diagnoses is usually made in adulthood and most patients are obese,

inactive, and have poor blood lipid profiles [58]. Type 2 diabetes can be controlled with a combination of diet and exercise, as well as pharmacological intervention with different drug classes, including: insulin secretagogues, insulin sensitizers, and gastrointestinal glucose uptake inhibitors [62]. Poorly controlled type 2 diabetes can eventually result in patients requiring exogenous insulin to control blood glucose levels. Risk factors for developing type 2 diabetes include metabolic syndrome, physical inactivity, family history, and African-American, American Indian, Hispanic or Asian-American decent. Unlike the monogenetic disease, maturity onset diabetes of the young (MODY), type 2 diabetes is a polygenic disease with currently over 36 genes identified to have an association with its development [75].

Type 2 mouse models: Common mouse models of type 2 diabetes are the leptin-deficient *ob/ob* mouse, the leptin receptor null *db/db* mouse, and the high fat fed mouse [76]. In the absence of leptin signaling, mice do not reach satiation and display hyperphagia [76], however, other factors beyond over eating may be contributing to the obesity and type 2 diabetes in *ob/ob* and *db/db* mice. *Ob/ob* mice display obesity, extreme hyperinsulinemia, and insulin resistance with transient hyperglycemia (by 14-16 weeks of age, glucose levels return to baseline), although the leptin mutation on different background strains can produce different phenotypes. With respect to neuropathy, *ob/ob* mice display mechanical hyperalgesia, thermal hypoalgesia, reduced epidermal nerve fibers, and nerve conduction deficits [77]. Similar to *ob/ob* mice, *db/db* mice show obesity, hyperinsulinemia and insulin resistance. However, diabetes appears to be more severe in *db/db* mice and glucose levels remain elevated throughout their lifetime. With respect to neuropathy *db/db* mice display mechanical and thermal hypoalgesia, and reduced nerve conduction velocity [78, 79].

A growing model of glucose intolerance, insulin resistance, and type 2 diabetes is diet-induced obesity, which may better model the human condition. C57Bl/6 mice on a high fat diet display characteristics similar, albeit milder, to *ob/ob* and *db/db* mice such as hyperinsulinemia, insulin resistance, dyslipidemia, glucose intolerance and hyperglycemia [80]. With respect to neuropathy, mice

on a high fat diet display an increased mechanical sensitivity with mild changes in nerve conduction velocity [80].

1.3 Diabetic Neuropathy

Neuropathy is the most common complication of diabetes. Every division of the nervous system is affected (peripheral, autonomic and central nervous systems), but this project will focus primarily on peripheral neuropathy. Damage to the peripheral nervous system due to diabetes is associated with a particularly high level of morbidity and afflicts 40-50% of all diabetic patients [14, 60]. Diabetic neuronal complications first present in the distal extremities and can result in either numbness or chronic pain; and is one of the major factors in the development of Charcot joints, foot ulcers, and limb amputation in diabetic patients [14]. The current treatment for DN involves only symptomatic relief, and often the results are disappointing [81-83]. Defining the pathogenic mechanisms that contribute to diabetic neuropathy (DN) is essential to establish both appropriate pharmacological and nonpharmacological treatments for this devastating diabetic complication.

Epidemiology: The Rochester Diabetic Neuropathy Study enrolled 380 diabetic patients from Rochester, MN. The cohort had 102 type 1 and 278 type 2 patients. The prevalence of polyneuropathy was similar between patients with type 1 (54%) and type 2 (45%) diabetes [84]. As approximately 50% of patients develop DN, it is estimated that by 2030 over 230 million people worldwide will be affected and DN will have a health care cost of over $10 billion in the United States alone [85]. Identified risk factors for DN development from the EURODIAB Prospective Complications Study include smoking, hypertension, diabetes duration, HbA1C, body mass index (BMI), and blood lipid levels [86].

Diagnosis: DN most often presents as a symmetric sensorimotor polyneuropathy, however focal neuropathies are also increased in diabetic patients [85]. Invariably, the symptoms of DN first manifest at the distal extremities, affecting the hands and feet. This is termed a “stocking and glove” distribution and

highlights the susceptibility of the body's longer axons. The small fibers of the PNS appear to be the most effected by diabetes and are the first to be involved in DN [87]. Changes in large fiber sensory modalities occur in later stages, and motor deficits can be seen in severe cases [84]. DN presents with a combination of positive and negative symptoms. Positive symptoms include chronic pain, increased sensitivity to either mechanical or thermal stimuli, or parasthesias/burning sensations. Negative symptoms include thermal or mechanical hypoalgesia, numbness, and reduced proprioception [14]. The combination of all these symptoms can result in chronic neuropathic pain, unawareness to injury, increased risk of falls, and foot ulcers leading to amputation. Patients are diagnosed using a combination of health history, neurological exam, electrophysiology, and intraepidermal nerve fiber density (IENF).

The neurological exam for diabetic neuropathy involves testing the patient's reflexes, observing gait, examining the patient's feet for non-healing ulcers and assessing the patient's ability to feel distinct modalities, normally starting with the feet and working up the leg. Sensory modalities commonly tested include vibration, discriminative touch, proprioception, and the response to a Semmes–Weinstein 10 g monofilament [14]. Additionally, computerized quantitative sensory testing is commonly used to help determine the patient's specific sensory deficit [88].

The gold standard for DN diagnosis is alterations in nerve electrophysiology. Two of the most important electrophysiological changes are a decrease in sensory nerve action potential amplitude and sensory nerve conduction velocity [89]. These parameters are measured on the sural nerve, a predominantly sensory nerve of the lower leg. Electrophysiology is also commonly implemented in mouse models to characterize DN; however results are more variable.

DN is a "dying back" neuropathy, in that, axons regress from their proper innervation site [14]. This results from the inability of peripheral sensory neurons to maintain their distal axons. Axons innervating the distal limb must project from the DRG and travel out to the distal limb, creating a large distance between the supporting cell body and the axon tip. The "dying back" of sensory neurons can be quantified by counting the epidermal nerve fibers stained with PGP 9.5 in punch skin biopsies [90]. A reduction in intraepidermal nerve fiber density (IENF) is characteristic of DN. Recently, a new method

has been developed to quantify nerve fiber density in the cornea, corneal confocal microscopy (CCM). Patients with DN show reduced corneal fibers similar to IENF. CCM has proven to be less invasive and time consuming than IENF and is currently being implemented in clinics throughout the world [91].

Deficits in the aforementioned areas in the presence of diabetes and absence of other insulting factors (chemotherapy, nutrient deficiencies, etc) warrant a diagnosis of DN.

Pathogenesis: The development and progression of DN is multifactorial [14, 92, 93]. Currently investigated and proposed mechanisms are briefly discussed below. Unfortunately, treatments targeting many these mechanisms have shown limited success, indicating that further research is needed [81-83].

Diabetes is associated with several pathogenic changes in vascularization. Changes in blood flow and microvasculature have been demonstrated to be important mechanisms in the development of several diabetes complications, including nephropathy [94] and retinopathy [95]. Furthermore, cardiovascular risk factors (such as smoking, hypertension, and lipid levels) are associated with an increased risk of developing DN. Alterations in nerve blood flow have been demonstrated in DN [96] and it is likely that the biochemical changes associated with diabetes has direct effects on sensory neurons as well blood vessels, and that the development of DN is a result of changes in both neuronal function and nerve blood flow. Several recent clinical trials have addressed interventions to improve neuronal microcirculation and a combination therapy of pentoxifylline and pentosan polysulphate has demonstrated improvement in vibration thresholds [97].

Polyol pathway activation resulting in increased intracellular sorbitol accumulation is a longstanding proposed mechanism of DN. The increase in intracellular sorbitol causes an influx of extracellular fluid, due to poor membrane permeability of sorbitol, resulting in osmotic stress on neurons and an increase in reactive oxygen species (ROS). In rodent models, inhibition of aldose reductase, the first enzyme in the polyol pathway, has shown promising results [98]. Furthermore, upregulation of aldose reductase in Schwann cells has been shown to potentiate reductions in nerve conduction velocity,

indicating an important role for both the polyol pathway as well as Schwann cells in DN [99]. Unfortunately, clinical trials with aldose reductase inhibitors have demonstrated limited success [83].

Advanced glycation endproducts (AGEs) are the result of nonenzymatic glycation of proteins, lipids, and nucleic acids due to hyperglycemia. AGEs have been demonstrated to alter cell biology by reducing protein function and signaling through the receptor for advanced glycation endproducts (RAGE), which appears to cause an upregulation of proinflammatory pathways via NFκB and increase ROS [100]. In experimental diabetes, both neurons and Schwann cells upregulate RAGE. Furthermore, RAGE knockout mice show attenuated features of DN [101] and treatment of diabetic mice with benfotiamine, an AGE inhibitor, showed reduced DN symptoms [102].

A common downstream mechanism between all of the aforementioned pathways is increased production of ROS. In fact, the antioxidant α-lipoic acid has recently been approved for treatment of DN in Germany [103]. Mitochondrial dysfunction is considered one of the major contributing factors to increased ROS in DN. Due to hyperglycemia, an overload of metabolites are shunted to the mitochondria causing increased production of ROS. The increase in ROS causes cellular as well as mitochondrial damage which can eventually result in reduced electron transport activity and ATP synthesis, as well as neuronal calcium dysregulation [104].

Changes in neurotrophic support has been demonstrated in DN and, as mentioned earlier, several clinical trials have investigated neurotrophic factors as treatments for DN. Deficits in signaling, production, transport, and receptor expression have been demonstrated for a number of neurotrophic factors, including NGF, GDNF, BDNF, NT3 and IGF1. While the mechanism through which reduced neurotrophic support contributes to DN remains unclear, several possibilities have been proposed. These mechanisms include reduced neuropeptide production, reduced regeneration capacity, altered mitochondrial support, deficits in ion channels resulting in membrane potential disruptions, decreased cytoskeleton support of the distal axon, and blunted transport of intracellular signaling molecules [16, 67, 105-109]. Similar to the “neurotrophic hypothesis” during development, a disruption in adult sensory neuron growth factors is believed to inhibit the neurons ability to withstand the underlying injury in DN,

thus resulting in axonal degeneration. While treatments with neurotrophic factors have shown promise in rodent models of DN, successful translation into human treatments has not been achieved [82]. Based on the observations that sensory neurons have reduced neurotrophic support in DN, that insulin has recently been demonstrated to have neurotrophic actions, and that insulin signaling is altered in diabetes, a growing mechanism of interest in DN is reduction in sensory neuron insulin support.

Treatment: Evidence from the Diabetes Control and Complication Trial (DCCT) as well as a recent comprehensive review of 17 randomized studies indicate that enhanced glycemic control is the best treatment for prevention of DN [110, 111]; unfortunately, often a significant number of patients will still develop neuropathy. Furthermore, strict glycemic control is associated with a significant increase in hypoglycemic events. After symptoms develop, treatments are primarily focused on controlling severely uncomfortable symptoms such as chronic pain. According to the American Academy of Neurology, first line pharmacological interventions for painful DN include anticonvulsants (pregabalin and gabapentin), serotonin-noradrenaline reuptake inhibitors (duloxetine) and tricyclic antidepressants (amitriptyline) [112]. Additional medications that have been shown to be effective include sodium valproate, oxycodone, and capsaicin.

1.4 Insulin

Structure, Production and Release: Insulin is a 5.8 KDa peptide hormone that is secreted from the beta cells of the pancreas. The beta cells are located within the islets of Langerhans. The morphology of islets of Langerhans is characterized by an inner cell mass of beta cells (insulin producing) and an outer ring of cells consisting mainly of alpha cells (glucagon producing) with interspersed delta cells (somatostatin producing). The islets of Langerhans make up the endocrine portion of the pancreas which accounts for about 2% of the pancreas, the remainder is exocrine tissue.

The insulin gene (Ins) is located on chromosome 11 in humans [113]. Interestingly, mice have 2 insulin genes, Ins2 is the murine homologue to the human insulin gene and is located on chromosome 7,

whereas Ins1 lacks exon 2 of the Ins2 gene and is located on chromosome 19 [114]. Insulin is initially translated as preproinsulin, consisting of the A, C, and B chains of the insulin peptide and a 24 amino acid (AA) rough endoplasmic reticulum (RER) localizing signal. In the RER, the signaling peptide is cleaved and proinsulin undergoes proper folding so that the A and B chains are linked by disulfide bonds. Proinsulin is then transported to the Golgi apparatus where the C-peptide is cleaved, leaving the 51 amino acids of the A and B chains connected by disulfide bonds [115, 116]. In the presence of zinc ions, insulin is then packaged into hexamers, which increases its half-life. Upon release, insulin is separated into the active monomer form and it has a half-life of 5-6 minutes in the blood. Degradation usually occurs after internalization of the insulin-insulin receptor complex via the insulin degrading enzyme [117].

Blood glucose levels predominantly regulate the release of insulin from pancreatic beta cells; however amino acid levels as well as parasympathetic nervous system activity can stimulate insulin release. The steps of insulin release in response to elevated glucose levels are as follows: 1) beta cells take up glucose through the specialized glut2 glucose transporter 2) glucose metabolism in the beta cells produces ATP 3) the cellular increase in the ATP/ADP ratio causes closure of the SUR/Kir6.2 potassium channel resulting in elevated intracellular K^+ 4) increased intracellular K^+ causes depolarization and the opening of voltage-gated calcium channels 5) Ca^{2+} enters the beta cell through opened calcium channels causing membrane fusion and insulin release. Insulin is released in two phases, a rapid first phase (secretion of preformed vesicles) and a prolonged second phase (newly synthesized insulin release) [116, 118].

Insulin Receptor: The insulin receptor is a disulfide-linked heterodimer consisting of 2 alpha and 2 beta subunits. The 120 KDa alpha subunit is extracellular and contains the insulin-binding domain. The 95 KDa beta subunit is a transmembrane tyrosine kinase [119]. The insulin receptor gene is located on chromosome 19 [120] in humans and chromosome 8 [121] in mice. The insulin receptor is conserved across several species, from *C. elegans* (*daf-2*) [122] to *Drosophila melanogaster* (*dInR*) [123] to humans. The gene is comprised of 22 exons, with exons 1-11 corresponding to the alpha subunit and exons 12-22

corresponding to the beta subunit [124]. The insulin receptor is initially translated as a 190 KDa pro-insulin receptor containing both the alpha and beta subunits; however, during posttranslational processing the alpha and beta subunits cleaved. Differential splicing of exon 11 results in 2 insulin receptor isoforms, that are expressed in a tissue specific manner [125, 126]. IR-A results from exclusion of exon 11 and shows increased affinity for insulin-like growth factors. IR-A is primarily expressed in fetal tissues and parts of the CNS. IR-B includes exon 11 and is termed the "high affinity" insulin receptor. IR-B is highly expressed in muscle, liver, and adipose [127, 128].

Mice with a systemic knockout of the insulin receptor are born at term with a mild 10% reduction in birth weight. However, immediately upon feeding, glucose levels and insulin levels rise dramatically and mice die from diabetic ketoacidosis within 3-4 days after birth [129]. While extremely rare, homozygous deletion of the insulin receptor has been observed in humans. A deletion of the inulin receptor in humans results in leprechaunism and is characterized by severe intrauterine growth retardation, several developmental delays, hyperinsulinemia, and post-prandial hyperglycemia, but fasting hypoglycemia [130]. In 1998, exon 4 of the insulin receptor was flanked by loxp sites enabling the conditional knockout of the insulin receptor using tissue specific cre recombinase expression and a more targeted understanding of insulin signaling [131]. Results from conditional knockout in several tissues have been published. Mice with muscle specific insulin receptor knockout using a muscle creatine kinase (MCK) promoter, displayed dyslipidemia, increased fat pads, but normal glucose, insulin levels and normal glucose tolerance [131]. A specific knockout of the insulin receptor in all adipose tissue using the aP2 promoter produced a mouse phenotype with reduced fat pads, resistance to obesity, and increased lifespan [132, 133]. However, mice with a conditional knockout of in the insulin receptor in brown adipose (uncoupling protein-1 promoter) demonstrated brown adipose atrophy and beta cell failure [134]. Mice with an insulin receptor knockout in the beta cells (rat Ins2 promoter) showed impaired glucose-induced insulin release and glucose intolerance [135]; whereas liver knockout (albumin promoter) produced severe glucose intolerance, hyperinsulinemia and transient hyperglycemia [136]. Finally, a conditional knockout of the insulin receptor in the CNS has also been generated using the nestin promoter

[137]. These mice demonstrated increased food intake, diet-sensitive obesity, insulin resistance, and hypogonadotropic hypogonadism resulting in subfertility.

Insulin receptor signaling pathway: The insulin signaling cascade is propagated by phosphorylation events beginning with activation of the insulin receptor tyrosine kinase upon insulin binding. After activation, the insulin receptor kinase phosphorylates tyrosine residues on both the receptor and docking proteins, such as insulin receptor substrate (IRS). Tyrosine phosphorylation allows downstream mediators with src homology-2 (Sh2) domains to bind IRS and localize to the plasma membrane. Two key Sh2 containing mediators are PI3-kinase, which activates the Akt cascade, and Grb2/SOS, which activates the MAPK cascade [18, 19]. These effectors eventually lead to increased transcription, translation, and translocation of the proteins necessary to carry out insulin's actions (Figure 1.1).

Physiological functions of insulin: Insulin has numerous effects throughout the body, mostly relating to energy storage and glucose homeostasis. In peripheral "insulin-sensitive" tissues (liver, muscle, and adipose), insulin mediates glucose metabolism by stimulating glucose uptake through translocation of glut4, as well as controlling glucose breakdown and synthesis via its effects on glycolysis and gluconeogenesis. Additionally, insulin promotes glycogen synthesis through inhibition of glycogen synthetase kinase, increases protein production through mTor activation, as well as promotes fatty acid synthesis and inhibits lipolysis through activation of Acetyl-CoA Carboxylase and inhibition of hormone sensitive lipase, respectively. Furthermore, insulin can mediate gene transcription through the MAPK pathway or through Akt-mediated phosphorylation of FOXO transcription factors which results in nuclear exclusion [138, 139]. Beyond energy balance, insulin plays a role in several other aspects of physiology, including: fertility, blood lipid levels, blood pressure, as well as, growth and survival of beta cells, bone, retina, and neurons [18, 140-142].

Figure 1.1

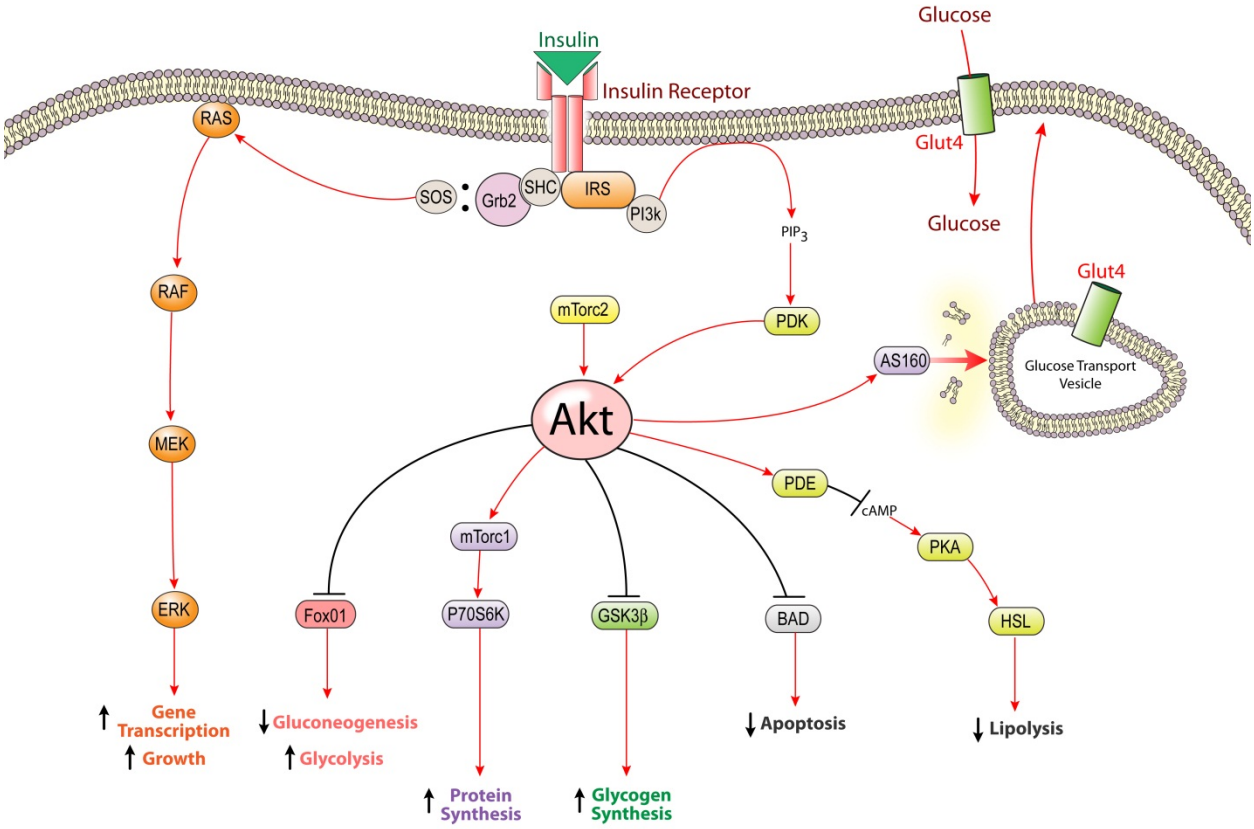
Insulin
Insulin Receptor
Glucose
Glut4
Glucose
RAS
SOS
Grb2
SHC
IRS
PI3k
PIP3
RAF
mTorc2
PDK
Glut4
AS160
Glucose Transport Vesicle
MEK
Akt
PDE
cAMP
PKA
mTorc1
ERK
Fox01
P70S6K
GSK3β
BAD
HSL
Gene Transcription
Growth
Gluconeogenesis
Glycolysis
Protein Synthesis
Glycogen Synthesis
Apoptosis
Lipolysis

Figure 1.1. The insulin signaling pathway: Intracellular insulin signaling is initiated by insulin receptor tyrosine kinase activity leading to the activation of both the PI3K-Akt pathway and the MAPK pathway. The most well characterized function of insulin signaling is glucose homeostasis; however insulin stimulates several other cellular mechanisms including the biosynthesis of proteins, glycogen, and lipids. Insulin receptor substrate (IRS), glycogen synthetase kinase β (GSK3β), extracellular signal-related kinase (ERK), Srchomology-2-containing protein (Shc), forkhead box protein O1 (FOXO1), Akt substrate of 160 kDa (AS160), mammalian target of rapamycin complex (mTorc), p70 ribosomal protein S6 kinase (p70S6K), hormone sensitive lipase (HSL), phosphodiesterase (PDE), protein kinase A (PKA), phosphoinositide dependent kinase (PDK), Growth factor receptor-bound protein 2 (Grb2), son of sevenless (SOS). Illustration by Stanton Fernald.

1.5 Insulin and the Nervous System:

Throughout history, insulin signaling in the nervous system has been fairly ignored, because unlike muscle and adipose tissues, neurons do not take up glucose in an insulin dependent manner [143, 144]. However, neurons do express insulin receptors [145]. Neurons primarily express the glut1 and glut3 glucose transporters and take up glucose via a concentration gradient receptor mediated process [146]. However, it has recently been demonstrated that certain areas of the brain, such as the olfactory bulb, hippocampus, and hypothalamus express glut4 transports [147]. Glucose is the main energy supply for neurons; however, in states of extreme starvation neurons can utilize ketone bodies [148].

Insulin crosses the blood-brain barrier (BBB) through a saturable receptor mediated transport system, termed receptor-mediated transcytosis [149]. During this process, serum insulin binds the insulin receptor on the endothelial cells of the blood brain barrier; the ligand-receptor complex is internalized and transported to the opposite side of the cell where insulin is released. Insulin receptor-mediated transcytosis is currently one of the most targeted systems in drug development to transport chemicals across the BBB [150].

Diabetes has recently been implicated as a risk factor for several neurological diseases, including Alzheimer's and Parkinson's disease [151, 152]. This has led to a spiked interest in the role that insulin might play in the nervous system. Many of the CNS changes associated with diabetes are similar to those observed in Alzheimer's disease, including increased beta amyloid and tau phosphorylation [153]. Additionally, the brains from Alzheimer's patients show characteristic signs of insulin resistance [154] and the insulin sensitizing drugs, thiazolidinediones, have been shown to improve memory in both mice [155] and human patients [156]. Furthermore, both intracerebroventricular and intrahippocampal insulin administration has been demonstrated to improve memory formation in rats [157-159], and insulin has been demonstrated to regulate synapse number and plasticity [160]. Recently, in phase 1 clinical trials, Alzheimer's patients that received intranasal insulin treatment demonstrated improved memory and activities of daily living [161].

Beyond a role in memory, insulin is involved in centrally regulating glucose metabolism and food intake via signaling in the hypothalamus. Insulin inhibits neuronal firing of the NP-Y/AgRP neurons of the arcuate nucleus by activating K_{ATP} leading to neuronal hyperpolarization, resulting in decreased release of the orexigenic hormone NP-Y [162, 163]. Additionally, this process has been demonstrated to centrally regulate liver gluconeogenesis, and is hypothesized to be a major mechanism contributing to obesity and insulin resistance [164, 165]. Intriguingly, insulin also activates K_{ATP} channels on pancreatic beta cells, causing hyperpolarization and reduced insulin release in a negative feedback mechanism [166].

Insulin has also been demonstrated to regulate AMPA-induced neuronal damage [167] and modulate AMPA excitatory currents in the spinal cord dorsal horn [168]. Additionally, insulin receptor signaling in the CNS has been shown be involved in regulating neuronal development [169].

These observations suggest that although neurons do not take up glucose in an insulin dependent manner, neurons do seem to be insulin responsive and insulin may be important to maintaining proper neuronal function.

Insulin as a neurotrophic factor in sensory neurons: Insulin is a member of the insulin-like super family that includes Insulin, IGF1, and IGF2. While IGF1 has been a well-defined neurotrophic factor for some time, insulin's effect on neurons has only gained significant attention over the past 15-20 years. A growing body of literature has now established insulin as a potent neurotrophic factor that appears essential to promoting proper neuronal function.

Insulin receptors are expressed on both the DRG neuron soma as well as in the peripheral nerve [170-172]. Several reports have indicated that the insulin receptor is predominantly expressed in small nociceptive neurons. Baiou et. al. indicated that approximately 40% of DRG neurons express the insulin receptor and that approximately 75% of insulin receptor expressing neurons were co-labeled with peripherin [173]. Furthermore, insulin receptor expression was not confined to one c-fiber subtype, as insulin receptor expressing neurons were co-labeled with either CGRP or IB4. However, and in contrast, a number of reports have also reported strong co-labeling with neurofilament-H, a marker of large myelinated neurons [174, 175].

In primary culture models of peripheral neurons, insulin supplementation has been shown to have many functional effects. Insulin stimulation appears to increase neuritogenesis, as well as neurite length and area. Recio-Pinto et al. showed that the percent of both sympathetic and sensory neurons bearing neurites increased in a dose dependent manner with insulin supplementation, with an ED_{50} of 0.4nM for sympathetic neurons and an ED_{50} of 30nM for sensory neurons [142]. Similarly, Fernyhough et al. reported that insulin increased the rate of neurite regeneration in DRG cultures 3.5 fold compared to control cultures without insulin supplementation [176]. Interestingly, this effect appears to be additive with NGF supplementation [177, 178]. One possible mechanism through which insulin may be promoting an increase in neurite outgrowth is through stabilization of tubulin microtubule mRNA, an essential part of neurite formation, as suggested by Fernyhough et al. [179]. Beyond neurite outgrowth, many reports also noted an apparent increase in neuronal survival with insulin supplementation [142, 180], and insulin is characterized to be one of the few essential molecules required for cultured primary peripheral neurons [141]. Furthermore, stimulation of the PNS with insulin has shown strong activation of the PI3K-Akt pathway, a pathway that is directly related to axonal growth and neuronal survival [181]. Thus, a possible molecular mechanism of increased neuronal survival with insulin supplementation may be through insulin-induced Akt activation, which in turn shuts down apoptosis through inhibition of both BAD and caspase 9 [182].

Additionally, recent evidence has demonstrated that insulin may play an important role in Schwann cell physiology. Schwann cells express the insulin receptor in the basal lamina, plasma membrane and cytoplasmic processes [183]. Furthermore, insulin receptor expression in Schwann cells during development parallels myelin glycoprotein P zero (P0) expression and growth of the myelin sheath. Moreover, insulin supplementation can induce P0 expression in primary Schwann cell culture, indicating that insulin could have crucial roles in myelination and peripheral nerve support via Schwann cell signaling [172].

Beyond its effects on neurons *in vitro*, insulin has also been shown to have dramatic neurotrophic qualities *in vivo*. In nerve injury models (nerve transection or nerve crush), recovery from the ensuing pathological changes is accelerated by insulin supplementation. Q.G. Xu et al. showed that intraperitoneal

(IP) injections of insulin (0.02 IU Humulin R) twice daily increased both the rate of motor endplate reinnervation (measured by M wave amplitude) and hindpaw motor function recovery after sciatic nerve transection. Furthermore, in these studies it was also demonstrated that systemic insulin treatment through IP injections increased the number of mature regenerating myelinated fibers after nerve crush. Mice in the insulin treated group displayed significantly increased axonal and fiber diameter as well as increased axonal area [184]. Similar results were reported in a comprehensive study comparing the effects of intrathecal (through mini-osmotic pump) or near nerve insulin treatment on peripheral nerve regeneration after nerve crush injury by Toth et al [185]. In the experimental paradigm of this study, the most dramatic effects of insulin treatment were observed in the group receiving intrathecal insulin. In separate experiments of sural (mostly sensory axons) and peroneal (mostly motor axons) nerve crush, insulin supplementation prevented degeneration of axons proximal to the nerve injury and accelerated regeneration of axons distal to the crush site. These changes were associated with an increase in axonal fiber density, size, and regenerating fiber clusters in both the sural and peroneal nerve with intrathecal insulin treatment. Furthermore, these observed morphological differences were coupled with an increase in CGRP and translated into an accelerated recovery of thermal sensation after nerve injury in insulin treated rats.

Collectively, these studies have established insulin as a key component of neuronal support and have led to the assumption that disruptions in insulin availability (reduced circulating levels or reduced signaling) could have detrimental effects on neuronal function.

1.6 Insulin and Diabetic Neuropathy:

As previously discussed, the currently investigated pathways of DN pathogenesis mainly focus on the cellular damage associated with the various cascades activated in response to hyperglycemia. However, there are 2 major insults in diabetes. The first is the loss of insulin signaling, either due to insulinopenia (type 1) or insulin resistance (type 2), and secondly, the resultant elevated blood glucose levels. While it is reasonable to assume that the sequela of hyperglycemia does contribute to the

development of DN, it is also reasonable to consider that the loss of insulin signaling directly on sensory neurons may also be a contributing factor.

Epidemiologic data from the Diabetes Control and Complications Trial (DCCT) provided very strong evidence of the link between poor glucose control and DN [186]. Results from this trial indicated that patients with intensive glycemic control (3 or 4 daily insulin injections or external pump) showed a 64% percent reduction in neuropathy over a 5-year period as compared to patients on conventional therapy (1 or 2 daily insulin injections with mixed rapid and intermediating acting insulin). Furthermore, patients on conventional therapy experienced a steady deterioration in nerve conduction velocity, while patients in the intensive treatment group displayed no change and even a slight improvement [186, 187]. Accordingly, the best known treatment for prevention of neuropathic complications is strict glycemic control. Interpretation of this clinical data has led to a large emphasis on the role of hyperglycemia in DN, however another interpretation of this data reveals that strict glycemic control also means a more balanced, steady, and physiological insulin exposure. Thus, the reduction in DN in intensive treatment group may be a result of restoration of the lost neuronal insulin signaling key to maintaining proper sensory function rather than just the control of hyperglycemia.

Low insulin without hyperglycemia causes signs of DN: Do to the intimate connection between insulin and blood glucose levels; teasing out the consequences of changes in one variable without disruptions in the other is difficult. However, several studies have demonstrated that in instances of low serum insulin, yet euglycemia, abnormalities in sensory function develop. Correspondingly, strong evidence has also shown that low dose insulin treatment of animals with DN can reverse many of the abnormal morphologic and behavioral changes associated with the disease, without significantly altering glucose levels.

A common animal model of type 1 diabetes is to use the beta-cell toxin STZ to induce severe insulinopenia and thus hyperglycemia. However, there is a variable response to STZ and not all animals will develop hyperglycemia and diabetes. In 2010, Romanovsky et al. characterized a cohort of these euglycemic-STZ injected rats, and showed that while they did not have elevated glucose levels, they did

have a significant decrease in serum insulin concentrations as compared to rats that received vehicle. Interestingly, euglycemic-STZ rats did display mechanical hyperalgesia indicated by a reduced threshold on a paw-pressure withdrawal test. These changes were similar to that of hyperglycemic-STZ rats, although hyperglycemic rats did maintain a lower threshold [188]. In an earlier study, it was also demonstrated that this observed change in paw-pressure threshold correlated significantly with insulin deficiency in euglycemic-STZ rats and could be ameliorated with low-dose insulin treatment [189]. Surprisingly, the euglycemic-STZ rats showed no alterations in mechanical sensitivity in response to von Frey filaments, no change in thermal sensation, or decreases in nerve conduction velocity. Perhaps indicating that the loss of neuronal insulin support and hyperglycemia contribute to different features of DN.

Similar results of neuropathy without overt hyperglycemia have also been demonstrated in the Goto-Kakizaki (GK) rat. Murakawa et al. evaluated the effect of continued impaired glucose tolerance (IGT) and progressive insulinopenia, without severe hyperglycemia on peripheral neurophysiology and neuromorphology in the GK rat [190]. While no differences in PNS function were observed in the 2-month-old GK rat with IGT and hyperinsulinemia, 18-month-old GK rats with IGT and insulinopenia displayed classical features of diabetic neuropathy (reduced NCV, loss of unmyelinated axons, and increased frequency of regenerating fibers). Surprisingly, these neuropathic changes developed without overt fasting hyperglycemia in 18 month old GK rats (control=3.2±0.4 mM and GK=4.4±1.3 mM) and the authors suggest that these changes appear to be more related to the decrease in neuronal insulin support. Furthermore, in conjunction with the increase in CGRP expression with insulin treatment observed by Toth et al., Murakawa et al. noted a significant decrease in CGRP expression in insulinopenic 18-month-old GK rats. Together these results suggest that one of the mechanisms through which insulin may promote proper sensory function is by maintaining synthesis of key neuromodulator proteins and peptides.

It has also been demonstrated that sequestering of endogenous intrathecal insulin in nondiabetic rats by intrathecally infusing anti-insulin antibodies produces slowed motor nerve conduction and atrophy of axonal fibers, similar to that seen in models of diabetic neuropathy [191]. Once again suggesting that

non-glycemic triggers of DN exist and that the loss of PNS insulin signaling may be one of the initiating events.

Finally, it has recently been demonstrated that STZ-diabetic rats show reduced insulin receptor activation in the sciatic nerve [192]. The rapid change in insulin receptor signaling was correlative with the rapid onset of mechanical hyperalgesia. This was one of the first publications investigating insulin signaling in the sciatic nerve and the authors speculate that the change in sciatic nerve insulin signaling may help explain the change in nociceptive behavior associated with DN.

Low dose insulin reverses signs of DN: As discussed earlier, many studies have shown that a loss of PNS insulin signaling may contribute to DN, similarly, several reports have demonstrated that low-dose insulin (insufficient to reduce hyperglycemia) can have beneficial effects on the signs and symptoms of DN. Brussee et. al. demonstrated that intrathecal delivery of insulin or equimolar IGF1 daily for 4 weeks could not only restore both motor and sensory nerve conduction deficits, but also prevent axonal atrophy in type 1 diabetic rats [191]. Furthermore, in a similar experiment, both intrathecal insulin and IGF1 were able to reverse the loss of epidermal nerve fiber density and length in diabetic rats [193], which is a well-documented and quantifiable consequence of the "dying back" neuropathy associated with diabetes. Surprisingly, subcutaneous insulin deliver within these same experimental paradigms did not alter the investigated neuronal parameters. This is in contrast to the results from Hoybergs and Meert, which demonstrated that low-dose insulin delivered through subcutaneous insulin pellet can nearly normalize diabetes-induced tactile allodynia and mechanical hyperalgesia, despite persistent hyperglycemia (blood glucose levels dropped from 600mg/dl to approximately 400mg/dl 2 weeks after insulin pellet insertion) [194]. Thus, some controversy still exist as the appropriate dosing regimen and delivery method most appropriate for beneficial effects on the PNS, however it does appear that insulin treatment can relieve symptoms of DN through mechanisms other than reducing elevated blood glucose levels.

Most recently, Guo et. al reported that intraplantar delivery of insulin at sub-glucose lowering levels not only reversed the loss of intraepidermal nerve fiber density but also slightly ameliorated some

of the symptoms of DN [174]. This study demonstrated the efficacy of local insulin administration on epidermal innervation in several mouse models of diabetic neuropathy, including type 1 diabetes induced by STZ in C57BL/6J, CD-1, and CFW as well as *db/db* type 2 diabetic mice. Intraplantar insulin showed a benefit on epidermal axons over vehicle control in each of these DN models and in diabetic C57BL/6J mice the increase in epidermal innervation with insulin treatment was also associated with upregulation of GAP43/B50, a growth associated protein. Along with changes in innervation, local insulin administration improved deficits in mechanical but not thermal sensation. These results further corroborate the neuronal growth promoting qualities of insulin and the potent affects that insulin treatment *in vivo* has on symptoms of DN.

Beyond its effects on sensorimotor behavior and epidermal innervation, some subcellular pathological changes associated with DN can be alleviated with insulin treatment. Defects in sensory neuron mitochondrial function is believed to be a possible mechanism contributing to DN through several different pathways, including the over-production of ROS and reduced respiration through defects in the electron transport chain. Insulin and mitochondria are intimately connected through numerous metabolic pathways, and proper insulin signaling is essential for proper mitochondrial function [195]. Interestingly, insulin treatment has been shown to improve many of the mitochondrial defects associated with DN [196-198]. Huang et al. reported that in a STZ model of type 1 diabetes, DRG neuronal mitochondria display increased depolarization and Chowdhury et. al. reported that diabetes can induce deficits in mitochondrial respiration as well as mitochondrial protein expression [196, 198]. In both of these reports, insulin supplementation restored the mitochondrial parameters back to the levels observed in control animals. These results suggest that a loss of insulin signaling may be one of the compounding factors affecting proper mitochondrial function.

Similar to the beneficial roles of insulin treatment on sensory deficits associated with DN, insulin treatment has been shown to protect against late-stage diabetes-induced motor neuropathy as well [199]. Intranasal insulin (and subcutaneous insulin to a lesser extent) showed beneficial effects on motoneuron morphology and function. Insulin treated diabetic mice (8 month old CD1) showed protection against electrophysiological decline, loss of neuromuscular junctions, and loss of motor function (as measured

with forelimb and hindlimb grip testing as well as rearing activity). These results provided further evidence of the neurotrophic qualities of insulin and the potential impact it may have on proper neuronal function.

1.7 Purpose and central hypothesis of dissertation:

While substantial evidence is mounting in support of a role of dysfunctional neuronal insulin support in DN pathogenesis, several crucial areas still need to be investigated. 1) Unlike muscle, adipose, and liver, essentially nothing is known about neuronal insulin signaling pathways and this has greatly impeded the understanding of how reduced neuronal insulin support may lead to neuronal dysfunction. 2) Patients with type 1 and type 2 diabetes develop neuropathy with similar incidence and present with common symptoms. However, most early research surrounding the role of insulin in diabetic neuropathy has focused on type 1 insulinopenic diabetes, where decreased PNS insulin signaling is plausible do to the systemic lack of insulin. However, how this idea applies to type 2 diabetes, where patients are usually severely hyperinsulinemic is not well characterized. 3) Due to the intimate connection between blood glucose and insulin levels; separating the contribution to DN pathogenesis from either variable is nearly impossible using currently available models.

The purpose of this project was to investigate the role of reduced insulin signaling in DN pathogenesis by delineating the PNS insulin signaling cascade, outlining the changes in PNS insulin signaling associated with type 2 diabetes and establishing a new model to study reduced sensory neuron insulin signaling independent of blood glucose changes.

Central hypothesis: Reduced sensory neuron neurotrophic support resulting from disrupted insulin signaling contributes to the pathogenesis of diabetic neuropathy irrespective of hyperglycemia.

Chapter 2: *In vivo* Peripheral Nervous System Insulin Signaling

2.1 Abstract

Diabetes-induced damage to the peripheral nervous system (PNS) is associated with several debilitating symptoms, including chronic pain, numbness, and foot ulcers. Unfortunately, the pathogenesis of diabetic neuropathy (DN) is not fully understood and current treatment options are unsatisfactory. Alterations in PNS insulin support is a proposed mechanism contributing to DN development. However, a comprehensive study of insulin signaling in the PNS is lacking. The purpose of this study was to investigate PNS insulin signaling in response to exogenous insulin and to identify possible differences in PNS insulin signaling compared to muscle, liver, and adipose. Nondiabetic male mice were administered an insulin dose curve. PNS insulin signaling was quantified with Western blots of Akt activation in the DRG and sciatic nerve. Resulting EC50 doses were used to characterize the PNS insulin signaling time course as well as make comparisons between insulin signaling in the PNS and other peripheral tissues (i.e. muscle, liver, adipose) at a therapeutically relevant insulin dose. The results reveal that the PNS in insulin responsive and that differences in insulin signaling pathway activation may exist within the PNS compartments. At a therapeutically relevant dose, Akt was significantly activated in the muscle, liver, and adipose at 30 minutes, correlating with the observed change in glucose levels. Interestingly, the sciatic nerve showed a similar signaling profile as muscle, liver, and adipose, however there did not appear to be significant activation in the DRG or spinal cord. These results begin to outline the *in vivo* PNS insulin signaling pathway and will help determine how disruption of PNS insulin signaling may contribute to the development of DN.

2.2 Introduction

An interesting mechanism of DN that is currently receiving additional attention is the loss of insulin signaling in the nervous system, either through insulinopenia or insulin resistance [175, 181, 188, 191, 193, 200]. Mounting evidence has established that insulin plays an important neurotrophic role in both the central nervous system (CNS) and peripheral nervous system (PNS). Insulin has been shown to induce neurite outgrowth [142, 179], facilitate *in vivo* nerve regeneration [174, 184, 185], and improve memory formation [159, 161].

Insulin signaling begins with activation of the insulin receptor tyrosine kinase which then phosphorylates tyrosine residues on docking proteins, such as insulin receptor substrate (IRS). Tyrosine phosphorylation of IRS allows downstream mediators to bind and propagate the signal. Insulin activates both the PI3K-Akt pathway as well as the MAPK pathway. Cellular actions of insulin in "insulin sensitive tissues" (i.e. muscle, liver, and adipose) include: increased glucose uptake, decreased gluconeogenesis, increased glycogen synthesis, increased protein synthesis, and increased lipid synthesis (for review [138]).

Unfortunately, a comprehensive study of *in vivo* insulin signaling in the PNS has not been completed, and has hindered the understanding of the exact role that disrupted insulin signaling may play in DN. Varying results have been published with respect to the timing, dose, and delivery method needed for proper insulin signaling and functional results [184, 185, 201]. Additionally, insulin signaling has been investigated in primary DRG culture, but these studies are incomplete and translation of these results is difficult due to a complete disruption of the *in vivo* environment. Furthermore, culture models do not allow for the simultaneous comparison between tissues or provide information about the physiological effects of insulin signaling [181, 200]. The aim of the current study was to begin to establish PNS insulin signaling physiologic parameters in response to systemically delivered insulin. Delineating the PNS insulin signaling pathway will reveal possible mechanisms contributing to insulin's neurotrophic effect and how disruptions in those mechanisms may lead to DN.

Our results indicate that while PNS insulin signaling is dose dependent, very high doses of intraperitoneal insulin were needed. In fact, only moderate insulin signaling was observed in the PNS as compared to the robust response of muscle, liver, and adipose when a therapeutically relevant insulin dose was administered. These studies provide a much needed baseline of PNS insulin signaling in comparison to other tissues and will be crucial in guiding future research aimed at delineating the role of insulin in DN pathogenesis.

2.3 Experimental Procedures

Animals: All experiments were approved by the University of Kansas Medical Center Institutional Animal Care and Use Committee. Male nondiabetic C57bl/6 mice aged 8 to 11 weeks were used for all studies. Mice were given access to food and water ad libitum and housed on a 12-hour light/dark cycle. Mice were fasted 3 hours prior to the start of all experiments and data collection. Tissues collected included the lumbar dorsal root ganglia (DRG), sciatic nerve, lumbar enlargement of spinal cord, liver, gastrocnemius muscle, and epididymal fat pad.

Antibodies and Reagents: Humulin R insulin (Eli Lilly, Indianapolis, IN) was used for all experiments. Blood glucose levels were measured vial tail clip with a glucose diagnostic assay (Sigma, St. Louis, MO). All antibodies for Western blot analysis were purchased from Cell Signaling (Danvers, MA) unless otherwise noted: total Akt, p-(Ser473)Akt, p-(Thr308)Akt, total GSK3β, p-(Ser9)GSK3β, total p44/42 MAPK (ERK1/2), p-(Thr202/Tyr204)p44/42 MAPK (ERK1/2), total mTor, p-(Ser2448)mTor, total AS160 (Millipore, Billerica, MA), and p-(Thr642)AS160 (Millipore). Secondary antibodies included: HRP-conjugated anti-mouse and anti-rabbit (Santa Cruz, Santa Cruz, CA).

Insulin dosing: Insulin was delivered via intraperitoneal injection for all experiments and sterile PBS was used as a vehicle control. To establish an insulin dose curve, doses were increased from the minimal dose of 0.01 U/kg to the maximal dose of 10000 U/kg. Accordingly, minimum and maximum doses given were approximately 0.00025 and 250 units, respectively (assuming a 25 gram mouse). A 30 minute insulin stimulation timeframe was used for these studies based on previous observations of PNS

insulin signaling, and this was later confirmed with a time course study. Blood glucose levels were measured immediately prior to insulin administration and directly following the 30 minute insulin stimulation.

Based on the results of the dose curve and time course studies, an additional experiment was run to investigate PNS insulin signaling at a "therapeutically relevant" insulin dose, defined as a dose sufficient to decrease blood glucose levels without causing signs of hypoglycemia. An insulin dose of 1.29 U/kg (3 times the EC50 for glucose percent change in dose curve experiments) was delivered via IP injection and mice were sacrificed at 30 minutes, 2 hours, 4 hours, and 6 hours thereafter. Glucose levels were measured before insulin administration and at every subsequent time point. Sterile PBS was used as a vehicle control.

Western blot analysis: At sacrifice, tissues were harvested and snap frozen in liquid nitrogen and stored at -80°C until further use. Samples were homogenized in Cell Extraction Buffer (Invitrogen, Carlsbad, CA) containing 55.55 µl/ml protease inhibitor cocktail, 200mM Na_3VO_4, and 200mM NaF. After homogenization, samples were incubated on ice for 60 minutes and vortexed every 10 minutes to allow for complete protein extraction. Samples were then centrifuged for 10 minutes at 10000 rpm and the protein concentration of the supernatant was measured with a Bradford assay (Bio-Rad, Hercules, CA). Before samples were used for Western blot analysis, they were boiled with Lane Marker Reducing Sample Buffer (Thermo Scientific, Waltham, MA) for 3 minutes. 30 µg of protein was loaded per lane and samples were separated on a 4-15% gradient tris-glycine gel (Bio-Rad). After gel electrophoresis, samples were transferred to a nitrocellulose membrane and blocked in 5% milk. Following incubation with primary and secondary antibodies, resultant bands were visualized with film and analyzed with ImageJ (NIH). All Western blot data is reported as the band density of the phospho-protein normalized to the band density of the total protein.

Statistical Analysis: All data is expressed as means ± standard error of the mean. Insulin dose curve data was analyzed with a non-linear fit curve (Sigmoidal dose-response (variable slope)). The resultant EC50's and R squared values are reported. In addition, dose curve data was also analyzed with a

1-way ANOVA and Dunnett's post-hoc to compare all groups back to control (PBS). Experiments investigating signaling time courses and 1.29 U/Kg insulin doses were also analyzed with a 1-way ANOVA and Dunnett's post-hoc to compare all groups back to control (PBS or 0 time point). Outliers greater than or less than 2 standard deviations from the mean were not included in the analysis. All statistical tests were performed using GraphPad Prism software and a P value <0.05 was considered significant.

2.4 Results

Insulin induced Akt activation is dose and time dependent in the PNS:

Akt is a major downstream mediator of insulin signaling and Akt phosphorylation (ser 473 via mTorc2 and thr 308 via PDK1) can be used to quantify insulin signal transduction. Here, insulin was delivered via IP injection in increasing doses and PNS insulin signaling was quantified with Western blots of activated Akt (p-(Ser473)Akt/ total Akt and p-(Thr308)Akt/total Akt) in the DRG and sciatic nerve. Analysis of dose response curves indicated that insulin induced Akt ser473 and thr308 phosphorylation is dose dependent in both the DRG and sciatic nerve (Figure 2.1). At the maximum dose of 10,000 U/kg the fold change for Akt ser473 phosphorylation as compared to baseline in the DRG and sciatic nerve was 9.2 and 30.5, respectively. Analysis of Akt thr308 phosphorylation indicates the fold change at 10,000 U/Kg as compared to baseline was 14.0 in the DRG and 18.1 in the sciatic nerve.

Beyond dosing, insulin signaling in the PNS is time sensitive. To establish the PNS insulin signaling time course profile, mice were given IP injections of insulin at 33.05 U/kg (the EC50 for DRG Akt ser473 phosphorylation) and the DRG and sciatic nerve were harvested at 0, 5, 15, 30, and 60 minutes after insulin administration. At this dose, Akt activation was evident 5 minutes after insulin injection and appeared to be maximal at approximately 30 minutes in the DRG at both activation sites,

Figure 2.1

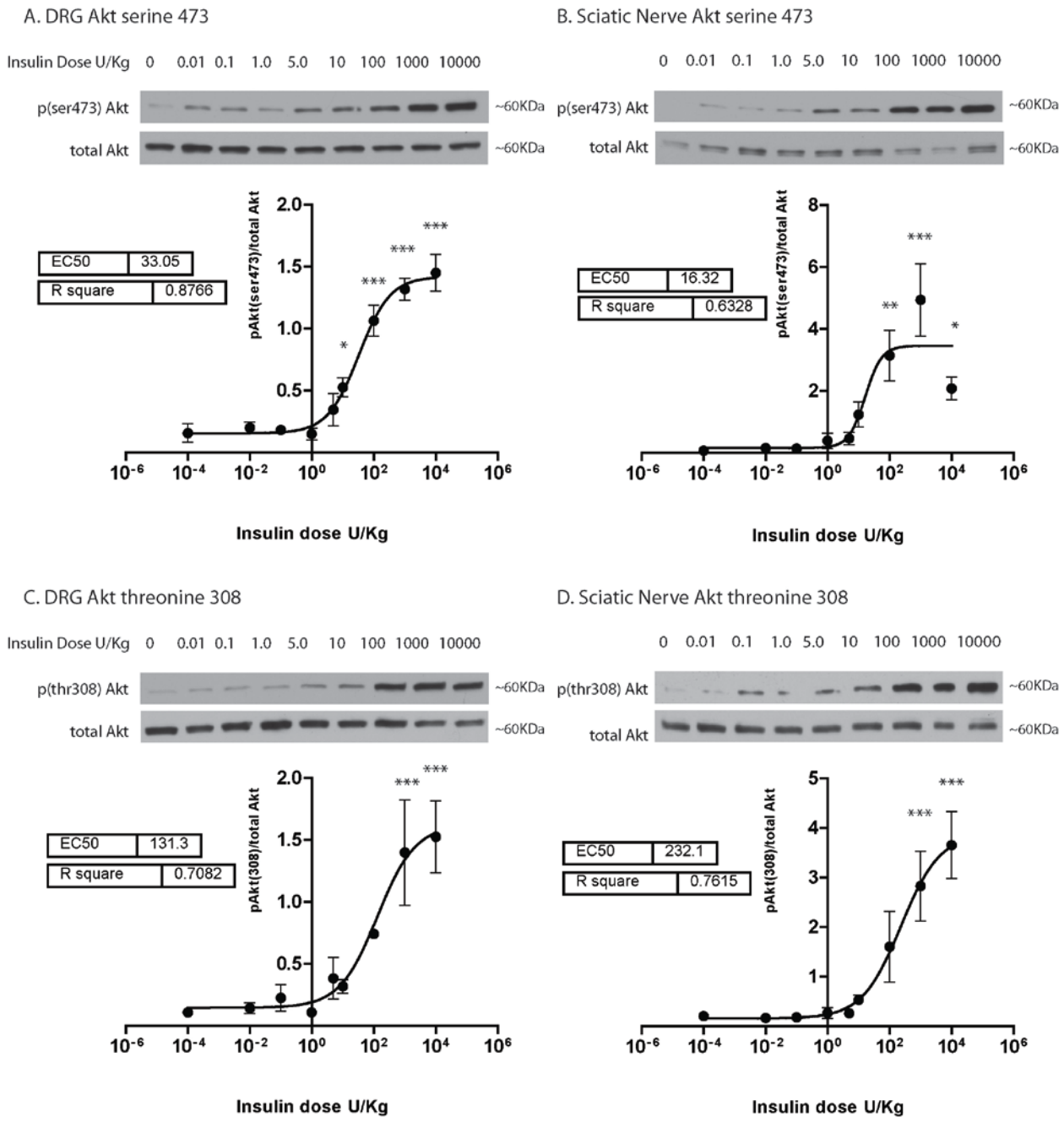
A. DRG Akt serine 473
Insulin Dose U/Kg 0 0.01 0.1 1.0 5.0 10 100 1000 10000
p(ser473) Akt
total Akt
~60KDa
EC50 33.05
R square 0.8766
pAkt(ser473)/total Akt
Insulin dose U/Kg
B. Sciatic Nerve Akt serine 473
EC50 16.32
R square 0.6328
C. DRG Akt threonine 308
p(thr308) Akt
EC50 131.3
R square 0.7082
pAkt(308)/total Akt
D. Sciatic Nerve Akt threonine 308
EC50 232.1
R square 0.7615

Figure 2.1: Insulin-induced Akt activation is dose dependent in the DRG and sciatic nerve. Mice were administered insulin via IP injections at doses of 0.01, 0.1, 1.0, 5.0, 10.0, 100.0, 1000.0 and 10000 U/kg. Sterile PBS was used as a vehicle control. Akt phosphorylation at sites serine 473 (A and B) and threonine 308 (C and D) were then analyzed in the DRG and sciatic nerve and normalized to total Akt levels. Data was fit with a sigmoidal dose response curve and analyzed with a 1-way ANOVA and Dunnet's post hoc. Results indicate that Akt activation in the DRG (A and C) and sciatic nerve (B and D) increased in a dose dependent manner with insulin. n=4-5 mice per dose. *=$p<0.05$, **=$p<0.01$, ***=$p<0.001$.

ser473 (6.5 fold change from baseline) (Figure 2.2 A) and thr308 (5.7 fold change from baseline) (Figure 2.2 C). In the sciatic nerve, Akt activation appeared to continue increasing out to the 60 minute time point at both phosphorylation sites, ser473 (14.0 fold change from baseline) (Figure 2.2 B) and thr308 (15.1 fold change from baseline) (Figure 2.2 D). For comparison, blood glucose levels were also collected at these time points (Figure 2.2 E). Glucose levels decreased throughout the study; however the rate of decrease was much slower from 15 to 60 minutes after an initial steep decline from 0 to 15 minutes. Experiments were not carried out past 60 minutes at this dose due to possible hypoglycemic events.

Downstream insulin signaling pathway activation in the PNS:

The insulin signaling cascade results in the activation of several cellular pathways, including pathways dependent on Akt activation and Akt independent pathways. Several proteins known to be modulated by insulin induced Akt activation in muscle, liver, and adipose tissue were investigated in the PNS via Western blot analysis including inhibition of GSK3β (glycogen synthesis), activation of mTor (protein synthesis), and activation of AS160 (glucose uptake). In addition, ERK activation was tested to evaluate Akt independent pathways (results are summarized in Table 2.1). All proteins investigated appeared to be respond to insulin in a dose dependent manner in the sciatic nerve (Figure 2.3). However, in the DRG, GSK3β (Figure 2.3A) and ERK (Figure 2.3G) signaling did not show a dose dependent relationship with insulin. In the sciatic nerve, it appeared that although both GSK3β (Figure 2.3B) and ERK (Figure 2.3H) signaling was dose dependent; a plateau level was not reached. Dunnet's post hoc suggests that at a dose of 10000 U/Kg GSK3β in the DRG (Figure 2.3A) and mTor in sciatic nerve (Figure 2.3F) were the only points that did not show significant change as compared to baseline.

The time course of downstream mediator activation was also investigated at an insulin dose of 33.05 U/Kg. Only GSK3β serine 9 phosphorylation in the sciatic nerve showed significant changes under these experimental conditions (Figure 2.4), suggesting that either a longer time frame or higher insulin doses are needed to effectively study downstream insulin signaling in the PNS. These results correlate

Figure 2.2

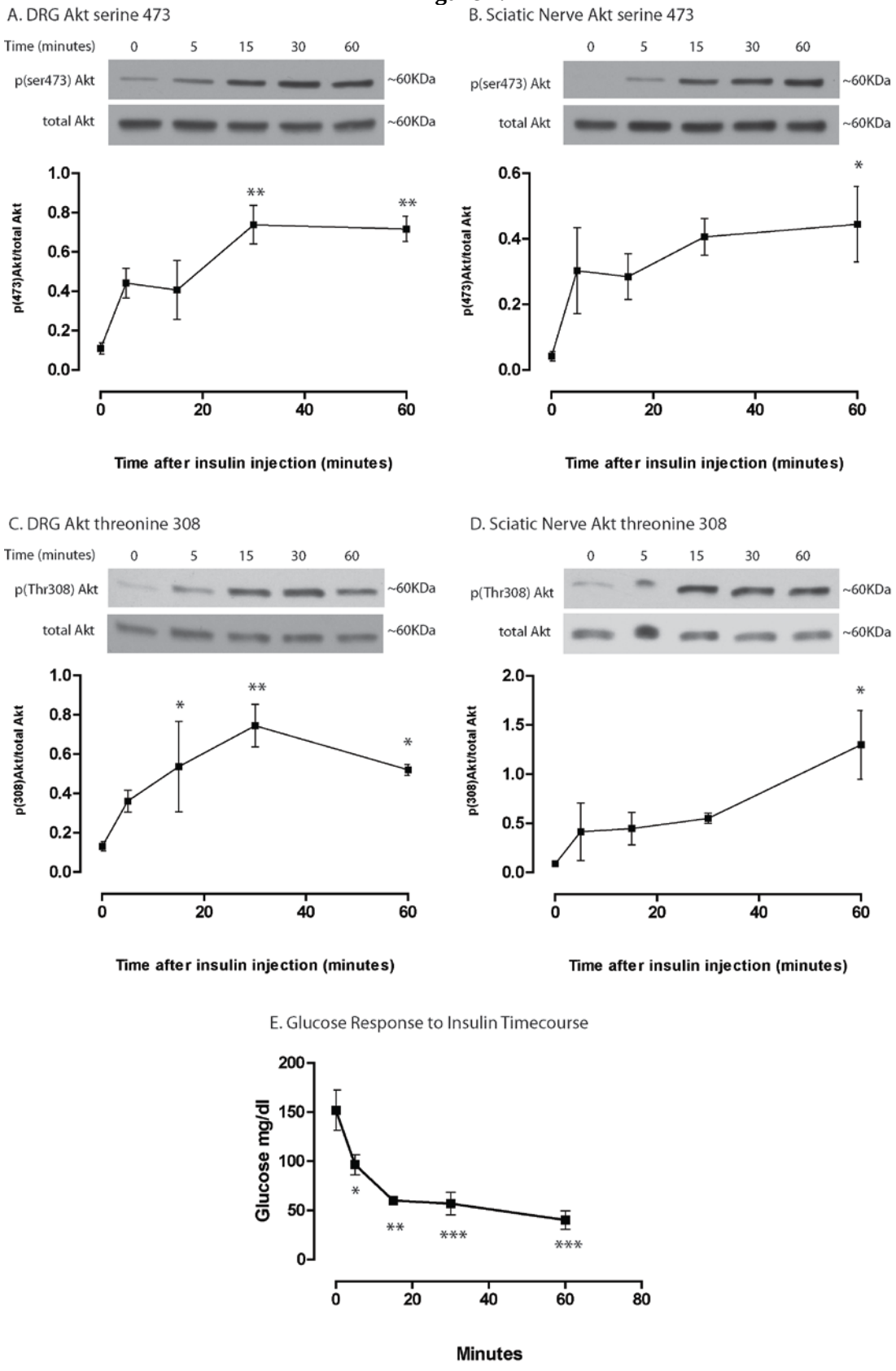
A. DRG Akt serine 473
Time (minutes) 0 5 15 30 60
p(ser473) Akt
total Akt
~60KDa
~60KDa
p(473)Akt/total Akt
Time after insulin injection (minutes)
B. Sciatic Nerve Akt serine 473
0 5 15 30 60
p(ser473) Akt
total Akt
~60KDa
~60KDa
p(473)Akt/total Akt
Time after insulin injection (minutes)
C. DRG Akt threonine 308
Time (minutes) 0 5 15 30 60
p(Thr308) Akt
total Akt
~60KDa
~60KDa
p(308)Akt/total Akt
Time after insulin injection (minutes)
D. Sciatic Nerve Akt threonine 308
0 5 15 30 60
p(Thr308) Akt
total Akt
~60KDa
~60KDa
p(308)Akt/total Akt
Time after insulin injection (minutes)
E. Glucose Response to Insulin Timecourse
Glucose mg/dl
Minutes

Figure 2.2: Insulin-induced Akt activation time course in DRG and sciatic nerve. Mice were administered 33.05 U/Kg insulin and Akt activation in the DRG (A and C) and sciatic nerve (B and D) was analyzed via Western blot at 5, 15, 30, and 60 minutes post insulin injection. Akt activation appears to be maximal around 30 minutes in the DRG and 60 minutes in the sciatic nerve. Glucose levels were significantly decreased 5 minutes after insulin injection. Results were analyzed with a 1-way ANOVA and Dunnett's post hoc. N=3 mice per time point. *=$p<0.05$, **=$p<0.01$, ***=$p<0.001$.

Figure 2.3

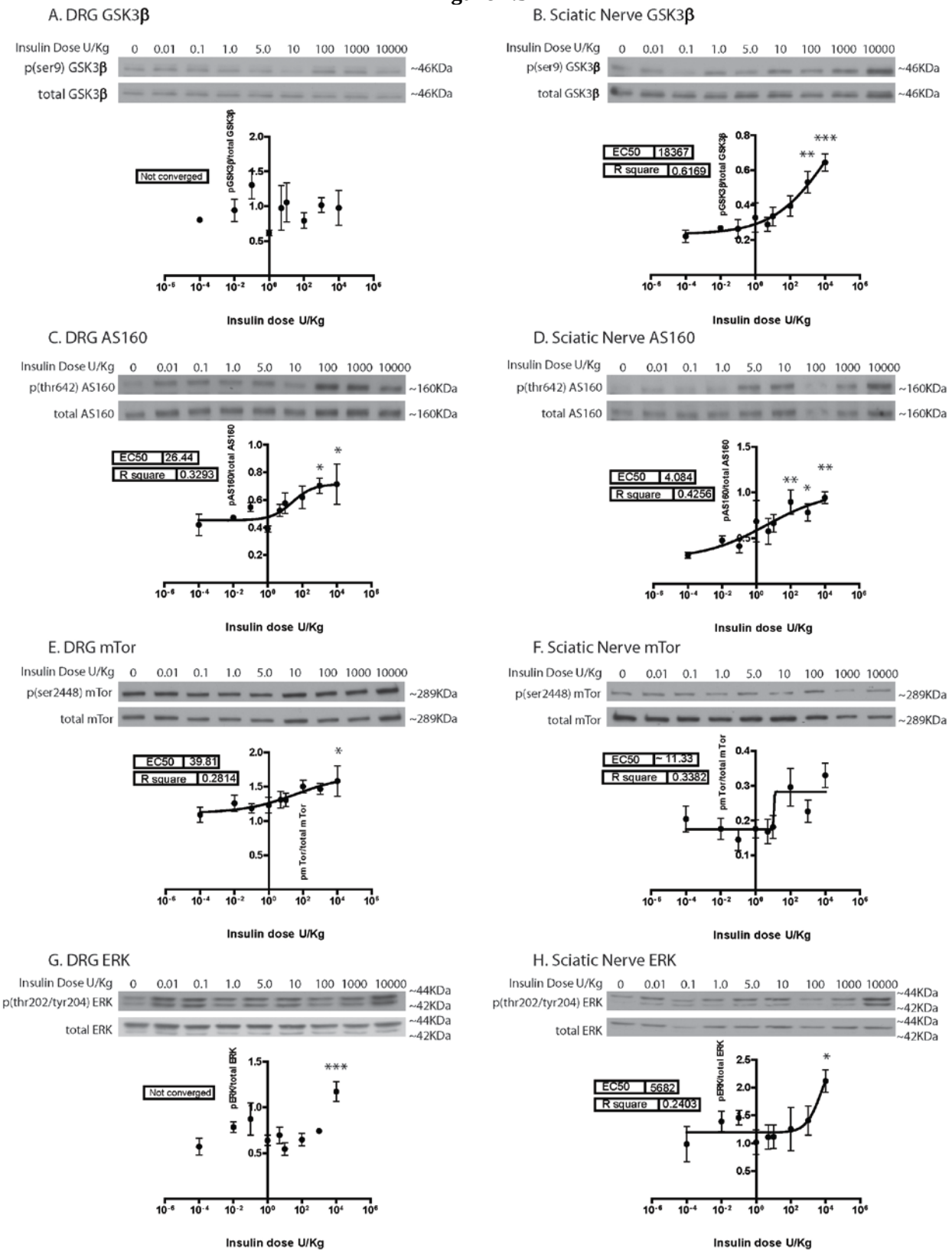
A. DRG GSK3β
Insulin Dose U/Kg 0 0.01 0.1 1.0 5.0 10 100 1000 10000
p(ser9) GSK3β
total GSK3β
~46KDa
~46KDa
Not converged
pGSK3β/total GSK3β
Insulin dose U/Kg
B. Sciatic Nerve GSK3β
Insulin Dose U/Kg 0 0.01 0.1 1.0 5.0 10 100 1000 10000
p(ser9) GSK3β
total GSK3β
~46KDa
~46KDa
EC50 18367
R square 0.6169
pGSK3β/total GSK3β
Insulin dose U/Kg
C. DRG AS160
Insulin Dose U/Kg 0 0.01 0.1 1.0 5.0 10 100 1000 10000
p(thr642) AS160
total AS160
~160KDa
~160KDa
EC50 26.44
R square 0.3293
pAS160/total AS160
Insulin dose U/Kg
D. Sciatic Nerve AS160
Insulin Dose U/Kg 0 0.01 0.1 1.0 5.0 10 100 1000 10000
p(thr642) AS160
total AS160
~160KDa
~160KDa
EC50 4.084
R square 0.4256
pAS160/total AS160
Insulin dose U/Kg
E. DRG mTor
Insulin Dose U/Kg 0 0.01 0.1 1.0 5.0 10 100 1000 10000
p(ser2448) mTor
total mTor
~289KDa
~289KDa
EC50 39.81
R square 0.2814
pm Tor/total m Tor
Insulin dose U/Kg
F. Sciatic Nerve mTor
Insulin Dose U/Kg 0 0.01 0.1 1.0 5.0 10 100 1000 10000
p(ser2448) mTor
total mTor
~289KDa
~289KDa
EC50 11.33
R square 0.3382
pm Tor/total m Tor
Insulin dose U/Kg
G. DRG ERK
Insulin Dose U/Kg 0 0.01 0.1 1.0 5.0 10 100 1000 10000
p(thr202/tyr204) ERK
total ERK
~44KDa
~42KDa
~44KDa
~42KDa
Not converged
pERK/total ERK
Insulin dose U/Kg
H. Sciatic Nerve ERK
Insulin Dose U/Kg 0 0.01 0.1 1.0 5.0 10 100 1000 10000
p(thr202/tyr204) ERK
total ERK
~44KDa
~42KDa
~44KDa
~42KDa
EC50 5682
R square 0.2403
pERK/total ERK
Insulin dose U/Kg

Figure 2.3. Insulin dose curve downstream mediator activation. In addition to Akt, the *in vivo* signaling of several other proteins in the insulin pathway was investigated in the DRG and sciatic nerve in response to an IP insulin dose curve. Data was fit with a sigmoidal dose response curve and analyzed with a 1-way ANOVA and Dunnet's post hoc. The sigmoidal dose response curve was unable to fit the GSK3β (A) and ERK (F) results in the DRG (not converged). All other proteins appear to have a dose dependent relationship with insulin. The overall ANOVA p-value was significant for all proteins investigated except mTor and GSK3β in the DRG and ERK in the SN. Results of Dunnet's post hoc are denoted with *. n=4-5 mice per dose. *=$p<0.05$, **=$p<0.01$, ***=$p<0.001$.

Table 2.1

Protein of Interest	Dose Curve EC50		Dose Curve R^2 Value		10000U/Kg Insulin-induced fold change as compared to baseline	
	DRG	Sciatic Nerve	DRG	Sciatic Nerve	DRG	Sciatic Nerve
Akt (t308)	33.05	16.3	0.71	0.76	13.9***	18.1***
Akt (s473)	131.3	232.1	0.88	0.63	9.2***	30.5*
GSK3β (s9)	not converged	18367.0	not converged	0.62	1.2	2.9***
AS160 (t642)	26.4	4.1	0.33	0.43	1.7*	3.0**
mTor (s2448)	39.8	~11.3	0.28	0.34	1.4*	1.6
ERK (Thr202/Tyr204)	not converged	5682.0	not converged	0.24	2.1***	1.8*

Table 2.1: Summary of insulin dose curve insulin signaling pathway activation in the DRG and sciatic nerve. Analyzed results of *in vivo* insulin signaling in the DRG and sciatic nerve in response to an insulin dose curve indicate that both sensory neuron cell bodies and the peripheral nerve are insulin responsive. Interestingly, differences in downstream signaling may exist between the DRG and sciatic nerve. Data was fit with a sigmoidal dose response curve and analyzed with a 1-way ANOVA and Dunnet's post hoc. "not converged" indicates that the sigmoidal dose response curve equation was unable to fit the data. *=$p<0.05$, **=$p<0.01$, ***=$p<0.001$.

Figure 2.4

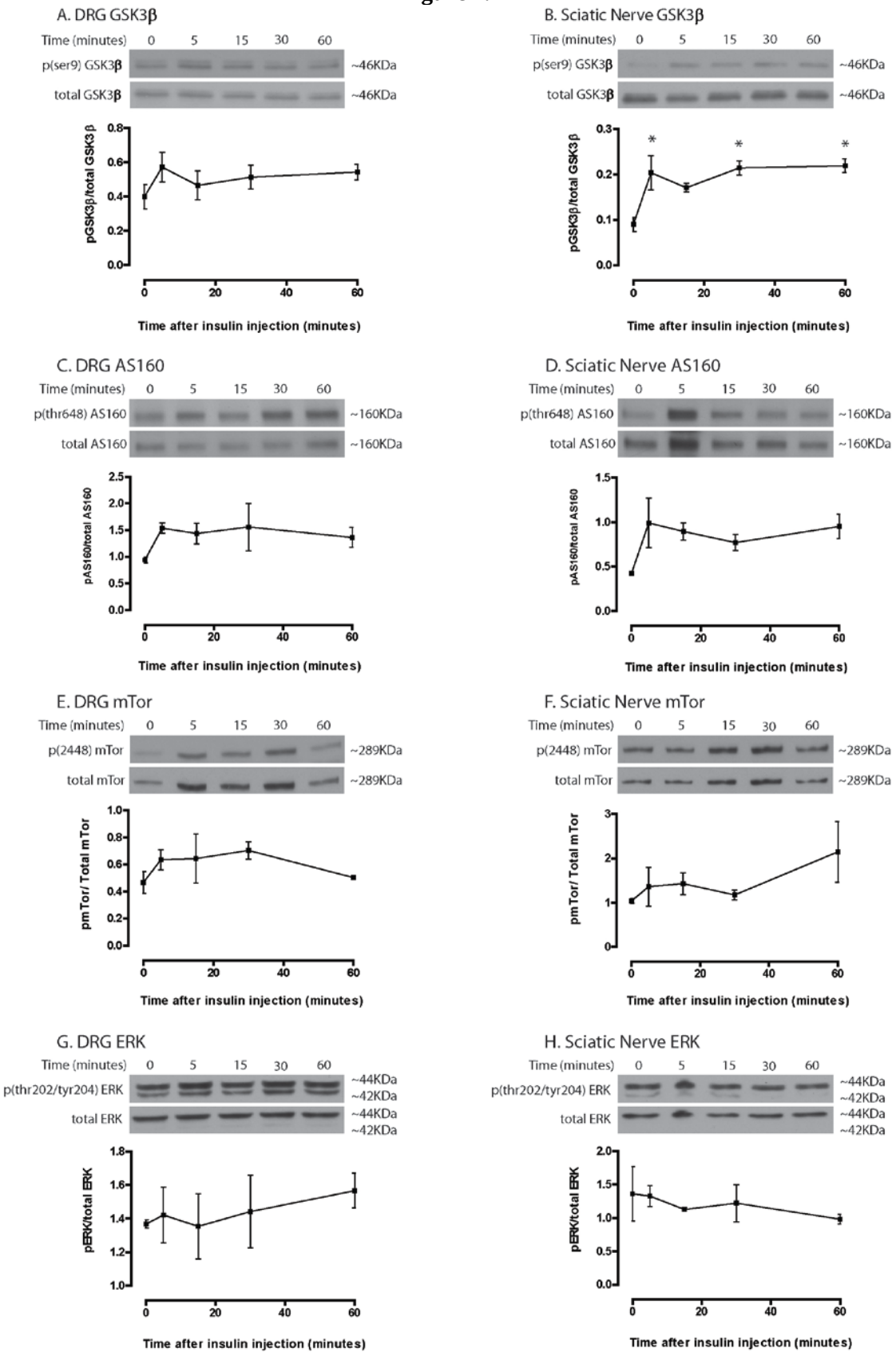
A. DRG GSK3β
Time (minutes) 0 5 15 30 60
p(ser9) GSK3β ~46KDa
total GSK3β ~46KDa
pGSK3β/total GSK3β
Time after insulin injection (minutes)
B. Sciatic Nerve GSK3β
Time (minutes) 0 5 15 30 60
p(ser9) GSK3β ~46KDa
total GSK3β ~46KDa
pGSK3β/total GSK3β
Time after insulin injection (minutes)
C. DRG AS160
Time (minutes) 0 5 15 30 60
p(thr648) AS160 ~160KDa
total AS160 ~160KDa
pAS160/total AS160
Time after insulin injection (minutes)
D. Sciatic Nerve AS160
Time (minutes) 0 5 15 30 60
p(thr648) AS160 ~160KDa
total AS160 ~160KDa
pAS160/total AS160
Time after insulin injection (minutes)
E. DRG mTor
Time (minutes) 0 5 15 30 60
p(2448) mTor ~289KDa
total mTor ~289KDa
pmTor/ Total mTor
Time after insulin injection (minutes)
F. Sciatic Nerve mTor
Time (minutes) 0 5 15 30 60
p(2448) mTor ~289KDa
total mTor ~289KDa
pmTor/ Total mTor
Time after insulin injection (minutes)
G. DRG ERK
Time (minutes) 0 5 15 30 60
p(thr202/tyr204) ERK ~44KDa ~42KDa
total ERK ~44KDa ~42KDa
pERK/total ERK
Time after insulin injection (minutes)
H. Sciatic Nerve ERK
Time (minutes) 0 5 15 30 60
p(thr202/tyr204) ERK ~44KDa ~42KDa
total ERK ~44KDa ~42KDa
pERK/total ERK
Time after insulin injection (minutes)

Figure 2.4. Time course of insulin signaling downstream mediator activation. In contrast to Akt results, few significant changes were observed in downstream insulin signaling throughout the time course at a dose of 33.05 U/Kg. Only GSK3β in the sciatic nerve showed significant differences from baseline when analyzed with a 1-way ANOVA and Dunnet's post hoc (Figure 4B). n=3 mice per time point. *=$p<0.05$, **=$p<0.01$, ***=$p<0.001$.

with those observed in the dose curve, where GSK3β in the sciatic nerve had the best fit with the sigmoidal dose response analysis (R square=0.6169) (Figure 3B).

Differences in insulin signaling exist between PNS and "classically" insulin sensitive tissues:

An interesting observation from the dose curve experiments was the large difference between the EC50 for glucose percent change (0.43 U/kg) (Figure 2.5A) and the EC50 for Akt activation in the DRG (33.05 U/kg) (Figure 2.1A), approximately a 77 fold difference. Furthermore, it is recognized that 33.05 U/Kg is supraphysiological insulin dose and potentially lethal. To further explore the difference in glucose percent change and PNS insulin signaling as well as to investigate PNS insulin signaling at a more physiological insulin dose; Akt activation was tested over a 6 hour period in the PNS as well as in muscle, liver, and adipose at a "therapeutically relevant" dose. An insulin dose 3 times the EC50 for glucose percent change, 1.29 U/kg; was used for these experiments. Time points chosen were based on a previous publication investigating the delivery of insulin to neural structures via intranasal or subcutaneous injections [201]. It was indicated that intranasal insulin had greater deliver to neural structures at early time points, but that later time points showed increased insulin levels with systemic deliver. As expected, significant increases in Akt activation were seen in the liver (21.8 fold change) (Figure 2.5C), muscle (4.6 fold change) (Figure 2.5D), and adipose (21.5 fold change) (Figure 2.5E) at 30 minutes, correlating with the change in glucose levels (Figure 2.5B). However, of the neural tissues investigated only the sciatic nerve demonstrated a significant increase in Akt activation (2.5 fold change) at 30 minutes (Figure 2.5F). No significant changes in Akt activation were observed in the DRG or spinal cord at all-time points investigated (Figures 2.5G and 2.5H, respectively). These results differ from previous results presented using higher insulin doses; indicating the dose and timeframe of insulin signaling in the PNS are codependent, an important consideration when trying to establish outcome measures for *in vivo* quantification of PNS insulin signaling.

Figure 2.5

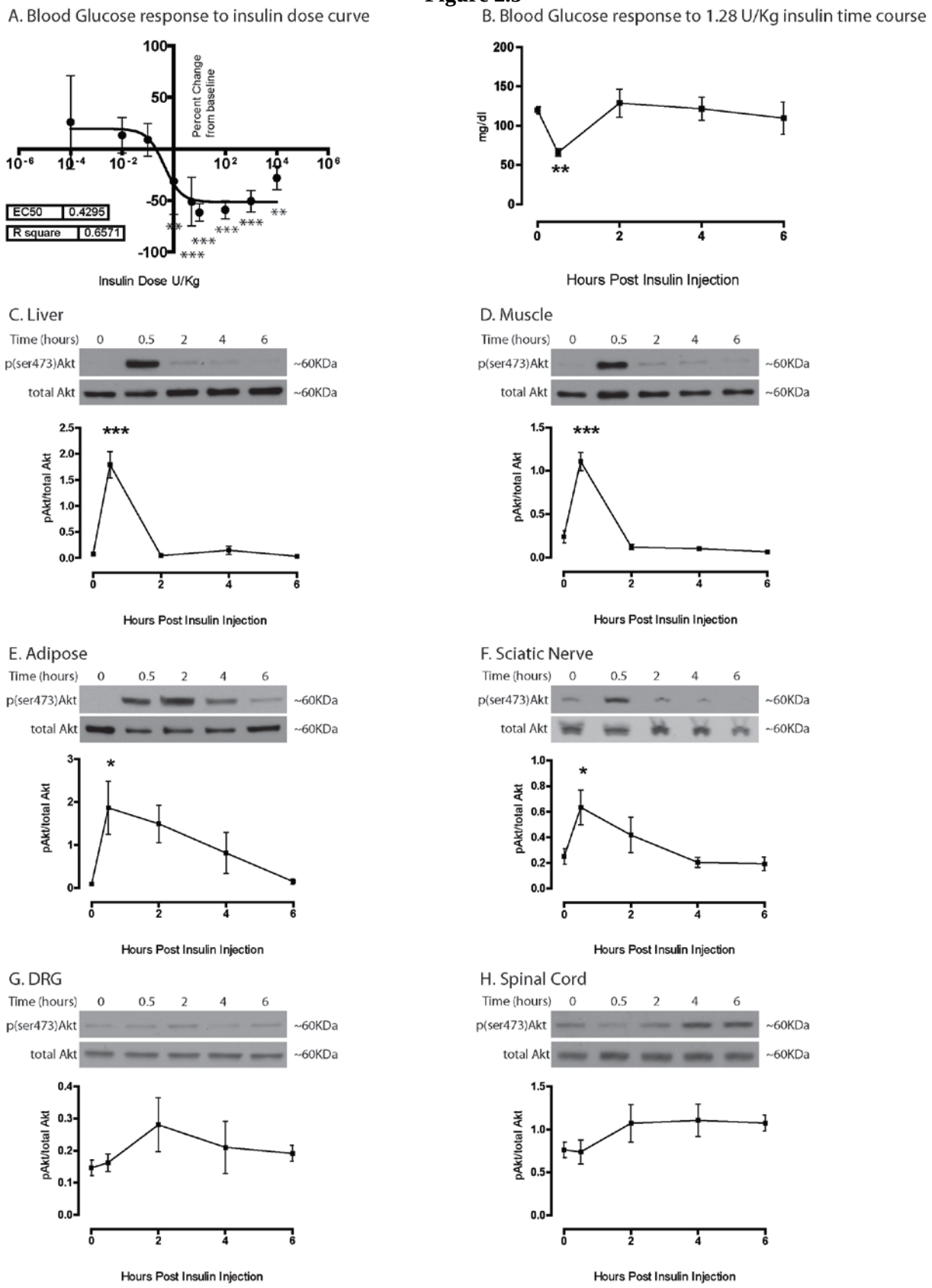
A. Blood Glucose response to insulin dose curve
Percent Change from baseline
EC50 0.4295
R square 0.6571
Insulin Dose U/Kg
B. Blood Glucose response to 1.28 U/Kg insulin time course
mg/dl
Hours Post Insulin Injection
C. Liver
D. Muscle
E. Adipose
F. Sciatic Nerve
G. DRG
H. Spinal Cord
Time (hours) 0 0.5 2 4 6
p(ser473)Akt
total Akt
~60KDa
pAkt/total Akt
Hours Post Insulin Injection

Figure 2.5. "Therapeutic" insulin dose Akt activation time course in liver, muscle, adipose, sciatic nerve, DRG, and spinal cord. Analysis with sigmoidal dose response curve indicates that the EC50 for glucose percent change was 0.4295 U/Kg in insulin dose curve studies (A). A 6-hour time course study using 1.29 U/Kg insulin showed a significant decrease in glucose levels 30 minutes after insulin injection, with a return to baseline by 2 hours (B). Significant Akt activation was observed at 30 minutes post insulin in the liver (C), muscle (D), adipose (E), and sciatic nerve (F). No significant changes were seen in the DRG (G) or lumbar spinal cord (H). Data was analyzed with a 1-way ANOVA and Dunnet's post hoc. n=6 at 0 time point, n=6 at 30 minute time point, n=4 at 2 hour time point, n=5 at 4 hour time point, n=3 at 6 hour time point. *=$p<0.05$, **=$p<0.01$, ***=$p<0.001$.

2.5 Discussion

Due to the growing cases of diabetes, diabetic complications are becoming increasingly prevalent. DN occurs with an elevated incidence as compared to other complications and is associated with dramatic decreases in patient quality of life. The goal of this study was to establish the profile of insulin signaling in the PNS *in vivo* in order to better understand how disruptions in PNS insulin signaling may impact sensory neuron function. Our results indicate that the PNS is clearly insulin responsive and that differences in insulin signaling may exist between PNS compartments. Furthermore, it also appears that PNS insulin signaling is muted as compared to muscle, liver, and adipose at a therapeutically relevant dose. Importantly, these results will further guide researchers when completing *in vivo* studies evaluating the impact of altered insulin signaling on DN pathogenesis.

A consistent theme throughout the presented data was an increased insulin response in the sciatic nerve as compared to the DRG. For several of the investigated proteins, a higher fold change in activation (inhibition for GSK3β) was observed in the sciatic nerve. These results closely mimic previous observations of insulin signaling in the PNS using intrathecal injections (unpublished observation, Figure 4.3). Moreover, at a "therapeutically relevant" insulin dose, only the sciatic nerve showed a significant increase in Akt activation. It is plausible that the post mitotic DRG neurons are buffered from large swings in insulin levels and rely more on basal insulin for support; whereas the Schwann cells of the peripheral nerve readily react to changing insulin levels via Akt activation to induce proliferation [202], differentiation [203] and myelination [204]. In fact, it has been recently discovered that not only do Schwann cells express insulin receptors [183], but that insulin receptor signaling is important in regulating glycoprotein P0 expression [172]. Furthermore, Schwann cell dysfunction has been implicated in diabetic neuropathy [205]. Thus, we propose that reductions in insulin signaling associated with diabetes not only impacts the sensory neuron cell body, but also the axons and Schwann cells of the peripheral nerve which severely diminishes the regenerative/repair capacity of distal axons. In DN, reduced PNS insulin signaling may be more of a propagating event than an inciting event, such that nerves cannot recover from hyperglycemia injury due to the lack of insulin support.

One important consideration when interpreting the data presented here is that this was a one-time IP injection of Humulin R insulin, differences in delivery (insulin pumps) or insulin formulations may give differing results. Furthermore, it should be noted that cross talk between insulin and the IGF1 receptor does occur [176]. Insulin at high concentrations can signal through the IGF1 receptor and activate many of the same intracellular pathways (namely Akt). Thus, the signaling observed cannot be solely attributed to signaling through the insulin receptor.

While these studies have provided a new understanding of insulin signaling in the PNS, they do not provide much indication of what amount of signaling is needed for a biological/cellular response or what exactly that response maybe. It can be extrapolated from the proteins investigated and the understanding of these pathways in "classically" insulin sensitive tissues, however further research is needed to completely understand the physiologic role of insulin in the PNS. The results of two downstream mediators were of particular interest, GSK3β and AS160. Inhibition of GSK3β was dose dependent in the sciatic nerve but not the DRG; suggesting that insulin may have divergent downstream signaling within different compartments of the PNS. Interestingly, inhibition of GSK3β has been shown to play a pivotal role in peripheral nerve remyelination [206] and that this may occur via the PI3K-Akt pathway [203]. Reductions in insulin-induced GSK3β inhibition in the peripheral nerve may contribute to pathological changes in DN. AS160 is predominantly thought to be involved in glucose uptake via translocation of Glut4 to the plasma membrane [207]. DRG neurons and Schwann cells of the peripheral nerve do not take up glucose in an insulin dependent manner [144, 208]. Thus, a dose dependent increase in AS160 activation was surprising. These results suggest that either high dose insulin may trigger glucose uptake in the PNS or that AS160 may have a previously undiscovered function in these tissues. Further experiments are needed to fully elucidate these possibilities.

A growing trend in the literature indicates that direct administration of insulin to the nervous system has a much greater neurotrophic potency as compared to systemic insulin administration [191, 201]; an idea first proposed by Kan et. al., [209]. The results presented here may explain some of this observed effect, in that a majority of systemically delivered insulin is quickly metabolized in the muscle,

liver, and adipose possibly contributing to a blunted neurotrophic effect. Furthermore, it appears that only the peripheral nerve is responsive to low doses of systemic insulin; whereas, both the neuronal cell body and peripheral nerve are responsive to intrathecal insulin (unpublished observation, Figure 4.3). Insulin stimulation of both PNS compartments may produce a greater neurotrophic effect as compared to just peripheral nerve signaling. These results suggest that while current insulin formulations and delivery methods are very adequate for reducing elevated glucose levels, they may not reach the nervous system appropriately, and thus fail to deliver the needed neurotrophic support. Perhaps the development and integration of better insulin delivery to the nervous system either through different routes (i.e. intranasal) or through insulin peptide modification is warranted.

In conclusion, these studies have established that the PNS is insulin responsive *in vivo* and that the peripheral nerve and DRG may have different insulin signaling profiles. This information provides a new basis for future experiments designed to explore the role of insulin in the PNS and how disruptions in PNS insulin signaling may be contributing to DN pathogenesis.

Chapter 3: Insulin Receptor Substrate 2 Expression and Involvement in Neuronal Insulin Resistance in Diabetic Neuropathy

3.1 Abstract

Insulin signaling depends on tyrosine phosphorylation of insulin receptor substrates (IRS) to mediate downstream effects; however, elevated serine phosphorylation of IRS impairs insulin signaling. Here, we investigated IRS protein expression patterns in dorsal root ganglia (DRG) of mice and whether their signaling was affected by diabetes. Both IRS1 and IRS2 are expressed in DRG, however IRS2 appears to be the prevalent isoform and is expressed by many DRG neuronal subtypes. Phosphorylation of Ser(731)IRS2 was significantly elevated in DRG neurons from diabetic mice. Additionally, Akt activation and neurite outgrowth in response to insulin were significantly decreased in DRG cultures from diabetic *ob/ob* mice. These results suggest that DRG neurons express IRS proteins that are altered by diabetes similar to other peripheral tissues, and insulin signaling downstream of the insulin receptor may be impaired in sensory neurons and contribute to the pathogenesis of diabetic neuropathy.

3.2 Introduction

Insulin receptor substrate (IRS) is a key mediator of intracellular insulin signaling. IRS is a docking protein known to be composed of 3 structural significant areas, an N-terminal pleckstrin homology (PH) domain, a phosphotyrosine-binding (PTB) domain, and a C-terminal tail with multiple tyrosine, serine, and threonine phosphorylation sites [18, 19, 210]. The PH domain plays a role in binding IRS to the plasma membrane and the insulin receptor, the PTB domain binds IRS directly to the juxtamembrane domain of the insulin receptor, and the phosphorylation sites regulate the binding of effectors to IRS [18, 19, 210]. In addition, IRS2 also has a kinase regulatory-loop binding (KRLB) domain that plays a role in regulating IRS2 tyrosine phosphorylation [211].

Four mammalian isoforms of IRS have been described thus far, with IRS1 and IRS2 being the most physiologically relevant [212, 213]. IRS1 appears to be the main isoform expressed in muscle and adipose tissue [212-214], whereas IRS2 seems to be more relevant in liver and brain [212, 213, 215]. Mice with systemic IRS1 knockouts demonstrate growth retardation, insulin resistance, and beta-cell hyperplasia without diabetes [213]. IRS2 knockout mice develop insulin resistance, decreased beta-cell proliferation, overt diabetes, and female sterility [212, 213].

Serine phosphorylation of IRS has emerged as a key regulatory step for insulin signaling in both physiological and pathological situations. A large body of work suggests that elevated IRS serine phosphorylation inhibits insulin signal transduction [18, 19, 210, 214, 216-222]. Under normal conditions, IRS is tyrosine phosphorylated upon insulin binding, but following accumulation of activated downstream mediators, IRS is phosphorylated on serine residues, impairing insulin signaling through a negative feedback mechanism. In an insulin-resistant state, agents that promote IRS serine phosphorylation are upregulated, resulting in pathological elevation of IRS serine phosphorylation and impaired insulin signaling [18, 19, 210, 216, 217, 222-224].

To address whether these same regulatory mechanisms affect sensory neurons, we examined IRS expression and signaling *in vivo* and *in vitro* in DRG neurons from streptozotocin (STZ)-induced type 1 and *ob/ob* type 2 diabetic mice. Our results suggest that IRS proteins are expressed by sensory DRG

neurons and undergo elevated serine phosphorylation in diabetic mice. Cultured DRG neurons from *ob/ob* animals had blunted responses to insulin as indicated by decreased Akt activation and neurite outgrowth. These findings support the hypothesis that insulin resistance due to increased serine phosphorylation of IRS2 could contribute to alterations in neuronal insulin support and promote peripheral nerve dysfunction.

3.3 Experimental Procedures

Animals: All experiments were approved by the University of Kansas Medical Center Institutional Animal Care and Use Committee. Mice were subjected to a 12-hour light/dark cycle and had ad libitum access to food and water. For determination of IRS expression, 8-week old male C57Bl/6 mice were purchased from Charles River (Wilmington, MA). DRG were harvested for reverse transcriptase-PCR, Western blot analysis, and immunohistochemistry. To determine the effects of diabetes on insulin signaling in peripheral neurons, male *ob/ob* mice and colony controls were ordered at 8 weeks of age from Jackson Laboratories (Bar Harbor, Maine). The *ob/ob* leptin knockout mice have been previously characterized as a model of insulin resistance, type 2 diabetes, and DN [77].

In addition, diabetes was induced in 8 week-old C57BL/6 male mice using a single intraperitoneal injection of streptozotocin (STZ), a pancreatic beta cell toxin, (Sigma, St. Louis, MO) at 180 mg/kg body weight. The STZ was dissolved in 10mM sodium citrate buffer (pH 4.5) and the nondiabetic mice were injected with 400 μl of the vehicle buffer. Mice were fasted for 3 hours pre and post injection to improve STZ uptake in pancreatic β cells. Body weights and blood glucose levels via tail clip were checked weekly to monitor diabetes progression.

Adult DRG Culture: Mice were anesthetized with an intraperitoneal (IP) injection of cold Avertin (2-2-2 Tribromoethanol) 20μL g^{-1} and transcardially perfused with ice-cold HBSS without Ca^{++}/Mg^{++} (Sigma-Aldrich) to reduce protease activity and increase cell survival [225]. The DRG were harvested and transferred to 3 mL of ice-cold HBSS without Ca^{++}/Mg^{++}. Adult mouse DRG were cultured

according to a protocol published by Molliver et al [225]. All procedures were performed in a tissue hood with appropriate sterile technique. DRG were partially digested with 2 separate enzyme solutions, one containing papain (Worthington, Lakewood, NJ) and another containing collagenase type II (Worthington) and dispase type II (Roche, Basel, Switzerland). Neurons were then triturated with a fire-polished glass Pasteur pipette to dissociate neuronal cell bodies. Neurons were grown on laminin/poly-D-lysine coated coverslips (BD Biosciences, Bedford, MA) placed in 24 well culture plates (Sigma-Aldrich). The media consisted of insulin-free B27 supplement (Invitrogen, Carlsbad, CA), penicillin/streptomycin (Invitrogen), and F12 culture medium (Invitrogen). Neurons were then allowed to adhere to coverslips for 2 hours. After this time, either 1mL fresh insulin-free media or media containing 100nM insulin (Sigma-Aldrich), depending on the experimental group and assay was added. For hyperglycemia experiments, DRG neuronal cultures from wildtype C57Bl/6 mice were grown in 25mM glucose and control cultures were maintained at 10mM glucose [226, 227].

Reverse Transcriptase-Polymerase Chain Reaction: RT-PCR was performed to determine mRNA levels of different IRS isoforms. Total RNA was isolated from DRG tissue using TRI Reagent (Ambion, Foster City, CA) as indicated in the manufacturer's protocol. The RNA concentration was determined using a Bio Rad spectrophotometer and the quality of RNA was tested with an electrophoretic separation technique (Agilent 2100 bioanalyzer tracer with the Eukaryote Total RNA Nano assay). RNA was then reverse transcribed to cDNA using iScript cDNA synthesis kit (Bio Rad). The thermal cycler conditions were as follows: 25°C for 5 minutes, 42°C for 30 minutes, and 85°C for 5 minutes. Real time PCR amplification of IRS1, IRS2, IRS3, and IRS4 was performed using 2.0µg of cDNA and SYBR green master mix (Bio-Rad). Glyceraldehyde 3-phosphate dehydrogenase (GAPDH) was used as a reference gene and all reactions were run in triplicate. The thermal cycler conditions for PCR were 95°C and 60°C for 40 cycles. IRS isoform mRNA levels were normalized to GAPDH and the ΔΔCt method was used for relative expression analysis. The primer sequences used for real time PCR were as follows:

IRS1 forward: 5'-CTCTACACCCGAGACGAACAC-3'

IRS1 reverse: 5'-TGGGCCTTTGCCCGATTATG-3'

IRS2 forward: 5'-CTGCGTCCTCTCCCAAAGTG-3'

IRS2 reverse: 5'-GGGGTCATGGGCATGTAGC-3'

IRS3 forward: 5'-TCCTCCAAAGAGTGTTCCTGC-3'

IRS3 reverse: 5'-GGGGCTTGAAGTAGTCCTGC-3'

IRS4 forward: 5'-TCCTGTACCAATGCTTCTCCG-3'

IRS4 reverse: 5'-AGCTTTCTTGTTCCGACTCGT-3'

GAPDH forward: 5'-AGGTCGGTGTGAACGGATTTG-3'

GAPDH reverse: 5'-TGTAGACCATGTAGTTGAGGTCA-3'

Western Blots: Protein from primary DRG cultures was harvested after 3 days in insulin-free media by removing growth media, adding CEB (Invitrogen), and then scraping the coverslips. Cell Extraction Buffer (CEB) (Invitrogen) contained 55.55 µl/ml protease inhibitor cocktail, 200mM Na_3VO_4, and 200mM NaF. Three coverslips per treatment group were combined into a single sample. The samples were incubated on ice for 1 hour with light vortexing every 10 minutes and then centrifuged at 7000 rpm for 10 minutes at 4°C. Protein concentration of the supernatant was measured with a Bradford assay (Bio-Rad, Hercules, CA). Samples were then boiled with Lane Marker Reducing Sample Buffer (Thermo Scientific, Waltham, MA) for 3 minutes. For normalization purposes, equal amounts of protein were loaded for each sample. The samples were separated on a 4-15% gradient tris-glycine gel (Bio-Rad) and then transferred to a nitrocellulose membrane. After transfer, the membrane was stained with Ponceau S and cut so that IRS (180kDA) and Akt (60kDA) are separated, producing 2 membranes that could be probed independently. Primary antibodies were used at the following dilutions and incubations: total IRS1 (Santa Cruz, Santa Cruz, CA) 1:1000 overnight at 4°C, total IRS2 (Millipore, Billerica, MA) 1:500 overnight at 4°C, pSer(731)IRS2 (Abcam, Cambridge, MA) 1:1000 overnight at 4°C, insulin receptor β subunit (Santa Cruz) 1:500 overnight at 4°C, pSer(473)Akt (Cell Signaling, Danvers, MA) 1:500 overnight at 4°C, total Akt (Cell Signaling) 1:500 overnight at 4°C, and actin (Millipore) 1:100,000 at room temperature for 1 hour. Anti-mouse and anti-rabbit secondary antibodies conjugated to HRP (Santa

Cruz) were diluted 1:10,000 and incubated for 1 hour at room temperature. Band density was analyzed with ImageJ (NIH).

Immunohistochemistry: DRG were harvested and immediately frozen in Tissue Tek (Sakura Fineteck, Torrance, CA). The tissue was sectioned at 10µm with a cryostat and placed in serial order on glass slides. Slides were blocked at room temperature for 1 hour with pre-incubation solution (1.5% Normal Goat or Donkey Serum, 0.5% Porcine Gelatin, 0.5% Triton X-100, and 450 µL Superblock (Thermo Scientific)). Primary antibodies were used at the following dilutions and incubations: total IRS2 (Millipore) 1:400 overnight at 4°C, mouse monoclonal Peripherin (Millipore) 1:2000 overnight at 4°, and mouse monoclonal Neurofilament 200 (Sigma) 1:2000 overnight at 4°C. Donkey anti-Rabbit Alexa-488 and donkey anti-mouse Alexa-555 conjugated secondary antibodies (Invitrogen) were diluted 1:2000 and incubated for 1 hour at 4°C. Images were photographed using a Nikon Eclipse E800 microscope and analyzed with ImageJ (NIH).

Neurite Outgrowth: To assess potential changes in the functional neurotrophic effect of insulin on DRG neurons, neurite outgrowth was quantified in dissociated cultures of *ob/ob* mice and controls. After 5 days in culture with either insulin-free media or media containing 100nM insulin the neurons were fixed with 4% paraformaldehyde for 10 minutes. Immunohistochemistry was performed with SMI-312 (Covance, Emeryville, CA), a pan-axonal marker, to visualize neurites, and counterstained with nuclear marker, Hoechst 33342 (Invitrogen). Coverslips were mounted on slides and imaged. Neurite outgrowth area was quantified using Image J. A stereological grid was superimposed on images of the cultures and the number of neurites crossing exactly through intersections of the grid was counted, as were the number of neuronal cell bodies producing neurites. Six coverslips per group were counted and the neurite area per neuron was calculated according to the following equation [228]:

Statistical

$$\frac{\left(\frac{\text{neurite intersections}}{\text{total grid intersections}}\right) X \text{ total grid area}}{\text{neurons extending neurites}} = \text{neurite area } (\mu m^2) \text{ per neuron}$$

Analysis: All data were expressed as means ± standard error of the mean. Data were analyzed using a student's t-test or 2-factor analysis of variance (ANOVA). ANOVAs were followed up with post hoc comparisons using Fisher's least significance difference where appropriate. A P value < 0.05 was considered statistically significant.

3.4 Results

IRS2 is the predominant IRS isoform in the DRG:

RT-PCR was used to determine which mRNAs encoding IRS isoforms were expressed in lumbar DRG from young adult C57Bl/6 mice. Comparisons of mRNA levels for the 4 different IRS isoforms in the DRG of nondiabetic C57Bl/6 mice revealed that IRS2 mRNA is abundantly expressed within the lumbar DRG (Figure 3.1A, B). In fact, IRS2 mRNA was expressed nearly 27-fold higher relative to IRS1. In comparison, both IRS3 and IRS4 mRNAs were barely detectable in relation to IRS1 (Figure 3.1A, B). Western blots of DRG from nondiabetic C57Bl/6 mice showed that both IRS1 and IRS2 proteins were detectable in the DRG (Figure 3.1C, D). Together, these results suggest that insulin signals may be mediated through IRS substrates in the DRG and IRS2 is expressed at much higher levels similar to other neural tissues [215, 229-231].

Because IRS2 was expressed at higher levels than other IRS isoforms, we focused on IRS2 expression and signaling in DRG neurons. Characterization of IRS2 expression patterns in the lumbar DRG revealed widespread IRS2-immunoreactivity throughout the ganglia (Figure 3.2A, D). IRS2-immunoreactivity was predominantly observed in the cytoplasm of neurons and not in satellite cells or Schwann cells (Figure 3.2A, D). Accordingly, identification of sensory neuron populations using antibodies to neurofilament heavy chain (NF-200, myelinated neurons, Figure 3.2B) and peripherin (unmyelinated neurons, Figure 3.2E) revealed that IRS2 was expressed by a majority of DRG neurons, and these IRS2-positive neurons included both unmyelinated and myelinated neuronal populations (Figure 3.2B, C, E, F).

Figure 3.1

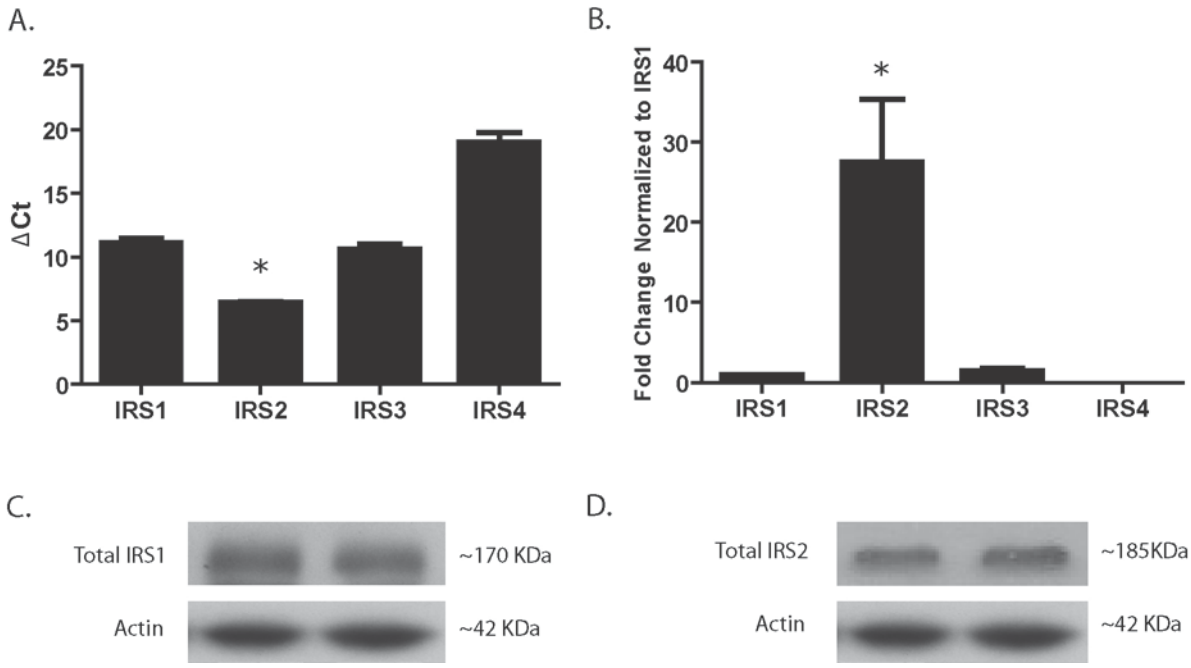
A.
ΔCt
25
20
15
10
5
0
*
IRS1
IRS2
IRS3
IRS4
B.
Fold Change Normalized to IRS1
40
30
20
10
0
*
IRS1
IRS2
IRS3
IRS4
C.
Total IRS1
~170 KDa
Actin
~42 KDa
D.
Total IRS2
~185KDa
Actin
~42 KDa

Figure 3.1. IRS isoform expression in murine lumbar DRG. IRS isoforms were examined using RT-PCR (A, B) and Western blot (C, D). A) RT-PCR was performed on adult C57Bl/6 mouse lumbar DRG (n=3 mice) and comparisons were made among IRS1, IRS2, IRS3, and IRS4. GAPDH was used as the housekeeping gene. ΔCt values for IRS2 were significantly lower than any other isoform. B) Analysis of IRS mRNA levels that were normalized to IRS1 mRNA levels revealed that IRS2 mRNA expression was 27-fold higher than IRS1 in the DRG. * denotes $P<0.05$ n=3 mice. C, D) Representative Western blots of IRS1 and IRS2 protein in mouse lumbar DRG. Equal amounts of protein (20μg) were loaded for each lane and samples were separated on 4-15% tris-glycine gel. Both IRS1 (C) and IRS2 (D) protein were readily detectable. All mice were 8-week old nondiabetic C57Bl/6 males.

Figure 3.2

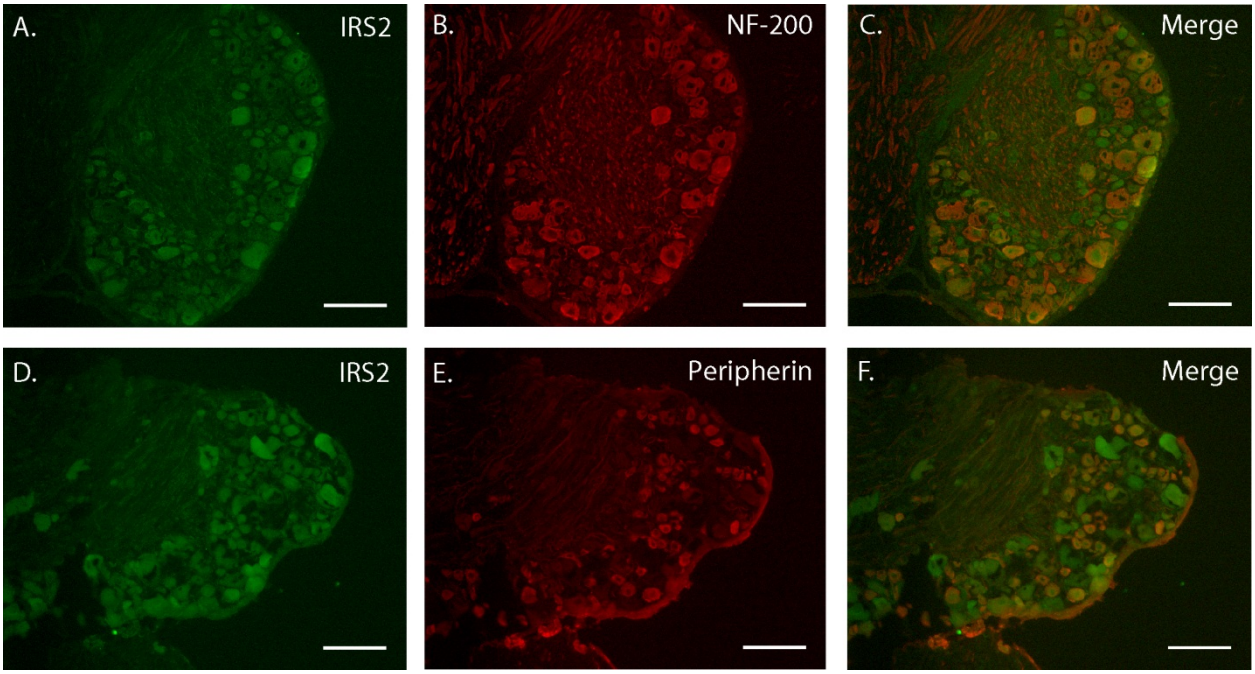

Figure 3.2. IRS2 protein expression pattern in murine lumbar DRG. Fluorescence immunohistochemistry was used to examine IRS2 expression in adult C57Bl/6 mouse lumbar DRG. A, D) Photomicrographs of IRS2 immunoreactivity in DRG neurons. IRS2 was expressed in most neurons of the DRG in mice. B, E) Photomicrographs of the same sections stained with antibodies to NF–200 (B), which labels large, myelinated neurons in the DRG or peripherin (E), which labels unmyelinated small DRG neurons. C, F) Merged images of IRS2 and NF-200 (C) labeling illustrates that many IRS2-positive neurons also express NF-200, suggesting many IRS2-positive neurons are large myelinated neurons. Similarly, merged images of IRS2 and peripherin (F) labeling illustrate that many IRS2-positive neurons coexpress peripherin, suggesting many IRS2-positive neurons are small unmyelinated neurons. Scale bar=100μm.

Diabetes elevates IRS2 serine phosphorylation in mouse DRG:

To determine whether IRS2 in the DRG is prone to diabetes-induced elevations in serine phosphorylation similar to other peripheral tissues, DRG neurons from type 2 diabetic and nondiabetic mice were cultured without insulin for 3 days and then harvested for Western blot analysis. Membranes were probed with antibodies selective for p*S*er(731)IRS2 and then stripped and probed for total IRS2 (Figure 3.3A). Quantification of p*S*er(731)IRS2 normalized to total IRS2 revealed that IRS2 serine phosphorylation was significantly increased in neurons from diabetic *ob/ob* mice compared to their nondiabetic controls ($P < 0.05$, Figure 3.3A). Moreover, similar elevations in p*S*er(731)IRS2 were observed in freshly harvested DRG neurons after 6 weeks of STZ-induced type 1 diabetes in C57Bl/6 mice ($P < 0.05$, Figure 3.3B). These results reveal that IRS2 phosphorylation of serine residues is elevated in multiple models of diabetes and like other peripheral tissues, this serine phosphorylation could lead to suppressed insulin signaling in DRG neurons.

To investigate whether the elevated serine phosphorylation of IRS2 observed in DRG neurons harvested from diabetic mice was possibly caused by the elevated glucose levels, cultures from nondiabetic control mice were grown in hyperglycemic conditions (25mM glucose) for 3 days and pSer(731)IRS2 levels were quantified. Results from these experiments revealed that p*S*er(731)IRS2 was not elevated in hyperglycemic cultures as compared to control cultures grown in 10mM glucose ($P > 0.05$ Figure 3.3C). Thus, short-term elevations in glucose levels do not appear to modify serine phosphorylation of IRS2, suggesting that the mechanisms responsible for this effect are not simply due to elevated glucose.

It has been proposed that elevated serine phosphorylation of IRS proteins can lead to increased protein degradation of IRS. Thus, degradation of IRS proteins may also contribute to insulin resistance [232]. To address this possibility, we quantified total IRS2 expression in neuronal cultures from *ob/ob* diabetic mice and normalized them to the housekeeping protein actin. This analysis revealed that total IRS2 expression appeared to be decreased in DRG cultures from diabetic *ob/ob* mice, although this

Figure 3.3

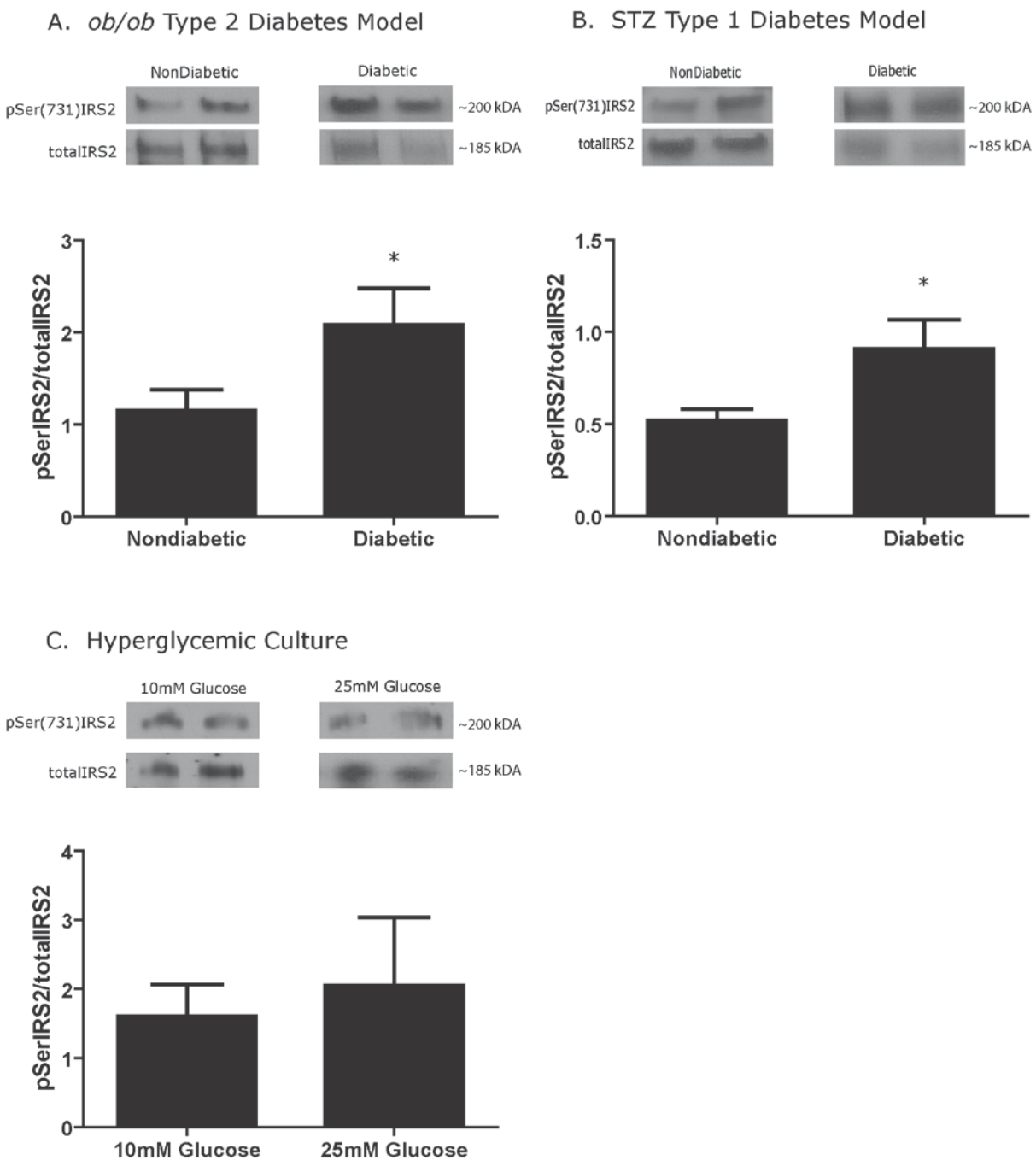
A. ob/ob Type 2 Diabetes Model
NonDiabetic
Diabetic
pSer(731)IRS2
totalIRS2
~200 kDA
~185 kDA
pSerIRS2/totalIRS2
Nondiabetic
Diabetic
B. STZ Type 1 Diabetes Model
NonDiabetic
Diabetic
pSer(731)IRS2
totalIRS2
~200 kDA
~185 kDA
pSerIRS2/totalIRS2
Nondiabetic
Diabetic
C. Hyperglycemic Culture
10mM Glucose
25mM Glucose
pSer(731)IRS2
totalIRS2
~200 kDA
~185 kDA
pSerIRS2/totalIRS2
10mM Glucose
25mM Glucose

Figure 3.3. pSer(731)IRS2 is elevated in DRG neurons from type 1 and type 2 diabetic mice. Protein was harvested from adult mouse DRG culture from diabetic *ob/ob* and nondiabetic mice (A),freshly isolated DRG from STZ-injected diabetic and nondiabetic C57Bl/6 mice (B), and from DRG neurons grown in hyperglycemic and control conditions (C). Western blots were performed using antibodies that recognized phosphorylated ser731 resides on IRS2, and levels of Ser(731)IRS2 were normalized to total IRS2. A) Comparisons of pSer(731)IRS2 levels in nondiabetic and diabetic *ob/ob* mice revealed a significant increase in pSer(731)IRS2 levels in diabetic mice. * denotes $P<0.05$ vs nondiabetics. n=6 for nondiabetic mice and n=7 for diabetic mice. B) Diabetes was induced in 8-week old C57Bl/6 male mice with STZ and diabetes was allowed to progress for 6 weeks. Similar to *ob/ob* diabetic mice, pSer(731)IRS2 levels were significantly elevated in STZ-injected diabetic mice. * denotes $P < 0.05$ vs nondiabetics. n=5 for nondiabetic mice and n=8 for diabetic mice. C) DRG neurons from nondiabetic animals were grown in 10mM (control) and 25mM (hyperglycemic) glucose concentrations. There was no significant change in IRS2 serine phosphorylation levels between groups. n=6 for 10mM glucose and n=7 for 25mM glucose,

Figure 3.4

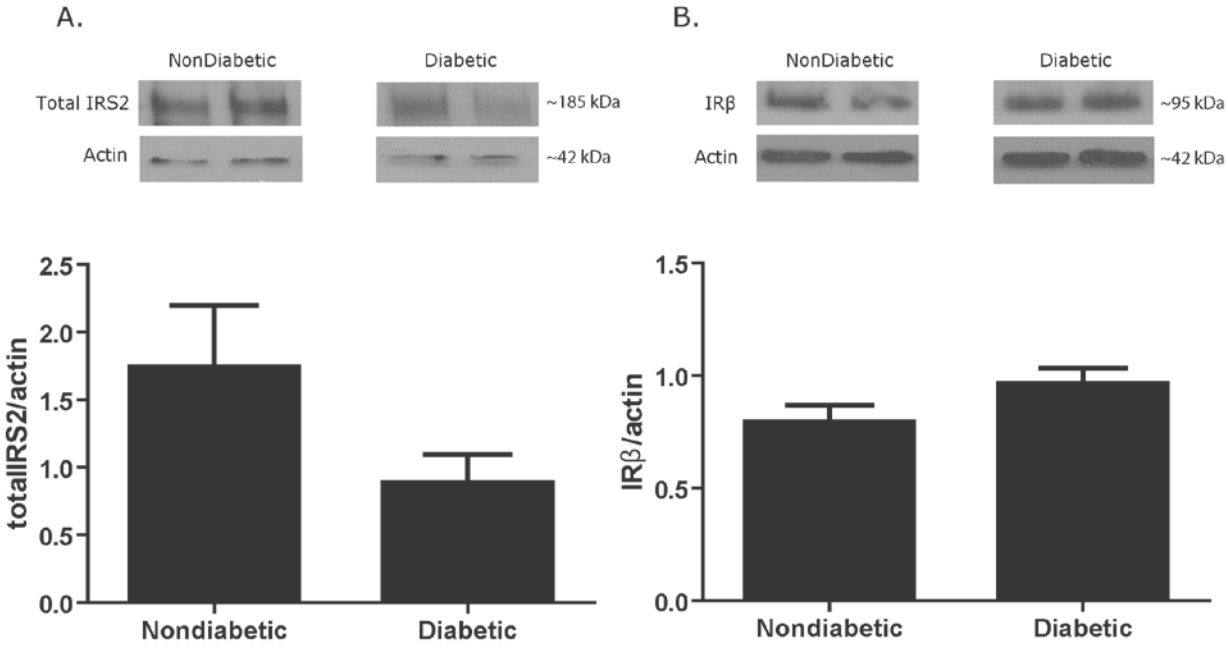
A.
NonDiabetic
Diabetic
Total IRS2
~185 kDa
Actin
~42 kDa
B.
NonDiabetic
Diabetic
IRβ
~95 kDa
Actin
~42 kDa
totalIRS2/actin
2.5
2.0
1.5
1.0
0.5
0.0
Nondiabetic
Diabetic
IRβ/actin
1.5
1.0
0.5
0.0
Nondiabetic
Diabetic

Figure 3.4. Total IRS2 and IR protein levels in primary DRG culture. Protein was harvested from adult mouse DRG culture from diabetic *ob/ob* and nondiabetic mice. Western blots were performed using antibodies that recognized total IRS2 (A), or IR β subunit levels (B). In both cases protein levels were normalized to actin. A) Total IRS2 levels were slightly decreased in diabetic *ob/ob* mice, although this trend was not statistically significant ($P > 0.05$). n=7 for nondiabetic mice and n=7 for diabetic mice. B) IR β subunit protein levels were not statistically different between diabetic and nondiabetic mice. ($P > 0.05$). n=5 for nondiabetic mice and n=6 for diabetic mice.

decrease was not statistically significant ($P > 0.05$, Figure 3.4A). However, this finding is consistent with the view that elevated IRS2 degradation may play a role in diminished insulin signaling.

One alternative possibility for decreased insulin signaling is a down regulation of the insulin receptor (IR) in DRG of diabetic *ob/ob* mice. To examine this possibility, we measured total IR protein levels in DRG cultures from diabetic *ob/ob* mice. There were no significant differences in IR levels between DRG cultures from diabetic *ob/ob* mice and cultures from nondiabetic mice ($P > 0.05$, Figure 3.4B).

Insulin-stimulated Akt activation is blunted in DRG neurons from diabetic mice.

Akt is a serine kinase that is one of the major downstream mediators activated in insulin signaling in both peripheral tissues and neurons [18, 219]. In neurons, neurotrophic factor activation of the Akt pathway has been shown to promote survival and growth of neurons [177, 233]. In its activated form, Akt is phosphorylated (pAkt) on serine residue 473, and pAkt is decreased in settings of insulin resistance [234]. Here, DRG from diabetic *ob/ob* and control mice were grown in insulin-free media for 3 days and then stimulated with 100nM insulin for 15 minutes. Cultures were then harvested for Western blot analysis to determine Akt activation in response to insulin. No significant differences were observed in baseline levels of Akt activation between diabetic and nondiabetic mice. Insulin significantly elevated activated pSer(473) Akt in cultures from both nondiabetic and diabetic mice ($P < 0.05$, Figure 3.5). However, Akt activation in response to insulin was significantly lower in cultures from diabetic *ob/ob* mice as compared to nondiabetic controls ($P < 0.05$, Figure 3.5), suggesting that the insulin signaling pathway is not being activated appropriately in the DRG of diabetic *ob/ob* mice.

Figure 3.5

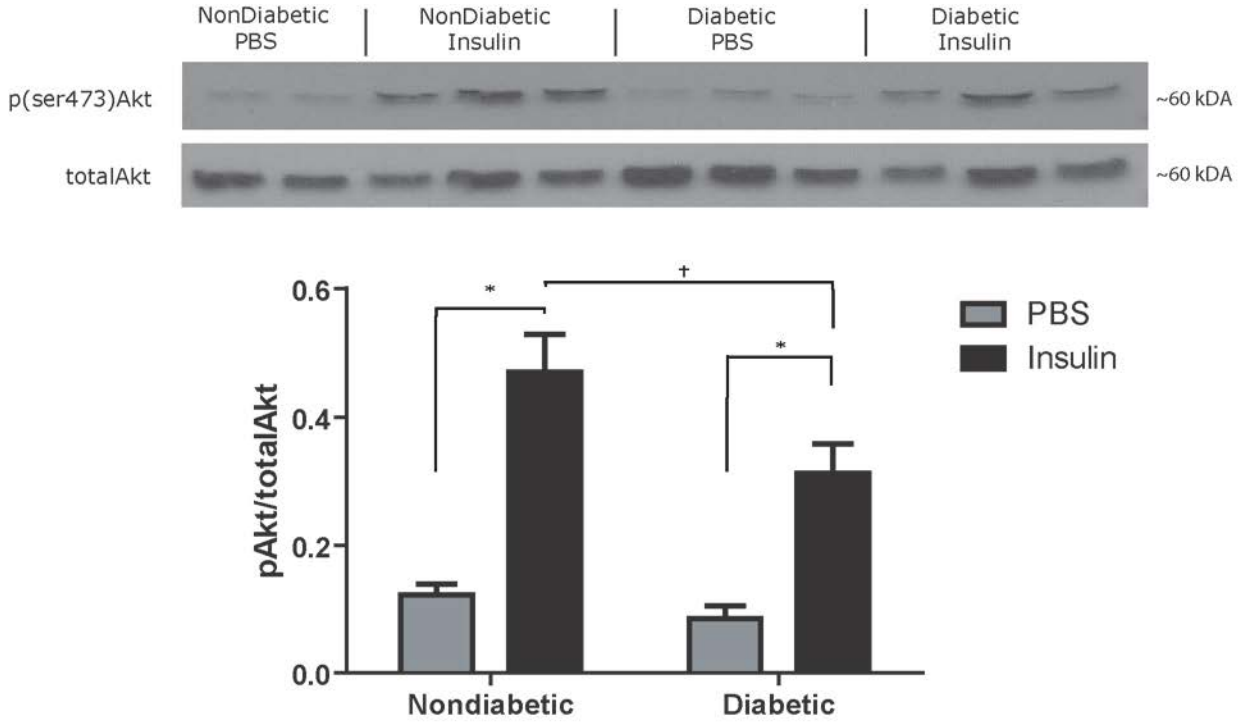
NonDiabetic PBS
NonDiabetic Insulin
Diabetic PBS
Diabetic Insulin
p(ser473)Akt
totalAkt
~60 kDA
~60 kDA
pAkt/totalAkt
0.6
0.4
0.2
0.0
*
*
†
PBS
Insulin
Nondiabetic
Diabetic

Figure 3.5. Diabetes decreases insulin-stimulated Akt activation in DRG neurons. Primary cultures of lumbar DRG neurons from *ob/ob* diabetic mice and nondiabetic controls were stimulated with 100nM insulin for 15 minutes and harvested for Western blot. Membranes were probed for activated Akt (pSer(473)Akt) and normalized to total Akt levels. Insulin significantly increased Akt activation in both nondiabetic and diabetics cultures (* = $P < 0.05$). In contrast, insulin-stimulated Akt activation in cultures from diabetic *ob/ob* mice was significantly suppressed in comparison to nondiabetic controls, († = $P < 0.05$). There were no significant differences in baseline pAkt levels between nondiabetic and diabetic mice. * and † denote $P < 0.05$; n=5 for nondiabetic without insulin, n=6 for nondiabetics with insulin, n=6 for diabetics without insulin, and n=6 for diabetics with insulin.

Insulin-stimulated neurite outgrowth is diminished in DRG neurons from diabetic mice.

One common feature of neurotrophic factors is their ability to stimulate neurite outgrowth in culture. Insulin increases the percentage of neurons that produce neurites (neuritogenesis) and promotes overall growth of neurites in culture [142, 176]. Here, neurite outgrowth in response to insulin supplementation was used to determine whether suppressed insulin signaling correlated with alterations in neurite outgrowth. DRG cultures from diabetic *ob/ob* mice and nondiabetic controls were grown in insulin-free media or media supplemented with 100nM insulin. After five days, the cultures were fixed and stained with SMI-312, a pan-axonal marker (Figure 3.6A-D). Quantification of cultures harvested from nondiabetic and diabetic *ob/ob* mice revealed that neurite outgrowth was significantly elevated in nondiabetic cultures following insulin supplementation ($P < 0.05$, Figure 3.6A, C). In contrast, insulin supplementation did not affect neurite outgrowth in cultures from diabetic *ob/ob* mice. These differences suggest that cultures from diabetic *ob/ob* mice have impaired responses to insulin related to neurite outgrowth, a finding that is consistent with the hypothesis that insulin-signaling pathways in DRG neurons may be impaired by diabetes.

3.5 Discussion

The current study demonstrates that similar to other neural tissues, IRS2 appears to be the predominant isoform of IRS in DRG neurons. Furthermore, insulin signaling in DRG neurons from diabetic mice undergoes similar modifications that have been proposed to underlie insulin resistance in adipose and muscle. These signaling alterations are consistent with blunted responses of sensory neurons to insulin stimulation, including diminished activation of downstream molecules and morphological changes. Collectively, these results provide an important step towards understanding how abnormalities in insulin signaling may impact sensory neurons, and may also contribute to the development and/or progression of diabetic neuropathy.

Figure 3.6

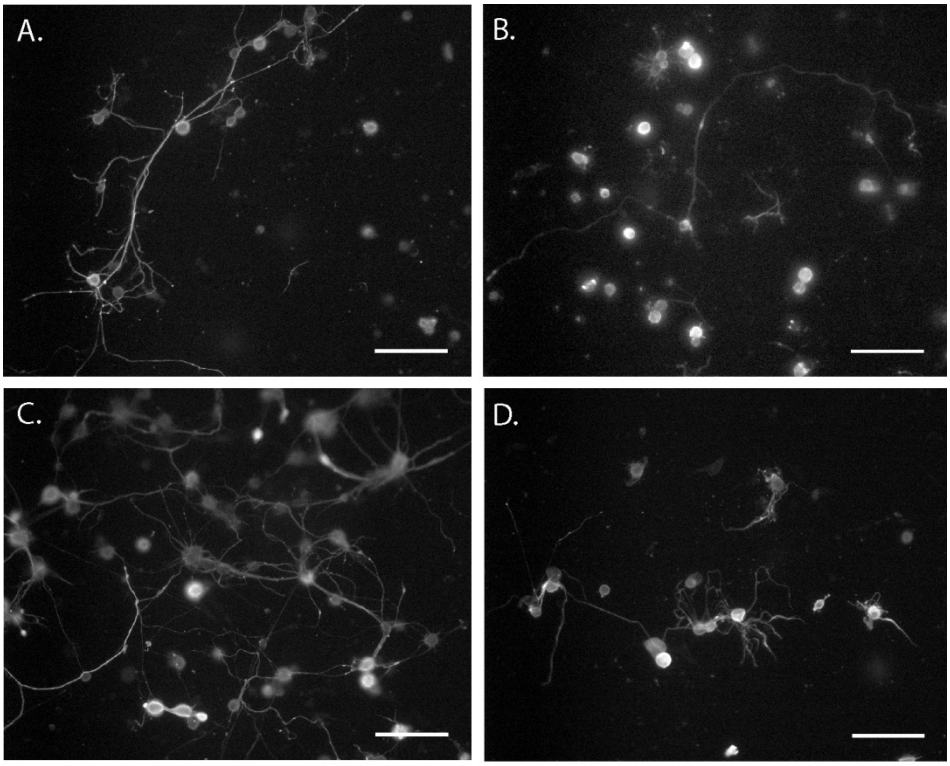
A.
B.
C.
D.

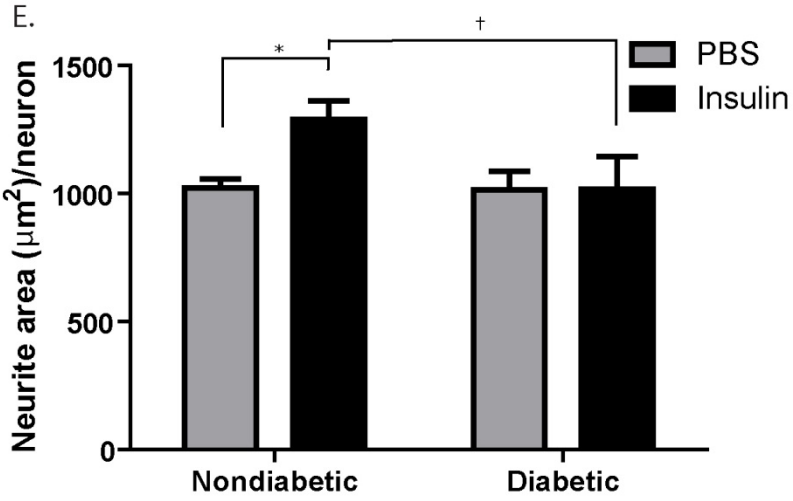
E.
*
†
PBS
Insulin
Neurite area (μm²)/neuron
1500
1000
500
0
Nondiabetic
Diabetic

Figure 3.6: Diabetes decreases insulin-stimulated neurite outgrowth in DRG neurons. Primary cultures of lumbar DRG neurons from diabetic *ob/ob* and nondiabetic mice were grown in either insulin-free media or with media containing 100nM insulin for 5 days. Neurites were then stained with SMI 312, a pan-axonal marker. Neurite area was quantified using a stereological grid applied overtop photomicrographs of cultured wells. Photographs of representative wells are show on the top panel A) nondiabetics without insulin (n=5), B) diabetics without insulin (n=6), C) nondiabetics with insulin (n=6), D) diabetics with insulin (n=5). E) Quantification of neurite outgrowth in the different treatment groups. Insulin significantly increased neurite outgrowth in nondiabetic animals, whereas there was no effect of insulin on neurite outgrowth in neurons from diabetic mice. * and † denote $P < 0.05$. Scale bar=100μm.

Although insulin resistance is a major focus in type 2 diabetes associated with adipose and muscle tissue, our understanding of the effects of reduced insulin support to sensory neurons is surprisingly lacking. A number of studies have reported expression patterns of the insulin receptor and IGF-1 receptor in DRG, but little is known about the expression of IRS isoforms in DRG. Previous studies reported that the insulin receptor is expressed primarily by small nociceptive unmyelinated neurons [170, 171, 173]. Similar expression patterns were described for the IGF-1 receptor [235], suggesting that insulin and IGF-1 may preferentially modulate small nociceptive neurons in the DRG [173]. In the current study, IRS2 protein appears to be expressed by both small and large DRG neurons, suggesting that insulin and/or IGF-1 may support a broader scope of neuronal subtypes than previously thought. Additionally, several reports have documented IRS as key docking proteins in many signaling cascades other than insulin, including neurotrophins such as brain-derived neurotrophic factor [20, 236, 237]. Thus, inhibitory IRS serine phosphorylation may be blunting the signaling of several neurotrophic factors.

Studies are currently underway to determine if changes in IRS serine phosphorylation also leads to altered IGF1 signaling. IRS proteins are a major component of both insulin and IGF1 pathways, so it is possible that the reductions in insulin signaling through IRS serine phosphorylation may also affect proper IGF1 function. It will be important to identify these relationships, as a better understanding of how IRS proteins integrate trophic signals may shed light on mechanisms associated with neurotrophin deficiency in diabetic neuropathy [16]. Finally, although the current study focused primarily on IRS2, IRS1 was clearly detectable in the DRG. It is plausible that DRG neurons can utilize multiple IRS proteins to signal, and compensation and cooperation between IRS proteins likely exist in the DRG and should be considered in future investigations.

Schwann cell dysfunction leading to demyelination, decreased neurotrophic support, and altered protection of neurons is a known factor in the pathogenesis of DN [205]. Schwann cells express insulin receptors [183], however the docking protein profile has not been completely characterized. In this study, we did not observe IRS2 expression in Schwann cells, raising the possibility that insulin signaling in

Schwann cells may be mediated through another IRS isoforms or an additional docking protein such as, growth factor receptor-bound protein 2 (Grb2), Grb2-associated binding protein 1 (GAB1), or src homology 2 domain containing transforming protein 1 (SHC1).

One interesting finding from this study was that IRS2 serine phosphorylation was increased in DRG from both type 1 and type 2 diabetic animals. This result was not entirely surprising as a growing body of literature has documented altered insulin responses in type 1 diabetic patients [238-241]. Most recently, Schauer et. al. demonstrated that type 1 patients are insulin resistant compared to nondiabetic subjects and that the degree of insulin resistance correlated with cardiovascular disease risk [239]. This suggests that mechanisms associated with insulin resistance thought to be exclusive to type 2 diabetes may also be at work in type 1 diabetes.

In the current study, experiments were carried out *in vitro* to determine whether elevated glucose may underline the increases in serine phosphorylation of IRS2. At this point, our results do not support this view, as we saw no change in serine phosphorylation of IRS2 in neurons grown in high glucose. A failure to see insulin signaling changes in cultures exposed to abnormally high glucose levels could be a result of the short time frame, such that agents associated with hyperglycemia and increased IRS serine phosphorylation, including advanced glycation endproducts and reactive oxygen species, did not sufficiently alter the stress kinase activity level. Further research is required to determine the interplay of DRG IRS serine phosphorylation and hyperglycemia.

If the efficacy of insulin signaling does indeed play an important role in DRG function, it is reasonable to propose that factors common to both diabetes models could play an important role in modulating IRS2 signaling regardless of available insulin levels. In that vein, chronic inflammation, increased free fatty acids, and elevated oxidative stress associated with diabetes inhibits insulin signaling by increasing serine phosphorylation of IRS1 in muscle and adipose tissue [18, 19, 210, 216, 217, 219, 222-224, 242-244]. These various cellular stressors drive IRS serine phosphorylation by activating serine/threonine kinases. Evidence has targeted several kinases involved in this pathway, including inhibitor of kappa B kinase b (IKKb), c-Jun N-terminal kinase (JNK), mammalian target of rapamycin

(mTOR), and glycogen synthetase kinase-3 β (GSK-3β) [18, 210, 212]. Further reports have shown that both IRS1 and IRS2 have a JNK binding motif [18, 220], and that JNK and GSK-3β knockout mice display increased insulin sensitivity [243, 245]. In addition, rapamycin, an mTOR inhibitor, has been shown to improve insulin sensitivity in an *in vivo* human study and a neuronal cell line [219, 246]. Moreover, anti-oxidant or anti-inflammatory approaches can decrease stress kinase activity, leading to improved insulin action in muscle [234, 247]. These studies provide important links between inflammation, oxidative stress and insulin signaling, and it will be important to determine if these relationships exist and are relevant to sensory nerve dysfunction.

Although it is likely that the inhibitory effect of IRS serine phosphorylation may be more dependent on the number of residues involved than a specific phosphorylation site [210, 248, 249], the question of how IRS serine phosphorylation may be affecting insulin signaling is not clear. Several mechanisms have been proposed, including dissociation from either the insulin receptor or plasma membrane, increased IRS proteosome degradation, interference with binding of downstream mediators, and finally, decreased tyrosine phosphorylation of the IRS protein [210]. Our finding that IRS2 appears to be slightly decreased in neuronal cultures from diabetic *ob/ob* mice is consistent with the idea that elevated serine phosphorylation can lead to IRS degradation, thus limiting the ability of insulin to stimulate downstream effectors.

In addition to effects of insulin in the peripheral nervous system, insulin signaling in the central nervous system (CNS) is gaining considerable attention. Insulin is known to promote learning and memory [158], metabolic homeostasis [137], and have effects on aging [250]. Consequently, CNS insulin resistance has been shown to play a critical role in the development of Alzheimer's disease [251], Parkinson's disease [252], and metabolic syndrome [162]. It is now becoming evident that insulin resistance is not restricted to muscle and adipose tissue, but that it also occurs in nervous tissue and can potentially be detrimental to proper neuron function.

Conclusion

The current study provides evidence that IRS proteins are expressed in the DRG and could play an important role in the ability of insulin to support peripheral neurons. Elevated serine phosphorylation of IRS proteins is a major contributing mechanism underlying insulin resistance in muscle and adipose tissue. Our results support a similar mechanism of insulin-signaling disruption within DRG neurons, and this modulatory step should be considered as an additional component contributing to diabetic neuropathy. Future studies should address mechanisms that can promote insulin sensitivity in sensory neurons, as these may be an avenue to develop therapeutic interventions that could improve sensory nerve function in both type 1 and type 2 diabetic patients.

Chapter 4: *In vivo* Peripheral Nervous System Insulin Resistance

4.1 Abstract

A reduction in peripheral nervous system (PNS) insulin signaling is a proposed mechanism that may contribute to sensory neuron dysfunction and diabetic neuropathy. While decreased PNS insulin signaling is plausible in type 1 diabetic (insulinopenic) models due to the paucity of insulin, a loss of insulin signaling within PNS neurons in type 2 (hyperinsulinemic) models has not been explored. Here, experiments were performed to test the hypothesis that the PNS of insulin-resistant mice displays altered insulin signal transduction similar to other peripheral tissues. For these studies, nondiabetic control and type 2 diabetic *ob/ob* mice were challenged with an intrathecal injection of insulin or insulin-like growth factor 1 (IGF-1) and downstream signaling was evaluated in the dorsal root ganglion (DRG) and sciatic nerve using Western blot analysis. The results indicate that insulin signaling abnormalities documented in other "insulin sensitive" tissues (i.e. muscle, fat, liver) of *ob/ob* mice are also present in the PNS. A robust increase in Akt activation was observed with insulin and IGF-1 stimulation in nondiabetic mice in both the sciatic nerve and DRG; however this response was blunted in both tissues from *ob/ob* mice. The results also suggest that upregulated JNK activation and reduced insulin receptor expression could be contributory mechanisms of PNS insulin resistance within sensory neurons. These findings contribute to the growing body of evidence that alterations in insulin signaling occur in the PNS and may be a key factor in the pathogenesis of diabetic neuropathy.

4.2 Introduction

Diabetes and metabolic syndrome are risk factors for several neurological diseases and emerging evidence has indicated that neuronal insulin resistance may be involved in disease pathogenesis [253]. While altered insulin signaling is known to be the key factor in the development of diabetes, the role that it plays in DN is not well understood. Recent evidence suggests that cultured sensory neurons from insulin-resistant mice display classic signs of insulin resistance and that insulin resistance may be contributing to mitochondrial dysfunction and increased ROS in DN [181, 200]. Furthermore, clinical evidence has also reported that insulin resistance appears to be an independent risk factor for both autonomic and peripheral neuropathy [254].

Cellular mechanisms of insulin resistance include downregulation of the insulin receptor, inhibitory serine phosphorylation of insulin receptor substrate (IRS), and upregulation of tyrosine phosphatases (PTPs). Many of these mechanisms are negative feedback pathways to regulate insulin signaling and can be potentiated by hyperinsulinemia. While mutations in the insulin receptor can result in insulin resistance, these events are rare [255]. However, a common observation is that chronic insulin treatment and hyperinsulinemia can induce blunted insulin receptor expression. The decreased insulin receptor expression seems to be due to increased receptor internalization and degradation [256, 257]. IRS serine phosphorylation is upregulated by several kinases downstream in the insulin signaling pathway (i.e. GSK3β), and IRS serine phosphorylation can blunt insulin signaling through several different mechanisms (discussed in Chapter 3). Like IRS serine phosphorylation, PTP downregulates insulin signal transduction. PTPs dephosphorylate the tyrosine residues on the insulin receptor and IRS, causing signaling deactivation. Several PTPs have been implicated in insulin resistance, however the role of PTP1B is most well characterized. Cell lines that overexpress PTP1B demonstrate reduced insulin sensitivity [258] and PTP1B knockdown in insulin resistant *ob/ob* mice caused significant decreases in glucose and insulin levels and an increase in insulin sensitivity [259]. Furthermore, PTP1B knockout mice demonstrate increased insulin sensitivity and resistance to obesity [260].

Growing evidence suggests that neurons may become insulin resistant similar to other tissues and that insulin is a neuronal growth factor. However, no *in vivo* evidence of PNS insulin resistance has been presented and the cellular mechanisms associated with PNS insulin resistance have not been thoroughly investigated. The aim of the current study was to investigate insulin and IGF-I signaling in PNS sensory neurons *in vivo* and determine if signaling is disrupted in insulin-resistant type 2 diabetic mice.

4.3 Experimental Procedures

Animals: All experiments were approved by the University of Kansas Medical Center Institutional Animal Care and Use Committee. Male *ob/ob* leptin null mutant and age-matched control mice (*ob/+*) were purchased from Jackson Laboratories (Bar Harbor, Maine) at 8 weeks of age. Mice were given access to food and water ad libitum and housed on a 12-hour light/dark cycle. Weekly blood glucose levels and weights were monitored and mice were sacrificed at 11 weeks of age.

Glucose Tolerance Test: At 9 weeks of age, an intraperitoneal glucose tolerance test (IPGTT) was used to assess the response of mice to a glucose challenge. After a 6-hour fast, mice were given an intraperitoneal injection of glucose at 1g of glucose per kg body weight. Blood glucose levels were measured via tail clip immediately prior to the glucose bolus and then at 15, 30, 60, and 120 minutes after injection.

Insulin Tolerance Test: At 10 weeks of age, mice underwent an insulin tolerance test (ITT). Mice were fasted for 6 hours and then administered IP insulin (Humulin R, Lilly, Indianapolis, Indiana) at a dosage of 1.5U per kg body weight. Blood glucose levels were monitored immediately prior to insulin injection and then at 15, 30, 60, and 120 minutes thereafter.

HOMA-IR: Fasting insulin and fasting glucose levels were used to calculate the homeostatic model assessment of insulin resistance (HOMA-IR). Scores were calculated with the following equation: (Blood Glucose (mg/dl) X (Serum Insulin (uU/mL))/405) [261].

Mechanical Sensitivity: Mechanical behavioral responses to Semmes Weinstein-von Frey monofilaments (0.07 to 5.0 g) were assessed at 8, 9, 10, and 11 weeks of age. Mice underwent acclimation 2 days prior to the first day of behavioral testing. Mice were placed in individual clear plastic cages (11x5x3.5 cm) on a wire mesh grid 55 cm above the table and were acclimated for 30 minutes prior to behavioral analysis. The filaments were applied perpendicularly to the plantar surface of the hindpaw until the filament bent. Testing began with the 0.7 g filament, and in the presence of a response, the next smaller filament was applied. If no response was observed, the next larger filament was used. Filaments were applied until there was a change in response, followed by an additional 4 more applications. The withdrawal threshold was calculated using the formula from the up-down method previously described [262].

Insulin and IGF-1 Injections: Sterile PBS (vehicle), 0.1U (~0.7 nmol) Humulin R insulin, or recombinant IGF-1 equimolar to 0.1U insulin was directly administered to both nondiabetic and *ob/ob* type 2 diabetic mice via a one-time intrathecal injection. Previously, intrathecal 0.1U insulin and equimolar IGF-1 have been shown to have beneficial effects on the symptoms of DN [185]. All injections were 50μL and administered with a 1cc 28½ gauge insulin syringe between the L6 and S1 vertebrae. In an additional preliminary study, sterile PBS or insulin was delivered through an intraperitoneal injection at a dose of 3.33U/kg, such that the total insulin administered was approximately 0.1U for nondiabetic mice and 0.17U (~1.2 nmol) for *ob/ob* mice.

Western Blots: After a 30 minute insulin stimulation period, the lumbar DRG and sciatic nerve were harvested from 11 week old mice and frozen at -80°C. Tissues were sonicated in Cell Extraction Buffer (Invitrogen, Carlsbad, CA) containing 55.55 μl/ml protease inhibitor cocktail, 200mM Na_3VO_4, and 200mM NaF. Following sonication, protein was extracted on ice for 60 minutes and vortexed every 10 minutes. After centrifugation, protein concentration of the supernatant was measured with a Bradford assay (Bio-Rad, Hercules, CA). Samples were then boiled with Lane Marker Reducing Sample Buffer (Thermo Scientific, Waltham, MA) for 3 minutes. Equal amounts of protein (30 μg) were loaded per lane and samples were separated on a 4-15% gradient tris-glycine gel (Bio-Rad), and then transferred to a

nitrocellulose membrane. Membranes were probed with the following primary antibodies and all antibodies were purchased from Cell Signaling (Danvers, MA) unless otherwise noted: total Akt, p-(Ser473)Akt, total p70S6K, p-(Thr389)p70S6K, total GSK3β, p-(Ser9)GSK3β, total JNK, p-(Thr183/Tyr185)JNK, total mTor, p-(Ser2448)mTor, Insulin-like growth factor 1 receptor β subunit, PTP1B (Abcam, Cambridge, MA), total AS160 (Millipore, Billerica, MA), p-(Thr642)AS160 (Millipore), Insulin Receptor β subunit (Santa Cruz, Santa Cruz, CA), and α-tubulin (Abcam). Bands were visualized with either anti-mouse or anti-rabbit HRP-conjugated secondary antibodies (Santa Cruz) and ECL with X-ray film. Densitometry with ImageJ (NIH) was then used to analyze each lane.

Statistical Analysis: All data is expressed as means ± standard error of the mean. IPGTT, ITT, and behavior data were analyzed with a repeated measures analysis of variance (RM-ANOVA). In addition, the area under the curve (AUC) for IPGTT and ITT was analyzed using a Student's t-test. Western blot results were analyzed with 2-way ANOVA and Bonferroni's post hoc analysis when appropriate. Outliers greater than or less than 2 standard deviations from the mean were not included in the analysis. All statistical tests were performed using SigmaPlot software and a P value <0.05 was considered significant.

4.4 Results

Ob/ob insulin resistance:

To quantify the extent of systemic insulin resistance in *ob/ob* mice, nondiabetic and diabetic *ob/ob* mice underwent an IPGTT at 9 weeks of age (Figure 4.1A). Blood glucose levels of the *ob/ob* mice were significantly higher than nondiabetic mice throughout the course of the experiment and the area under the curve (AUC) was also significantly elevated for *ob/ob* mice (Figure 4.1B). Results from the ITT indicated that nondiabetic, insulin-injected mice exhibited an expected physiological decrease in blood glucose in response to insulin; however, *ob/ob* mice displayed a transient elevation of glucose

Figure 4.1

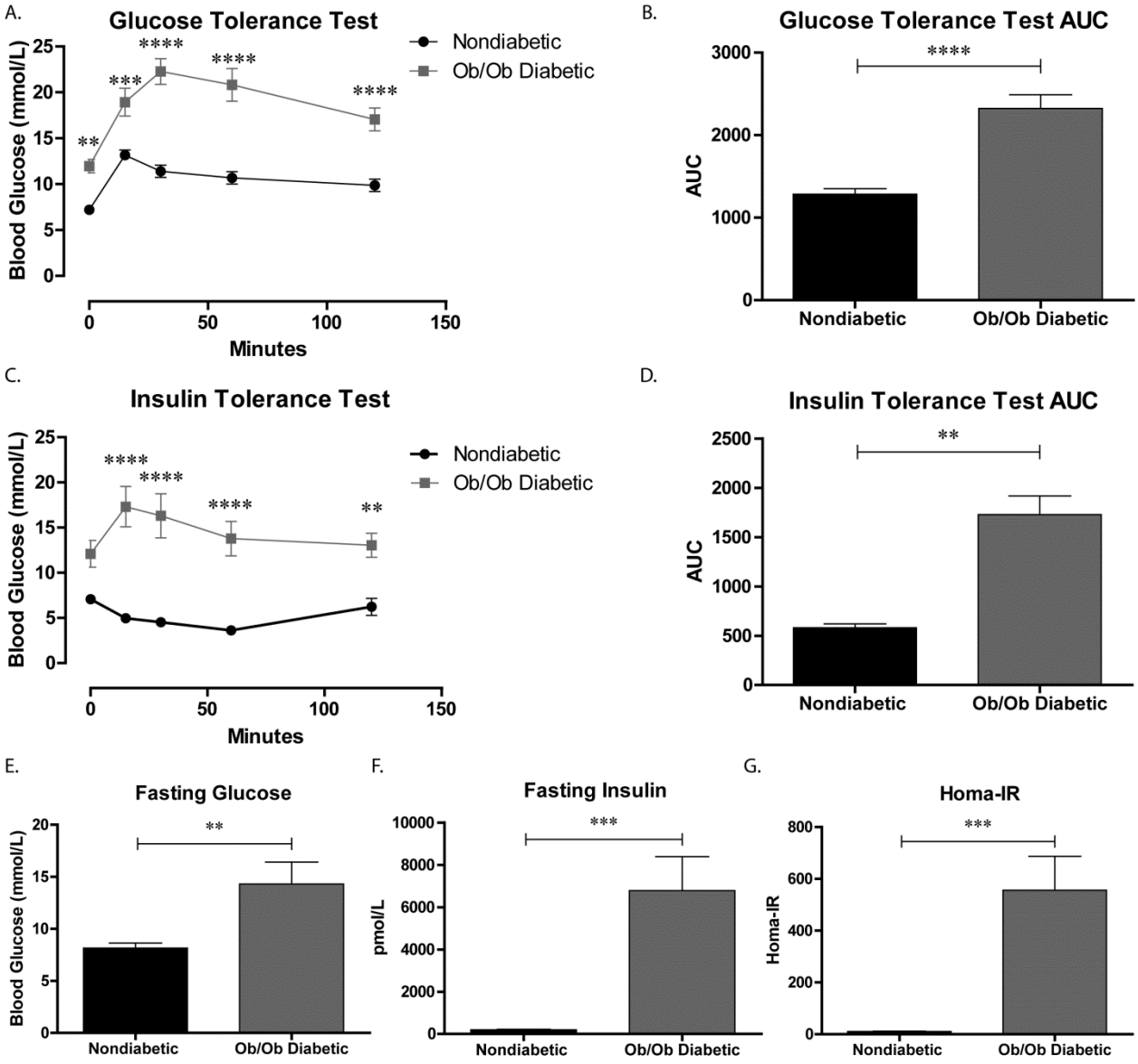
A.
Glucose Tolerance Test
Blood Glucose (mmol/L)
Minutes
Nondiabetic
Ob/Ob Diabetic
B.
Glucose Tolerance Test AUC
AUC
Nondiabetic
Ob/Ob Diabetic
C.
Insulin Tolerance Test
Blood Glucose (mmol/L)
Minutes
Nondiabetic
Ob/Ob Diabetic
D.
Insulin Tolerance Test AUC
AUC
Nondiabetic
Ob/Ob Diabetic
E.
Fasting Glucose
Blood Glucose (mmol/L)
Nondiabetic
Ob/Ob Diabetic
F.
Fasting Insulin
pmol/L
Nondiabetic
Ob/Ob Diabetic
G.
Homa-IR
Homa-IR
Nondiabetic
Ob/Ob Diabetic

Figure 4.1. **Ob/ob mice display classic signs of insulin resistance:** A, B) An IPGTT showed significantly elevated blood glucose levels in *ob/ob* mice throughout the test. The blood glucose of *ob/ob* mice increased more than 10 mmol/L at its maximal level as opposed to nondiabetic mice that elevated less than 6 mmol/L after glucose injection, indicating severe glucose intolerance in *ob/ob* mice. C, D) Similar to the IPGTT, data from the ITT showed reduced insulin sensitivity in *ob/ob* mice. In fact, an insulin dose of 1.5U/Kg did not decrease the blood glucose level of *ob/ob* mice, whereas this dose lowered the blood glucose of nondiabetic controls by approximately 3.6 mmol/L. E-G) At 10 weeks of age, *ob/ob* mice had significantly elevated blood glucose and serum insulin levels. Accordingly, the HOMA-IR measure of insulin resistance was significantly higher in *ob/ob* mice. **=$p<0.01$, ***=$p<0.001$, ****=$p<0.0001$. IPGTT n=7 nondiabetic mice, n=6 *ob/ob*. ITT n=4 nondiabetic mice, n=4 *ob/ob*.

levels (Figure 4.1C). Statistical analysis of the data revealed that *ob/ob* mice maintained elevated glucose levels as compared to nondiabetic controls throughout most of the study, and that the AUC was significantly higher for diabetic *ob/ob* mice (Figure 4.1D). The HOMA-IR, a measure of insulin resistance, was also calculated using fasting blood glucose and serum insulin levels from 10 week old mice. *Ob/ob* mice had significantly higher blood glucose levels (14.3±2.1 mmol/L) as compared to nondiabetic mice (8.2 ±0.5 mmol/L) (Figure 4.1E). Fasting insulin levels were also significantly higher in diabetic *ob/ob* mice (6780±1610 pmol/L) compared to nondiabetic mice (198±25 pmol/L, Figure 4.1F). As such, *ob/ob* mice had a significantly elevated HOMA-IR as compared to nondiabetic mice (557±130 compared to 10.1±1.4, respectively, Figure 4.1G). These results demonstrate significant glucose intolerance and insulin resistance in *ob/ob* mice at this age.

Mechanical allodynia in ob/ob mice:

To quantify a known behavioral abnormality associated with neuropathy in mice, mechanical sensitivity was assessed in nondiabetic and diabetic *ob/ob* mice at 8, 9, 10, and 11 weeks of age. There were no differences in mechanical thresholds between nondiabetic and *ob/ob* diabetic mice at 8, 9, or 10 weeks of age. However, at 11 weeks, there was a significant decrease in the mechanical thresholds of diabetic *ob/ob* mice compared to nondiabetic mice (Figure 4.2), consistent with sensory aberrations associated with peripheral neuropathy as previously reported in this genetic mouse strain [77].

Blunted insulin and IGF-1 Akt activation in ob/ob DRG and sciatic nerve:

Insulin stimulation causes a robust activation of Akt in “insulin-sensitive” tissues like muscle and adipose, as well as in neurons of both the peripheral and central nervous system. Moreover, reduced insulin-induced activation of Akt is a hallmark of insulin resistance [181, 200, 214, 263]. Here, nondiabetic and diabetic *ob/ob* mice were administered either intrathecal PBS or insulin and the DRG and sciatic nerve were harvested for Western blot analysis to assess Akt activation 30 minutes later. In

Figure 4.2

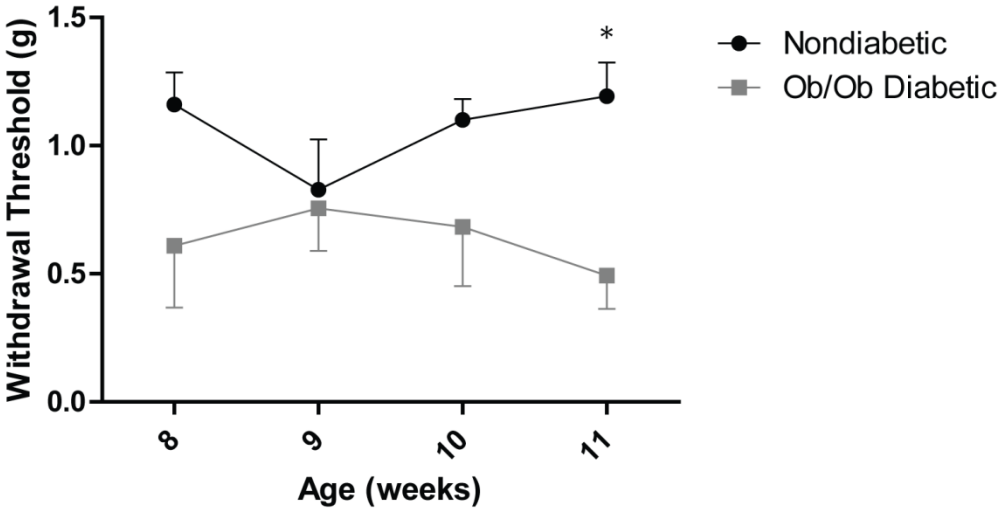
Withdrawal Threshold (g)
1.5
1.0
0.5
0.0
*
8
9
10
11
Age (weeks)
Nondiabetic
Ob/Ob Diabetic

Figure 4.2: Ob/ob mice develop mechanical allodynia: Mechanical thresholds were tested using von Frey monofilaments at 8, 9, 10, and 11 weeks of age. *Ob/ob* mice did not display significant differences from nondiabetic controls at 8, 9, or 10 weeks. However, at week 11, *ob/ob* mice had a significant decrease in their mechanical withdrawal thresholds. *=$p<0.05$. n=6 nondiabetic mice, n=6 *ob/ob* diabetic mice.

Figure 4.3

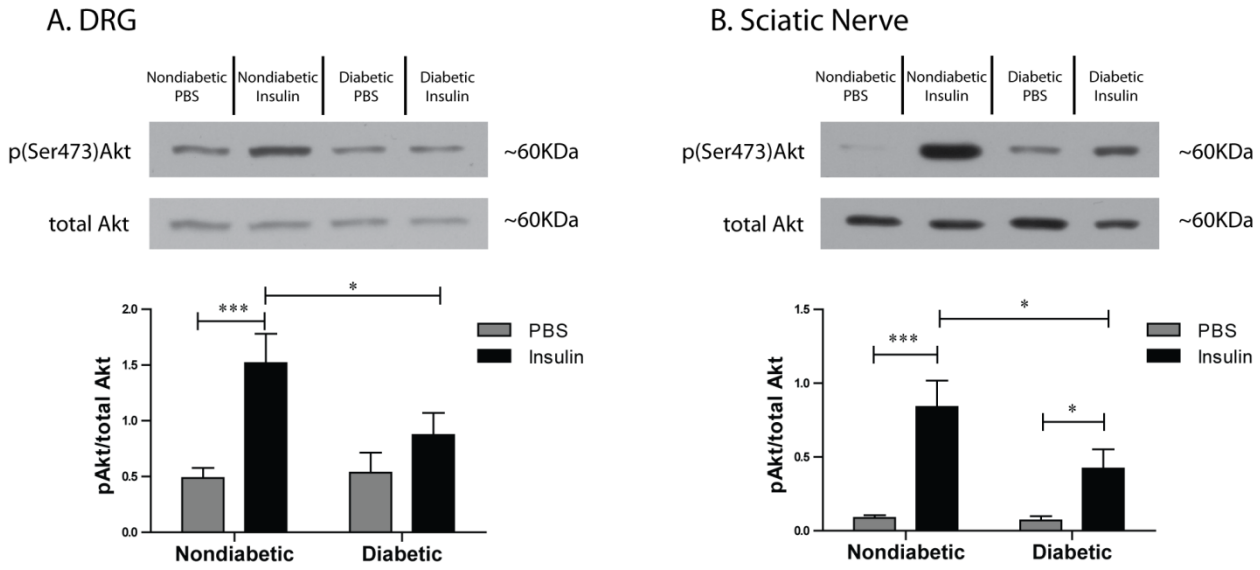
A. DRG
Nondiabetic PBS
Nondiabetic Insulin
Diabetic PBS
Diabetic Insulin
p(Ser473)Akt
~60KDa
total Akt
~60KDa
pAkt/total Akt
PBS
Insulin
Nondiabetic
Diabetic
B. Sciatic Nerve
Nondiabetic PBS
Nondiabetic Insulin
Diabetic PBS
Diabetic Insulin
p(Ser473)Akt
~60KDa
total Akt
~60KDa
pAkt/total Akt
PBS
Insulin
Nondiabetic
Diabetic

Figure 4.3: Intrathecal insulin-induced Akt activation is blunted in the PNS of ob/ob mice: DRG (A) and sciatic nerve (B) were harvested after an intrathecal injection of PBS (nondiabetic n=10, *ob/ob* n=7) or insulin (nondiabetic n=10, *ob/ob* n=9) was administered to nondiabetic control and *ob/ob* mice. Nondiabetic mice displayed a robust and significant increase in Akt activation with insulin stimulation; however insulin failed to significantly activate Akt in the DRG of *ob/ob* mice. Furthermore, the maximal increase in Akt activation with insulin stimulation was significantly lower in both the DRG and sciatic nerve of *ob/ob* mice. There were no differences in mice that received PBS in either the DRG or sciatic nerve. *=$p<0.05$, ***=$p<0.001$.

nondiabetic mice, insulin produced a strong elevation in levels of activated Akt (p(ser473)Akt/total Akt) in both the DRG and sciatic nerve (Figure 4.3A, B). However in *ob/ob* mice, Akt activation was significantly lower in the DRG and sciatic nerve. In fact, insulin failed to significantly increase Akt activation over baseline in the DRG of *ob/ob* mice. For comparison, Akt activation in the DRG was increased 3.1 fold in nondiabetic mice and 1.6 fold in *ob/ob* diabetic mice. In the sciatic nerve, insulin produced a 9.7 and 6.1 fold increase in Akt activation in nondiabetic and *ob/ob* mice, respectively.

To confirm that these results were not dependent on the intrathecal route of delivery, a small number of mice were administered intraperitoneal insulin at a dose of 3.33U/kg. Similar to the intrathecal delivery route, a significant increase in Akt activation was observed in the DRG and sciatic nerve of nondiabetic mice stimulated with insulin; however, no significant change was observed in either tissue from *ob/ob* mice. (Figure 4.4A, B). In the DRG, nondiabetic mice displayed a 2.4 fold change in Akt activation, compared to a 1.5 fold change in *ob/ob* mice. IP insulin induced a 3.8 fold change in Akt in the sciatic nerve of nondiabetic mice, but only a 1.4 fold change in *ob/ob* in the sciatic nerve from *ob/ob* mice.

IGF-1 and insulin activate many of the same intracellular pathways, and utilize many of the same signaling machinery [195], and altered IGF-1 signaling has been demonstrated in states of insulin resistance [264]. Furthermore, IGF-1 resistance has recently been demonstrated to be associated with brain insulin resistance and cognitive decline in Alzheimer's patients [154]. To investigate IGF-1 signal transduction in the PNS of *ob/ob* mice, a dose of IGF-1 equimolar to 0.1U insulin was administered via an intrathecal injection. Akt was significantly activated in the DRG from both nondiabetic (13.3 fold) and *ob/ob* diabetic mice (6.0 fold). However, Akt activation was significantly lower in the DRG from *ob/ob* mice as compared to nondiabetic mice (Figure 4.5A). In the sciatic nerve of nondiabetic mice, IGF stimulation produced a significant 2.8 fold increase in Akt activation. In contrast, Akt was not significantly activated in the sciatic nerve of *ob/ob* mice (Figure 4.5B).

Figure 4.4

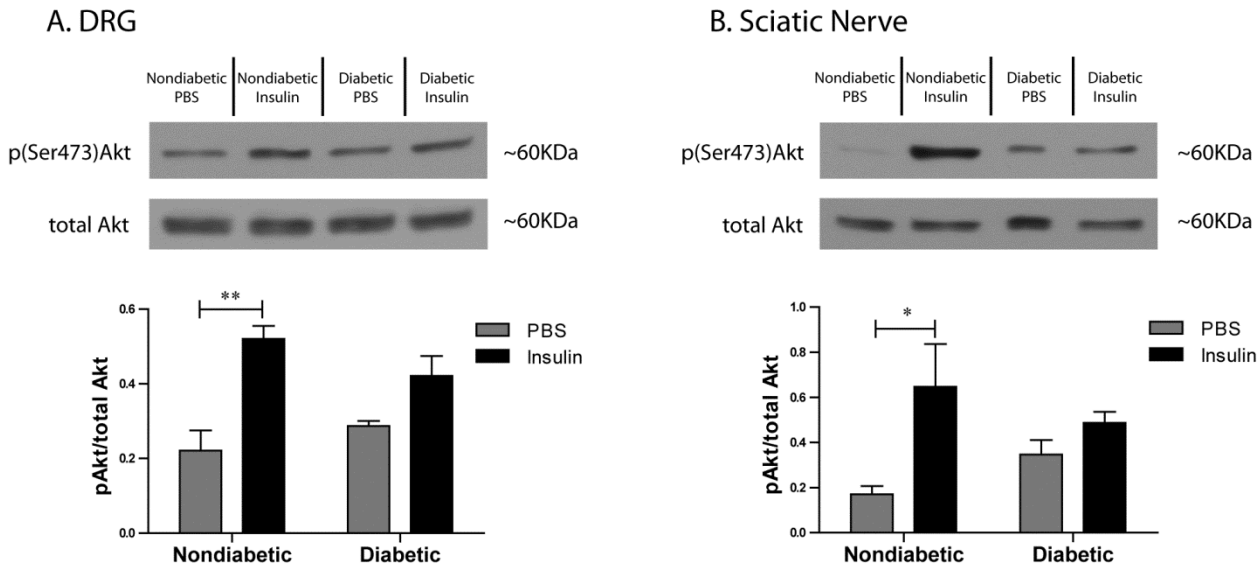
A. DRG
Nondiabetic PBS
Nondiabetic Insulin
Diabetic PBS
Diabetic Insulin
p(Ser473)Akt
~60KDa
total Akt
~60KDa
**
pAkt/total Akt
0.6
0.4
0.2
0.0
PBS
Insulin
Nondiabetic
Diabetic
B. Sciatic Nerve
Nondiabetic PBS
Nondiabetic Insulin
Diabetic PBS
Diabetic Insulin
p(Ser473)Akt
~60KDa
total Akt
~60KDa
*
pAkt/total Akt
1.0
0.8
0.6
0.4
0.2
0.0
PBS
Insulin
Nondiabetic
Diabetic

Figure 4.4: The PNS of ob/ob mice showed reduced insulin-induced Akt activation in response to intraperitoneally-delivered insulin, similar to that observed with IT insulin. Nondiabetic and *ob/ob* diabetic mice were given intraperitoneal injections of PBS (nondiabetic n=3, *ob/ob* n=3) or insulin at a dose of 3.33U/kg (nondiabetic n =3 and *ob/ob* n=3). In both the DRG (A) and sciatic nerve (B) of nondiabetic mice, there was a significant increase in Akt activation in the insulin stimulated group as compared to mice that received PBS, yet no statistically significant changes were observed in the PNS from *ob/ob* mice. *=$p<0.05$, **=$p<0.01$.

Figure 4.5

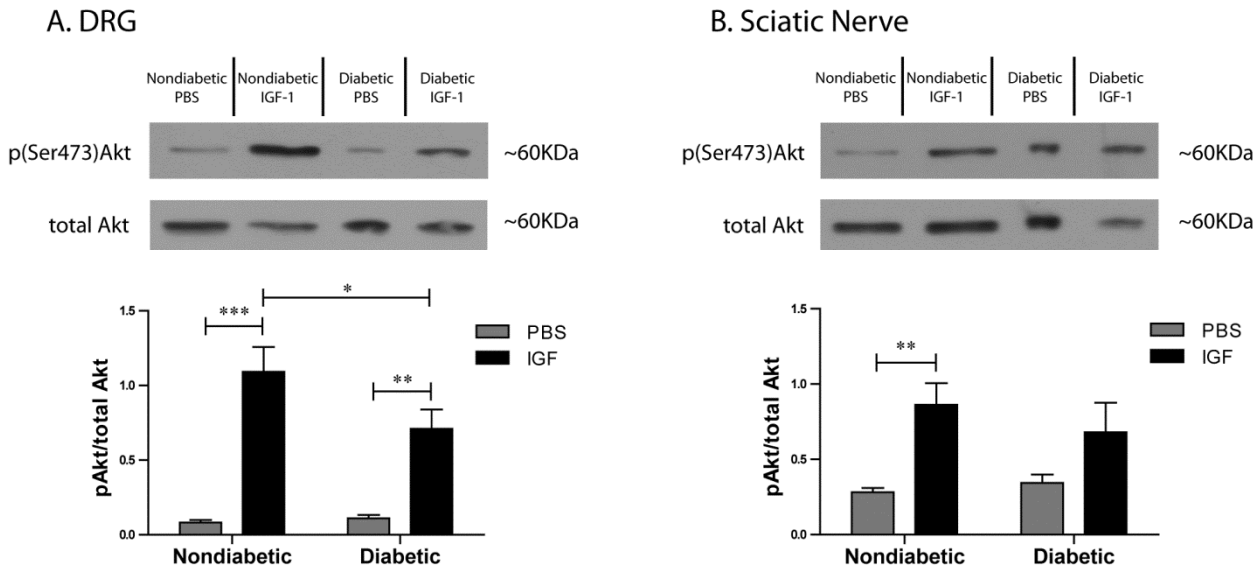
A. DRG
Nondiabetic PBS
Nondiabetic IGF-1
Diabetic PBS
Diabetic IGF-1
p(Ser473)Akt
~60KDa
total Akt
~60KDa
***
*
**
PBS
IGF
pAkt/total Akt
1.5
1.0
0.5
0.0
Nondiabetic
Diabetic
B. Sciatic Nerve
Nondiabetic PBS
Nondiabetic IGF-1
Diabetic PBS
Diabetic IGF-1
p(Ser473)Akt
~60KDa
total Akt
~60KDa
**
PBS
IGF
pAkt/total Akt
1.5
1.0
0.5
0.0
Nondiabetic
Diabetic

Figure 4.5: The PNS of ob/ob mice displayed reduced Akt activation in response to intrathecal IGF-1 as compared to nondiabetic mice. Similar to the results shown for intrathecal insulin, an intrathecal injection of IGF-1 produced a strong activation of Akt in both the DRG and sciatic nerve of nondiabetic mice, but the response was somewhat blunted in the PNS of *ob/ob* mice. In the DRG (A), there was a significant increase in Akt activation in both the nondiabetic and *ob/ob* mice; however, the activation level was significantly lower in the DRG from *ob/ob* mice. In the sciatic nerve (B), IGF-1 stimulation resulted in a significant Akt activation in nondiabetic mice, but not in the *ob/ob* mice. *=$p<0.05$, **=$p<0.01$, ***=$p<0.001$. n=8 nondiabetic PBS, n=9 nondiabetic IGF-1, n=7 diabetic PBS, n=10 diabetic IGF-1.

Insulin signaling downstream of Akt in the DRG and sciatic nerve:

To assess whether diabetes-induced blunting of Akt activation was maintained downstream, several other insulin-responsive proteins were investigated via Western blot analysis, including mTor (protein synthesis), p70S6K (protein synthesis), AS160 (glucose uptake), and GSK3β (glycogen synthesis). At the insulin dose (0.1U) and time point (30 minute stimulation) that were investigated, no statistical differences ($p>0.05$) were observed in the activation of these proteins even in control mice (Table 4.1). However, it is interesting to note that in both the DRG and sciatic nerve from *ob/ob* mice, there is a consistent pattern of a reduced fold change in response to insulin for most proteins compared to responses in nondiabetic mice.

The PNS of ob/ob mice display reduced insulin receptor expression and increased JNK activation:

To explore possible mechanisms responsible for reduced PNS insulin sensitivity, we investigated several pathways known in other insulin-resistant tissues. One contributor to reduced insulin signaling is a downregulation of insulin receptor expression induced by hyperinsulinemia [265]. As shown in Fig. 4.6A, protein levels of the insulin receptor subunit β were significantly lower in the DRG of *ob/ob* mice compared to nondiabetic mice. However, there was no statistical difference in the expression of insulin receptor between nondiabetic and *ob/ob* mice in the sciatic nerve (Fig. 4.6B). No significant differences between groups were observed in IGF-1 receptor expression in either the DRG or sciatic nerve (data not shown).

Our previous studies in primary DRG cultures reported an upregulation of IRS serine phosphorylation [200], a recognized mechanism of insulin resistance in muscle and adipose. In the current study, we investigated both IRS1 (muscle and adipose isoform) [213] and IRS2 (neural isoform) [200, 231] serine phosphorylation. In contrast to neurons *in vitro*, IRS serine phosphorylation does not appear to be significantly affected in the PNS *in vivo* within this model, (data not shown). Interestingly, there was significant activation of the stress kinase, JNK (p(Thr183/Tyr185)JNK/total JNK), in the sciatic

Table 4.1

Protein of Interest	DRG		Sciatic Nerve	
	Control Nondiabetic	*ob/ob* Diabetic	Control Nondiabetic	*ob/ob* Diabetic
	Insulin-induced fold change	Insulin-induced fold change	Insulin-induced fold change	Insulin-induced fold change
mTor	1.52	1.00	1.13	0.98
AS160	1.47	1.28	2.13	1.22
p70S6K	1.00	1.04	1.09	0.93
GSK3β	1.26	1.17	1.56	0.88

Table 4.1: Downstream Akt pathway activation in the DRG and sciatic nerve after intrathecal insulin stimulation. Four proteins downstream of Akt that are known to be involved in the intracellular actions of insulin signaling were investigated in the PNS of nondiabetic and *ob/ob* mice. In both the DRG and sciatic nerve, there were no significant changes in the activation of mTor, p70S6K, or AS160 in either nondiabetic or *ob/ob* mice, nor was there a significant change in the inhibition of GSK3β. Data presented is the fold change of protein modification (measured with Western blot analysis) induced by insulin as compared to that observed in mice that received PBS. n=7-10 for all groups.

Figure 4.6

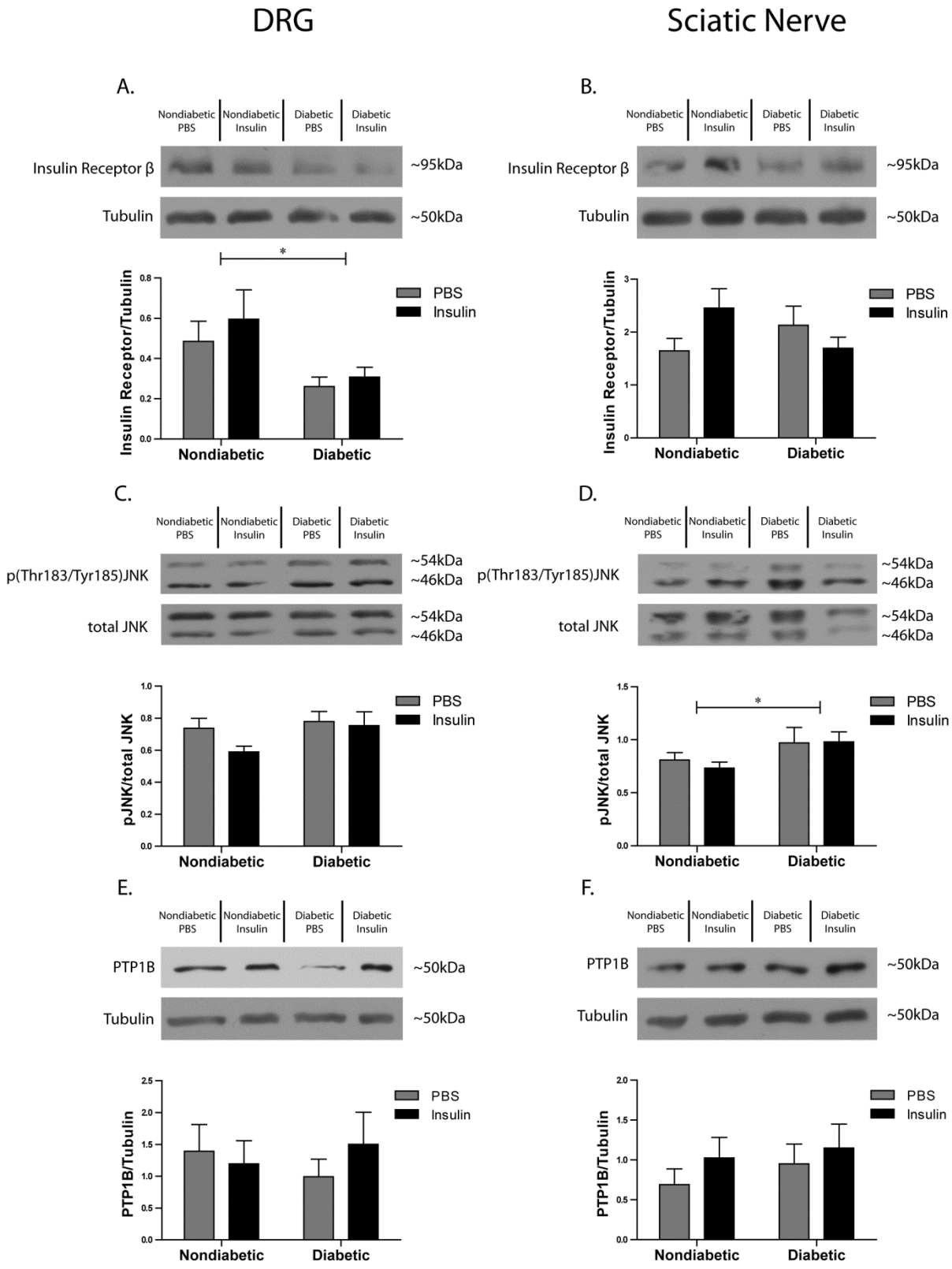
DRG
Sciatic Nerve
A.
B.
Nondiabetic PBS
Nondiabetic Insulin
Diabetic PBS
Diabetic Insulin
Insulin Receptor β
~95kDa
Tubulin
~50kDa
*
Insulin Receptor/Tubulin
PBS
Insulin
Nondiabetic
Diabetic
C.
D.
p(Thr183/Tyr185)JNK
~54kDa
~46kDa
total JNK
pJNK/total JNK
E.
F.
PTP1B
PTP1B/Tubulin

Figure 4.6: Possible mechanisms that may be contributing to insulin resistance in the PNS. A) In this study the expression of the beta subunit of the insulin receptor was significantly reduced in the DRG of *ob/ob* mice as compared to nondiabetic controls. B) No significant change in insulin receptor expression was observed in the sciatic nerve. C) The stress kinase, JNK, was not significantly activated in the DRG of *ob/ob* mice; however in the sciatic nerve (D) there was a significant upregulation of JNK in *ob/ob* mice. E, F) No differences in PTP1B expression profiles were observed in either the DRG or sciatic nerve between nondiabetic and diabetic groups. *=$p<0.05$. n=9 nondiabetic PBS, n=9 nondiabetic insulin, n=7 diabetic PBS, n=9 diabetic insulin.

nerve of *ob/ob* mice compared to nondiabetic mice (Fig. 4.6D) and a similar pattern of activated JNK was observed in the DRG of *ob/ob* mice, however significance was not reached (nondiabetic vs. diabetic p=0.122) (Fig. 4.6C).

In addition to stress kinase activation and reduced insulin receptor expression, insulin resistance can also be induced by over activation of tyrosine phosphatases [258]. Here, however, PTP1B expression was not elevated in the DRG or sciatic nerve of *ob/ob* mice, nor did insulin stimulation appear to alter its expression levels (Fig. 6E, F, respectively).

4.5 Discussion

Diabetic neuropathy is associated with profound loss of distal limb sensation and/or pain, causing significant decline in the quality of life and potential morbidity and mortality for patients. Currently, there are no clinical treatments that successfully improve neuropathic damage to peripheral sensory nerve fibers, likely due to the multifactorial etiology of neuropathy development and progression. Here, we have demonstrated *in vivo* PNS insulin resistance in *ob/ob* mice. These results are consistent with recent *in vitro* studies and supports the view that altered insulin signaling may contribute to DN. In general, a robust activation of insulin-sensitive pathways was observed in the DRG and sciatic nerve of nondiabetic mice, with a blunted response in both tissues from insulin resistant *ob/ob* mice. While no one mechanism of insulin resistance was clearly prevalent, significant changes were seen in two known pathways of insulin resistance, including increased JNK activity and reduced insulin receptor expression. Although more research is needed to fully elucidate the pathways leading to PNS insulin resistance; these results suggest that cellular mechanisms of insulin resistance that have been defined in muscle may also play an important role in the PNS. Collectively, this study supports the hypothesis that altered insulin neurotrophic support may be a key factor in the pathogenesis of DN.

Importantly, these experiments used an *in vivo* approach to support the mounting *in vitro* evidence identifying PNS insulin resistance. This *in vivo* approach also made it difficult to completely assess cellular signaling. Thus, insulin-induced Akt activation was used as a focal point to assess PNS

insulin sensitivity. Interestingly, Akt activation was very prominent in the DRG and sciatic nerve of nondiabetic mice, yet very few significant changes were seen in downstream signaling molecules. This may be due to a temporal effect, as downstream mediators of the Akt pathway may have not yet been activated during the 30-minute stimulation period used for this study. However, it is also plausible that the downstream Akt signaling proteins explored in this study do not play a prominent role in insulin pathways within the DRG. Thus, beyond protein synthesis through mTor and p70S6K or regulation of GSK3β actions, insulin may be playing a more important role in lipid and glucose metabolism, gene regulation, or mitochondrial maintenance in peripheral neurons. It is clear that further studies are necessary to succinctly define the temporal components of this signaling pathway. As such, further experiments are underway to define *in vivo* PNS physiologic insulin signaling with respect to appropriate dosing, timing, and pathway activation.

An additional caveat to this study is the use of leptin-deficient *ob/ob* mice. Leptin's role in the nervous system is receiving increasing attention, and it may have a neuroprotective role [266]. It is not known how reduced neuronal leptin may have contributed to our results. Thus, confirming these results in a high-fat diet model of obesity will be an important step to further investigating PNS insulin resistance.

In experiments presented here, it appeared that insulin produced a stronger Akt activation in the sciatic nerve as compared to the DRG (Figure 3), whereas IGF-1 produced a stronger Akt activation in the DRG as compared to the sciatic nerve (Figure 5). These results point to an apparent separation in insulin/IGF-1 signaling support within the PNS. One plausible explanation may be that insulin and IGF-1 have different actions on the DRG soma and satellite cells compared to sensory axons, motor axons and Schwann cells in the peripheral nerve. These different cellular components likely respond differently to insulin and IGF-1 and would provide alternative signaling profiles. However, how this divergence in signaling may affect sensory neuron function is yet to be determined and ongoing research is targeted at delineating the differential roles that insulin and IGF-1 may play in sensory nerve biology.

In *ob/ob* mice, both the DRG and sciatic nerve displayed reduced insulin-induced Akt activation, a classic indication of insulin resistance. Several mechanisms of insulin resistance outlined in muscle also

appear to be altered in the PNS, and may be contributing to the observed reduction in insulin signal transduction. However, these results must be interpreted with caution as significant changes were not seen consistently across PNS tissues, and further research will need to be completed to fully establish a clear mechanism.

Hyperinsulinemia can promote insulin resistance through downregulation of the insulin receptor [219]. This effect was demonstrated in our data. The *ob/ob* mice in this cohort had serum insulin levels 34.3 fold higher than nondiabetic mice and the DRG of *ob/ob* mice displayed significantly lower insulin receptor expression. Thus, the extreme hyperinsulinemia in the *ob/ob* mice may be promoting insulin receptor downregulation and contributing to PNS insulin resistance. This idea is supported by a recent study that reported a significant decrease in insulin receptor mRNA in cultured DRG neurons that displayed insulin resistance when treated with high levels of insulin [175].

An alternative mediator of insulin resistance is the stress kinase JNK, which is activated in response to various cellular stressors, including low grade chronic inflammation induced by obesity [218, 267]. In fact, *ob/ob* mice with a JNK null mutation have improved whole body glucose tolerance and insulin sensitivity [243]. JNK activation is proposed to promote insulin resistance through upregulation of IRS serine phosphorylation, and IRS is a key common signaling component of both the insulin and IGF-1 pathways. Interestingly though, in the current study we observed increased JNK activation without a significant elevation in either IRS1 or IRS2 serine phosphorylation. Some controversy does exist as to which serine sites are most important in insulin resistance, thus the serine sites that we probed (p(ser731)IRS2 and p(ser307)IRS1) may not be heavily involved in inhibiting insulin signaling in the PNS, resulting in our studies not seeing a significant effect. More powerful approaches such as mass spectrometry, may be needed to establish a global change in the IRS phosphorylation profile within the PNS [268].

Another possible component of the insulin receptor signaling pathway that could be affected in insulin resistance is PTP1B. PTP1B is the canonical member of protein tyrosine phosphatases and serves an important role in insulin signaling regulation [258]. Overexpression of PTP1B has been linked to

insulin resistance in peripheral tissues of *ob/ob* mice [259] and PTP1B knockout mice display increased insulin sensitivity [260]. In the current study, we did not detect significant upregulation of PTP1B in the DRG or sciatic nerve of insulin resistant mice. While there was no change in PTP1B expression, there still could be alterations in phosphatase activity and further studies are underway to explore this possibility.

It will be important to put the current results in context with other contributory mechanisms of DN, including glucose and/or lipid mediated toxicity as well as oxidative stress [92]. We postulate that the metabolic dysfunction associated with hyperglycemia and dyslipidemia in concert with reduced neurotrophic support promotes deterioration and reduced regeneration of the distal axon. Furthermore, the loss of appropriate insulin signaling could make neurons even more susceptible to these pathogenic cascades. Further research into disrupted PNS insulin signaling relative to other pathogenic mechanisms is needed, as this will be a key step in translating these basic science results into clinical applications.

Insulin resistance is emerging as a potential mediator of several neurological syndromes (reviewed in [253]). This study along with recent data of *in vitro* DRG insulin resistance strongly supports altered insulin signaling as a pathogenic mechanism in DN. While insulinopenia has been a proposed contributor to DN in type 1 models for some time [190, 191, 193, 196], how this translated to type 2 (hyperinsulinemic) models of DN remained elusive. Here, we outline reduced insulin signaling *in vivo* in the PNS of type 2 diabetic *ob/ob* mice and possible mechanisms that may be contributing to these changes. It is now becoming evident that decreased insulin neurotrophic support in the PNS is an integral part of DN and may be a congruent mechanism between type 1 and type 2 diabetic models of DN, as both have reduced insulin signaling either due to insulinopenia or neuronal insulin resistance.

Future studies will focus on mechanisms through which insulin supports proper PNS function, as revealing these pathways may provide insight into how decreased insulin support contributes to the pathogenesis of DN. Furthermore, delineating the details of PNS insulin signaling may open new avenues for therapeutic intervention in patients with DN.

Chapter 5: Sensory Neuron Insulin Receptor Knockout Mice

5.1 Abstract

Insulin is known to have neurotrophic properties and it has been proposed that loss of direct sensory neuron insulin signaling, irrespective of glucose neurotoxicity, is a major contributing factor to the development of peripheral diabetic neuropathy (DN). However, current *in vivo* models of DN are not sufficient to fully assess the role and function of sensory neuron insulin signaling. To determine if disrupted sensory neuron insulin signaling plays a crucial role in the development of DN we used Cre-loxP technology to generate sensory neuron insulin receptor knockout (SNIRKO) mice. These mice display euglycemia, yet reduced sensory neuron insulin signaling. We predicted under these conditions that SNIRKO mice would develop signs of DN due to the reduced insulin neurotrophic support. However, SNIRKO mice did not have significant changes in sensorimotor behavior, nerve conduction velocity or intraepidermal nerve fiber density. Interestingly though, SNIRKO mice display significantly elevated serum insulin levels as well as glucose intolerance, and the pancreas from SNIRKO mice displays elevated insulin content in the islets of Langerhans. These results contribute to the growing idea that sensory innervation of pancreatic islets is key to regulating islet function and that a negative feedback loop of sensory neuron insulin signaling keeps this regulation in balance. While it appears that reduced neuronal insulin support does not independently lead to DN, SNIRKO mice will be a powerful tool to investigate sensory neuron insulin signaling and may give a unique insight into the role that sensory neurons play in modifying islet physiology.

5.2 Introduction

The pathogenesis of DN is ill defined, although it appears to develop from a combination of hyperglycemia neurotoxicity and reduced neurotrophic support. One neurotrophic agent that is of increased interest in diabetes is insulin. A growing body of literature suggests that direct neuronal insulin signaling plays a key role in maintaining proper neuronal function and that disruption of this neuronal insulin signaling may contribute to DN.

Unfortunately, the role of insulin signaling in sensory neurons is not well understood. There are inherent difficulties in studying the role of sensory neuron insulin signaling *in vivo.* With current DN models, neither hyperglycemia nor reductions in PNS insulin signaling can be isolated to establish the pathogenesis arising from either insulting factor. For example, STZ-induced diabetic mice are hyperglycemic and hypoinsulinemic and *ob/ob* mice are hyperglycemic and insulin resistant; thus, both models have elevated glucose levels and reduced insulin signaling. Furthermore, *in vivo* insulin stimulations to study signaling or physiological function generally cause a reduction in blood glucose levels. Even when low dose insulin is "directly" applied to neurons via intrathecal injections or near-nerve pumps, interpreting if the observed result was due to neuronal signaling or effects on the surrounding tissue is difficult.

The previous generation of tissue specific insulin receptor knockout mice has greatly increased our understanding of the physiological role of insulin [213]. Conditional knockout mice are one of the most powerful tools available to establish an understanding of *in vivo* protein function. The growing interest in the role of insulin signaling in sensory neurons, the possibility that reductions in insulin independent of hyperglycemia drives DN, and the paucity of models available to study insulin signaling in sensory neurons provided a strong rationale to develop sensory neuron insulin receptor knockout (SNIRKO) mice. The purpose of this study was to characterize the metabolic and sensorimotor phenotype of SNIRKO mice with the hypothesis that SNIRKO mice would develop neuropathy similar to other mouse models of DN due to the absent neurotrophic support from insulin despite euglycemia. Our results suggest that reductions in sensory neuron insulin signaling alone do not contribute to the symptoms of

DN. However, it does appear that an important negative feedback mechanism may exist between sensory neuron insulin signaling and beta cell insulin production. These results contribute to a recently proposed model by Razavi et. al. [38] suggesting that TRPV1 positive sensory neurons modulate the function of pancreatic beta cells.

5.3 Experimental Procedures

Animals and Genotyping:

SNIRKO mice were generated using Cre/Loxp technology [269]. Advillin$^{Cre/+}$ mice have been previously characterized to demonstrate sensory neuron specific cre recombinase activity [270-274] and this was confirmed in our lab using a fluorescent reporter line *Gt(ROSA)26Sor$^{tm4(ACTB-tdTomato,-EGFP)Luo}$*/J (Tomato) (Jackson Laboratories, Bar Harbor, ME). These tomato mice constitutively express td tomato in all cell membranes; however, in the presence of cre recombinase green fluorescent protein (GFP) will be expressed. Thus, green fluorescence is a marker for cre recombinase expression and activity in this reporter line.

Mice with loxp sites flanking exon 4 of the insulin receptor gene (IR$^{lox/lox}$) were purchased from Jackson Laboratories (Bar Harbor, ME). In the presence of cre recombinase, exon 4 is deleted creating a frameshift mutation resulting in a stop codon. The resultant product would be a nonfunctional 308 amino acid truncated peptide. Male Advillin$^{Cre/+}$ mice were bred to female IR$^{lox/lox}$ to generate heterozygous Advillin$^{Cre/+}$, IR$^{lox/+}$ mice. Male Advillin$^{Cre/+}$, IR$^{lox/+}$ were bred to female IR$^{lox/lox}$ to produce SNIRKO mice with an Advillin$^{Cre/+}$, IR$^{lox/lox}$ genotype. Mice were genotyped via tail clip. Primers used for genotyping Advillin$^{Cre/+}$ were:

p1: 5′-CCCTGTTCACTGTGAGTAGG-3′,

p2: 5′-AGTATCTGGTAGGTGCTTCCAG-3’,

p3: 5′-GCGATCCCTGAACATGTCCATC-3’.

A wildtype allele produced a 500 bp fragment and a cre-expressing allele produced a 180 bp fragment. Primers used for genotyping IR$^{lox/lox}$ were:

p1: 5’-GATGTGCACCCCATGTCTG-3’,

p2: 5’-CTGAATAGCTGAGACCACAG-3’.

A wildtype allele produced a 279 bp fragment and an allele with loxp insertion produced a 313 bp fragment. All primers were added to a supermix to genotype SNIRKO mice and the PCR product was amplified for 35 cycles (94°C for 15 sec, 62°C for 15 sec, 72ºC for 90 sec) in a 40µL reaction. $IR^{lox/lox}$ were used as controls for all experiments. All experiments were approved by the University of Kansas Medical Center Institutional Animal Care and Use Committee. Mice were given access to food and water ad libitum and housed on a 12-hour light/dark cycle.

Conformation of Sensory Neuron Insulin Receptor Knockout:

RT-PCR: Total RNA was isolated from control and SNIRKO DRG to assess Cre/loxP recombination as described previously [134]. A reverse primer specific for exon 6 of the insulin receptor was used for reverse transcription: 5’-GTGATGGTGAGGTTGTGTTTGCTC-3’. The reaction was carried out using an iScript select kit (Bio-rad) at 42 degrees for 30 min, followed by 85 degrees for 5 min. The generated cDNA was then used for PCR template. Primers to exon 3, 5’-GCTGCACAGCTGAAGGCCTGT-3’, and exon 5, 5’-CTCCTCGAATCAGATGTAGCT-3’ were used to amplify the region corresponding to exon 4. PCR conditions were 94° for 30 secs followed by 35 cycles of 94° for 30 sec, 58° for 30 sec, 72 °for 1 min and a final extension at 72° for 7 min. A 585 bp fragment indicates an intact insulin receptor and a 435 bp fragment indicates cre/loxp recombination and deletion of the 150 bp exon 4.

Western blots: Insulin receptor protein expression was quantified in gastrocnemius muscle and DRG using Western blot analysis. Samples were homogenized in Cell Extraction Buffer (Invitrogen, Carlsbad, CA) containing 55.55 µl/ml protease inhibitor cocktail, 200mM Na_3VO_4, and 200mM NaF. After homogenization, samples were incubated on ice for 60 minutes and vortexed every 10 minutes to allow for complete protein extraction. Samples were then centrifuged for 10 minutes at 10000 rpm and the protein concentration of the supernatant was measured with a Bradford assay (Bio-Rad, Hercules,

CA). Before samples were used for Western blot analysis, they were boiled with Lane Marker Reducing Sample Buffer (Thermo Scientific, Waltham, MA) for 3 minutes. 30 µg of protein was loaded per lane and samples were separated on a 4-15% gradient tris-glycine gel (Bio-Rad). After gel electrophoresis, samples were transferred to a nitrocellulose membrane and blocked in 5% milk. Following incubation with primary (Insulin receptor β subunit (Santa Cruz), Actin (Millipore)) and secondary antibodies, bands were visualized with film and analyzed with ImageJ (NIH).

Additionally, Western blots were used to assess Akt activation in muscle and DRG following an intraperitoneal injection of insulin at 10.0 U/Kg to determine if insulin receptor knockout disrupted the insulin signaling pathway. Sterile PBS was used as vehicle control. Mice were fasted 3 hours prior to insulin injection. Thirty minutes after insulin stimulation mice were sacrificed and tissues were harvested. Western samples were then prepared and blots were probed with total Akt and p-(Ser473)Akt (Cell Signaling, Danvers, MA).

Sensorimotor Behavior Analysis:

SHIRPA: A modified SHIRPA analysis was used to assess gross motor and sensory function of SNIRKO mice at 6 weeks of age. SHIRPA is a semi-quantitative protocol used to assess genetically modified mice for defects in areas such as grooming, reflexes, strength, activity level, body position, and appearance [275]. Briefly, mice were placed in a glass viewing jar and undisturbed behaviors, such as body position, tremor, and spontaneous activities, were recorded for 5 minutes. Mice were then quickly transferred to an open arena to observe transfer arousal, gait, and tail position. After arena observation, mice were transferred to a grid and several different reflexes were assessed, including visual placing, righting reflex, limb grasping and pinna reflex. Throughout the observation period vocalization, excretion, appearance, and overall aggression level is recorded. Any sign of convulsion, disorientation, or stereotyped behavior was also documented.

Force plate Actometer: To further assess activity and undisturbed behavior, mice were placed in a force plate actometer as previously described [276]. Briefly, mice were placed in a light and sound

attenuated box on a 42 cm X 42 cm metal plate coupled to force transducers located on each of the 4 corners. The actometer is able to precisely determine the mouse's location based on the recordings of the force transducers and is capable of providing high resolution temporal and spatial behavior data. Types of data that can be acquired are total distance travelled, percent of distance in the perimeter, focused stereotypys, and bouts of low mobility. For experiments presented here, data was collected for 60 frames at 10.24 seconds/frame (approx. 10 minutes total) and analyzed using FPA Analysis software.

*Thermal sensitivity***:** Prior to collection of experimental data, mice were acclimated to the behavior facility and equipment for a minimum of 2 days. On test days, mice were acclimated to the behavior facility for 30 minutes and then the Hargreaves table for 30 minutes prior to data collection. The surface of the table was maintained at 30°C, and mice were housed in individual clear plastic cages. A 4.0V radiant heat source was applied to the mid plantar surface of the hind paw, and time to withdrawal was measured [277]. Four trials were recorded for each hindpaw, alternating paws between trials. To prevent damage to the skin of the paw, the heat source shut off automatically after 20.48 seconds. Thermal sensitivity was tested at 9, 13, and 28 weeks of age and data is presented as the average latency to withdrawal across both paws.

Mechanical sensitivity: Mice were acclimated to the procedure for 2 days prior to testing at each time point and behavioral testing was performed at 8, 12, and 27 weeks of age. On test day, mice were acclimated to the behavioral testing room for 30 minutes in their home cages and for 30 minutes on the mesh grid in individual clear plastic cages. The mesh grid was elevated 55 cm above the testing table. The up-down method was used to test mechanical sensitivity [278]. A set of standard von Frey monofilaments (Stoelting, Wood Dale, IL) capable of exerting forces of 0.0045, 0.02, 0.068, 0.158, 0.178, 1.2, 2.041, and 5.5 g were applied to the right hind paw of each mouse. The duration of each stimulus was approximately 1 s and the inter-stimulus interval was approximately 30-60 seconds. Beginning with the 0.158 g monofilament, the right hind paw of each mouse was tested for a withdrawal response. Depending on the response the next filament was selected, if there was a positive response (no paw withdrawal) the next filament with greater force was applied. In the case of a negative response (paw

withdrawal) the next filament with a lesser force was used. This method was continued in determining the next filament to test until four trials were completed after the first negative response for each mouse. The 50% threshold was calculated for each mouse as previously described [262].

Beamwalk: The ability of mice to traverse an elevated beam was used to test motor coordination and proprioception. Two days before testing, mice were acclimated to the behavior facility and trained to traverse a 1 m-long, 1.2 cm diameter, wooden beam [80]. On test day, mice were recorded with a digital video camera as they walked across the beam. Each mouse had 3 trials per testing period. Videos were later analyzed and the number of times either the left or right hindpaw slipped of the beam was counted as a footslip. The number of footslips was averaged across all 3 trails.

Rotorod: Mice were placed on a rotating rod to test motor coordination and balance [279]. The speed of rotation was gradually increased from 4.0 to 40 rpm over a 5 minute time period and the latency to fall was recorded. If a mouse did not fall throughout the testing period, the rod was stopped and latency was recorded as 5 minutes. Mice were acclimated for one 5 minute period before being tested in 3 separate trials with 5 minutes between trials. The average latency to fall across all 3 trials is reported.

Metabolic Characteristics:

Several metabolic characteristics with respect to somatic growth, glucose metabolism and insulin signaling were monitored throughout the course of SNIRKO development and testing. Mice weights were recorded at 3, 5, 6, 7, 8, 16, 22, and 28 weeks of age.

Glucose and Hemoglobin A1C: Blood glucose levels were determined using a glucose diagnostic assay (Sigma-Aldrich, St. Louis, MO). Mice were fasted 3 hours prior to glucose measurement and blood was collected via tail snip at 6, 10, 16, 22, and 29 weeks of age. In addition, long term glucose levels were assessed by determining hemoglobin A1C levels immediately prior to sacrifice at 29 weeks of age using A1CNow+ Meter (Bayer, Leverkusen, Germany).

Insulin and Insulin-like Growth Factor-1: After a 3-hour fast, whole blood was collected via tail snip and allowed to clot on ice for 30 minutes. Samples were then centrifuged at 3000g for 15 minutes.

The resultant serum supernatant was used for analysis. Serum insulin and IGF-1 levels were measured with ELISAs from ALPCO (Salem, NH). Serum insulin levels were measured alongside glucose at 6, 10, 16, 22, and 29 weeks of age and IGF-1 levels were determined at sacrifice.

Intraperitoneal Glucose Tolerance Test (IPGTT): At 28 weeks of age, both $IR^{lox/lox}$ and SNIRKO glucose tolerance was analyzed with an IPGTT. After a 6-hour fast, mice were administered a glucose bolus of 2g/kg body weight via IP injection. Blood glucose measurements were taken immediately prior to glucose stimulation and at 15, 30, 60 and 120 minutes thereafter.

Nerve Conduction Velocity: Nerve conduction velocity was conducted as previously described [280]. Briefly, mice were anesthetized with 200 mg/kg Avertin (1.25% v/v tribromoethanol, 2.5% tert-amyl alcohol, dH_2O). Mouse body temperature was monitored with rectal probe and maintained at 37°C via feed-back controlled heating pad. Motor nerve conduction velocities (MNCVs) were obtained by measuring compound muscle action potentials using 9.9 mA stimulation at the ankle distally and at the sciatic notch proximally. MNCVs are reported as the average of 3 independent recordings. Sensory nerve conduction velocity (SNCV) was measured behind the medial malleolus with a 2.4 mA stimulation of the second toe digital nerve. SNCVs are reported as the average of 10 recordings.

Fluorescent Microscopy:

Tomato mice cre expression: $Advillin^{+/+}$, $Tomato^{+/-}$ and $Advillin^{cre/+}$, $Tomato^{+/-}$ mice tissues were fixed via intracardial perfusion with Zamboni's fixative (4% paraformaldehyde and 15% picric acid) prior to dissection. After dissection, tissues were post-fixed in Zamboni's fixative for 1 hour. Tissues were then rinsed in PBS for 24 hours before being transferred to 30% sucrose. After sucrose saturation, tissues were imbedded in optimal cutting temperature compound and stored at -80°C until further use. Tissue sections were cut using a Leica CM 1950 cryostat and placed on slides in serial sections. Sections were then covered with PBS and cover slipped. Images were acquired using a Nikon Eclipse 90i microscope. Exposure times were kept constant between experimental groups.

Intraepidermal Nerve Fiber Density: At sacrifice, the skin of the hindpaw footpad was removed from $IR^{lox/lox}$ and SNIRKO mice and fixed in Zamboni's fixative for 1 hour. Tissues were then prepared and imbedded as described above. Hindpaw footpad skin was cut in sagittal sections with a Leica CM 1950 cryostat and placed on slides in serial sections. Slides were blocked at room temperature for 1 hour with pre-incubation solution (1.5% Normal Goat or Donkey Serum, 0.5% Porcine Gelatin, 0.5% Triton X-100, and 450 µL Superblock (Thermo Scientific)). Primary antibody to PGP 9.5 (Chemicon, Temecula, CA) and donkey anti-rabbit Alexa-488 conjugated secondary antibody (Molecular Probes) were then used to label and visualize epidermal nerve fibers. Images were acquired with a Nikon Eclipse 90i microscope. Fibers that crossed the dermal-epidermal border were quantified in 3 regions per section and 3 sections per mouse were evaluated. The length of the epidermal region was measured with NIH Image J software and the intraepidermal nerve fiber density (IENFD) is expressed as number of fibers per millimeter of epidermis.

Pancreas Morphology:

Tissue Preparation: Pancreata were removed and fixed in 4% paraformaldehyde in phosphate buffered saline (PBS), pH 7.2, for three days at +4°C. Tissue was embedded in paraffin using an automated vacuum tissue processor Leica ASP300S (Leica Microsystems Inc., Bannockburn, IL) and stored at +4°C. Tissue sections of 8 µm thickness were cut using a microtome RM2255 (Leica Microsystems Inc.) and mounted directly on Superfrost/Plus microscope slides (Fisher, Pittsburgh, PA, #12-550-12). After cutting, slides were dried at +40°C overnight in an oven and stored at +4°C until processing.

Paraffin embedded sections were deparaffinized/rehydrated in xylene followed by ethanol and PBS serial rehydration. Antigen retrieval was completed in a steamer using 0.01M citrate buffer, pH 6.2, with 0.002M EDTA, for 30 min. After cooling for 20 min, slides were washed in PBS 2 times and permeabilized in1% Triton X-100 in PBS for 30 min. Slides were rinsed again in PBS. After washing,

sections were encircled with a PAP pen. Sections were incubated in 10% normal donkey serum (NDS), 1% bovine serum albumin (BSA), 0.03% Triton X-100, all diluted in PBS, for 30 min to block nonspecific binding sites and rinsed in PBS. Blocked sections were used for immunofluorescence (IF) and immunohistochemistry (IHC) staining.

Immunofluorescence (IF): Blocked sections were incubated with the primary antibody mix at +4°C, overnight, in a wet chamber. Sections were rinsed in PBS 3 times, and incubated for 2 hr at room temperature in a mix of fluorophore conjugated secondary antibodies in a dark wet chamber. The following solution was used to dilute primary and secondary antibodies: 1% NDS, 1% BSA, 0.03% Triton X-100. After incubation with secondary antibodies, slides were washed in PBS 3 times, and mounted with anti-fading agent Gel/Mount (Biomeda, Foster City, CA). In some cases, DAPI (4'6-diamindino-2-phenylindole; 0.5 µg/ml; Molecular Probes, Eugene, OR, # D1306) staining was performed for 5 min at room temperature following the first wash after secondary antibody exposure.

The following primary antibodies were used to stain the pancreas: anti-insulin (1:200, Abcam, Cambridge, MA, # ab7842) or anti-insulin (1:100, Santa Cruz Biotechnology, Inc**.,** Santa Cruz, CA, # sc-9168), anti-glucagon (1:300, Abcam, # ab10988), anti-somatostatin (1:300, Abcam, # ab53165), and anti-Ki67 Proliferation Marker (1:200, Abcam, # ab16667). Appropriate secondary antibodies were used that were conjugated with DyLight 488 (1:400, Jackson ImmunoResearch Laboratories Inc., West Grove, PA, # 706-485-148), Alexa 555 (1:400, Molecular Probes, Eugene, OR, # A31570),or Alexa 647 (1:400, Molecular Probes, # A31573).

Images were captured on a Nikon C1Si or C1 Plus confocal microscopes (Nikon Instruments Inc, Melville, NY). IF images were analyzed using Nikon software EZ-C1 3.90 Free viewer. The cellular composition of islets was measured by counting the individual types of cells (β-cells labeled with anti-insulin, α-cells with anti-glucagon and δ-cells with anti-somatostatin) in each islet, and dividing the number of each cell type by the total number of all labeled cells per islet.

Immunohistochemistry (IHC): Anti-insulin (1:100, Santa Cruz Biotechnology, Inc**.,** Santa Cruz, CA, # sc-9168) or anti-glucagon (1:200, Santa Cruz Biotechnology, # sc-13091) primary antibodies were

used. Staining was developed using Histostain-*Plus* Broad Spectrum (AEC) Kit (Invitrogen, Frederick, MD, # 859943). The IHC procedure was conducted according to manufacturer instructions. Slides were counterstained with hematoxylin to identify cell nuclei.

After staining, slides were rinsed in deionized water and placed on coverslips in Clear Mount mounting medium (Electron Microscopy Sciences, Hatfield, PA, #17985-12). The specificity of immunoreactivity was confirmed by omitting the primary antibody from some sections. The staining was observed using a light microscope Nikon Eclipse 80i (Nikon Instruments Inc, Melville, NY.). Images were analyzed using Ps Adobe Photoshop CZ4 extended software. The relative insulin content was measured based on the intensity of staining of pancreatic sections with anti-insulin. The average pixel value of staining per cell or per islet was determined. Background staining was subtracted from each value.

Insulitis was determined by the presence of lymphocyte infiltration, which was defined as highly concentrated monocytic nuclei around islets. Infiltration was scored using images of hematoxylin staining combined with IHC with either insulin or glucagon antibody labeling. Islets were scored using the following criteria: peri-insulitis when infiltration had begun with peripherally observed immune cells; intra-insular insulitis when immune cells had clearly infiltrated the islet; and the islet destruction stage was determined when the islet area was completely infiltrated by immune cells. Infiltration was calculated as the percentage of the islet area comprised of infiltrating cells.

Statistical analysis:

All data is reported as the mean ± standard error of the mean. The statistical test and n for each experiment is listed in the legend for each figure. Male and female mice were included in analysis, as the pattern of differences between $IR^{lox/lox}$ and SNIRKO mice was consistent across both sexes. A p-value less than 0.05 was considered statistically significant. Graphpad Prism software was used for all statistical analysis.

5.4 Results

Cre recombinase expression is sensory neuron specific in Advillin$^{cre/+}$ mice:

Advillin is a member of the gelosin superfamily and has recently been demonstrated to have a selective sensory neuron specific expression [274] and cre recombinase expression under control of the advillin promoter shows a similar sensory neuron specific expression [272]. Advillin$^{cre/+}$ mice are unique as compared to previous developed mice that conditionally express cre in sensory neurons. Advillin$^{cre/+}$ show cre expression in almost all sensory neurons where as previously developed mice only had cre expression in specific neuronal subpopulations [281]. To confirm sensory neuron specific cre expression, Advillin$^{cre/+}$ male mice were bred to female Tomato mice and the expression of GFP was qualitatively analyzed across several different tissues (Figure 5.1-5.3). Sensory neuron cell bodies showed strong GFP expression in Advillin$^{cre/+}$, Tomato$^{+/-}$ mice in both the DRG and nodose ganglia (Figures 5.1A and 5.2A, respectively), little to no GFP is visible in Tomato$^{+/-}$ mice. In addition to sensory neuron cell bodies, sensory axons can also be visualized in the hindpaw footpad (Figure 5.1B), sciatic nerve (Figure 4.1C), and dorsal horn of the spinal cord (Figure 5.2B) of Advillin$^{cre/+}$, Tomato$^{+/-}$. No GFP expression was observed in axons of these tissues in Tomato$^{+/-}$ mice. GFP expression was not observed in sections of brain frontal cortex (Figure 5.2C), ventral spinal cord (Figure 5.2B), liver (Figure 5.3A) or muscle (Figure 5.3B) in either Advillin$^{cre/+}$, Tomato$^{+/-}$ or Tomato$^{+/-}$ mice.

SNIRKO mice have decreased insulin receptor expression the DRG:

Cre/lox recombination of the insulin receptor was confirmed in the DRG using RT-PCR (Figure 5.4A). An RT-PCR product of 585bp, suggesting intact insulin receptor RNA, was observed in DRG both from IR$^{lox/lox}$ and SNIRKO mice. A 435bp product, suggesting deletion of insulin receptor exon 4, was only observed in DRG from SNIRKO mice. The presence of a 585bp product in the DRG of SNIRKO mice is most likely due to non-sensory neuron cells within the DRG sample that express the insulin receptor, as the DRG is not solely comprised of sensory neurons. Possible contaminating cells include Schwann cells, endothelial cells, and satellite cells [170].

Figure 5.1

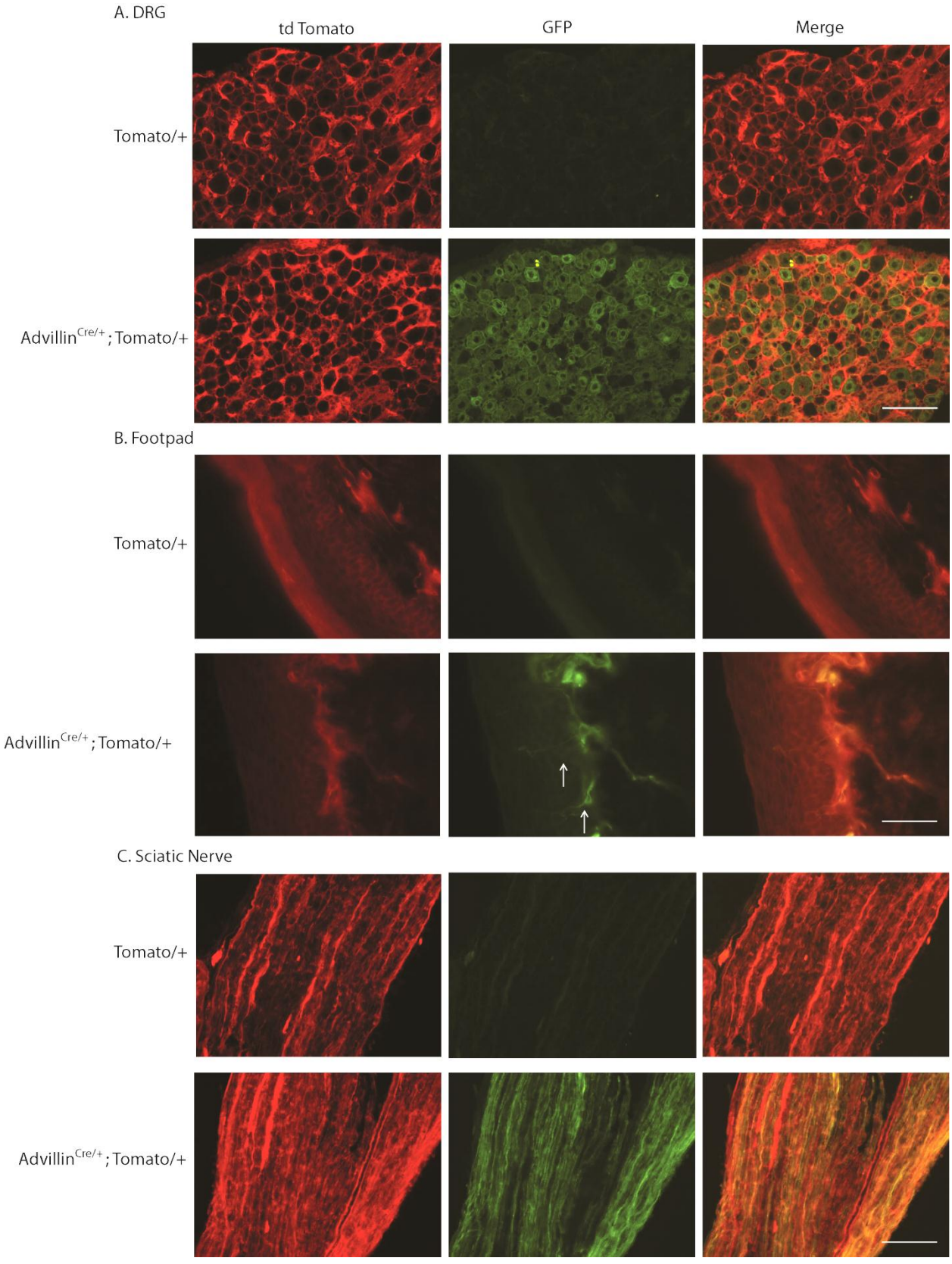
A. DRG
td Tomato
GFP
Merge
Tomato/+
Advillin$^{Cre/+}$; Tomato/+
B. Footpad
Tomato/+
Advillin$^{Cre/+}$; Tomato/+
C. Sciatic Nerve
Tomato/+
Advillin$^{Cre/+}$; Tomato/+

Figure 5.1. Cre recombinase expression in DRG, footpad, and sciatic nerve of Advillin$^{Cre/+}$ mice. A reporter line for cre recombinase activity (Tomato) was used to confirm sensory neuron specific cre expression in Advillin$^{Cre/+}$ mice. Images of red fluorescence, green fluorescence, and merged images are shown from Advillin$^{Cre/+}$; Tomato$^{+/-}$ and Tomato$^{+/-}$ mice. A) Sensory neurons in the DRG show GFP expression in Advillin$^{Cre/+}$; Tomato$^{+/-}$ mice but not Tomato$^{+/-}$ mice. Images were taken at 20x magnification. Scale bar=100µm. B) In the hindpaw footpad, GFP expression can be visualized in the axons of sensory neurons crossing the dermal-epidermal border (arrows) in Advillin$^{Cre/+}$; Tomato$^{+/-}$ mice, but not Tomato$^{+/-}$ mice. Images were taken at 40x magnification. Scale bar=50µm C) Strong GFP expression was visualized in the sciatic nerve of Advillin$^{Cre/+}$; Tomato$^{+/-}$ mice. GFP was not present in the sciatic nerve of Tomato$^{+/-}$ mice. Images were taken at 20x magnification. Scale bar=100µm.

Figure 5.2

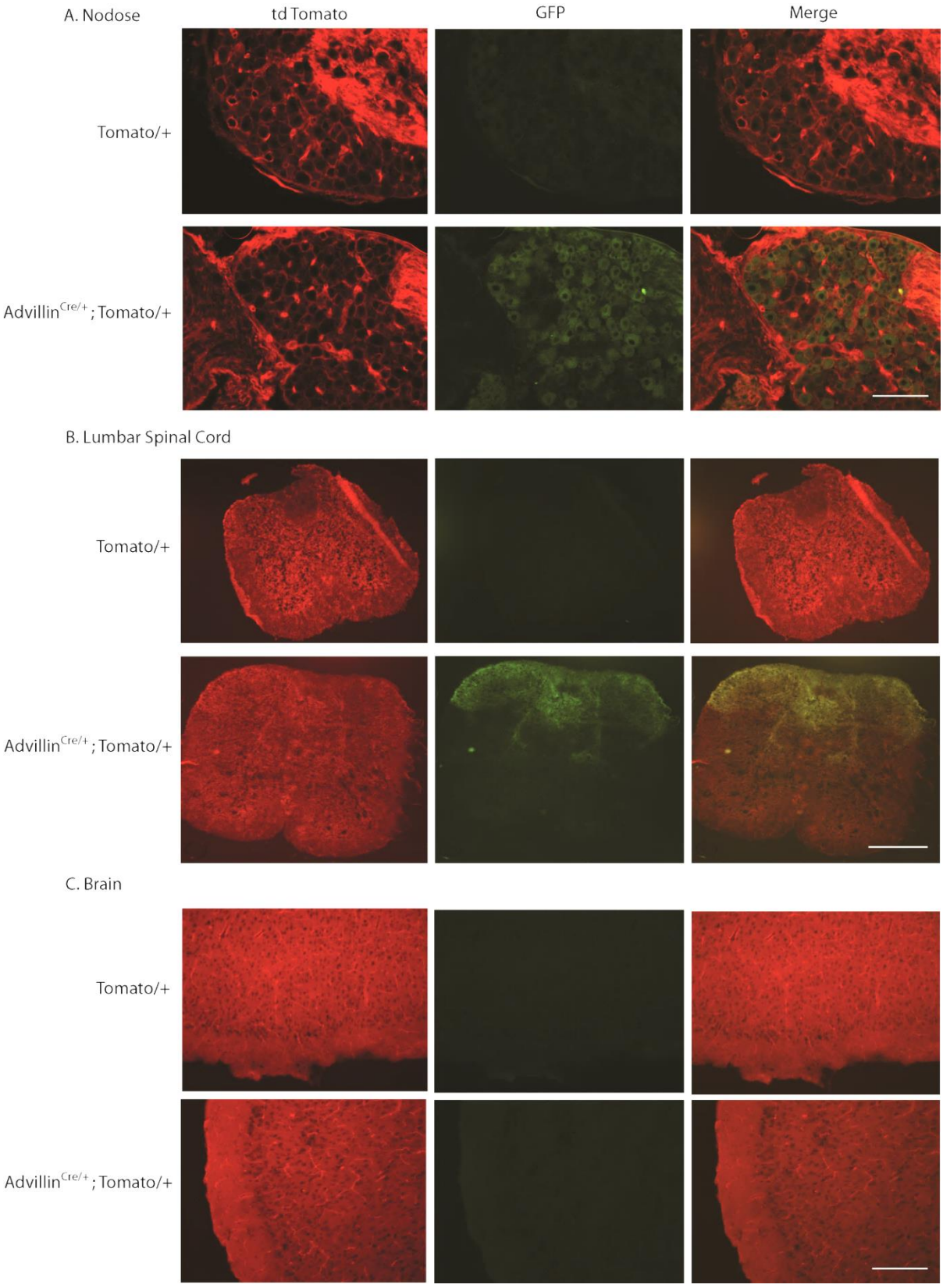
A. Nodose
td Tomato
GFP
Merge
Tomato/+
Advillin$^{Cre/+}$; Tomato/+
B. Lumbar Spinal Cord
Tomato/+
Advillin$^{Cre/+}$; Tomato/+
C. Brain
Tomato/+
Advillin$^{Cre/+}$; Tomato/+

Figure 5.2. Cre recombinase expression in nodose ganglia, lumbar spinal cord, and frontal cortex of Advillin$^{Cre/+}$ mice. A portion of pancreatic sensory innervation arises from the nodose ganglia [282]. Here, GFP expression is evident in the sensory neurons of the nodose ganglia of Advillin$^{Cre/+}$; Tomato$^{+/-}$, but not Tomato$^{+/-}$ mice (A). Images were taken at 20x magnification. Scale bar=100µm. B) GFP expression is present only in the dorsal horn of the spinal cord from Advillin$^{Cre/+}$; Tomato$^{+/-}$ mice, corresponding to the area of sensory neuron axon termination. No GFP expression is visible from either Advillin$^{Cre/+}$; Tomato$^{+/-}$ or Tomato$^{+/-}$ mice in the ventral portion of the spinal cord, an area predominantly associated with motor neurons. Images were taken at 4x magnification. Scale bar=400µm. C) Neither Advillin$^{Cre/+}$; Tomato$^{+/-}$ or Tomato$^{+/-}$ mice show GFP expression in the brain frontal cortex. Images were taken at 10x magnification. Scale bar=200µm.

Figure 5.3

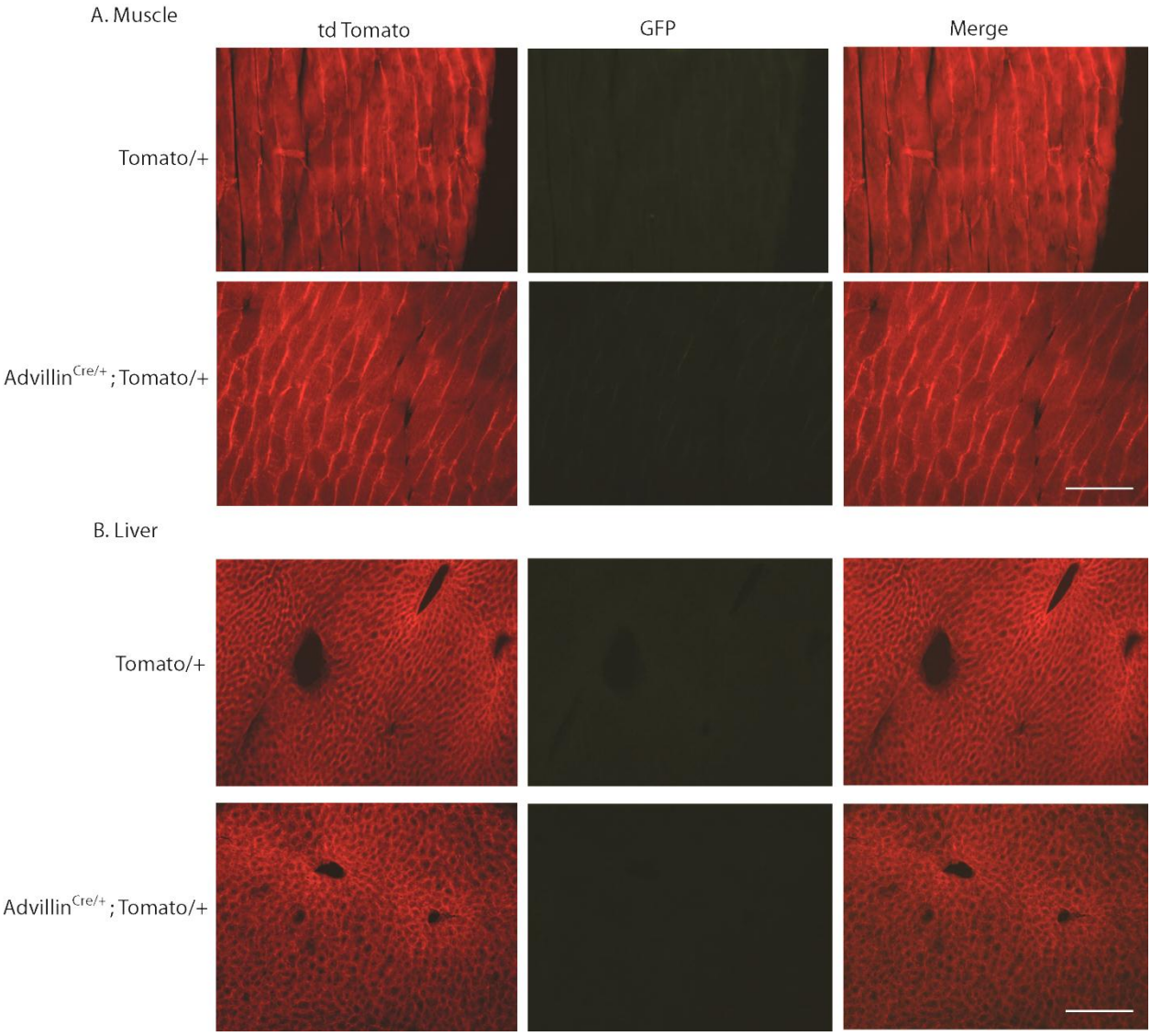
A. Muscle
td Tomato
GFP
Merge
Tomato/+
Advillin$^{Cre/+}$;Tomato/+
B. Liver
Tomato/+
Advillin$^{Cre/+}$;Tomato/+

Figure 5.3. Cre recombinase expression in muscle and liver of Advillin$^{Cre/+}$ mice. Neither muscle (gastrocnemius) nor liver cells from Advillin$^{Cre/+}$; Tomato$^{+/-}$ or Tomato$^{+/-}$ mice express GFP (A and B). Images were taken at 10x magnification. Scale bar=200μm. However, at higher magnification (40x) thin axons can be visualized expressing GFP in the muscle of Advillin$^{Cre/+}$; Tomato$^{+/-}$ mice (images not shown).

Western blot analysis was used to determine whether cre/lox recombination resulted in reduced insulin receptor protein levels in the DRG (Figure 5.4B). SNIRKO mice show a significant decrease in DRG insulin receptor expression. Insulin receptor levels in SNIRKO mice are approximately 60% lower than that observed in $IR^{lox/lox}$ mice. This observed significant decrease in insulin receptor expression was not present in the gastrocnemius muscle of SNIRKO mice (Figure 5.4C).

To determine if reductions in DRG insulin receptor expression affected insulin signaling transduction, DRG Akt activation was assessed via Western blot analysis after IP insulin injection. As expected, DRG from $IR^{lox/lox}$ mice showed a significant increase in Akt activation (p(ser473)/totalAkt) in response to insulin stimulation (Figure 5.4D). However, Akt activation in the DRG of SNIRKO mice was not significantly increased above baseline (PBS) and was significantly lower as compared to $IR^{lox/lox}$ mice. Insulin-induced Akt activation was significantly activated in the muscle from both $IR^{lox/lox}$ and SNIRKO mice as compared to baseline and there was no significant difference between groups (Figure 5.4E).

These data suggest that insulin receptor cre/lox recombination was specific to sensory neurons and that reduced insulin receptor expression is significantly blunting neuronal insulin signaling.

SNIRKO mice do not display gross changes in development:

Mice with systemic insulin receptor knockout are born 10% smaller and die within 72 hours from severe diabetic ketoacidosis [129]. SNIRKO mice were born with the expected frequency and showed no observable difference in appearance or weight gain through 28 weeks of age (Figure 5.5). SNIRKO development was also assessed with SHIRPA analysis. SNIRKO mice did not show significant differences in overall SHIRPA scores as compared to $IR^{lox/lox}$ and no significant difference was detected between male and female SNIRKO mice (Figure 5.5B and C). The only significantly different behavior observed during SHIRPA analysis between $IR^{lox/lox}$ and SNIRKO mice was related to biting. Results indicate that SNIRKO mice were more likely to bite as compared to $IR^{lox/lox}$ mice (Figure 5.5D and E). The complete list of behaviors tested, scoring, and results of SHIRPA analysis are listed in Table 5.1.

Figure 5.4

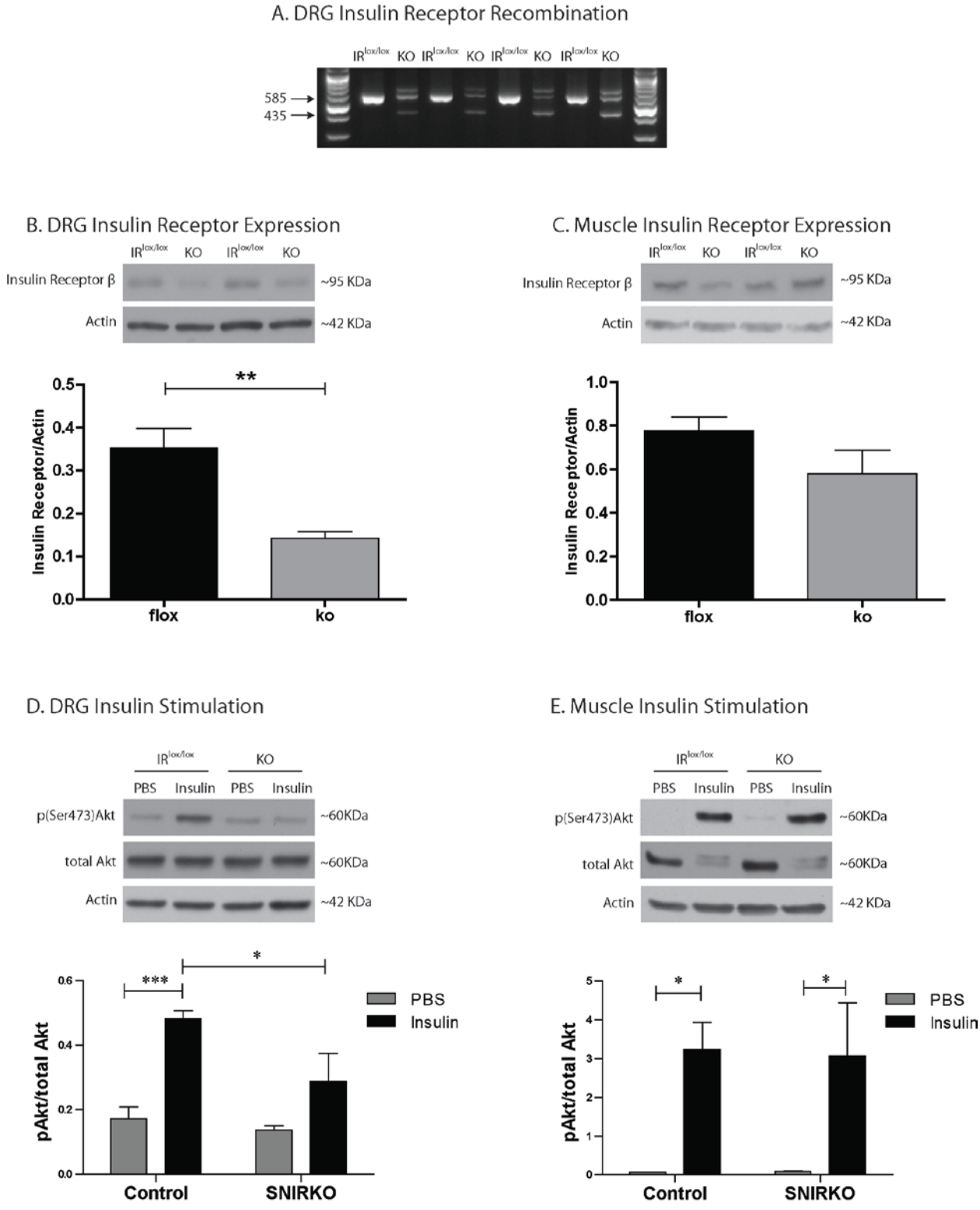
A. DRG Insulin Receptor Recombination
IRlox/lox KO IRlox/lox KO IRlox/lox KO IRlox/lox KO
585
435
B. DRG Insulin Receptor Expression
IRlox/lox KO IRlox/lox KO
Insulin Receptor β
~95 KDa
Actin
~42 KDa
**
Insulin Receptor/Actin
0.5
0.4
0.3
0.2
0.1
0.0
flox
ko
C. Muscle Insulin Receptor Expression
IRlox/lox KO IRlox/lox KO
Insulin Receptor β
~95 KDa
Actin
~42 KDa
Insulin Receptor/Actin
1.0
0.8
0.6
0.4
0.2
0.0
flox
ko
D. DRG Insulin Stimulation
IRlox/lox KO
PBS Insulin PBS Insulin
p(Ser473)Akt
~60KDa
total Akt
~60KDa
Actin
~42 KDa
***
*
pAkt/total Akt
0.6
0.4
0.2
0.0
PBS
Insulin
Control
SNIRKO
E. Muscle Insulin Stimulation
IRlox/lox KO
PBS Insulin PBS Insulin
p(Ser473)Akt
~60KDa
total Akt
~60KDa
Actin
~42 KDa
*
*
pAkt/total Akt
5
4
3
2
1
0
PBS
Insulin
Control
SNIRKO

Figure 5.4. SNIRKO Insulin Receptor Expression in DRG and Muscle. Cre recombinase excision of insulin receptor exon 4 flanked by loxp sites was confirmed in the DRG with RT-PCR (A). A 585 bp band was indicative of intact insulin receptor RNA and a 435 bp band suggested a recombination event and the excision of the 150 bp exon 4. A 435 bp band was only observed in DRG from SNIRKO mice. Western blots show a significant decrease in insulin receptor beta expression in the DRG of SNIRKO mice (B), however no significant change was observed in the muscle of SNIRKO mice (C). Results were analyzed with a student's t-test. n=15 $IR^{lox/lox}$ and n=8 SNIRKO. Insulin stimulation failed to significantly activate Akt over baseline in the DRG of SNIRKO mice and insulin-induced activated Akt levels were significantly lower as compared to $IR^{lox/lox}$ (D). Insulin stimulation significantly activated Akt over baseline in the muscle from both $IR^{lox/lox}$ and SNIRKO mice. No significant difference was observed between $IR^{lox/lox}$ and SNIRKO mice insulin-induced Akt activation levels in the muscle (E). Results were analyzed with a 2-way ANOVA and Bonferroni's post-hoc analysis. n=4 $IR^{lox/lox}$ PBS, n=4 $IR^{lox/lox}$ insulin, n=3 SNIRKO PBS and n=3 SNIRKO insulin. *=$p<0.05$, **=$p<0.01$, ***=$p<0.001$.

Figure 5.5

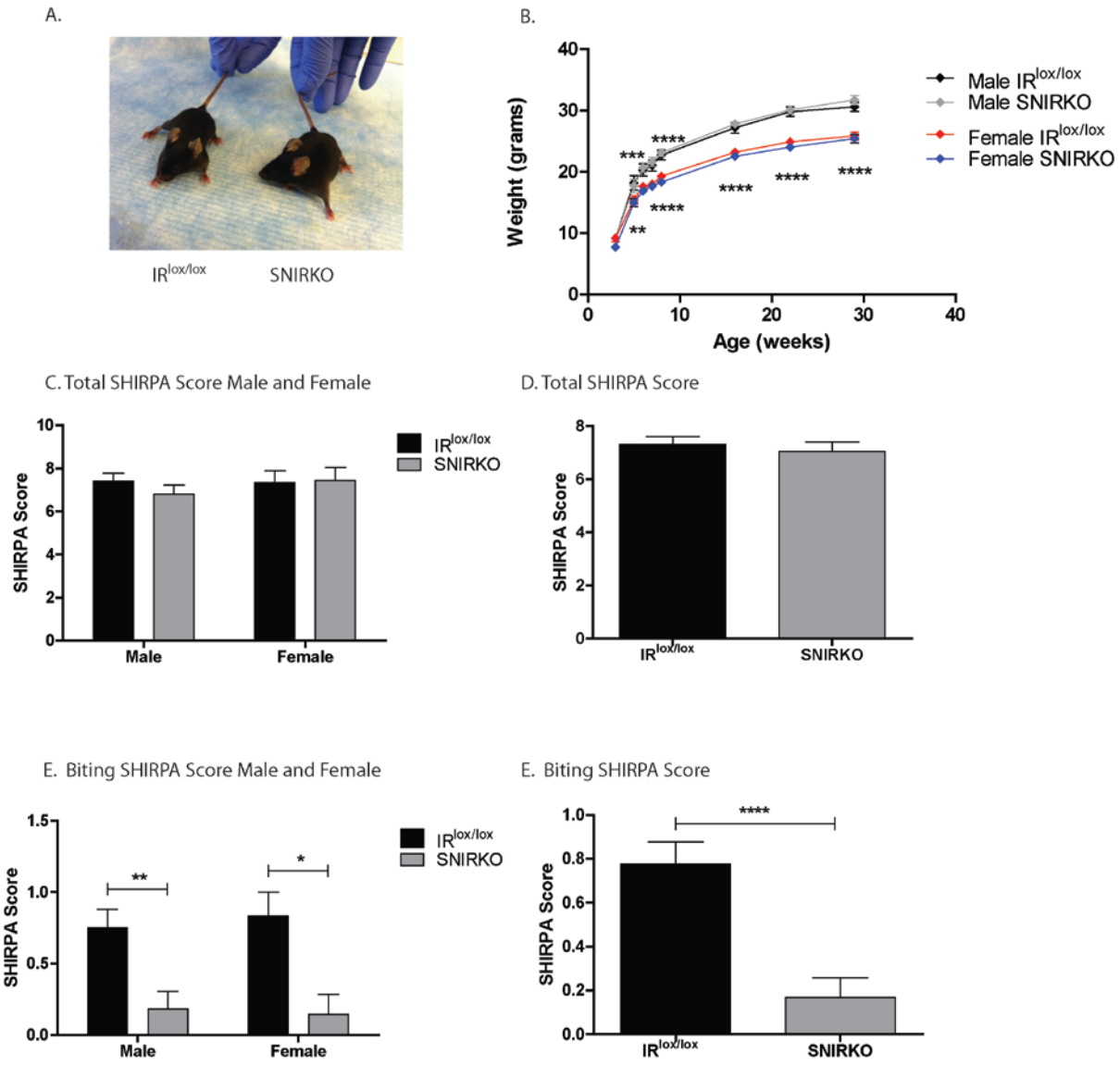
A.
IR lox/lox
SNIRKO
B.
Weight (grams)
Age (weeks)
Male IR lox/lox
Male SNIRKO
Female IR lox/lox
Female SNIRKO
C. Total SHIRPA Score Male and Female
SHIRPA Score
Male
Female
IR lox/lox
SNIRKO
D. Total SHIRPA Score
SHIRPA Score
IR lox/lox
SNIRKO
E. Biting SHIRPA Score Male and Female
SHIRPA Score
Male
Female
IR lox/lox
SNIRKO
E. Biting SHIRPA Score
SHIRPA Score
IR lox/lox
SNIRKO

Figure 5.5. SNIRKO mice do not have gross developmental defects. SNIRKO mice do not show signs of major birth defects and appear healthy from birth (A). SNIRKO mice weigh similar to $IR^{lox/lox}$ mice of the same sex (B). Results were analyzed with a repeated measures 2-way ANOVA and Bonferroni's post-hoc. There were no differences between $IR^{lox/lox}$ and SNIRKO mice. The differences indicated in the figure are between males and females only. n=9 $IR^{lox/lox}$ male, n=10 SNIRKO male, n=8 $IR^{lox/lox}$ female, and n=6 SNIRKO female. SNIRKO mouse development was also quantified with a SHIRPA analysis. SHIRPA analysis uses a battery of tests to roughly assess behaviors as well as morphology. No significant difference in total SHIRPA score was noted between male and female $IR^{lox/lox}$ and SNIRKO mice (C). Results were analyzed with a 2-way ANOVA and Bonferroni's post-hoc. n=12 $IR^{lox/lox}$ male, n=11 SNIRKO male, n=6 $IR^{lox/lox}$ female, and n=7 SNIRKO female. Additionally, no difference was observed when males and females were combined (D). Results were analyzed with a student's t-test. n=18 $IR^{lox/lox}$ and n=18 SNIRKO. The only significant difference in behavior noted between $IR^{lox/lox}$ and SNIRKO mice was in biting observed throughout the SHRIPA (E). SNIRKO mice displayed increased biting (0=biting present, 1=biting absent). Results were analyzed with a 2-way ANOVA and Bonferroni's post-hoc. n=12 $IR^{lox/lox}$ male, n=11 SNIRKO male, n=6 $IR^{lox/lox}$ female, and n=7 SNIRKO female. The significant difference was maintained when data from males and females was combined (F). Results were analyzed with a student's t-test. n=18 $IR^{lox/lox}$ and n=18 SNIRKO. *=$p<0.05$, **=$p<0.01$, ***=$p<0.001$, ****=$p<0.0001$.

Table 5.1

Behavior/Morphology Observed	Scoring	Male $IR^{lox/lox}$	Male SNIRKO	Female $IR^{lox/lox}$	Female SNIRKO
Body Position	0 = active 1 = inactive 2 = excessive activity	0.0 ± 0.0	0.18 ± 0.18	0.0 ± 0.0	0.0 ± 0.0
Tremor	0 = absent 1 = present	0.0 ± 0.0	0.0 ± 0.0	0.0 ± 0.0	0.0 ± 0.0
Prepebral Closure	0 = eyes open 1 = eyes closed	0.0 ± 0.0	0.0 ± 0.0	0.0 ± 0.0	0.0 ± 0.0
Coat Appearance	0 = Well groomed coat 1 = Irregularities such as piloerection	0.0 ± 0.0	0.0 ± 0.0	0.0 ± 0.0	0.0 ± 0.0
Whiskers	0 = present 1 = absent	0.0 ± 0.0	0.0 ± 0.0	0.0 ± 0.0	0.0 ± 0.0
Lacrimation	0 = absent 1 = present	0.0 ± 0.0	0.0 ± 0.0	0.0 ± 0.0	0.0 ± 0.0
Defecation	0 = present 1 = absent	0.25 ± 0.13	0.09 ± 0.09	0.17 ± 0.17	0.43 ± 0.20
Transfer Arousal	0 = extended freeze (over 5 sec) 1 = brief freeze followed by movement 2 = immediate movement	1.42 ± 0.20	1.45 ± 0.20	1.17 ± 0.31	1.57 ± 0.20
Gait	0 = fluid movement and pevis is off floor 1 = lack of fluidity, retropulsion, etc	0.0 ± 0.0	0.0 ± 0.0	0.0 ± 0.0	0.0 ± 0.0
Tail elevation	0 = dragging tail 1 = horizontal extension 2 = elevated/straub tail	1.0 ± 0.0	1.00 ± 0.0	1.0 ± 0.0	1.14 ± 0.14
Startle response	0 = none 1 = preyer reflex (backwards flick of pinnae) 2 = reaction in addition to Preyer response	1.17 ± 0.11	1.10 ± 0.09	1.17 ± 0.17	1.29 ± 0.18
Touch escape	0 = no response 1 = response to touch 2 = flees prior to touch	1.67 ± 0.14	1.64 ± 0.15	1.50 ± 0.22	1.86 ± 0.14
Positional passivity	0 = struggles when held by tail 1 = struggles when held by scruff 2 = struggles when laid supine 3 = no struggle	0.0 ± 0.0	0.0 ± 0.0	0.0 ± 0.0	0.0 ± 0.0
Skin color	0 = pale 1 = pink 2 = red	1.0 ± 0.0	1.0 ± 0.0	1.0 ± 0.0	1.0 ± 0.0
Trunk curl	0 = present 1 = absent	0.0 ± 0.0	0.0 ± 0.0	0.0 ± 0.0	0.0 ± 0.0
Limb grasping	0 = present 1 = absent	0.0 ± 0.0	0.0 ± 0.0	0.0 ± 0.0	0.0 ± 0.0
Visual placing	0 = present 1 = absent	0.0 ± 0.0	0.0 ± 0.0	0.0 ± 0.0	0.0 ± 0.0
Righting reflex	0 = present 1 = absent	0.0 ± 0.0	0.0 ± 0.0	0.0 ± 0.0	0.0 ± 0.0
Pinneal reflex	0 = present 1 = absent	0.0 ± 0.0	0.0 ± 0.0	0.0 ± 0.0	0.0 ± 0.0
Contact righting reflex	0 = present 1 = absent	0.0 ± 0.0	0.0 ± 0.0	0.0 ± 0.0	0.0 ± 0.0
Biting	0 = present 1 = absent	0.75 ± 0.13	0.18 ± 0.12 **	0.83 ± 0.17	0.14 ± 0.14 *
Vocalization	0 = present 1 = absent	0.17 ± 0.11	0.18 ± 0.12	0.5 ± 0.16	0.0 ± 0.0
Morphology	0 = normal 1 = abnormal	0.0 ± 0.0	0.0 ± 0.0	0.0 ± 0.0	0.0 ± 0.0
Tail pinch	0 = response 1 = no response	0.0 ± 0.0	0.0 ± 0.0	0.0 ± 0.0	0.0 ± 0.0
Total SHIRPA Score		7.42 ± 0.36	6.82 ± 0.40	7.33 ± 0.56	7.43 ± 0.61

Table 5.1. SNIRKO SHIRPA data. Complete data and scoring from SHIRPA analysis indicates that SNIRKO mice do not have major developmental defects. Results were analyzed with a 2-way ANOVA and Bonferroni's post-hoc. n=12 $IR^{lox/lox}$ male, n=11 SNIRKO male, n=6 $IR^{lox/lox}$ female, and n=7 SNIRKO female. *=$p<0.05$, **=$p<0.01$.

SNIRKO mice are euglycemic:

A central reason behind developing SNIRKO mice was the need to separate altered sensory neuron insulin signaling from hyperglycemia. Blood glucose levels were monitored for 6 months and no significant difference was observed between SNIRKO and $IR^{lox/lox}$ mice (Figure 5.6A and B). Independent of genotype, female mice did have a significantly lower blood glucose level as compared to males (not denoted in the figure). In addition, there was no significant difference in hemoglobin A1C levels between groups (Figure 5.6 C and D). The results indicate that in addition to reduce sensory neuron insulin signaling, SNIRKO mice maintain normal glucose levels.

SNIRKO mice do not show significantly different actometer-assessed behaviors:

A force plate actometer was used to assess several baseline behaviors. SNIRKO mice did not have a significant difference in total distance travelled and no significant difference was detected between the percent of distance travelled in the perimeter between $IR^{lox/lox}$ and SNIRKO mice (p-value=0.11). No significant difference between groups was observed in all other behaviors analyzed (Table 5.2).

SNIRKO mice do not show sensorimotor behavior changes as seen in DN:

A hallmark of DN in rodent models is changes in sensorimotor behavior, predominantly assessed by testing mechanical (large and small fiber) and thermal sensitivity (small fiber) using von Frey filaments or a Hargreaves table, respectively. SNIRKO mice have no significant difference in mechanical sensitivity (Figure 5.7 A). Analysis of thermal sensitivity with a repeated measures 2-way ANOVA indicates no main effect between $IR^{lox/lox}$ and SNIRKO mice throughout the testing periods (Figure 5.7 B), however Bonferroni's post-hoc indicates a significant difference at 13 weeks of age. Interestingly, this appears to be due more to an increase in $IR^{lox/lox}$ threshold at this time point rather than a decrease in SNIRKO threshold. For comparison, $IR^{lox/lox}$ thresholds were 7.0, 7.9, and 7.5 at 9, 13, and 28 weeks of age, respectively. SNIRKO thresholds were 7.2, 6.8, and 7.0 at 9, 13, and 28 weeks of age, respectively.

Figure 5.6

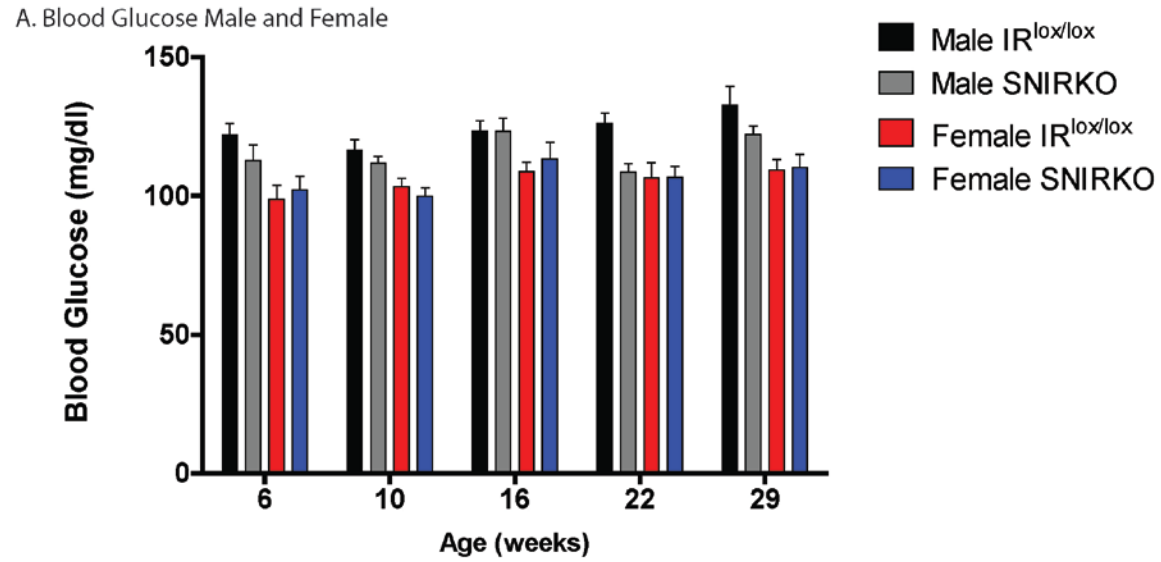
A. Blood Glucose Male and Female
Male IR lox/lox
Male SNIRKO
Female IR lox/lox
Female SNIRKO
Blood Glucose (mg/dl)
150
100
50
0
6
10
16
22
29
Age (weeks)

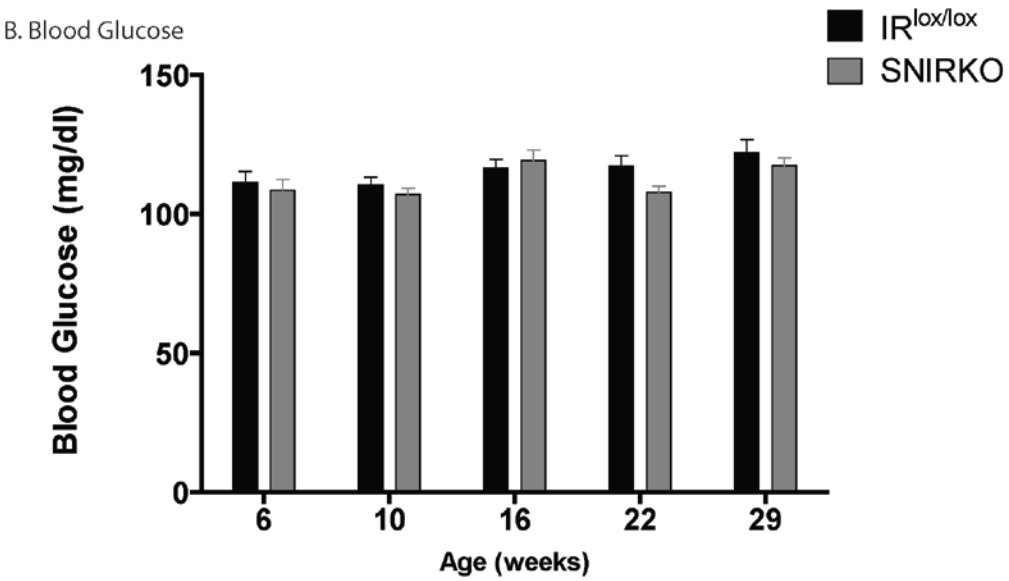
B. Blood Glucose
IR lox/lox
SNIRKO
Blood Glucose (mg/dl)
150
100
50
0
6
10
16
22
29
Age (weeks)

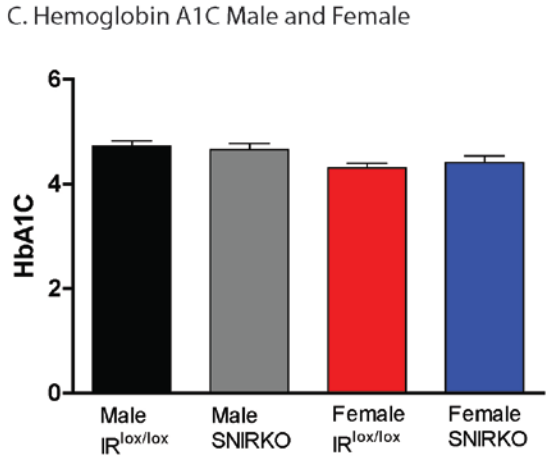
C. Hemoglobin A1C Male and Female
HbA1C
6
4
2
0
Male IR lox/lox
Male SNIRKO
Female IR lox/lox
Female SNIRKO

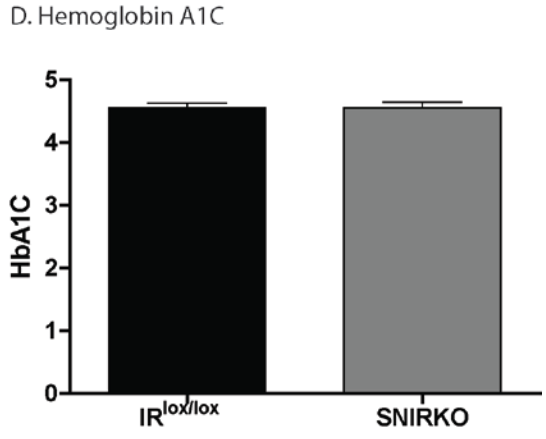
D. Hemoglobin A1C
HbA1C
5
4
3
2
1
0
IR lox/lox
SNIRKO

Figure 5.6. SNIRKO mice are euglycemic. Blood glucose levels were measured at 6, 10, 16, 22, and 28 weeks of age. Results were analyzed with a repeated measures 2-way ANOVA and Bonferroni's post-hoc. No significant differences were observed between male or female $IR^{lox/lox}$ and SNIRKO mice (A). Female mice independent of group did have significantly lower blood glucose levels than male mice (not denoted on the figure). n=12 $IR^{lox/lox}$ male, n=14 SNIRKO male, n=10 $IR^{lox/lox}$ female, and n=9 SNIRKO female. Furthermore, no significant difference was observed when data from males and females was combined (B). n=22 $IR^{lox/lox}$ and n=23 SNIRKO. Hemoglobin A1C levels were measured at 29 weeks of age. There were no significant differences noted in males or females between $IR^{lox/lox}$ and SNIRKO groups (C) or when data from females and males was combined (D). Results were analyzed with a 2-way ANOVA and Bonferroni's post-hoc (C) and student's t-test (D).

Table 5.2

Activity Measured	Male $IR^{lox/lox}$	Male SNIRKO	Female $IR^{lox/lox}$	Female SNIRKO
Distance Traveled(mm)	168707 ± 9840	174360 ± 14964	170640 ± 12205	167738 ± 15392
% Distance in perimeter	59.7 ± 4.1	69.7 ± 4.7	60.3 ± 4.6	63.3 ± 4.3
Bouts of Low Mobility	0.86 ± 0.39	1.43 ± 0.80	0.3 ± 0.15	0.11 ± 0.11
Area Measure	154779 ± 15228	160258 ± 17054	169889 ± 18957	152376 ± 20891
Spatial Statistic	28.5 ± 0.95	30.1 ± 1.74	25.9 ± 1.06	26.5 ± 1.10
Focused Stereotypy	0.25 ± 0.03	0.27 ± 0.02	0.20 ± 0.02	0.18 ± 0.03

Table 5.2. SNIRKO Mice do not have significant differences in activity behaviors assessed by force plate actometer. Force plate actometer is capable of precisely determining several behaviors related to activity and repetitive motion. All the behaviors assessed are listed and no significant difference was noted in any behavior. Results were analyzed with a 2-way ANOVA and Bonferroni's post-hoc. n=14 $IR^{lox/lox}$ male, n=14 SNIRKO male, n=10 $IR^{lox/lox}$ female, and n=9 SNIRKO female. The perimeter was defined as the outside 2 rows of squares when the force plate was divided into a grid of 16 by 16 squares. A bout of low mobility was defined as no movement outside a 15.0 mm radius for 10.24 seconds. Area measure is the amount of area covered by the mouse during 1 frame. The spatial statistic is an indication of the activity distribution across the actometer. A high spatial statistic indicates little movement around the actometer and a low spatial statistic indicates extensive of movement throughout the actometer. The focused stereotypy score is an indication of time spent doing repetitive motions.

Figure 5.7

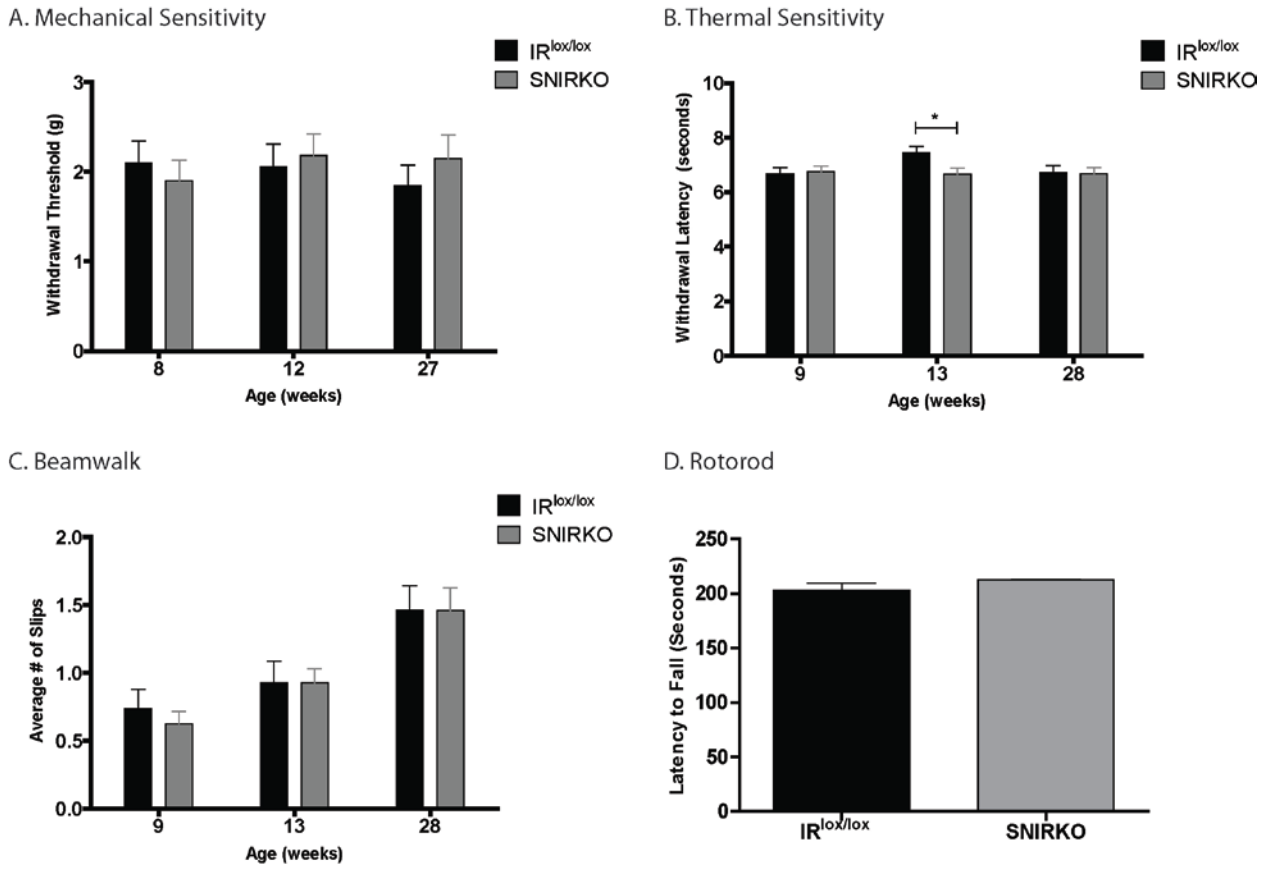
A. Mechanical Sensitivity
IRlox/lox
SNIRKO
Withdrawal Threshold (g)
3
2
1
0
8
12
27
Age (weeks)
B. Thermal Sensitivity
IRlox/lox
SNIRKO
Withdrawal Latency (seconds)
10
8
6
4
2
0
*
9
13
28
Age (weeks)
C. Beamwalk
IRlox/lox
SNIRKO
Average # of Slips
2.0
1.5
1.0
0.5
0.0
9
13
28
Age (weeks)
D. Rotorod
Latency to Fall (Seconds)
250
200
150
100
50
0
IRlox/lox
SNIRKO

Figure 5.7. SNIRKO mice do not display sensorimotor deficits characteristic of DN in murine models. It was hypothesized that the reduction in sensory neuron insulin signaling despite euglycemia would produce a phenotype similar to DN in mouse models. Similar patterns were observed across males and females between groups and data presented here is combined from males and females. No significant difference between $IR^{lox/lox}$ and SNIRKO was observed in mechanical sensitivity (A). For thermal sensitivity there was no significant difference of group between $IR^{lox/lox}$ and SNIRKO mice upon analysis with 2-way repeated measures ANOVA (B). However, Bonferroni's post-hoc does show a significant difference between $IR^{lox/lox}$ and SNIRKO mice at 13 weeks of age. Of note, the thermal threshold for SNIRKO mice appears to remain relatively constant throughout the time period tested, yet $IR^{lox/lox}$ mice show an increase in threshold at 13 weeks. No significant difference between $IR^{lox/lox}$ and SNIRKO mice was observed in beamwalk (C) or rotorod (D). Mechanical sensitivity, thermal sensitivity, and beamwalk were analyzed with a repeated measures 2-way ANOVA and Bonferroni's post-hoc. Rotorod was analyzed with a student's t-test. n=24 $IR^{lox/lox}$ and n=23 SNIRKO. *=$p<0.05$.

Two additional tests were performed to assess motor coordination and balance/proprioception (large fiber). SNIRKO mice showed no significant difference in the number of foot slips during beamwalk analysis (Figure 5.7 C) or in the latency to fall during rotorod analysis (Figure 5.7 D).

These results indicate that SNIRKO mice do not appear to have similar sensorimotor deficits to that seen in rodent models of DN.

SNIRKO mice do not show morphologic or physiologic changes as seen in DN:

DN neuropathy is characterized as a "dying back" neuropathy. This can be quantified by assessing the density of epidermal nerve fibers in the hindpaw footpad (IENF). Rodent models of DN display reduced IENF density [280]. SNIRKO mice do not have significantly different IENF density as compared to $IR^{lox/lox}$ (Figure 5.8 A-C).

The gold standard for diagnosing DN in human patients is electrophysiological changes [89]. Reduced NCV can also be observed in rodent models of DN [280]. SNIRKO mice show no significant difference in either SNCV or MNCV (Figure 5.8 D and E, respectively).

SNIRKO mice do not have a significant upregulation of the IGF-1 pathway:

A common caveat of transgenic knockout models is compensation through an alternate pathway. Due to strong overlap of intracellular signaling between insulin and IGF-1 and that IGF-1 is known to be a neurotrophic factor for sensory neurons [176], we reasoned that one of the most likely pathways that may be upregulated to compensate for reduced insulin signaling in sensory neurons was the IGF-1 pathway. However, no significant difference in serum IGF-1 levels (Figure 5.9 A) or IGFR protein levels in the DRG (Figure 5.9 B) were observed.

Figure 5.8

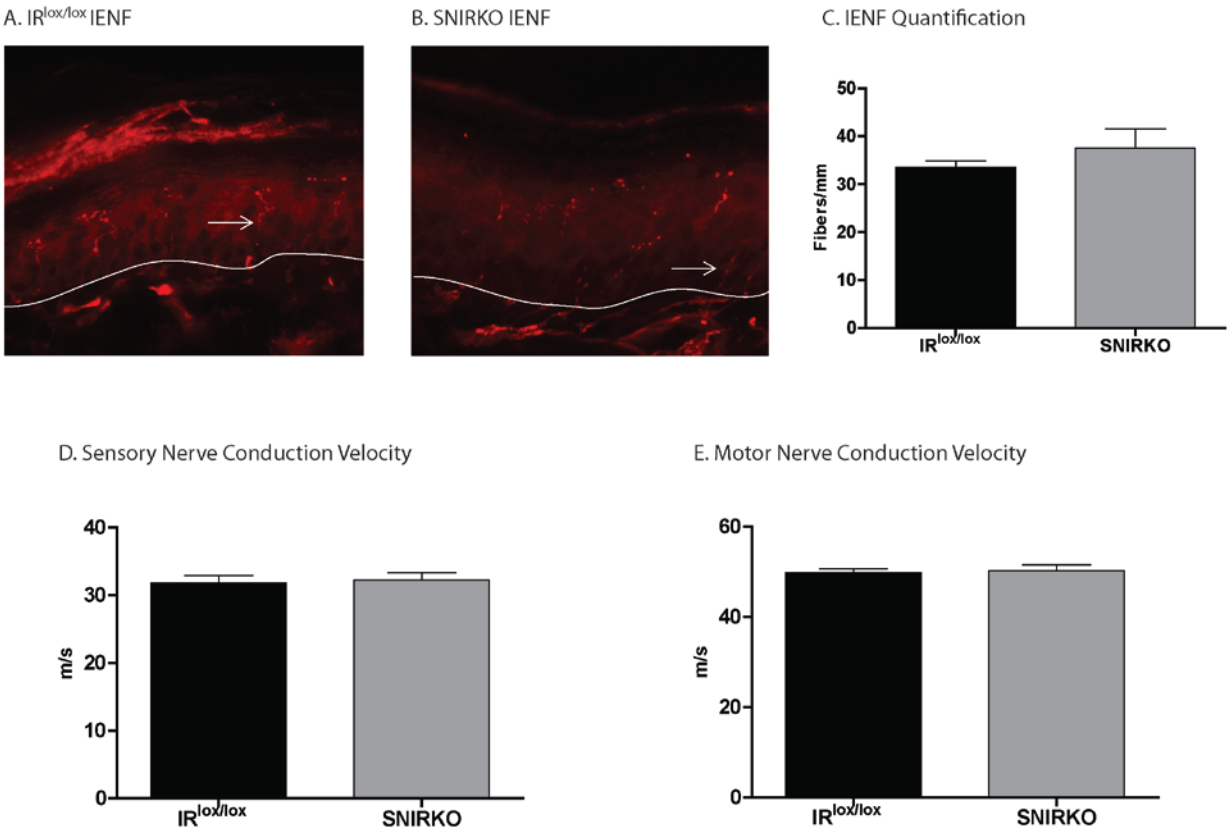
A. IR lox/lox IENF
B. SNIRKO IENF
C. IENF Quantification
Fibers/mm
50
40
30
20
10
0
IR lox/lox
SNIRKO
D. Sensory Nerve Conduction Velocity
m/s
40
30
20
10
0
IR lox/lox
SNIRKO
E. Motor Nerve Conduction Velocity
m/s
60
40
20
0
IR lox/lox
SNIRKO

Figure 5.8. SNIRKO mice do not show morphological or physiological changes characteristic of DN in murine models. Two characteristic signs of DN in mice are decreased IENF and reduced NCV. Nerve fibers (arrows) that cross the dermal-epidermal border (white line) were quantified in both $IR^{lox/lox}$ (A) and SNIRKO mice (B). No significant differences were noted (C). Results were analyzed with a student's t-test. n=4 $IR^{lox/lox}$ and n=4 SNIRKO. In addition, no differences were observed in either SNCV (D) or MNCV (E). Results were analyzed with a student's t-test. n=24 $IR^{lox/lox}$ and n=23 SNIRKO.

Figure 5.9

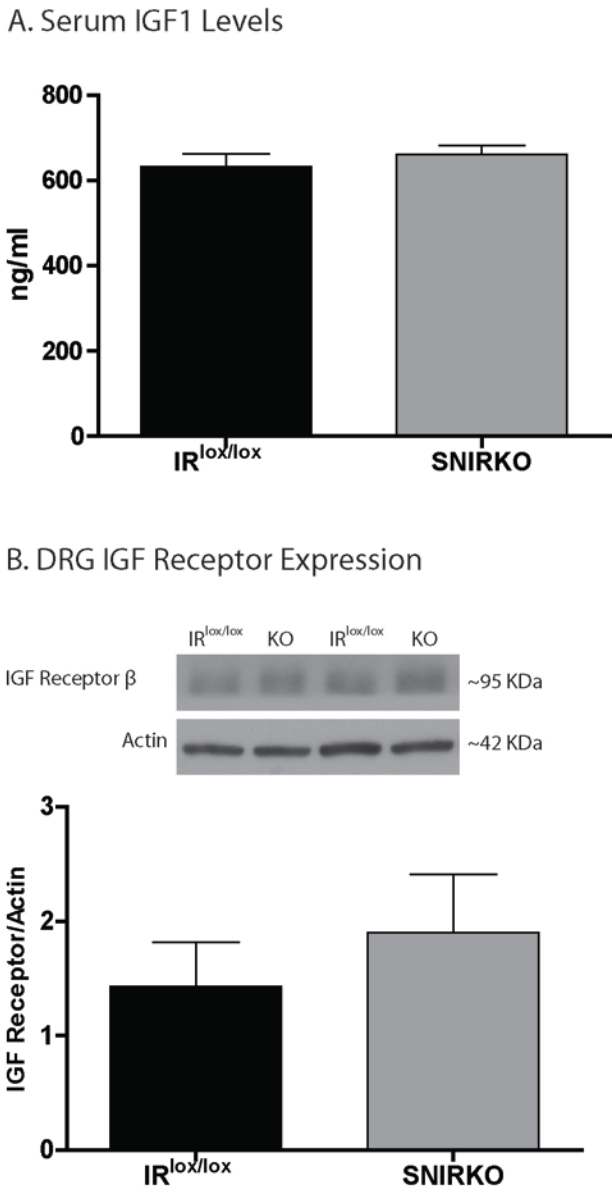
A. Serum IGF1 Levels
800
600
400
200
0
ng/ml
IR lox/lox
SNIRKO
B. DRG IGF Receptor Expression
IR lox/lox
KO
IR lox/lox
KO
IGF Receptor β
~95 KDa
Actin
~42 KDa
3
2
1
0
IGF Receptor/Actin
IR lox/lox
SNIRKO

Figure 5.9. The IGF1 pathway is not significantly upregulated in SNIRKO mice. One possible compensation pathway in SNIRKO mice is the IGF1 pathway. Here, IGF1 serum levels and IGF receptor expression levels in the DRG were assessed. No significant differences were observed between $IR^{lox/lox}$ and SNIRKO mice for either variable. Results were analyzed with a student's t-test. n=20 $IR^{lox/lox}$ and n=20 SNIRKO for IGF1 serum ELISA and n=14 $IR^{lox/lox}$ and n=10 SNIRKO for IGF receptor Western blot analysis.

SNIRKO mice display significantly elevated serum insulin levels and glucose intolerance:

A surprising observation made throughout the course of these studies was that SNIRKO mice displayed significantly elevated serum insulin levels (Figure 5.10). The difference between $IR^{lox/lox}$ and SNIRKO mice appeared to increase during the course of the testing period as well. For comparison, $IR^{lox/lox}$ mice had serum insulin levels of 0.93 ng/mL at 6 weeks of age and 1.00 ng/mL at 29 weeks of age. SNIRKO mice had serum insulin levels of 1.14 ng/mL at 6 weeks of age and 2.03 ng/mL at 29 weeks of age. Furthermore, when subjected to an IPGTT, SNIRKO mice maintained significantly higher blood glucose levels throughout the experiment (Figure 5.11 A and B) resulting in significantly different areas under the curve (AUC) between $IR^{lox/lox}$ and SNIRKO mice; suggesting that SNIRKO mice may show signs of hyperinsulinemia-induced insulin resistance.

These results suggest an interesting hypothesis in that sensory neuron insulin signaling plays a crucial role in regulating systemic insulin levels and glucose tolerance.

Proposed mechanism of the sensory neuron's role in beta cell modification:

In 2005 Razavi et. al. demonstrated that TRPV1 positive sensory neurons are critically involved in the pathogenesis of type 1 diabetes in non-obese diabetic (NOD) mice. NOD mice express a hypofunctional TRPV1 and it was demonstrated that embryological ablation of TRPV1 with capsaicin or substance P treatment could correct insulitis and diabetes in NOD mice [38]. Based on these observations, Tsui et. al proposed a mechanism of beta cell regulation via negative feedback of insulin signaling on sensory neurons (Figure 5.12, modified from [283]). TRPV1 stimulation results in the release of the neuropeptide substance P. Substance P plays an important role in regulating insulin production. It has previously been demonstrated that insulin may sensitize TRPV1 [34, 35]. Thus, in the NOD mouse which has a mutant TRPV1 receptor, there is a reduced release of substance P, resulting in an increase in insulin release from pancreatic beta cells in an effort to further sensitize TRPV1 and release more substance P (Figure 5.12 B). It is proposed that this results in beta cell stress and autoimmune attack. The observation that SNIRKO mice display hyperinsulinemia fits surprisingly well into this model. Whereas removal of

Figure 5.10

A. Serum Insulin Levels Male and Female

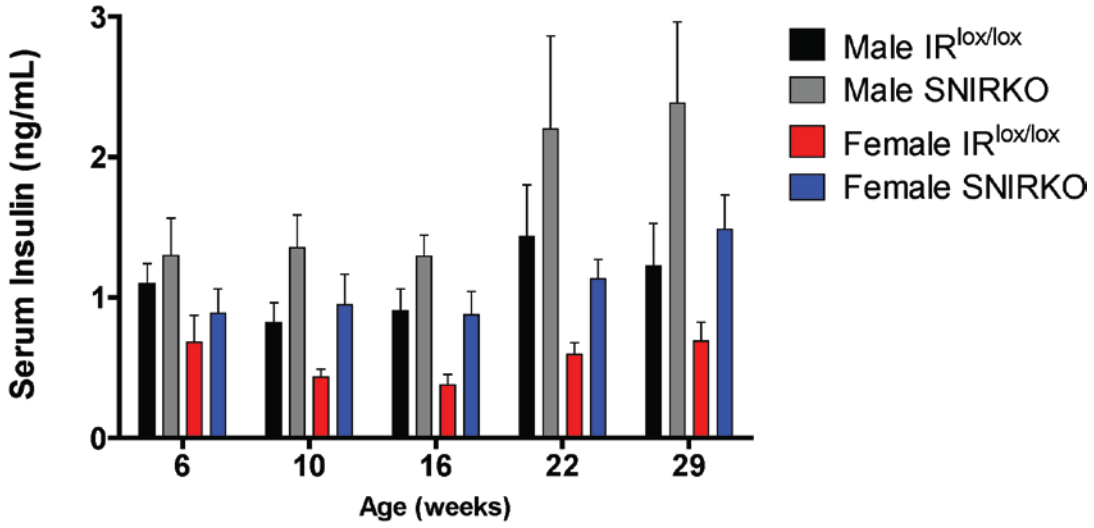

B. Serum Insulin Levels

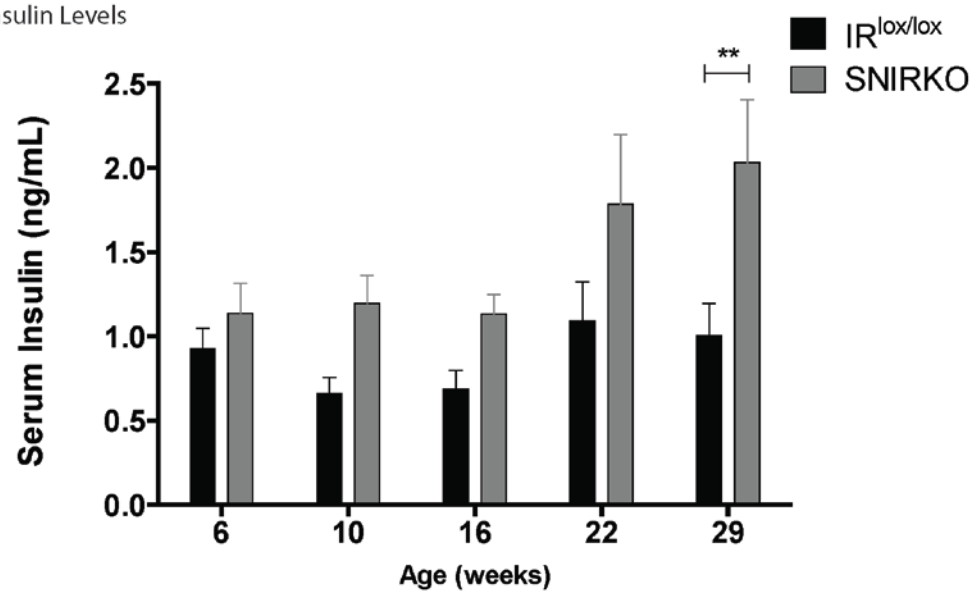

Figure 5.10. SNIRKO mice have significantly elevated serum insulin levels. Despite a conditional knockout of the insulin receptor specifically in sensory neurons, SNIRKO mice present with a systemic increase in serum insulin levels. A) A similar pattern of increased insulin levels in SNIRKO mice was observed between males and female throughout the experiment. n=12 $IR^{lox/lox}$ male, n=14 SNIRKO male, n=10 $IR^{lox/lox}$ female, and n=9 SNIRKO female. B) Combined male and female insulin data shows a significant main effect of group ($IR^{lox/lox}$ vs. SNIRKO) upon analysis with repeated measures 2-way ANOVA ($p=0.036$). Bonferroni's post-hoc indicates a significant difference at 29 weeks of age. n=22 $IR^{lox/lox}$ and n=23 SNIRKO. **=$p<0.01$.

Figure 5.11

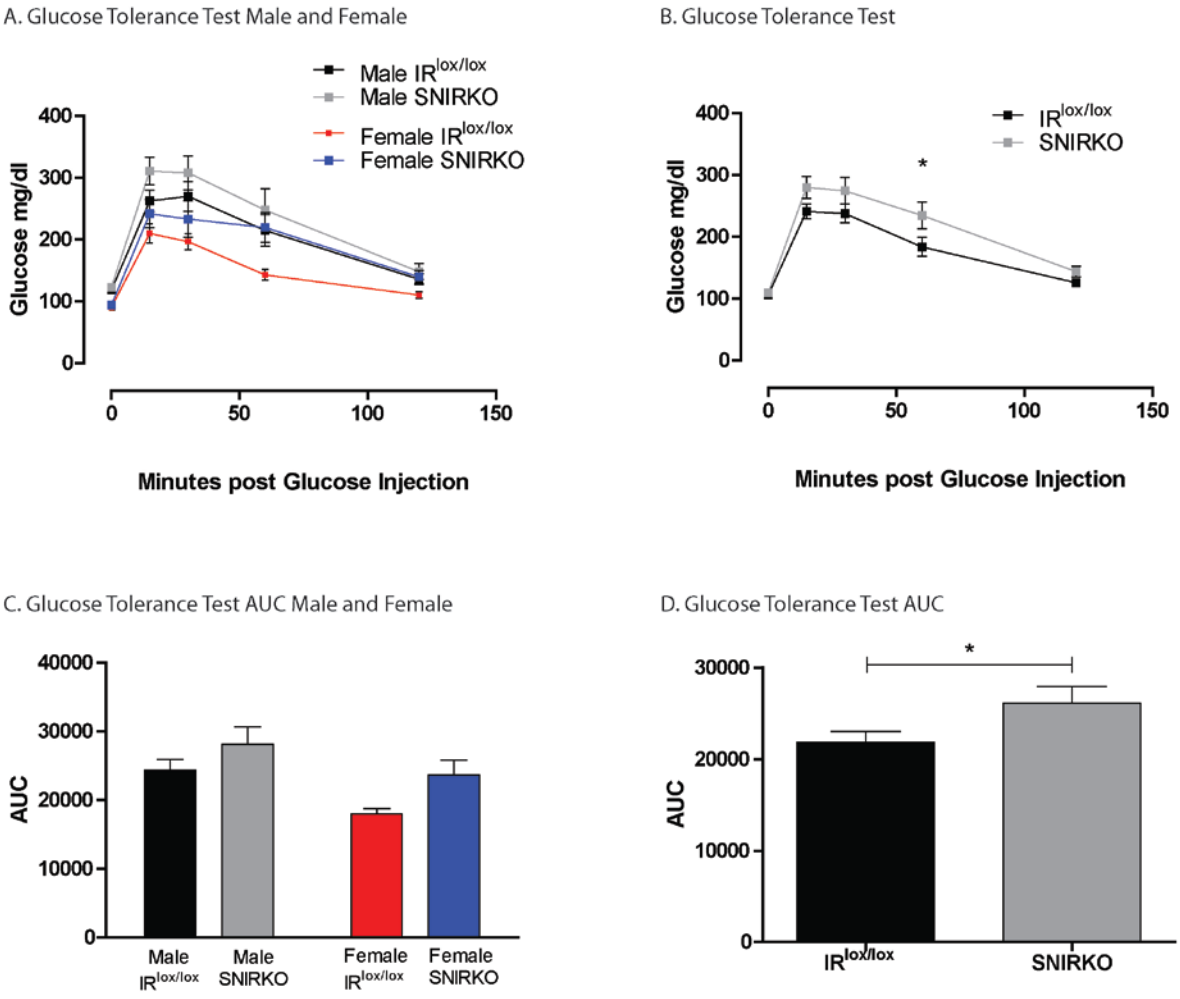
A. Glucose Tolerance Test Male and Female
Male IR lox/lox
Male SNIRKO
Female IR lox/lox
Female SNIRKO
Glucose mg/dl
400
300
200
100
0
0
50
100
150
Minutes post Glucose Injection
B. Glucose Tolerance Test
IR lox/lox
SNIRKO
*
Glucose mg/dl
400
300
200
100
0
0
50
100
150
Minutes post Glucose Injection
C. Glucose Tolerance Test AUC Male and Female
AUC
40000
30000
20000
10000
0
Male IR lox/lox
Male SNIRKO
Female IR lox/lox
Female SNIRKO
D. Glucose Tolerance Test AUC
*
AUC
30000
20000
10000
0
IR lox/lox
SNIRKO

Figure 5.11. SNIRKO mice display glucose intolerance. Elevated insulin levels are capable of producing signs of insulin resistance and glucose intolerance. $IR^{lox/lox}$ and SNIRKO mice were subjected to an IPGTT. Male and female SNIRKO mice show elevated glucose levels above $IR^{lox/lox}$ mice of the same sex (A). A combination of data from male and female mice shows that SNIRKO mice appear to maintain elevated glucose level throughout the IPGTT (B). Analysis with a 2-way repeated measure ANOVA indicates the p-value for group ($IR^{lox/lox}$ vs. SNIRKO) was 0.054. Bonferroni's post-hoc indicates at significant difference at 60 minutes post glucose injection. Calculation of the area under the curve (AUC) shows that male and female SNIRKO mice once again show similar patterns as compared to $IR^{lox/lox}$ mice (C) and the AUC was significantly elevated in SNIRKO mice as compared to $IR^{lox/lox}$ when data from male and females was combined. Results were analyzed with a student's t-test. n=20 $IR^{lox/lox}$ and n=18 SNIRKO. *=$p<0.05$.

Figure 5.12

A. Normal Physiological Condition

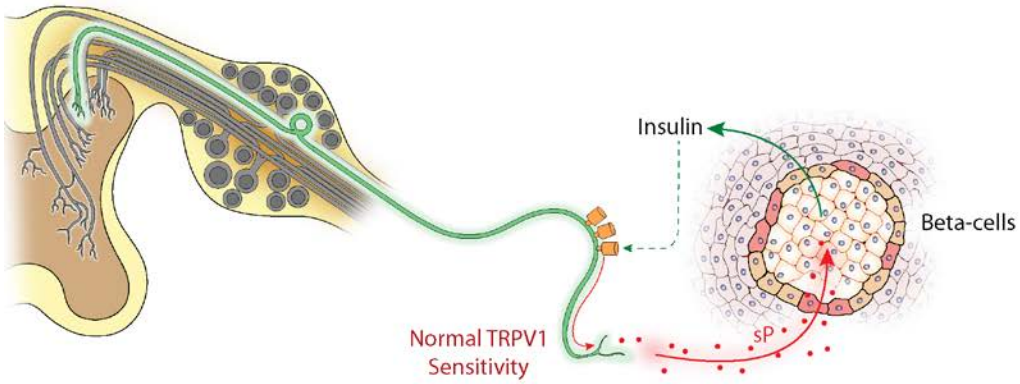

B. NOD mice with hypofunctional TRPV1

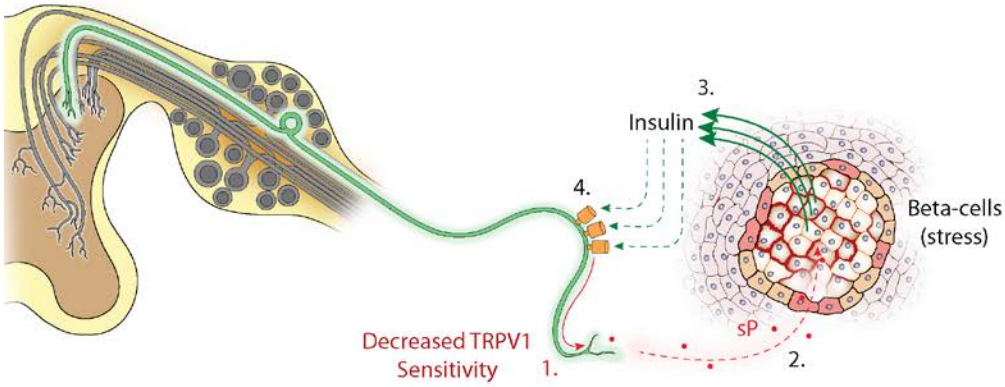

C. SNIRKO mice with disrupted sensory neuron insulin signaling

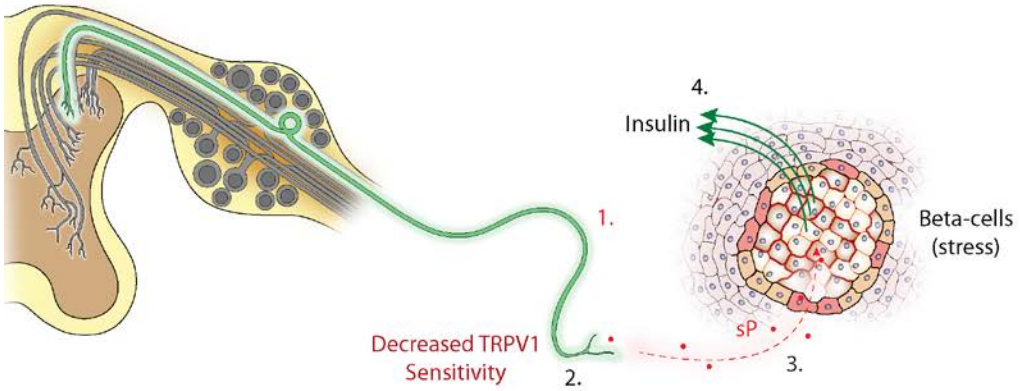

Figure 5.12. Proposed feedback mechanism between sensory neuron insulin signaling and beta cell function. A) Under normal physiologically conditions there is a finely tuned feedback mechanism between sensory neuron insulin signaling, TRPV1 sensitivity and neuropeptide release, and beta cell insulin production. B) In NOD mice, there is a primary defect in TRPV1 function (1), resulting in decreased substance P release (2). Due to decreased substance P support beta cells increase insulin production (3) in an effort to lower TRPV1 sensitivity and release more substance P via sensory neuron insulin signaling (4). This results in beta cell stress and in the autoimmune susceptible environment of NOD mice, diabetes. C) SNIRKO mice have a primary defect of reduced insulin receptor signaling (1) resulting in altered TRPV1 sensitivity (2) and reduced substance P release (3). Similar to young NOD mice, beta cells attempt to compensate for reduced neuropeptide signaling by increasing production of insulin (4), thus producing hyperinsulinemia in SNIRKO mice. Mechanism and figure adapted from Tsui et. al. [283]. Illustration by Stanton Fernald.

sensory neuron insulin receptors prevents sensitization of TRPV1, reducing the amount of substance P release, and causing the overproduction/release of insulin from beta cells in an effort to compensate (Figure 5.12 C). Based on these observations, preliminary studies were conducted to test these hypotheses in SNIRKO mice.

Pancreatic islets from SNIRKO mice show normal morphology, no insulitis, yet increased insulin content:

The proposed model suggests that the primary defect causing hyperinsulinemia in SNIRKO mice would be overproduction of insulin by the pancreatic beta cells. Beta cells are insulin producing cells of the pancreas and are located in the islets of Langerhans. The islets of Langerhans have a predictable morphology of centrally located beta cells surrounded by glucagon producing alpha cells and somatostatin producing delta cells. The islets of Langerhans are extensively vascularized [284] and innervated by both autonomic [285] and sensory nerves [282]. SNIRKO mice show no significant changes in islet morphology or cell composition as compared to $IR^{lox/lox}$ mice (Figure 5.13). Large islets have been demonstrated to have poorer function than small islets [286]. Islet size was quantified in $IR^{lox/lox}$ and SNIRKO mice, but no significant differences were noted (data not shown). Finally, insulitis (islet inflammation) and insulin content was assessed using immunohistochemistry. Based on the proposed model it was expected that SNIRKO mice would have mild insulitis resulting from increased beta cell stress. SNIRKO mice do not show signs of islet lymphocyte infiltration, which would have been noted by cells with small, densely stained nuclei (figure 5.14). However, islets for SNIRKO mice do display increased insulin content (Figure 5.14), consistent with proposed model.

SNIRKO mice do not show TRPV1 protein changes in lumbar DRG:

Unlike NOD mice, SNIRKO mice do not display decreased TRPV1 DRG expression (Figure 5.15). It should be noted that lumbar DRG were used for these experiments and that DRG sensory neurons that innervate the pancreas arise from DRG T9-T12, thus those DRG may have different expression profiles. Furthermore, TRPV1 electrophysiological parameters still need to be determined.

Figure 5.13

A. $IR^{Lox/lox}$ Islet of Langerhans

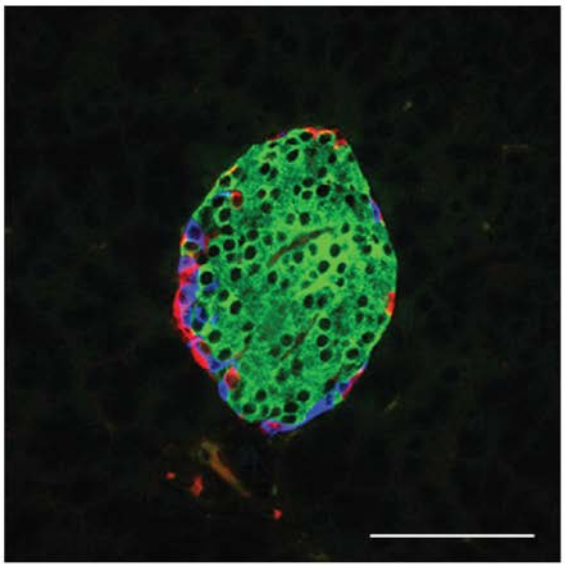

B. SNIRKO Islet of Langerhans

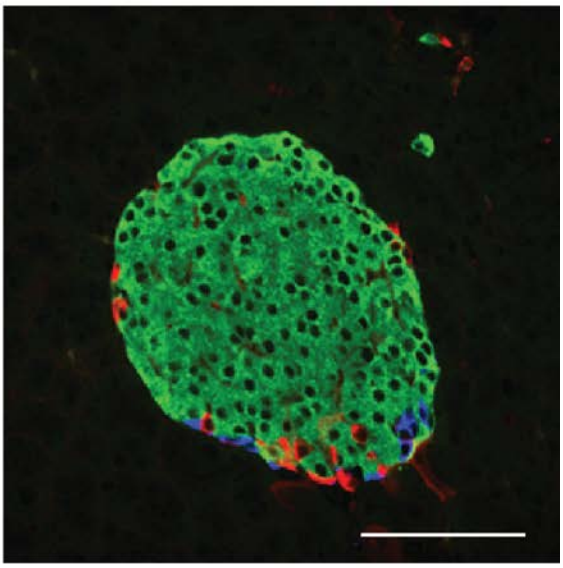

C. Quantification of Islet Composition

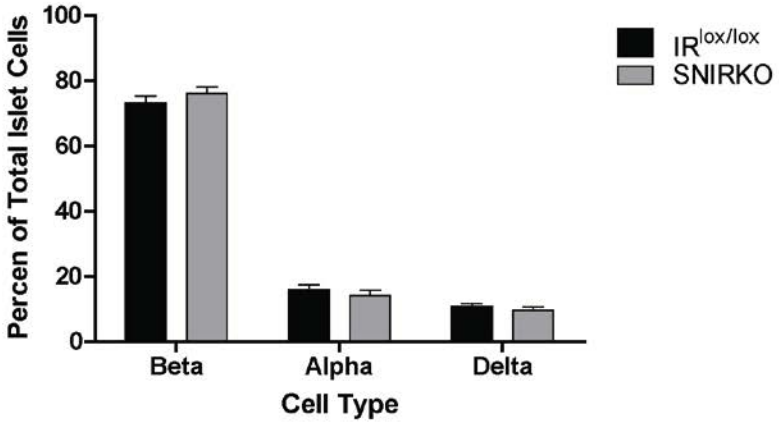

Figure 5.13. SNIRKO islet of Langerhans cell composition. Endocrine cells of the islets of Langerhans were labeled (green=beta cells, red=alpha cells, blue=delta cells) and cell composition was quantified (C). $IR^{lox/lox}$ (A) and SNIRKO (B) mice display similar islet of Langerhans cell composition, with no significant difference between beta, alpha, or delta cells. Data was analyzed with a 1-way nested ANOVA on ranks and Dunn's pairwise comparison. 42 islets from 3 $IR^{lox/lox}$ mice and 45 islets from 3 SNIRKO mice were analyzed.

Figure 5.14

A. $IR^{Lox/lox}$ Islet of Langerhans

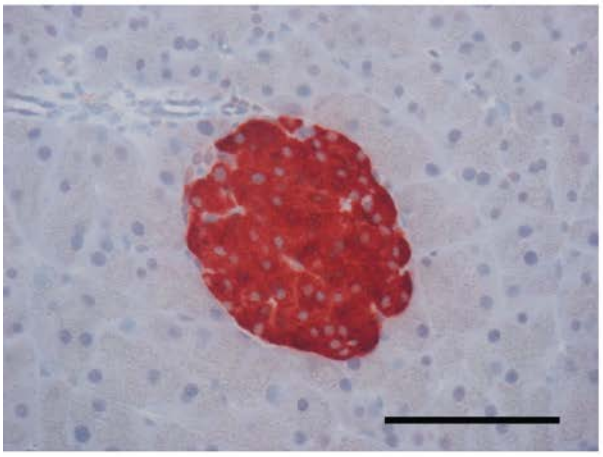

B. SNIRKO Islet of Langerhans

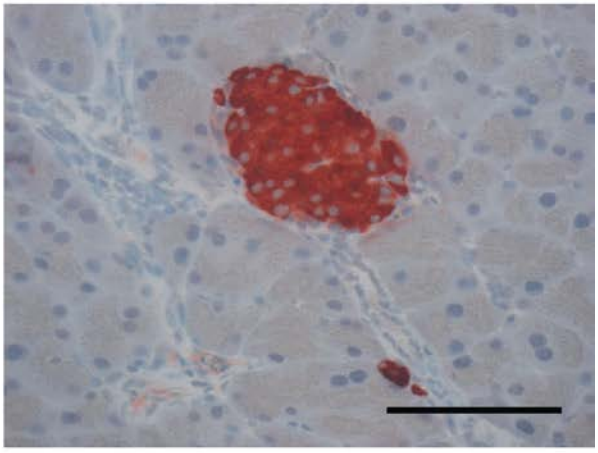

C. Quantification of Islet Insulin Content

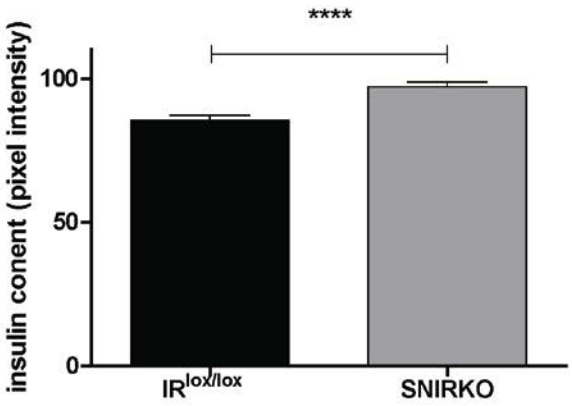

Figure 5.14. Islets of Langerhans from SNIRKO mice have increased insulin content and no lympocytic infiltrate. Insulitis was analyzed by assessing samples stained with hematoxylin for immune cell infiltration. No significant insulitis was observed in either islets from $IR^{lox/lox}$ (A) or SNIRKO (B) mice. Islet insulin content was analyzed be quantifying insulin staining intensity. Islets from SNIRKO mice have significantly elevated insulin content as compared to islets from $IR^{lox/lox}$ mice (C). Results were analyzed with a student's t-test. n=45 islets from 3 $IR^{lox/lox}$ mice and n=33 islets from 3 SNIRKO mice.

Figure 5.15

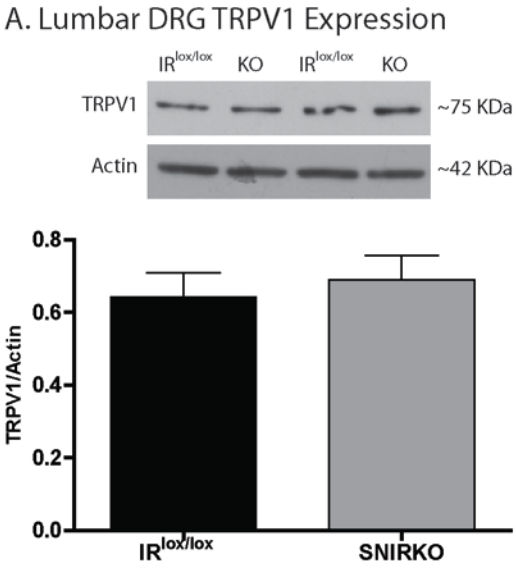
A. Lumbar DRG TRPV1 Expression
IRlox/lox
KO
IRlox/lox
KO
TRPV1
~75 KDa
Actin
~42 KDa
TRPV1/Actin
0.8
0.6
0.4
0.2
0.0
IRlox/lox
SNIRKO

Figure 5.15. SNIRKO mice do not have significantly altered lumbar DRG TRPV1 expression. An observation made in NOD mice that connected insulin signaling, pancreas function, and sensory neurons was a mutation in TRPV1. In addition to a mutation in TRPV1, protein levels were shown to be decreased in NOD mice [38]. No significant difference in DRG TRPV1 expression was observed between $IR^{lox/lox}$ and SNIRKO mice. Results were analyzed with a student's t-test. n=15 $IR^{lox/lox}$ and n=12 SNIRKO.

5.5 Discussion

While several studies have demonstrated the neurotrophic potential of insulin and suggested that reduced sensory neuron insulin support may be a major contributor to the pathogenesis of diabetic neuropathy, a model to specifically test sensory neuron insulin signaling *in vivo* without changes in other variables has been lacking. Here, we developed sensory neuron insulin receptor knockout mice to help better understand the role that insulin signaling plays in sensory neuron function. While the insulin receptor has been the target of several conditional knockouts, including the muscle [131], liver [136], pancreas [135], and central nervous system [137], these are the first mice to have a conditional knockout of the insulin receptor in sensory neurons. SNIRKO mice showed a tissue-specific decrease in DRG insulin receptor expression and reduced DRG insulin signaling, yet remained euglycemic.

SNIRKO mice do not show behavioral, physiological, or morphological signs of DN. Thus it appears that without hyperglycemia, a reduction in sensory neuron insulin signaling does not contribute to manifestations of neuropathy. Several possibilities may contribute to this result and they are discussed below.

1) While in primary culture, at supraphysiologic doses, or with direct administration to the nervous system insulin may act as a neurotrophic factor, it may be that under normal physiological conditions insulin does not provide support to the PNS. Perhaps the large fluctuations in insulin levels throughout the day in response to glucose intake makes it unsuitable for support of sensory neurons, which need to maintain a tonically high metabolic rate in order to support the distal axon and tightly maintain electrochemical gradients. Furthermore, although it does appear that there are non-glycemic mechanisms contributing to DN, the most effective treatment for prevention of DN is strict glycemic control, suggesting that hyperglycemia is the main driving force of DN pathogenesis.

2) In relation to hyperglycemia being the primary insult in DN; perhaps the PNS can function normally without insulin support in the absence of neuronal injury. Such that, the repair/regeneration of peripheral nerves is blunted and it is this loss of neurotrophic support during injury that contributes to DN. In support of this model is the repeated evidence indicating that insulin can promote nerve

regeneration after injury [174, 185]. Accordingly, SNIRKO mice may only show a difference in behavior or morphology after neuronal injury. Future experiments using models of nerve injury, such as nerve crush and spared nerve injury, as well as models using noxious agents such as formalin, complete Freund's adjuvant (CFA), and capsaicin are needed test this hypothesis.

3) It also possible that the behavioral tests used to assess the sensorimotor function in SNIRKO mice was not appropriate. For example, von Frey filaments assess mechanical allodynia (painful response to a non-painful stimulus), not hyperalgesia (an exaggerated response to a painful stimulus). If DN neuropathy is the result of reduced PNS insulin signaling and glucose neurotoxicity, it may be that deficits in only one area produce milder neuropathy (i.e. hyperalgesia as compared to allodynia). Thus, test of hyperalgesia, such as pin prick, Randal-Stilleto, colorectal distension, or the use of noxious agents (formalin, CFA, or capsacin) may delineate the differences between $IR^{lox/lox}$ and SNIRKO mice. Future studies are aimed at including these additional tests to fully characterize the sensorimotor function of SNIRKO mice.

4) An additional factor that may have contributed to the observed results is that SNIRKO mice do not perfectly model the reduced PNS insulin support present in diabetes. In diabetes, there is a global reduction in insulin support (reduced circulating levels or reduced signaling), such that not only will sensory neurons of the PNS have reduced insulin support, but so will the Schwann cells and satellite glia cells that also express insulin receptors [170]. Thus, while SNIRKO mice have reduced insulin support to sensory neurons, they should not have reduced insulin signaling in glia cells, which may confound the results. Based on these observations, a better model of reductions in PNS insulin support may be to knockout the insulin receptor in all cells of the PNS. Future studies are going to incorporate mice that specifically express cre recombinase in Schwann cells using the glycoprotein P 0 promoter with the goal of eventually having cre expression in both sensory neurons and Schwann cells simultaneously.

Along these same lines, SNIRKO mice would have a sensory neuron insulin receptor knockout early in development (Advillin is expressed at E12.5 [274]). Insulin has been documented to have an important role in central nervous system development [169], and it was recently demonstrated that IRS2

knockout mice have reduced trkA positive neurons and alterations in thermal sensitivity [287]. SNIRKO mice do not appear to have developmental defects, indicating that insulin may not be crucial developmental neurotrophic factor for sensory neurons. Thus, the changes in IRS2 knockout mice are most likely the result of reductions in signaling from several different growth factors as IRS2 is a docking protein involved in transduction of several different signaling pathways, not just insulin [236]. Nevertheless, neuronal development without insulin signaling may cause adaptations or subtle changes in set points that may cloud the results and a complete quantification of DRG sensory neuron composition needs to be completed. A better model of reduced sensory neuron insulin signaling post development would be to use an inducible-cre recombinase. This would better mimic the loss of mature sensory neuron insulin signaling in diabetic patients. Unfortunatley, tamoxifen inducible Advillin$^{cre/+}$ mice only show cre activation in about 20% of sensory neurons (personal communication with Dr. Fan Wang).

5) Finally, it is recognized that additional, uninvestigated pathways may be upregulated and compensating for the lack of sensory neuron insulin support. Beyond IGF-1, several other neurotrophins have signaling pathways similar to insulin, including NGF [13]. In fact, it was this observation that first indicated insulin may be a neurotrophic factor. Insulin has also been shown to promote neurotrophin actions [178]. Additional experiments are required to investigate other neurotrophic pathways.

An intriguing observation from these studies was the elevated insulin levels of SNIRKO mice. These results are consistent with recent publications indicating that the efferent actions of sensory neurons modify beta cell insulin production/release via a negative feedback mechanism [38, 283]. This also establishes a novel function for insulin signaling in sensory neurons beyond the neurotrophic effects that were previously discussed. Insulin signaling in sensory neurons may serve to help regulate systemic metabolism. Two possibilities through which sensory neuron insulin signaling may be affecting serum insulin levels are discussed below.

1) Sensory neuron insulin signaling modifies beta cell insulin production/release based on the model proposed by Ravazi et. al. [38]. Several studies have demonstrated that insulin can sensitize and potentiate TRPV1 signaling by lowering the threshold for activation and increasing membrane

translocation [34, 35, 288]. With the high concentration of insulin in the islet milieu it was recently proposed that TRPV1 would be tonically activated resulting in constant release of the neuropeptides CGRP and substance P [289]. CGRP and substance P are canonically considered to be potent proinflammatory regulators. However, these neuropeptides have also been demonstrated to have a trophic effect on beta cells [283, 290, 291] and treatment with CGRP and/or substance P causes normalization of insulin secretion and resolution of diabetes [38, 292]. It was also recently reported that capsaicin treatment can significantly reduce blood glucose levels in a mouse model of late phase type 1 diabetes [293]. Moreover, treatment with capsaicin and a capsaicin analog, resiniferatoxin, was shown to improve glucose homeostasis by increasing insulin secretion in type 2 diabetic Zucker rats [294, 295].

Unfortunately, until now, the involvement of sensory neuron insulin signaling in this model could not be directly tested. Prediabetic NOD mice display hyperinsulinemia which is thought to be due to dysfunctional TRPV1 and neuropeptide release [38, 296]. SNIRKO mice also demonstrate hyperinsulinemia as well as increased islet insulin content. In line with the recent understanding of the importance of insulin signaling in TRPV1 sensitivity and the role of neuropeptides in beta cell function, we postulate that hyperinsulinemia in SNIRKO mice is the result of altered TRPV1 sensitivity and altered local islet neuropeptide regulation of beta cells. The demonstration that multiple interventions associated with the insulin-TRPV1-neuropeptide-diabetes model results in similar and predictable outcomes is strong support for the existence of such a system *in vivo.* Several experiments remain to further investigate this hypothesis in SNIRKO mice. Specifically, it will be important to analyze the neuropeptide levels of islets and the innervating sensory neurons as well as assess the sensitivity of TRPV1. Additionally, a key proof of concept experiment will be to determine if CGRP and/or substance P treatment can reverse the observed hyperinsulinemia in SNIRKO mice.

2) Another previously unconsidered possibility that may contribute to elevated serum insulin levels in SNIRKO mice is a reduced insulin utilization or breakdown in the periphery. This may arise from 2 separate possibilities. First, a local system similar to that described in the islet involving insulin signaling, TRPV1 sensitivity, and neuropeptide release, may also be a factor in peripheral tissues. TRPV1

has been demonstrated to be an important factor in obesity, insulin resistance, and type 2 diabetes (reviewed in [297, 298]). In fact, TRPV1 null mice display resistance to diet-induced obesity and increased insulin sensitivity [38, 299].

Secondly, sensory neurons may act as a "sensor" for systemic insulin levels in the periphery. A subpopulation of "glucose sensing" sensory neurons was recently identified in the nodose ganglia [300, 301]. This novel population of neurons projects centrally to the nucleus tractus solitarius (NTS) in the medulla, a key area for integrating the afferent information from baroreceptors and chemoreceptors "sensing" blood pressure. Perhaps these "glucose-sensing" neurons have a dual purpose as "insulin-sensing" neurons, or perhaps an additional subpopulation of "insulin sensing" neurons exists within the nodose ganglia. While "glucose- and nutrient-sensing" neurons of the hypothalamus have been known for some time, "glucose-sensing" by sensory neurons is a novel concept. It is proposed that the nodose contains 2 different populations of glucose sensing neurons, excitatory or inhibitory and that glucose sensing occurs at the level of the stomach and portal vein. "Glucose-sensing" neurons that innervate the portal vein are more likely to be inhibitory, whereas neurons innervating the stomach are more likely to be excitatory. Interestingly, glucose-induced excitation is the result of closure of an ATP sensitive K^+ channel, similar to the mechanism for insulin release from beta cells [300]. Insulin has been demonstrated to open ATP sensitive K^+ channels in beta cells as a negative feedback mechanism and in populations of hypothalamic neurons to reduce food intake [163, 166]. Thus, insulin may act through a similar mechanism on neurons of the nodose ganglia. In this paradigm, SNIRKO mice would display hyperinsulinemia due to reduced uptake of systemic insulin by the "insulin-sensing" neurons. Furthermore, increased insulin production and reduced insulin sensing may be connected, in that a reduction in insulin "sensing" in the periphery may produce a signal to increase beta cell insulin production via islet sensory neuron innervation.

It is imperative to further confirm that the insulin receptor knockout is sensory neuron specific. Similar results of elevated insulin levels and glucose intolerance have previously been reported in mice with a conditional knockout of the insulin receptor in muscle in addition to a systemic heterozygous

insulin receptor knockout [131]. Thus, if SNIRKO mice have slight reductions in insulin receptor expression across multiple tissues, a similar phenotype of hyperinsulinemia may be evident. Techniques such as *in situ* hybridization and RT-PCR to visualize insulin receptor mRNA expression patterns and levels should be incorporated to compliment the presented protein expression data. Unfortunately, due to the presence of sensory neurons throughout the body, and the documented activation of Advillin$^{cre/+}$ in several peripheral sensory structures, such as free nerve endings, muscle spindles, Golgi tendon organs, Meissner's corpuscles, and Pacinian corpuscles [274], results will always have to be interpreted with caution.

The results presented here strongly indicate that sensory neuron insulin signaling is important in regulating systemic insulin levels, which may implicate sensory neuron involvement not only in DN, but in the development and progression of diabetes. Further research into these areas may help determine the pathogenic mechanisms of both DN and diabetes and open new pathways for treatment. In conclusion, SNIRKO mice do not appear to develop signs of DN, but do have systemic changes in serum insulin levels and glucose tolerance, supporting previous evidence of a connection between sensory neurons and pancreatic islet function.

Chapter 6: Dissertation Discussion and Conclusions

Experiments presented here were aimed at testing the hypothesis that DN pathogenesis is a result of reduced neurotrophic support from disrupted sensory neuron insulin signaling independent of hyperglycemia. These studies have 1) outlined the insulin signaling pathway in sensory neurons, 2) demonstrated that insulin signaling is modified in type 2 diabetes, and 3) characterized the phenotype of mice with a sensory neuron insulin receptor knockout. The PNS does respond to insulin in a dose-dependent manner and the PNS shows signs of insulin resistance similar to other tissues in type 2 diabetes. However, the physiological relevance of these results is challenged by our results demonstrating that supraphysiological insulin doses are needed to activate signaling and the absence of a neurological phenotype in SNIRKO mice. Based on these observations, the original hypothesis should be rejected. However, in light of the evidence that insulin is strongly neurotrophic, sensory neurons due respond to insulin, and there appears to be reduced signaling in both type 1 and type 2 diabetes a more suitable modified hypothesis would be that reduced sensory neuron insulin signaling in conjunction with the sequela of hyperglycemia contributes to DN pathogenesis.

The development of hyperinsulinemia in SNIRKO mice provides key information to a novel area of research suggesting that sensory neurons regulate pancreatic beta cell insulin production. Based on these results a new hypothesis was formed in that sensory neuron insulin signaling modulates beta cell insulin synthesis/release via a negative feedback mechanism, such that reduced sensory neuron insulin signaling results in an unchecked synthesis/release of insulin.

6.1 Caveats and Discrepancies

As with any large body of research, the experiments and methods of this project present several potential caveats that need to be considered when interpreting the presented data. They are discussed below in order of chapters presented.

The DRG are not solely sensory neurons. This is a common issue throughout the field of DN and sensory neuron biology, especially when using techniques such as Western blots and RT-PCR. Generally,

due to accessibility, several DRG are pooled together and the whole DRG homogenate is used for analysis. The results are then interpreted as alterations in sensory neurons, yet the results could be due to the other cells of the DRG, such as Schwann cells and satellite cells. Along those lines, all sensory neurons are not the same, there are several different subpopulations, and thus, using a DRG homogenate may mask the results that are specific to a subpopulation. In that vein, insulin receptor expression in the DRG has been characterized to be predominantly in small neurons of the DRG [173], however conflicting reports exist [174]. With respect to Akt activation in the DRG, several attempts were made to use immunohistochemistry to support the Western blot data, however results were inconclusive due to the poor quality of antibodies used for immunohistochemistry (data not shown).

The sciatic nerve is a mixed nerve with sensory and motor axons, thus results in the sciatic nerve cannot solely be attributed to sensory neurons. The sciatic nerve of a rat is composed of 8% motor axons, 23% sympathetic axons, and 69% sensory axons [302]. Additionally, a large percentage of the protein or RNA extracted from the sciatic nerve would be from Schwann cells. A more sensory-specific peripheral nerve is the sural nerve. However, once again due to accessibility, the sciatic nerve is most commonly used as a representative tissue of the peripheral nerve.

The insulin dose curve of PNS Akt activation provided strong evidence that DRG and sciatic nerve Akt activation *in vivo* is insulin dose dependent. However, for a better translation into how insulin may be signaling in the PNS of human patients, using subcutaneous (subq) injections rather than IP delivery would have been more useful, as insulin is delivered subq in diabetic patients. The pharmacokinetic profiles between subq and IP insulin are not drastically different, though, and IP insulin may even result in faster absorption and more physiological insulin levels [303, 304]. An additional complication of the dose curve experiments is the fact that Akt activation is both dose and time dependent. Thus, using a different time frame (experiment was done at 30 minutes) would shift the curve and generate different EC50s.

A “therapeutic” dose of exogenous insulin did not significantly activate Akt over baseline in the DRG or spinal cord. However, it still remains unknown if endogenously released insulin would activate

signaling in these tissues. In fact, very little is known about DRG insulin diffusion/transport, although it is assumed to fluctuate with serum insulin levels due to the reduced BBB at the DRG. Interestingly, it has been reported that tissue insulin level does not correlate with serum insulin level [305]. However, it has also been demonstrated that intrathecally, intranasally, and subcutaneously delivered insulin reaches the DRG [191, 201] and that systemically delivered insulin increases cerebrospinal fluid insulin levels [306]. Attempts were made to study both Akt activation and DRG insulin levels in response to endogenously released insulin (data not shown). Nondiabetic and type 1 diabetic (control for glucose effects alone) mice were given bolus injections of glucose to induce insulin release. Tissues were then harvested at 15, 30, 60, and 120 minutes post-glucose injection. While nondiabetic mice displayed a significant increase in insulin levels and diabetic mice did not, there appeared to be Akt activation in tissues from both groups suggesting the glucose bolus was interfering. Using insulin secretagues to induce insulin release may be a more controlled experiment. Additionally, an assay was developed using an insulin ELISA (Alpco) based on beta cell insulin extraction protocols and the method published by Agardh et. al [305] to measure DRG and sciatic nerve insulin levels. However, after several attempts it was concluded that either the interference from the extraction buffer was too high or the tissue insulin level was below detection in both nondiabetic and diabetic mice.

Insulin has been demonstrated to increase neurite outgrowth and similar results were demonstrated here (Figure 3.6), with a blunted growth in cultures from *ob/ob* mice. These results could have been more descriptive by looking at neurite outgrowth of different subpopulations using peripherin (small neurons) or NFH (large neurons). This would also have given an indication of the neuronal population supported by insulin. The culture system used may also have impacted the results. Neurons were allowed to adhere to coverslips in a small volume (approx. 100 µL) before wells were filled with media, this created a dense area of neurons and neuronal density is a major factor in neurite outgrowth [307]. Thus, although care was taken to maintain consistency across groups, and neurite area was normalized to number of cell bodies, it is possible that neurons from *ob/ob* mice had reduced survivability

in culture, similar to results published on type 1 DRG culture [308], which would have changed the neuronal density.

A discrepancy between the results presented in Chapters 3 and 4 is the expression of IRS2 serine phosphorylation and the insulin receptor. In primary DRG culture, IRS2 serine phosphorylation was significantly increased in cultures from *ob/ob* mice (Figure 3.3), however in freshly isolated DRG from *ob/ob* mice no change in IRS2 serine phosphorylation was observed (data not shown). The results suggest that the increased IRS2 serine phosphorylation may have been a result of the culture system. It is possible that the DRG of *ob/ob* mice are "primed" for stress kinases activation and IRS serine phosphorylation due to elevated adipokines and the added stress of dissociation and 3 day culture potentiated this system. However it may remain undetectable in freshly isolated tissue. Similarly, in primary DRG culture there was no change in insulin receptor protein expression; however, freshly isolated DRG from *ob/ob* mice display a significant decrease in expression (Figure 4.6). The difference in environment may have produced this effect. Freshly isolated DRG were surrounded by extremely elevated serum insulin levels which may have driven down insulin receptor expression. However, cultured DRG were in a hypoinsulinemic system for 3 days which may have allowed the insulin receptor expression levels to upregulate.

An area of research that has not been discussed thus far is the idea of *de novo* insulin synthesis in the nervous system. Rabbit brains express insulin mRNA [309] and neuronal culture from rat brains secrete insulin peptide [310]. Preproinsulin mRNA has also been characterized in the rat nervous system [311] and it has been suggested that *de novo* neuronal insulin synthesis may contribute to neurite outgrowth and differentiation [312, 313]. This could be a potential argument against reduced insulin neurotrophic support in diabetes, because the neuronal insulin level may be maintained. The role of neuronal insulin production is still ill-defined and its impact on DN has not been investigated.

Finally, as previously discussed the generation of SNIRKO mice is associated with several caveats and unfortunately due to time constraints many of them remain uninvestigated to date. A major concern when using conditionally expressed cre recombinase mouse lines is off-target cre expression.

Advillin$^{cre/+}$ mice do show cre activity in Mo5 trigeminal motor neurons [274] and mosaic expression in epidermal cells (personal communication with Dr. Fan Wang). How this expression may be affecting our results is yet to be determined. Additionally, although several tissues have been investigated for Cre activity using Tomato mice, it is possible that certain tissues have been overlooked or cre activity is too low to visualize with Tomato mice but high enough to cause recombination. One tissue that has not been investigated to date is the autonomic ganglia. Advillin does not appear to be expressed in ganglia of the autonomic nervous system [274], however, due to the importance of autonomic control over insulin secretion the cre activity and insulin receptor expression in autonomic ganglia needs to be further investigated. In addition, IR$^{lox/lox}$ mice are an appropriate control for loxp site interference. However, using Advillin$^{cre/+}$ mice as an additional control in future experiments will insure that differences are not the result of cre recombinase expression alone.

As mentioned earlier, using DRG homogenates presents several issues. This is particularly true for the SNIRKO mice, because although they showed significantly decreased insulin receptor expression and evidence of cre/lox recombination (Figure 5.4), it does appear that some intact insulin receptor expression remains. This is most likely due to non-sensory neuron cells in the DRG, however this has not yet been confirmed. Insulin receptor *in situ hybridization* would help clear up these discrepancies. Probes would have to be designed past exon 4 to be confident not to hybridize the early portions of the insulin receptor RNA that are still transcribed in the SNIRKO mice. Additionally, experiments could be performed using laser microdissection to isolate sensory neurons or primary DRG culture to assess single neuron characteristics.

6.2 Future directions

As expected, extensive work remains not only to further characterize the results presented, but to push this research forward. Several experiments are outlined below in order of chapters presented.

Akt activation in the PNS is insulin sensitive and the downstream signaling pathway was investigated here. However, the physiological result of PNS insulin signaling has yet to be clearly

defined. Future experiments need to be targeted at the function of insulin signaling in the PNS, this will provide important information about how loss of PNS insulin signaling may contribute to DN pathogenesis. A preliminary experiment used focused insulin signaling microarrays to assess genes modified by insulin in the DRG, however due to low numbers and high variability results are not presented here. Follow up on these experiments using additional microarrays and RT-PCR to confirm the results will be important to determine the role of insulin signaling in PNS gene transcription.

Insulin has been shown to have important roles in nerve regeneration and neurite outgrowth, yet the mechanisms through which insulin promotes these functions have not be revealed. The expression of key mediators of nerve regeneration, such as Gap43, in response to insulin needs to be investigated. Using nerve crush models, the difference in regenerative mediators in response to insulin could be characterized with immunohistochemistry, Western blots, and RT-PCR. Furthermore, samples already acquired from dose curve experiments may be helpful in answering these questions. Additionally, while immunohistochemistry of Akt activation was not useful in delineating the location of insulin signaling in the PNS, the discovery of a protein that is increased in response to insulin will be helpful in localizing the action of insulin to either a certain subpopulation of sensory neurons or perhaps glia cells.

Furthermore, although insulin has been characterized to modify TRPV1 sensitivity, its actions on other receptors and channels of the PNS remain largely uninvestigated. The internal calcium levels in response to different agonists, such as ATP for P2Y receptors or mustard oil for TRPA1, could be quantified using Calcium imaging or patch-clamp in DRG cultures with or without insulin. Additional studies could also investigate the membrane translocation of different receptors in response to insulin. As discussed earlier, insulin has been characterized to modify the K_{ATP} channels in the hypothalamus and beta cell. The expression of K_{ATP} channels in sensory neurons was recently characterized [314, 315] and thus may be a pathway through which insulin is acting on sensory neurons that has not be previously investigated.

Another area of insulin's suggested role on sensory neurons in modifications of neuropeptides, however direct evidence is lacking. Recent developments at the Microfabrication and Microfluidics Core

in Lawrence, KS may provide important data in this area. DRG neurons that innervate the pancreatic beta cells could be cultured and stimulated with increasing doses of insulin and the neuropeptide concentration changes quantified in real time. Similar studies could also be performed investigating neuropeptide mRNA levels and accumulation in sensory neurons in response to insulin stimulation.

Brussee et. al. [191] showed that sequestering of CSF insulin with intrathecal infusion of an insulin receptor antibody caused manifestations of neuropathy. A complimentary experiment to those studies and the data presented here would be to intrathecally infuse an insulin receptor antagonist and assess the resultant sensorimotor behavior. However, leakage out of the CSF would have to be tightly monitored as systemic insulin receptor antagonism would cause metabolic disturbances.

It was demonstrated that IRS2 serine phosphorylation was upregulated in the DRG of type 1 diabetic mice (Figure 3.3). Insulin resistance in type 1 diabetes has received increased attention recently [316] and insulin resistance in type 1 diabetes may be independently linked to cardiovascular disease [239]. Further studies should be completed to follow up on the increased IRS2 serine phosphorylation in type 1 diabetic mice. DRG Akt activation in response to insulin in both a culture and *in vivo* setting could be tested in STZ-diabetic mice. In fact, using an insulin dose curve to assess PNS insulin sensitivity in both type 1 and type 2 mice would provide an additional degree of evidence about diabetes-induced PNS insulin signaling changes. It would be predicted that the dose curve would show a significant rightward shift in diabetic mice as compared to nondiabetic mice.

An additional study that would have helped demonstrate resistance specifically to the insulin/IGF pathway in the PNS of *ob/ob* mice would have been to administer an additional growth factor whose signaling has been shown not to be disrupted in diabetes, such as fibroblast growth factor. This experiment would have helped demonstrate that the observed decrease in Akt activation was due to changes in insulin sensitivity, not a global change in Akt activation, although that result may have been of interest as well. Furthermore, a similar Akt activation in the PNS from nondiabetic and *ob/ob* mice in response to an alternative growth factor would demonstrate that the reduced PNS signaling was not due to

reduced delivery of insulin to the PNS in *ob/ob*. Although similar results were demonstrated with both IT and IP injections, it still remains possible that the severe obesity of *ob/ob* mice confounded the results.

The majority of future experiments are related to further characterization of the SNIRKO mice, in fact several of the previously discussed experiments (such as neuropeptide levels or nociceptive receptor modifications) should also be analyzed in SNIRKO mice. The list of possible future experiments on SNIRKO mice is extensive; several of them are discussed here in relation to the discussion points established in chapter 5.

Changes in sensory function may not be evident until the system is challenged or injured. As discussed earlier this can be tested with several different experimental paradigms. The behavior and physiological response to noxious agents such as formalin, capsaicin, and CFA can be quantified by assessing injection site edema and erythema, or by observing the time spent attending to the injections, or by using tests of mechanical and thermal sensitivity to assess changes in threshold. Similarly, assessing the recovery/response of sensory function in models of physical injury such as nerve crush and spared nerve injury in SNIRKO mice will provide important information about the role of sensory neuron insulin support in nerve regeneration and repair. Investigation of mediators of nerve regeneration in this paradigm will also provide evidence of the pathways through which insulin acts. Diabetic mice have been characterized to have a reduced nerve regeneration capacity [317], similarly it is predicted that SNIRKO mice will have a poor recovery in response to nerve injury resulting from reduced neuron insulin signaling.

Diabetic patients have been characterized to have a reduced axon mediated flare response [318]. The neurogenic flare response is mediated by substance P and CGRP vasodilation upon c-fiber activation with exogenous heat. The increase in blood flow can be analyzed with laser Doppler imaging. Assessing the flare response in SNIRKO mice would be an additional way to test the role of insulin signaling on sensory neuron function and neuropeptides. It may also delineate if the reduced neurogenic flare in diabetic patients is due to hyperglycemia or reduced sensory neuron insulin signaling.

Peripheral nerves of diabetic patients and mice show changes in ultrastructure morphology such as increased axon-myelin separations [319]. Although SNIRKO mice do not display changes in sensory behavior, they may have alterations in nerve morphology. Electron microscopy (EM) could be used to analyze ultrastructure morphology in SNIRKO mice and will also be important in studies assessing nerve regeneration. Furthermore, as previously discussed SNIRKO mice have a development sensory neuron insulin receptor knockout and while SNIRKO mice do not display developmental defects, the DRG composition may be altered. Thus, careful analysis and quantification of sensory neuron subpopulations are needed.

Diabetic patients have reduced would healing and it has been demonstrated that deficits in sensory neurons play an important role in regulating this process [320]. An interesting possibility is that the reduction in sensory neuron insulin signaling alters the neuro-immune axis needed for proper wound healing. SNIRKO mice are a powerful tool to test this hypothesis and this may give further insight into the function of neuropeptides in SNIRKO mice as the neuronal regulation of wound healing is through neuropeptide immune modification. The rate of healing, biomechanical properties, and collagen content of circular wounds on either side of the spine could be assessed in control and SNIRKO mice [321].

As previously discussed, to better model reduced insulin signaling in the PNS of diabetic patients, insulin signaling may have to be disrupted in glia cells in addition to sensory neurons. Mice with Schwann cell specific cre expression under control of the glycoprotein P0 ($P0^{cre/+}$) promoter are available for Jackson Laboratories. Two separate lines of insulin receptor knockout mice could be generated using $Advillin^{cre/+}$, $P0^{cre/+}$ and $IR^{lox/lox}$ mice. One line would be a conditional knockout of the insulin receptor in Schwann cells and the other line would have a knockout of the insulin receptor in Schwann cells and sensory neurons simultaneously by breeding the $P0^{cre/+}$ into the $Advillin^{cre/+}$ line. After generation of the new knockout lines, the phenotypes would have to be characterized with respect to development, metabolism, sensorimotor function, and PNS morphology. Interestingly, it has recently been demonstrated that the islets of Langerhans are surrounded by Schwann cells [322], thus a Schwann cell insulin receptor knockout and a knockout in both Schwann cells and sensory neurons may potentiate the

metabolic disturbance that have been observed in SNIRKO mice. Generation of these new mouse lines will be crucial in further delineating the role of insulin in the PNS and how disruptions in PNS insulin signaling may contribute to DN and/or diabetes pathogenesis.

A modified hypothesis from these studies is that reduced neuronal insulin signaling in conjunction with the sequelae of hyperglycemia contributes to DN pathogenesis. SNIRKO mice are a powerful tool to analyze this hypothesis. Pathogenic cascades associated with hyperglycemia include, reactive oxygen species, polyol pathway activation, advanced glycation endproducts, and mitochondrial dysfunction. Several of these mechanisms can be upregulated independently of hyperglycemia via pharmacological mediators. An experiment to test if the combination of RAGE activation and reduced neuronal insulin support cause neuropathy would be to administer SNIRKO mice a RAGE agonist, such as S100b or AGE-bovine albumin. However, no reports of RAGE agonists and DN are currently available. The prediction for these experiments would be that RAGE activation in $IR^{lox/lox}$ mice would not induce neuropathy; however RAGE activation in SNIRKO mice would cause a neuropathic phenotype. Suggesting that DN is a result of insults from both AGE and reduced insulin support. Furthermore, glyoxalase 1 (Glo1) activity has recently been demonstrated to have a role in DN [68]. Glo1 is the rate limiting enzyme in AGE breakdown, and differential expression of Glo1 may dictate if patients develop positive or negative symptoms. Studies with SNIRKO mice will help determine if there is a connection between Glo1 and insulin. Glo1 expression could be characterized with RT-PCR, Western blots, and immunohistochemistry in SNIRKO and $IR^{lox/lox}$ mice. Furthermore, inhibition of Glo1 with s-p-bromobenzylglutathione cyclopentyl diester produces thermal hyperalgesia in nondiabetic mice [323]. Inhibition of Glo1 in SNIRKO mice may give a better understanding of how Glo1 dysfunction may contribute to DN in human patients, as SNIRKO mice have the added defect of reduced sensory neuron insulin support. Similar experiments could be repeated for other factors, including ROS, which could be upregulated with the superoxide anion-inducing agent LY83583.

Surprisingly, SNIRKO mice displayed hyperinsulinemia, suggesting that sensory neuron insulin signaling may play a role in systemic metabolism regulation. Several experiments remain to fully

characterize the metabolic profile of SNIRKO mice including serum cholesterol and lipid levels, glucose uptake, insulin release in response to glucose bolus, and food intake. A high fat diet is regularly used to induce metabolic syndrome in mice, and it has recently been demonstrated that high fat diet can induce neuropathic changes [80]. Thus, a high fat diet would be a reasonable way to metabolically stress SNIRKO mice. Based on the proposed model (figure 5.12) it is predicted that SNIRKO mice will quickly progress to diabetes because of the underlying beta cell stress.

It has been demonstrated that administration of substance P can reduce the islet inflammation in NOD mice [38]. Accordingly, a proof of concept experiment would be to administer SNIRKO mice substance P, with the expectation that substance P would correct the SNIRKO hyperinsulinemia. Furthermore, Razavi et. al. proposed that the increased islet stress and insulin production induces autoimmunity in NOD mice. SNIRKO mice do not display insulitis, but have hyperinsulinemia and increased islet insulin content. Based on these observations, SNIRKO mice may be "primed" for diabetes development, such that a "second hit" would lead to rapid development of diabetes mellitus. As previously discussed, a high fat diet could be used as an environmental "second hit", however viral infection is one of main environmental factors implicated in diabetes development. Diabetes progression in $IR^{lox/lox}$ and SNIRKO mice could be monitored after administered of polyinosinic-polycytidylic acid, a mimic of double-stranded viral RNA [324] with the hypothesis that SNIRKO mice would develop diabetes earlier and at a higher incidence than $IR^{lox/lox}$ mice due to their "primed" state.

Sensory neuron innervation of the pancreas originates from both the nodose ganglia and the T9-T12 DRG [282]. Ablation of pancreatic sensory neurons with capsaicin has been previously demonstrated to alter insulin levels [38], however, it is not possible to determine if those changes were due to neuronal death in the nodose or DRG. Establishing the sensory neuron population that is involved in modulation of pancreatic beta cells will be important in understanding the underlying mechanism. To determine which sensory neurons modulate insulin release, neurons from either the nodose or DRG could be selectively ablated with saporin. Saporin is toxic upon endocytosis and when conjugated to a cell specific marker can target unique cell populations and it is currently being investigated for cancer treatment [325]. It was

recently demonstrated that 67% of DRG neurons innervating the pancreas express GDNF family receptor alpha-3, the coreceptor for artemin, whereas only 1% of nodose neuron innervating the pancreas express GDNF family receptor alpha-3 [282]. Thus, one way to specifically target DRG neurons innervating the pancreas maybe to give pancreatic injections of artemin conjugated to saporin. Characterization of the resultant phenotype will provide information about which sensory population has a larger role in regulating beta cells. While no publications are available, it has been proposed that selective surgical transection of DRG nerves innervating the pancreas can alter NOD mouse insulitis and diabetes (first proposed by Ravazi et. al. [38]). If so, this may be another way to investigate the selective role of sensory neuron innervation on beta cell function.

Beyond increased insulin production; it is also possible that SNIRKO hyperinsulinemia was a result of decreased uptake or breakdown. In light of recent evidence outlining vagal afferent "glucose sensing" sensory neurons of the nodose ganglia [300], it is possible that these neurons or a different subpopulation of neurons are "insulin sensing", thus an insulin receptor knockout would reduce insulin uptake and lead to hyperinsulinemia. In fact, Advillin$^{cre/+}$ do show cre activity in the nodose ganglia (Figure 5.2).

Experiments to test the hypothesis of "insulin sensing" neurons of the nodose ganglia would include a combination of anatomical and physiological characterizations. Expression of the insulin receptor on nodose cell bodies and axons would be confirmed using a combination of Western blots, immunohistochemistry, RT-PCR, and *in situ* hybridization. Furthermore, FITC-labeled insulin could be systemically delivered and axonal binding and neuronal uptake monitored in nodose ganglia. Insulin sensitivity of nodose ganglia could also be assessed using an insulin dose curve and analyzing activated Akt. Similar techniques used to analyze "glucose sensing" neurons could be employed to assess the electrochemical response to insulin, such as patch clamp analysis and intracellular ion imaging (K^+ or Ca^{2+}). SNIRKO mice will be a valuable control in many of these experiments.

6.3 Potential impact to the field and patients:

Prior to the experiments presented here, several areas in the field of DN were lacking support. Several studies had indicated the neurotrophic potency of insulin and established that under varying conditions reduced insulin support may contribute to DN. However, a basic understanding of PNS insulin signaling had not been completed. Historically, the nervous system has been considered nonresponsive to insulin. Studies presented here clearly demonstrate that the PNS does in fact show signaling activation in response to insulin. Interestingly though, it appears that differences between DRG and peripheral nerve insulin sensitivity exist. Furthermore, using both primary culture and *in vivo* models it was demonstrated that insulin signal transduction is blunted in the PNS from insulin resistant mice. This result has subsequently been demonstrated by 2 independent publications using similar primary culture techniques [175, 181]. Finally, SNIRKO mice have already provided important information on the role of insulin signaling on sensory neurons and should prove to be a powerful model for both DN and diabetes. These results will help push the field of DN forward and hopefully establish new treatments and relief for patients.

The outlining of the PNS insulin signaling pathway will greatly aid in establishing the role that insulin plays in PNS support and how this differs from its role in muscle, liver, and adipose. It also provides direction for future researchers to pursue. Akt activation was significantly activated in the sciatic nerve and not the DRG at a “therapeutic” insulin dose, suggesting that an increased emphasis should be placed on Schwann cell and peripheral nerve insulin support. This idea could also be applied to other mechanisms being investigated in DN pathogenesis, in that dysfunction in the entire PNS needs to be considered, not just the sensory neurons. Furthermore, supraphysiological insulin doses were needed to activate signaling in the DRG and SNIRKO mice do not display signs of neuropathy. These results suggest that reduced sensory neuron insulin signaling in the absence of other insults does not cause DN. This brings up a basic, but often overlooked aspect of DN, in that DN development/progression is multifactorial. Thus, treatments need to be multifaceted, targeting glucose neurotoxicity, reduced

neurotrophic support, ischemia and reduced insulin support simultaneously. This may help explain the poor success rates of DN treatments that make it to clinic trial.

The recent understanding that insulin has important functions in the CNS and PNS suggests that insulin may also be important in other tissues previously thought to be insulin insensitive. Based on this observation, other complications associated with diabetes, such as retinopathy and nephropathy, could be a result of changes in insulin signaling in addition to hyperglycemia. In fact, recent studies have demonstrated that insulin mediates a pro-survival pathway in retinal neurons and diabetes downregulates retinal insulin signaling [326]. Additionally, insulin receptors have been localized to the proximal and distal tubules in the renal cortex and a diabetes appears to downregulate kidney insulin receptor expression [327]. These studies and the ones presented here are starting to establish that insulin has roles beyond glucose metabolism in the muscle, liver, and adipose. This will be important information in designing new treatments for diabetes and diabetic complications.

One possible new treatment for DN may be to modify insulin therapy. Two possible areas of modification are changes in delivery or insulin peptide structure. In fact it has previously been demonstrated that intranasal insulin treatments improves Alzheimer's symptoms in patients [161] and signs of DN in diabetic rats [201]. The latter study demonstrated that insulin delivered intranasally had a more rapid and concentrated delivery to the spinal cord and DRG than subcutaneous insulin. Furthermore, the peak insulin concentration in the blood with intranasal delivery was nearly 1000 fold lower than that obtained with subcutaneous delivery. Accordingly, the incidence of hypoglycemic events was significantly lower in the intranasal insulin group. With the advanced deliver of insulin to the nervous system, significant improvements in signs of DN were observed in the intranasal insulin group as compared to not only placebo groups, but subcutaneous insulin groups as well. These results suggest that while the delivery of subcutaneous insulin (the currently most utilized route) may be sufficient to control blood glucose, it may not be sufficient to completely protect against the development of DN.

Another modification to insulin deliver may be to co-administer c-peptide. Currently patients only receive insulin, however it has been demonstrated that c-peptide and insulin have synergistic cellular

effects on neurite outgrowth and survival in the SH-SY5Y neuronal cell line [180]. Beyond cultured neurons, c-peptide treatment in patients with DN has been demonstrated to improve deficits in NCV as well as signs of sensory and autonomic neuropathy in a recent clinical trial [328]. Therefore, it is possible that the delivery of synthetic insulin without c-peptide does not provide the necessary combination of support to spare patients from developing diabetic complications.

Intense blood glucose control is the best known preventative treatment for diabetic complications. As expected though, hypoglycemia is the most common side effect of intense glycemic control. Perhaps the reduced complications with intense glycemic control are in part due to increased insulin support to other "off-target" tissues (kidney, retina, PNS, etc.). Thus, direct modification of the insulin peptide to increase delivery to tissues beyond muscle, liver, and adipose may decrease diabetic complications. This could be completed by trying to specifically target certain tissues or by decreasing the potency of insulin at muscle, liver, and adipose, thus enabling increased insulin dosing without causing hypoglycemia. The difference between currently delivered insulin formulations results from slight changes in insulin peptide sequence. For example, the rapid acting analog lispro has an aspartic acid residue in replace of a proline residue at site 29 of the beta chain. This weakens the tendency to form hexamer aggregates and increases the rate of absorption and action [329]. Accordingly, perhaps insulin modifications that direct increased delivery to certain tissues would show benefits in decreasing diabetes complications. It has also been shown that different tissues express different insulin isoforms, IR-B in muscle, liver, and adipose and IR-A in the CNS and Schwann cells [183], thus maybe modifications that create a higher binding to isoform A over isoform B may also be beneficial.

It was recently demonstrated that the insulin sensitizing drug, Pioglitazone, improves memory formation in a mouse model of Alzheimer's disease [330]. Furthermore, studies have shown that treatment with rosiglitazone reduces DN in diabetic STZ-mice independent of its effects on hyperglycemia [331]. With the growing evidence that insulin resistance may be present in both type 1 and type 2 diabetes and that insulin support to other tissues may be beneficial in preventing complications, adding insulin sensitizing drugs as first line therapy for all diabetic patients may be warranted.

The recent evidence that sensory neurons may regulate beta cell function, as well as autoimmunity in NOD mice and that SNIRKO mice display hyperinsulinemia opens new possibilities for diabetes treatment. Several intriguing question to consider are: 1) Can neuronally-targeted treatments be utilized as treatments for diabetes? 2) Can mutations in previously uninvestigated neuronal genes dictate susceptibility to diabetes? 3) Is the sensory neuron interaction with beta cells key to improving islet transplants and synthetic beta cell production?

1) Can neuronally-targeted treatments be utilized as treatments for diabetes? The idea that diabetes may be neuronal driven is not new. It has been documented that several of the characterized autoimmune antigens of type 1 diabetes are coexpressed in neuronal tissues [283] and in 2001 Winer et. al. detailed an associated between the neuronal autoimmune disease, multiple sclerosis (MS), and type 1 diabetes [332]. These results have been further supported by 2 population studies demonstrating an increased risk of MS in patients with type 1 diabetes and vice versa [333, 334]. Moreover, in 2005 Carrillo et. al. characterized islet-infiltrating B-cells of NOD mice to predominantly target neuronal antigens [335]. The development of hyperinsulinemia in SNIRKO mice further promotes the idea that neuronal elements may be involved in diabetes. The long term goal of this research is to positively impact patient care; thus based on these results and observations, one new avenue for patient treatment may be neuronally-targeted treatments. It may be possible to repurpose treatments that have shown beneficial impact on peripheral neuropathies or other neurological diseases. In fact, it has already been demonstrated that capsaicin can have beneficial effects on diabetes in mice [38]. Thus, through the modification of neuronal ion channels, neurotransmitters, or neuropeptides it may be possible to modify islet innervation and promote beta cell function and/or reduce autoimmune attack. Due the growing evidence that sensory neurons are playing a role in beta cell function, the first line medications to investigate would be ones that can modify sensory neuropeptide release beyond capsaicin, or too target neuropeptide administration to the pancreas. Intriguingly, angiotensin-converting-enzyme (ACE) inhibitors have recently been shown to have beneficial effects on diabetes and ACE inhibitors are known to cause an increase in the neuropeptide, substance P [336, 337]. Neuropeptide modulation by ACE inhibitors may be a possible

mechanism of diabetes regulation. Additional medications of interests are the anti-seizure and anti-depression drugs that have shown beneficial effects on peripheral neuropathy. However, it should be noted that in the clinical trials investigating pregabalin as a treatment for DN, no change in metabolic profiles were observed [338]. Along these lines, repurposing of drugs can be difficult due to known side effects. Intense research would have to be done fine tuning the delivery, timing, and dosing of these drugs in order to specifically target pancreas innervation and measure beta cell function as an outcome. Branching out even farther, other nervous system modifying drugs could be investigated including medications for Alzheimer's, anxiety, analgesia, or anesthesia.

Beyond pharmacology, other neurologically targeted treatments may be of use, including electrical nerve stimulation. Interestingly, it has already been reported that vagal nerve stimulation helps curb obesity and type 2 diabetes [339], as well as promote insulin release [340] although it was concluded that this effect was through ANS regulation. A more targeted approach based on the evidence presented here would be to stimulate the sensory neurons of the pancreas. In fact, in 2012 the Neural Diabetes Foundation, Inc. filed a patent for an implantable neural stimulation device to activate the pancreatic c-fibers and modulate islet function/inflammation via neuropeptide release [341].

Recent clinical trials have demonstrated that the use of nonreplicating herpes simplex virus (HSV) vectors can specifically target treatments or growth factors to the DRG. HSV is particularly useful for gene deliver to sensory neurons as HSV is retrogradely transported to sensory ganglia where the virus lays dormant. HSV vectors encoding encephalin, NT-3, and NGF have shown efficacy for treating polyneuropathy [342]. Specifically, targeting treatments to the sensory neurons of the pancreas to modify channel expression, neuropeptide release, or insulin sensitivity via viral vectors may prove effective for diabetes and DN treatment. This also may be a feasible option to increase insulin deliver to the PNS without inducing hyperglycemia. Furthermore, this approach may be associated with fewer side effects than the methods previously discussed.

Finally, optogenetic control over sensory neurons may also be a way to modify beta cell function via sensory neurons. Optogenetics use light sensitive ion channels to either excite or inhibit neurons.

Optogenetics are now been widely investigated in several different model organisms and in several different neurological diseases [343]. It may be possible to specifically express light sensitive ion channels in the sensory nerves of the pancreas via targeted gene therapy to modulate beta cell function. Light would most likely have to be delivered via an implanted device. Although, optogenetic treatments have not reached clinical trials yet, this powerful technique has intriguing potential and may be relevant to diabetes treatment based on the apparent role of sensory neurons.

2) Can mutations in previously uninvestigated neuronal genes dictate susceptibility to diabetes? Recently, NOD mice were demonstrated to express a hypofunctional TRPV1 and TRPV1 was mapped to the Idd4.1 diabetes risk locus on chromosome 11 [38]. Furthermore, TRPV1 null mice have increased insulin sensitivity. These results suggest that other unexplored neuronal genes may also be candidate genes for predicting diabetes susceptibility. In fact, 1 gene implicated in development of maturity onset diabetes in the young (MODY) is neuroD1, a transcription factor involved in neuronal development [344]. Thus, recent advancements in the understanding of neuronal involvement in beta cell function may expose new candidate genes for diabetes development and present new treatment or prevention options.

3) Is beta cell/sensory neuron interaction a key to improving islet transplant and synthetic islet production? Some of the first evidence indicating an important relationship between islets and neurons and the potential neurotrophic property of insulin was from islet transplantations. Upon transplantation under the kidney capsule of mice islets are innervated by sensory neurons [345]. Furthermore, coculture of beta cells with DRG neurons demonstrated increased survival of DRG neurons and reduced insulin output from beta cells (once again suggesting a negative feedback mechanism with sensory neuron insulin signaling) [346]. Thus, simply understanding that a necessary relationship between sensory neurons and beta cells exists may be able to revolutionize some current diabetes treatments.

Islet transplantation has demonstrated several promising results. According to the 2012 Collaborative Islet Transplant Registry report 66% of patients were insulin independent 1 year after transplantation in the 2007-2010 era, and even if patients were not completely insulin independent they showed reduced insulin need and better glucose control [347]. Additionally, islet transplant has been

demonstrated to greatly improve hypoglycemia unawareness. Unfortunately, several problems still exist with islet transplantation. Two major problems are immune rejection of transplanted islets and poor availability of islets for transplantation. However, using the recent evidence on sensory neuron and beta cell interaction may help improve outcomes. One possible change may be to give sensory neuron neurotrophic factors during islet transplantation to promote earlier innervation. As most evidence is demonstrating a role for TRPV1 positive neurons, which are primarily peptidergic c-fibers, NGF may be the best candidate neurotrophin. Furthermore, it may be possible to improve islet survival during transplantation by using media's or extraction procedures that include neuropeptides to help mimic the *in vivo* nerve regulation.

An additional area where sensory innervation may play an important role is in the creation of glucose-sensitive insulin releasing beta cells from multi-potent stem cells. Obviously the potential of stem cell therapy is astronomical, but for many applications it remains too unpredictable for human patients. Diabetes treatment has been at the center of stem cell research for several years, with the hope that *in vitro* generation of beta cells would eventually lead to an endless supply of transplantable insulin secreting cells. While reports of insulin-producing cell generations have been published, translation into patient care is still not achievable [348]. Once again, it may be that without the finely tuned input from sensory neurons; that beta cells cannot survive or function properly. Thus, perhaps cocultures with sensory neurons or the use of neuropeptides in differentiation protocols may establish a more stable stem-cell-derived beta cell.

6.4 Conclusions:

The experiments presented here were designed to investigate insulin signaling in the PNS and how disruption of PNS insulin support may contribute to DN pathogenesis. Akt activation is insulin dose responsive in the both the DRG and sciatic nerve. Furthermore, insulin signaling appears blunted in the PNS of insulin resistant *ob/ob* mice, establishing a commonality of decreased neuronal insulin signaling in both type 1 and type 2 diabetes. However, it does not appear the reduced sensory neuron insulin

signaling is the only contributor to DN as SNIRKO mice with reduced DRG insulin signaling and euglycemia did not display neuropathy. Future directions will explore the possibility that reduced PNS insulin support potentiates glucose neurotoxicity and the effects of reduced insulin signaling on sensory neurons and Schwann cells simultaneously. Continued research in these areas will further the understanding of mechanisms impacting neuronal function in diabetes and hopefully present new treatment options.

Results of hyperinsulinemia and increased islet insulin content in SNIRKO mice fits well into a proposed model of negative feedback regulation of beta cell insulin production by sensory neuron insulin signaling. This newly proposed model has been met with much skepticism and these results help confirm previous reports. The combination of earlier results and those presented here expose new ways to investigate diabetes development and establish potentially uninvestigated avenues for treatment, such as neuronally-targeted pathways.

In conclusion, further research into the interplay between sensory neuron insulin signaling, DN, and beta cell function has conceivable translational benefits that may improve patient outcomes.

Chapter 7: References

1. Farinas, I., et al., *Regulation of neurogenesis by neurotrophins in developing spinal sensory ganglia.* Brain Res Bull, 2002. **57**(6): p. 809-16.
2. Acloque, H., et al., *Epithelial-mesenchymal transitions: the importance of changing cell state in development and disease.* J Clin Invest, 2009. **119**(6): p. 1438-49.
3. Kirstein, M. and I. Farinas, *Sensing life: regulation of sensory neuron survival by neurotrophins.* Cell Mol Life Sci, 2002. **59**(11): p. 1787-802.
4. Blesch, A., *Neurotrophic factors in neurodegeneration.* Brain Pathol, 2006. **16**(4): p. 295-303.
5. Miller, F.D. and D.R. Kaplan, *Neurotrophin signalling pathways regulating neuronal apoptosis.* Cell Mol Life Sci, 2001. **58**(8): p. 1045-53.
6. Bennet, M.R., W.G. Gibson, and G. Lemon, *Neuronal cell death, nerve growth factor and neurotrophic models: 50 years on.* Auton Neurosci, 2002. **95**(1-2): p. 1-23.
7. Levi-Montalcini, R. and V. Hamburger, *Selective growth stimulating effects of mouse sarcoma on the sensory and sympathetic nervous system of the chick embryo.* J Exp Zool, 1951. **116**(2): p. 321-61.
8. Crowley, C., et al., *Mice lacking nerve growth factor display perinatal loss of sensory and sympathetic neurons yet develop basal forebrain cholinergic neurons.* Cell, 1994. **76**(6): p. 1001-11.
9. Ernfors, P., K.F. Lee, and R. Jaenisch, *Mice lacking brain-derived neurotrophic factor develop with sensory deficits.* Nature, 1994. **368**(6467): p. 147-50.
10. Ernfors, P., et al., *Lack of neurotrophin-3 leads to deficiencies in the peripheral nervous system and loss of limb proprioceptive afferents.* Cell, 1994. **77**(4): p. 503-12.
11. Indo, Y., *Nerve growth factor and the physiology of pain: lessons from congenital insensitivity to pain with anhidrosis.* Clin Genet, 2012. **82**(4): p. 341-50.
12. Sah, D.W., M.H. Ossipo, and F. Porreca, *Neurotrophic factors as novel therapeutics for neuropathic pain.* Nat Rev Drug Discov, 2003. **2**(6): p. 460-72.
13. Pittenger, G. and A. Vinik, *Nerve growth factor and diabetic neuropathy.* Exp Diabesity Res, 2003. **4**(4): p. 271-85.
14. Zochodne, D.W., *Diabetes mellitus and the peripheral nervous system: manifestations and mechanisms.* Muscle Nerve, 2007. **36**(2): p. 144-66.
15. Zochodne, D.W., *Diabetic polyneuropathy: an update.* Curr Opin Neurol, 2008. **21**(5): p. 527-33.
16. Apfel, S.C., *Neurotrophic factors and diabetic peripheral neuropathy.* Eur Neurol, 1999. **41 Suppl 1**: p. 27-34.
17. Bibel, M. and Y.A. Barde, *Neurotrophins: key regulators of cell fate and cell shape in the vertebrate nervous system.* Genes Dev, 2000. **14**(23): p. 2919-37.
18. White, M.F., *IRS proteins and the common path to diabetes.* Am J Physiol Endocrinol Metab, 2002. **283**(3): p. E413-22.
19. White, M.F., *Regulating insulin signaling and beta-cell function through IRS proteins.* Can J Physiol Pharmacol, 2006. **84**(7): p. 725-37.
20. Yamada, M., et al., *Insulin receptor substrate (IRS)-1 and IRS-2 are tyrosine-phosphorylated and associated with phosphatidylinositol 3-kinase in response to brain-derived neurotrophic factor in cultured cerebral cortical neurons.* J Biol Chem, 1997. **272**(48): p. 30334-9.
21. Fundin, B.T., et al., *Differential dependency of cutaneous mechanoreceptors on neurotrophins, trk receptors, and P75 LNGFR.* Dev Biol, 1997. **190**(1): p. 94-116.
22. Baudet, C., et al., *Positive and negative interactions of GDNF, NTN and ART in developing sensory neuron subpopulations, and their collaboration with neurotrophins.* Development, 2000. **127**(20): p. 4335-44.

23. Christianson, J.A., et al., *Development, plasticity and modulation of visceral afferents.* Brain Res Rev, 2009. **60**(1): p. 171-86.
24. Molliver, D.C. and W.D. Snider, *Nerve growth factor receptor TrkA is down-regulated during postnatal development by a subset of dorsal root ganglion neurons.* J Comp Neurol, 1997. **381**(4): p. 428-38.
25. Molliver, D.C., et al., *IB4-binding DRG neurons switch from NGF to GDNF dependence in early postnatal life.* Neuron, 1997. **19**(4): p. 849-61.
26. Zylka, M.J., F.L. Rice, and D.J. Anderson, *Topographically distinct epidermal nociceptive circuits revealed by axonal tracers targeted to Mrgprd.* Neuron, 2005. **45**(1): p. 17-25.
27. Braz, J.M., et al., *Parallel "pain" pathways arise from subpopulations of primary afferent nociceptor.* Neuron, 2005. **47**(6): p. 787-93.
28. Johnson, M.S., J.M. Ryals, and D.E. Wright, *Early loss of peptidergic intraepidermal nerve fibers in an STZ-induced mouse model of insensate diabetic neuropathy.* Pain, 2008. **140**(1): p. 35-47.
29. Coutaux, A., et al., *Hyperalgesia and allodynia: peripheral mechanisms.* Joint Bone Spine, 2005. **72**(5): p. 359-71.
30. Lee, Y., C.H. Lee, and U. Oh, *Painful channels in sensory neurons.* Mol Cells, 2005. **20**(3): p. 315-24.
31. Caterina, M.J., et al., *The capsaicin receptor: a heat-activated ion channel in the pain pathway.* Nature, 1997. **389**(6653): p. 816-24.
32. Chung, M.K., S.J. Jung, and S.B. Oh, *Role of TRP channels in pain sensation.* Adv Exp Med Biol, 2011. **704**: p. 615-36.
33. Caterina, M.J., et al., *Impaired nociception and pain sensation in mice lacking the capsaicin receptor.* Science, 2000. **288**(5464): p. 306-13.
34. Van Buren, J.J., et al., *Sensitization and translocation of TRPV1 by insulin and IGF-I.* Mol Pain, 2005. **1**: p. 17.
35. Lilja, J., F. Laulund, and A. Forsby, *Insulin and insulin-like growth factor type-I up-regulate the vanilloid receptor-1 (TRPV1) in stably TRPV1-expressing SH-SY5Y neuroblastoma cells.* J Neurosci Res, 2007. **85**(7): p. 1413-9.
36. Hong, S. and J.W. Wiley, *Early painful diabetic neuropathy is associated with differential changes in the expression and function of vanilloid receptor 1.* J Biol Chem, 2005. **280**(1): p. 618-27.
37. Pabbidi, R.M., et al., *Influence of TRPV1 on diabetes-induced alterations in thermal pain sensitivity.* Mol Pain, 2008. **4**: p. 9.
38. Razavi, R., et al., *TRPV1+ sensory neurons control beta cell stress and islet inflammation in autoimmune diabetes.* Cell, 2006. **127**(6): p. 1123-35.
39. Brain, S.D., *Sensory neuropeptides: their role in inflammation and wound healing.* Immunopharmacology, 1997. **37**(2-3): p. 133-52.
40. Benarroch, E.E., *CGRP: sensory neuropeptide with multiple neurologic implications.* Neurology, 2011. **77**(3): p. 281-7.
41. O'Connor, T.M., et al., *The role of substance P in inflammatory disease.* J Cell Physiol, 2004. **201**(2): p. 167-80.
42. Chiu, I.M., C.A. von Hehn, and C.J. Woolf, *Neurogenic inflammation and the peripheral nervous system in host defense and immunopathology.* Nat Neurosci, 2012. **15**(8): p. 1063-7.
43. Woolf, C.J. and R.J. Mannion, *Neuropathic pain: aetiology, symptoms, mechanisms, and management.* Lancet, 1999. **353**(9168): p. 1959-64.
44. Fuller, G., *Focal peripheral neuropathies.* J Neurol Neurosurg Psychiatry, 2003. **74 Suppl 2**: p. ii20-ii24.
45. Campbell, W.W., *Evaluation and management of peripheral nerve injury.* Clin Neurophysiol, 2008. **119**(9): p. 1951-65.

46. Chaudhry, V., J.D. Glass, and J.W. Griffin, *Wallerian degeneration in peripheral nerve disease.* Neurol Clin, 1992. **10**(3): p. 613-27.
47. Fawcett, J.W. and R.J. Keynes, *Peripheral nerve regeneration.* Annu Rev Neurosci, 1990. **13**: p. 43-60.
48. Heumann, R., et al., *Changes of nerve growth factor synthesis in nonneuronal cells in response to sciatic nerve transection.* J Cell Biol, 1987. **104**(6): p. 1623-31.
49. Funakoshi, H., et al., *Differential expression of mRNAs for neurotrophins and their receptors after axotomy of the sciatic nerve.* J Cell Biol, 1993. **123**(2): p. 455-65.
50. Fu, S.Y. and T. Gordon, *The cellular and molecular basis of peripheral nerve regeneration.* Mol Neurobiol, 1997. **14**(1-2): p. 67-116.
51. Jimenez-Andrade, J.M., et al., *Vascularization of the dorsal root ganglia and peripheral nerve of the mouse: implications for chemical-induced peripheral sensory neuropathies.* Mol Pain, 2008. **4**: p. 10.
52. Wolf, S., et al., *Chemotherapy-induced peripheral neuropathy: prevention and treatment strategies.* Eur J Cancer, 2008. **44**(11): p. 1507-15.
53. Kayser-Gatchalian, M.C. and B. Neundorfer, *Peripheral neuropathy with vitamin B12 deficiency.* J Neurol, 1977. **214**(3): p. 183-93.
54. Viaene, M.K., et al., *Cadmium: a possible etiological factor in peripheral polyneuropathy.* Neurotoxicology, 1999. **20**(1): p. 7-16.
55. Ikeda, Y., et al., *Long-term toxicity study of methylmercuric chloride in monkeys (first report).* Toxicology, 1973. **1**(4): p. 361-75.
56. Robinson-Papp, J., *Infectious neuropathies.* Continuum (Minneap Minn), 2012. **18**(1): p. 126-38.
57. Martyn, C.N. and R.A. Hughes, *Epidemiology of peripheral neuropathy.* J Neurol Neurosurg Psychiatry, 1997. **62**(4): p. 310-8.
58. Centers for Disease Control and Prevention, C., *National diabetes fact sheet: general information and national estimates on diabetes in the United States, 2007*, C. US Department of Health and Human Services, Editor 2008: Atlanta, GA.
59. Whiting, D.R., et al., *IDF diabetes atlas: global estimates of the prevalence of diabetes for 2011 and 2030.* Diabetes Res Clin Pract, 2011. **94**(3): p. 311-21.
60. Centers for Disease Control and Prevention, C., *National Diabetes Fact Sheet: National Estimates and General Information on Diabetes and Prediabetes in the United States, 2011*, C. US Department of Health and Human Services, Editor 2011, Centers of Disease Control and Prevention, 2011: Atlanta, GA.
61. Wild, S., et al., *Global prevalence of diabetes: estimates for the year 2000 and projections for 2030.* Diabetes Care, 2004. **27**(5): p. 1047-53.
62. *Standards of medical care in diabetes--2012.* Diabetes Care, 2012. **35 Suppl 1**: p. S11-63.
63. Bluestone, J.A., K. Herold, and G. Eisenbarth, *Genetics, pathogenesis and clinical interventions in type 1 diabetes.* Nature, 2010. **464**(7293): p. 1293-300.
64. Coppieters, K.T., A. Wiberg, and M.G. von Herrath, *Viral infections and molecular mimicry in type 1 diabetes.* APMIS, 2012. **120**(12): p. 941-9.
65. Roep, B.O. and M. Peakman, *Antigen targets of type 1 diabetes autoimmunity.* Cold Spring Harb Perspect Med, 2012. **2**(4): p. a007781.
66. Szkudelski, T., *The mechanism of alloxan and streptozotocin action in B cells of the rat pancreas.* Physiol Res, 2001. **50**(6): p. 537-46.
67. Christianson, J.A., et al., *Beneficial actions of neurotrophin treatment on diabetes-induced hypoalgesia in mice.* J Pain, 2003. **4**(9): p. 493-504.

68. Jack, M.M., J.M. Ryals, and D.E. Wright, *Characterisation of glyoxalase I in a streptozocin-induced mouse model of diabetes with painful and insensate neuropathy.* Diabetologia, 2011. **54**(8): p. 2174-82.
69. Makino, S., et al., *Breeding of a non-obese, diabetic strain of mice.* Jikken Dobutsu, 1980. **29**(1): p. 1-13.
70. Anderson, M.S. and J.A. Bluestone, *The NOD mouse: a model of immune dysregulation.* Annu Rev Immunol, 2005. **23**: p. 447-85.
71. Schmidt, R.E., et al., *Non-obese diabetic mice rapidly develop dramatic sympathetic neuritic dystrophy: a new experimental model of diabetic autonomic neuropathy.* Am J Pathol, 2003. **163**(5): p. 2077-91.
72. Salomon, B., et al., *Development of spontaneous autoimmune peripheral polyneuropathy in B7-2-deficient NOD mice.* J Exp Med, 2001. **194**(5): p. 677-84.
73. Kahn, S.E., R.L. Hull, and K.M. Utzschneider, *Mechanisms linking obesity to insulin resistance and type 2 diabetes.* Nature, 2006. **444**(7121): p. 840-6.
74. Muoio, D.M. and C.B. Newgard, *Mechanisms of disease: molecular and metabolic mechanisms of insulin resistance and beta-cell failure in type 2 diabetes.* Nat Rev Mol Cell Biol, 2008. **9**(3): p. 193-205.
75. Herder, C. and M. Roden, *Genetics of type 2 diabetes: pathophysiologic and clinical relevance.* Eur J Clin Invest, 2011. **41**(6): p. 679-92.
76. Srinivasan, K. and P. Ramarao, *Animal models in type 2 diabetes research: an overview.* Indian J Med Res, 2007. **125**(3): p. 451-72.
77. Drel, V.R., et al., *The leptin-deficient (ob/ob) mouse: a new animal model of peripheral neuropathy of type 2 diabetes and obesity.* Diabetes, 2006. **55**(12): p. 3335-43.
78. Sullivan, K.A., et al., *Mouse models of diabetic neuropathy.* Neurobiol Dis, 2007. **28**(3): p. 276-85.
79. Wright, D.E., et al., *Selective changes in nocifensive behavior despite normal cutaneous axon innervation in leptin receptor-null mutant (db/db) mice.* J Peripher Nerv Syst, 2007. **12**(4): p. 250-61.
80. Guilford, B.L., J.M. Ryals, and D.E. Wright, *Phenotypic changes in diabetic neuropathy induced by a high-fat diet in diabetic C57BL/6 mice.* Exp Diabetes Res, 2011. **2011**: p. 848307.
81. Habib, A.A. and T.H. Brannagan, 3rd, *Therapeutic strategies for diabetic neuropathy.* Curr Neurol Neurosci Rep, 2010. **10**(2): p. 92-100.
82. Apfel, S.C., et al., *Efficacy and safety of recombinant human nerve growth factor in patients with diabetic polyneuropathy: A randomized controlled trial. rhNGF Clinical Investigator Group.* JAMA, 2000. **284**(17): p. 2215-21.
83. Chalk, C., T.J. Benstead, and F. Moore, *Aldose reductase inhibitors for the treatment of diabetic polyneuropathy.* Cochrane Database Syst Rev, 2007(4): p. CD004572.
84. Dyck, P.J., et al., *The prevalence by staged severity of various types of diabetic neuropathy, retinopathy, and nephropathy in a population-based cohort: the Rochester Diabetic Neuropathy Study.* Neurology, 1993. **43**(4): p. 817-24.
85. Tesfaye, S. and D. Selvarajah, *Advances in the epidemiology, pathogenesis and management of diabetic peripheral neuropathy.* Diabetes Metab Res Rev, 2012. **28 Suppl 1**: p. 8-14.
86. Tesfaye, S., et al., *Vascular risk factors and diabetic neuropathy.* N Engl J Med, 2005. **352**(4): p. 341-50.
87. Hendriksen, P.H., et al., *Subclinical diabetic polyneuropathy: early detection of involvement of different nerve fibre types.* J Neurol Neurosurg Psychiatry, 1993. **56**(5): p. 509-14.
88. Gruener, G. and P.J. Dyck, *Quantitative sensory testing: methodology, applications, and future directions.* J Clin Neurophysiol, 1994. **11**(6): p. 568-83.

89. Vinik, A.I., et al., *Sural sensory action potential identifies diabetic peripheral neuropathy responders to therapy.* Muscle Nerve, 2005. **32**(5): p. 619-25.
90. Lauria, G., et al., *EFNS guidelines on the use of skin biopsy in the diagnosis of peripheral neuropathy.* Eur J Neurol, 2005. **12**(10): p. 747-58.
91. Hossain, P., A. Sachdev, and R.A. Malik, *Early detection of diabetic peripheral neuropathy with corneal confocal microscopy.* Lancet, 2005. **366**(9494): p. 1340-3.
92. Vincent, A.M., et al., *Diabetic neuropathy: cellular mechanisms as therapeutic targets.* Nat Rev Neurol, 2011. **7**(10): p. 573-83.
93. Tomlinson, D.R. and N.J. Gardiner, *Glucose neurotoxicity.* Nat Rev Neurosci, 2008. **9**(1): p. 36-45.
94. Zent, R. and A. Pozzi, *Angiogenesis in diabetic nephropathy.* Semin Nephrol, 2007. **27**(2): p. 161-71.
95. Murea, M., L. Ma, and B.I. Freedman, *Genetic and environmental factors associated with type 2 diabetes and diabetic vascular complications.* Rev Diabet Stud, 2012. **9**(1): p. 6-22.
96. Stevens, M.J., et al., *Effects of DL-alpha-lipoic acid on peripheral nerve conduction, blood flow, energy metabolism, and oxidative stress in experimental diabetic neuropathy.* Diabetes, 2000. **49**(6): p. 1006-15.
97. Laczy, B., et al., *Effects of pentoxifylline and pentosan polysulphate combination therapy on diabetic neuropathy in type 2 diabetes mellitus.* Acta Diabetol, 2009. **46**(2): p. 105-11.
98. Kuzumoto, Y., et al., *Effect of the aldose reductase inhibitor fidarestat on experimental diabetic neuropathy in the rat.* Diabetologia, 2006. **49**(12): p. 3085-93.
99. Song, Z., et al., *Transgenic mice overexpressing aldose reductase in Schwann cells show more severe nerve conduction velocity deficit and oxidative stress under hyperglycemic stress.* Mol Cell Neurosci, 2003. **23**(4): p. 638-47.
100. Bierhaus, A. and P.P. Nawroth, *Multiple levels of regulation determine the role of the receptor for AGE (RAGE) as common soil in inflammation, immune responses and diabetes mellitus and its complications.* Diabetologia, 2009. **52**(11): p. 2251-63.
101. Toth, C., et al., *Receptor for advanced glycation end products (RAGEs) and experimental diabetic neuropathy.* Diabetes, 2008. **57**(4): p. 1002-17.
102. Cameron, N.E., et al., *Inhibitors of advanced glycation end product formation and neurovascular dysfunction in experimental diabetes.* Ann N Y Acad Sci, 2005. **1043**: p. 784-92.
103. Ziegler, D., et al., *Oral treatment with alpha-lipoic acid improves symptomatic diabetic polyneuropathy: the SYDNEY 2 trial.* Diabetes Care, 2006. **29**(11): p. 2365-70.
104. Verkhratsky, A. and P. Fernyhough, *Mitochondrial malfunction and Ca2+ dyshomeostasis drive neuronal pathology in diabetes.* Cell Calcium, 2008. **44**(1): p. 112-22.
105. Andreassen, C.S., et al., *Expression of neurotrophic factors in diabetic muscle--relation to neuropathy and muscle strength.* Brain, 2009. **132**(Pt 10): p. 2724-33.
106. Calcutt, N.A., C.G. Jolivalt, and P. Fernyhough, *Growth factors as therapeutics for diabetic neuropathy.* Curr Drug Targets, 2008. **9**(1): p. 47-59.
107. Brewster, W.J., et al., *Diabetic neuropathy, nerve growth factor and other neurotrophic factors.* Trends Neurosci, 1994. **17**(8): p. 321-5.
108. Tomlinson, D.R., P. Fernyhough, and L.T. Diemel, *Role of neurotrophins in diabetic neuropathy and treatment with nerve growth factors.* Diabetes, 1997. **46 Suppl 2**: p. S43-9.
109. Christianson, J.A., et al., *Neurotrophic modulation of myelinated cutaneous innervation and mechanical sensory loss in diabetic mice.* Neuroscience, 2007. **145**(1): p. 303-13.
110. Callaghan, B.C., et al., *Enhanced glucose control for preventing and treating diabetic neuropathy.* Cochrane Database Syst Rev, 2012. **6**: p. CD007543.
111. Martin, C.L., et al., *Neuropathy among the diabetes control and complications trial cohort 8 years after trial completion.* Diabetes Care, 2006. **29**(2): p. 340-4.

112. Bril, V., et al., *Evidence-based guideline: Treatment of painful diabetic neuropathy: report of the American Academy of Neurology, the American Association of Neuromuscular and Electrodiagnostic Medicine, and the American Academy of Physical Medicine and Rehabilitation.* Neurology, 2011. **76**(20): p. 1758-65.
113. Owerbach, D., et al., *The insulin gene is located on chromosome 11 in humans.* Nature, 1980. **286**(5768): p. 82-4.
114. Wentworth, B.M., et al., *Characterization of the two nonallelic genes encoding mouse preproinsulin.* J Mol Evol, 1986. **23**(4): p. 305-12.
115. Steiner, D.F., et al., *A brief perspective on insulin production.* Diabetes Obes Metab, 2009. **11 Suppl 4**: p. 189-96.
116. Joslin, E.P. and C.R. Kahn, *Joslin's diabetes mellitus*. 14th ed2005, Philadelphia, Pa.: Lippincott Williams & Willkins. xiv, 1209 p.
117. Duckworth, W.C., R.G. Bennett, and F.G. Hamel, *Insulin degradation: progress and potential.* Endocr Rev, 1998. **19**(5): p. 608-24.
118. Hou, J.C., L. Min, and J.E. Pessin, *Insulin granule biogenesis, trafficking and exocytosis.* Vitam Horm, 2009. **80**: p. 473-506.
119. Levin, M.S., et al., *Developmental changes in the expression of genes involved in cholesterol biosynthesis and lipid transport in human and rat fetal and neonatal livers.* Biochim Biophys Acta, 1989. **1003**(3): p. 293-300.
120. Ebina, Y., et al., *The human insulin receptor cDNA: the structural basis for hormone-activated transmembrane signalling.* Cell, 1985. **40**(4): p. 747-58.
121. Wang, L.M., et al., *Chromosome assignment of mouse insulin, colony stimulating factor 1, and low-density lipoprotein receptors.* Genomics, 1988. **3**(2): p. 172-6.
122. Kaletsky, R. and C.T. Murphy, *The role of insulin/IGF-like signaling in C. elegans longevity and aging.* Dis Model Mech, 2010. **3**(7-8): p. 415-9.
123. Brogiolo, W., et al., *An evolutionarily conserved function of the Drosophila insulin receptor and insulin-like peptides in growth control.* Curr Biol, 2001. **11**(4): p. 213-21.
124. Seino, S., et al., *Structure of the human insulin receptor gene and characterization of its promoter.* Proc Natl Acad Sci U S A, 1989. **86**(1): p. 114-8.
125. Seino, S. and G.I. Bell, *Alternative splicing of human insulin receptor messenger RNA.* Biochem Biophys Res Commun, 1989. **159**(1): p. 312-6.
126. Moller, D.E., et al., *Tissue-specific expression of two alternatively spliced insulin receptor mRNAs in man.* Mol Endocrinol, 1989. **3**(8): p. 1263-9.
127. Mosthaf, L., et al., *Functionally distinct insulin receptors generated by tissue-specific alternative splicing.* EMBO J, 1990. **9**(8): p. 2409-13.
128. Sciacca, L., et al., *Signaling differences from the A and B isoforms of the insulin receptor (IR) in 32D cells in the presence or absence of IR substrate-1.* Endocrinology, 2003. **144**(6): p. 2650-8.
129. Accili, D., et al., *Early neonatal death in mice homozygous for a null allele of the insulin receptor gene.* Nat Genet, 1996. **12**(1): p. 106-9.
130. Wertheimer, E., et al., *Homozygous deletion of the human insulin receptor gene results in leprechaunism.* Nat Genet, 1993. **5**(1): p. 71-3.
131. Bruning, J.C., et al., *A muscle-specific insulin receptor knockout exhibits features of the metabolic syndrome of NIDDM without altering glucose tolerance.* Mol Cell, 1998. **2**(5): p. 559-69.
132. Bluher, M., et al., *Adipose tissue selective insulin receptor knockout protects against obesity and obesity-related glucose intolerance.* Dev Cell, 2002. **3**(1): p. 25-38.
133. Bluher, M., B.B. Kahn, and C.R. Kahn, *Extended longevity in mice lacking the insulin receptor in adipose tissue.* Science, 2003. **299**(5606): p. 572-4.

134. Guerra, C., et al., *Brown adipose tissue-specific insulin receptor knockout shows diabetic phenotype without insulin resistance.* J Clin Invest, 2001. **108**(8): p. 1205-13.
135. Kulkarni, R.N., et al., *Tissue-specific knockout of the insulin receptor in pancreatic beta cells creates an insulin secretory defect similar to that in type 2 diabetes.* Cell, 1999. **96**(3): p. 329-39.
136. Michael, M.D., et al., *Loss of insulin signaling in hepatocytes leads to severe insulin resistance and progressive hepatic dysfunction.* Mol Cell, 2000. **6**(1): p. 87-97.
137. Bruning, J.C., et al., *Role of brain insulin receptor in control of body weight and reproduction.* Science, 2000. **289**(5487): p. 2122-5.
138. Le Roith, D. and Y. Zick, *Recent advances in our understanding of insulin action and insulin resistance.* Diabetes Care, 2001. **24**(3): p. 588-97.
139. Taniguchi, C.M., B. Emanuelli, and C.R. Kahn, *Critical nodes in signalling pathways: insights into insulin action.* Nat Rev Mol Cell Biol, 2006. **7**(2): p. 85-96.
140. Takamoto, I., et al., *Crucial role of insulin receptor substrate-2 in compensatory beta-cell hyperplasia in response to high fat diet-induced insulin resistance.* Diabetes Obes Metab, 2008. **10 Suppl 4**: p. 147-56.
141. Skaper, S.D., I. Selak, and S. Varon, *Molecular requirements for survival of cultured avian and rodent dorsal root ganglionic neurons responding to different trophic factors.* J Neurosci Res, 1982. **8**(2-3): p. 251-61.
142. Recio-Pinto, E., M.M. Rechler, and D.N. Ishii, *Effects of insulin, insulin-like growth factor-II, and nerve growth factor on neurite formation and survival in cultured sympathetic and sensory neurons.* J Neurosci, 1986. **6**(5): p. 1211-9.
143. Greene, D.A. and A.I. Winegrad, *In vitro studies of the substrates for energy production and the effects of insulin on glucose utilization in the neural components of peripheral nerve.* Diabetes, 1979. **28**(10): p. 878-87.
144. Patel, N.J., et al., *Glucose and leucine uptake by rat dorsal root ganglia is not insulin sensitive.* J Neurol Sci, 1994. **121**(2): p. 159-62.
145. Plum, L., M. Schubert, and J.C. Bruning, *The role of insulin receptor signaling in the brain.* Trends Endocrinol Metab, 2005. **16**(2): p. 59-65.
146. Choeiri, C., W. Staines, and C. Messier, *Immunohistochemical localization and quantification of glucose transporters in the mouse brain.* Neuroscience, 2002. **111**(1): p. 19-34.
147. Leloup, C., et al., *Discrete brain areas express the insulin-responsive glucose transporter GLUT4.* Brain Res Mol Brain Res, 1996. **38**(1): p. 45-53.
148. Sokoloff, L., *Metabolism of ketone bodies by the brain.* Annu Rev Med, 1973. **24**: p. 271-80.
149. Baura, G.D., et al., *Saturable transport of insulin from plasma into the central nervous system of dogs in vivo. A mechanism for regulated insulin delivery to the brain.* J Clin Invest, 1993. **92**(4): p. 1824-30.
150. Wang, Y.Y., P.C. Lui, and J.Y. Li, *Receptor-mediated therapeutic transport across the blood-brain barrier.* Immunotherapy, 2009. **1**(6): p. 983-93.
151. Hu, G., et al., *Type 2 diabetes and the risk of Parkinson's disease.* Diabetes Care, 2007. **30**(4): p. 842-7.
152. Luchsinger, J.A., et al., *Diabetes mellitus and risk of Alzheimer's disease and dementia with stroke in a multiethnic cohort.* Am J Epidemiol, 2001. **154**(7): p. 635-41.
153. Akter, K., et al., *Diabetes mellitus and Alzheimer's disease: shared pathology and treatment?* Br J Clin Pharmacol, 2011. **71**(3): p. 365-76.
154. Talbot, K., et al., *Demonstrated brain insulin resistance in Alzheimer's disease patients is associated with IGF-1 resistance, IRS-1 dysregulation, and cognitive decline.* J Clin Invest, 2012. **122**(4): p. 1316-38.

155. Pedersen, W.A., et al., *Rosiglitazone attenuates learning and memory deficits in Tg2576 Alzheimer mice.* Exp Neurol, 2006. **199**(2): p. 265-73.
156. Sato, T., et al., *Efficacy of PPAR-gamma agonist pioglitazone in mild Alzheimer disease.* Neurobiol Aging, 2011. **32**(9): p. 1626-33.
157. Park, C.R., et al., *Intracerebroventricular insulin enhances memory in a passive-avoidance task.* Physiol Behav, 2000. **68**(4): p. 509-14.
158. McNay, E.C., et al., *Hippocampal memory processes are modulated by insulin and high-fat-induced insulin resistance.* Neurobiol Learn Mem, 2010. **93**(4): p. 546-53.
159. Haj-ali, V., G. Mohaddes, and S.H. Babri, *Intracerebroventricular insulin improves spatial learning and memory in male Wistar rats.* Behav Neurosci, 2009. **123**(6): p. 1309-14.
160. Chiu, S.L., C.M. Chen, and H.T. Cline, *Insulin receptor signaling regulates synapse number, dendritic plasticity, and circuit function in vivo.* Neuron, 2008. **58**(5): p. 708-19.
161. Craft, S., et al., *Intranasal Insulin Therapy for Alzheimer Disease and Amnestic Mild Cognitive Impairment: A Pilot Clinical Trial.* Arch Neurol, 2011.
162. Gerozissis, K., *Brain insulin, energy and glucose homeostasis; genes, environment and metabolic pathologies.* Eur J Pharmacol, 2008. **585**(1): p. 38-49.
163. Spanswick, D., et al., *Insulin activates ATP-sensitive K+ channels in hypothalamic neurons of lean, but not obese rats.* Nat Neurosci, 2000. **3**(8): p. 757-8.
164. Obici, S., et al., *Decreasing hypothalamic insulin receptors causes hyperphagia and insulin resistance in rats.* Nat Neurosci, 2002. **5**(6): p. 566-72.
165. Obici, S., et al., *Hypothalamic insulin signaling is required for inhibition of glucose production.* Nat Med, 2002. **8**(12): p. 1376-82.
166. Khan, F.A., et al., *Insulin activates ATP-sensitive K(+) channels in pancreatic beta-cells through a phosphatidylinositol 3-kinase-dependent pathway.* Diabetes, 2001. **50**(10): p. 2192-8.
167. Kim, S.J. and Y. Han, *Insulin inhibits AMPA-induced neuronal damage via stimulation of protein kinase B (Akt).* J Neural Transm, 2005. **112**(2): p. 179-91.
168. Spicarova, D. and J. Palecek, *Modulation of AMPA excitatory postsynaptic currents in the spinal cord dorsal horn neurons by insulin.* Neuroscience, 2010. **166**(1): p. 305-11.
169. Chiu, S.L. and H.T. Cline, *Insulin receptor signaling in the development of neuronal structure and function.* Neural Dev, 2010. **5**: p. 7.
170. Sugimoto, K., Y. Murakawa, and A.A. Sima, *Expression and localization of insulin receptor in rat dorsal root ganglion and spinal cord.* J Peripher Nerv Syst, 2002. **7**(1): p. 44-53.
171. Sugimoto, K., et al., *Insulin receptor in rat peripheral nerve: its localization and alternatively spliced isoforms.* Diabetes Metab Res Rev, 2000. **16**(5): p. 354-63.
172. Shettar, A. and G. Muttagi, *Developmental regulation of insulin receptor gene in sciatic nerves and role of insulin on glycoprotein P0 in the Schwann cells.* Peptides, 2012. **36**(1): p. 46-53.
173. Baiou, D., et al., *Neurochemical characterization of insulin receptor-expressing primary sensory neurons in wild-type and vanilloid type 1 transient receptor potential receptor knockout mice.* J Comp Neurol, 2007. **503**(2): p. 334-47.
174. Guo, G., et al., *Local insulin and the rapid regrowth of diabetic epidermal axons.* Neurobiol Dis, 2011. **43**(2): p. 414-21.
175. Singh, B., et al., *Resistance to trophic neurite outgrowth of sensory neurons exposed to insulin.* J Neurochem, 2012.
176. Fernyhough, P., et al., *Insulin and insulin-like growth factor I enhance regeneration in cultured adult rat sensory neurones.* Brain Res, 1993. **607**(1-2): p. 117-24.
177. Jones, D.M., et al., *The synergistic effects of NGF and IGF-1 on neurite growth in adult sensory neurons: convergence on the PI 3-kinase signaling pathway.* J Neurochem, 2003. **86**(5): p. 1116-28.

178. Recio-Pinto, E., F.F. Lang, and D.N. Ishii, *Insulin and insulin-like growth factor II permit nerve growth factor binding and the neurite formation response in cultured human neuroblastoma cells.* Proc Natl Acad Sci U S A, 1984. **81**(8): p. 2562-6.
179. Fernyhough, P., et al., *Stabilization of tubulin mRNAs by insulin and insulin-like growth factor I during neurite formation.* Brain Res Mol Brain Res, 1989. **6**(2-3): p. 109-20.
180. Li, Z.G., W. Zhang, and A.A. Sima, *C-peptide enhances insulin-mediated cell growth and protection against high glucose-induced apoptosis in SH-SY5Y cells.* Diabetes Metab Res Rev, 2003. **19**(5): p. 375-85.
181. Kim, B., et al., *Hyperinsulinemia Induces Insulin Resistance in Dorsal Root Ganglion Neurons.* Endocrinology, 2011.
182. Datta, S.R., et al., *Akt phosphorylation of BAD couples survival signals to the cell-intrinsic death machinery.* Cell, 1997. **91**(2): p. 231-41.
183. Shetter, A.R., G. Muttagi, and C.B. Sagar, *Expression and localization of insulin receptors in dissociated primary cultures of rat Schwann cells.* Cell Biol Int, 2011. **35**(3): p. 299-304.
184. Xu, Q.G., et al., *Insulin as an in vivo growth factor.* Exp Neurol, 2004. **188**(1): p. 43-51.
185. Toth, C., et al., *Rescue and regeneration of injured peripheral nerve axons by intrathecal insulin.* Neuroscience, 2006. **139**(2): p. 429-49.
186. *The effect of intensive diabetes therapy on the development and progression of neuropathy. The Diabetes Control and Complications Trial Research Group.* Ann Intern Med, 1995. **122**(8): p. 561-8.
187. *Effect of intensive diabetes treatment on nerve conduction in the Diabetes Control and Complications Trial.* Ann Neurol, 1995. **38**(6): p. 869-80.
188. Romanovsky, D., et al., *Comparison of metabolic and neuropathy profiles of rats with streptozotocin-induced overt and moderate insulinopenia.* Neuroscience, 2010. **170**(1): p. 337-47.
189. Romanovsky, D., et al., *Mechanical hyperalgesia correlates with insulin deficiency in normoglycemic streptozotocin-treated rats.* Neurobiol Dis, 2006. **24**(2): p. 384-94.
190. Murakawa, Y., et al., *Impaired glucose tolerance and insulinopenia in the GK-rat causes peripheral neuropathy.* Diabetes Metab Res Rev, 2002. **18**(6): p. 473-83.
191. Brussee, V., F.A. Cunningham, and D.W. Zochodne, *Direct insulin signaling of neurons reverses diabetic neuropathy.* Diabetes, 2004. **53**(7): p. 1824-30.
192. Sugimoto, K., et al., *Early changes in insulin receptor signaling and pain sensation in streptozotocin-induced diabetic neuropathy in rats.* J Pain, 2008. **9**(3): p. 237-45.
193. Toth, C., V. Brussee, and D.W. Zochodne, *Remote neurotrophic support of epidermal nerve fibres in experimental diabetes.* Diabetologia, 2006. **49**(5): p. 1081-8.
194. Hoybergs, Y.M. and T.F. Meert, *The effect of low-dose insulin on mechanical sensitivity and allodynia in type I diabetes neuropathy.* Neurosci Lett, 2007. **417**(2): p. 149-54.
195. Cheng, Z., Y. Tseng, and M.F. White, *Insulin signaling meets mitochondria in metabolism.* Trends Endocrinol Metab, 2010. **21**(10): p. 589-98.
196. Huang, T.J., et al., *Insulin prevents depolarization of the mitochondrial inner membrane in sensory neurons of type 1 diabetic rats in the presence of sustained hyperglycemia.* Diabetes, 2003. **52**(8): p. 2129-36.
197. Huang, T.J., A. Verkhratsky, and P. Fernyhough, *Insulin enhances mitochondrial inner membrane potential and increases ATP levels through phosphoinositide 3-kinase in adult sensory neurons.* Mol Cell Neurosci, 2005. **28**(1): p. 42-54.
198. Chowdhury, S.K., et al., *Mitochondrial respiratory chain dysfunction in dorsal root ganglia of streptozotocin-induced diabetic rats and its correction by insulin treatment.* Diabetes, 2010. **59**(4): p. 1082-91.

199. Francis, G.J., et al., *Motor end plate innervation loss in diabetes and the role of insulin.* J Neuropathol Exp Neurol, 2011. **70**(5): p. 323-39.
200. Grote, C.W., et al., *Insulin receptor substrate 2 expression and involvement in neuronal insulin resistance in diabetic neuropathy.* Exp Diabetes Res, 2011. **2011**: p. 212571.
201. Francis, G., et al., *Intranasal insulin ameliorates experimental diabetic neuropathy.* Diabetes, 2009. **58**(4): p. 934-45.
202. Fex Svenningsen, A. and M. Kanje, *Insulin and the insulin-like growth factors I and II are mitogenic to cultured rat sciatic nerve segments and stimulate [3H]thymidine incorporation through their respective receptors.* Glia, 1996. **18**(1): p. 68-72.
203. Ogata, T., et al., *Opposing extracellular signal-regulated kinase and Akt pathways control Schwann cell myelination.* J Neurosci, 2004. **24**(30): p. 6724-32.
204. Liang, G., G.W. Cline, and C.M. Macica, *IGF-1 stimulates de novo fatty acid biosynthesis by Schwann cells during myelination.* Glia, 2007. **55**(6): p. 632-41.
205. Eckersley, L., *Role of the Schwann cell in diabetic neuropathy.* Int Rev Neurobiol, 2002. **50**: p. 293-321.
206. Makoukji, J., et al., *Lithium enhances remyelination of peripheral nerves.* Proc Natl Acad Sci U S A, 2012. **109**(10): p. 3973-8.
207. Kramer, H.F., et al., *AS160 regulates insulin- and contraction-stimulated glucose uptake in mouse skeletal muscle.* J Biol Chem, 2006. **281**(42): p. 31478-85.
208. Magnani, P., et al., *Regulation of glucose transport in cultured Schwann cells.* J Peripher Nerv Syst, 1998. **3**(1): p. 28-36.
209. Kan, M., et al., *Glucagon-like peptide 1, insulin, sensory neurons, and diabetic neuropathy.* J Neuropathol Exp Neurol, 2012. **71**(6): p. 494-510.
210. Boura-Halfon, S. and Y. Zick, *Phosphorylation of IRS proteins, insulin action, and insulin resistance.* Am J Physiol Endocrinol Metab, 2009. **296**(4): p. E581-91.
211. Wu, J., et al., *Structural and biochemical characterization of the KRLB region in insulin receptor substrate-2.* Nat Struct Mol Biol, 2008. **15**(3): p. 251-8.
212. Sun, X.J. and F. Liu, *Phosphorylation of IRS proteins Yin-Yang regulation of insulin signaling.* Vitam Horm, 2009. **80**: p. 351-87.
213. Kahn, C.R., *Knockout mice challenge our concepts of glucose homeostasis and the pathogenesis of diabetes.* Exp Diabesity Res, 2003. **4**(3): p. 169-82.
214. Gupte, A.A., G.L. Bomhoff, and P.C. Geiger, *Age-related differences in skeletal muscle insulin signaling: the role of stress kinases and heat shock proteins.* J Appl Physiol, 2008. **105**(3): p. 839-48.
215. Freude, S., et al., *IRS-2 branch of IGF-1 receptor signaling is essential for appropriate timing of myelination.* J Neurochem, 2008. **107**(4): p. 907-17.
216. Werner, E.D., et al., *Insulin resistance due to phosphorylation of insulin receptor substrate-1 at serine 302.* J Biol Chem, 2004. **279**(34): p. 35298-305.
217. Paz, K., et al., *A molecular basis for insulin resistance. Elevated serine/threonine phosphorylation of IRS-1 and IRS-2 inhibits their binding to the juxtamembrane region of the insulin receptor and impairs their ability to undergo insulin-induced tyrosine phosphorylation.* J Biol Chem, 1997. **272**(47): p. 29911-8.
218. Lee, Y.H., et al., *c-Jun N-terminal kinase (JNK) mediates feedback inhibition of the insulin signaling cascade.* J Biol Chem, 2003. **278**(5): p. 2896-902.
219. Mayer, C.M. and D.D. Belsham, *Central insulin signaling is attenuated by long-term insulin exposure via insulin receptor substrate-1 serine phosphorylation, proteasomal degradation, and lysosomal insulin receptor degradation.* Endocrinology, 2010. **151**(1): p. 75-84.

220. Aguirre, V., et al., *The c-Jun NH(2)-terminal kinase promotes insulin resistance during association with insulin receptor substrate-1 and phosphorylation of Ser(307).* J Biol Chem, 2000. **275**(12): p. 9047-54.
221. Scioscia, M., et al., *Insulin resistance in human preeclamptic placenta is mediated by serine phosphorylation of insulin receptor substrate-1 and -2.* J Clin Endocrinol Metab, 2006. **91**(2): p. 709-17.
222. Tanti, J.F. and J. Jager, *Cellular mechanisms of insulin resistance: role of stress-regulated serine kinases and insulin receptor substrates (IRS) serine phosphorylation.* Curr Opin Pharmacol, 2009. **9**(6): p. 753-62.
223. Wellen, K.E. and G.S. Hotamisligil, *Inflammation, stress, and diabetes.* J Clin Invest, 2005. **115**(5): p. 1111-9.
224. Thomson, M.J., M.G. Williams, and S.C. Frost, *Development of insulin resistance in 3T3-L1 adipocytes.* J Biol Chem, 1997. **272**(12): p. 7759-64.
225. Malin, S.A., B.M. Davis, and D.C. Molliver, *Production of dissociated sensory neuron cultures and considerations for their use in studying neuronal function and plasticity.* Nat Protoc, 2007. **2**(1): p. 152-60.
226. Zherebitskaya, E., et al., *Development of selective axonopathy in adult sensory neurons isolated from diabetic rats: role of glucose-induced oxidative stress.* Diabetes, 2009. **58**(6): p. 1356-64.
227. Akude, E., et al., *Diminished superoxide generation is associated with respiratory chain dysfunction and changes in the mitochondrial proteome of sensory neurons from diabetic rats.* Diabetes, 2011. **60**(1): p. 288-97.
228. Blacklock, A.D., et al., *Estrogen increases sensory nociceptor neuritogenesis in vitro by a direct, nerve growth factor-independent mechanism.* Eur J Neurosci, 2005. **21**(9): p. 2320-8.
229. Ye, P., et al., *Deficient expression of insulin receptor substrate-1 (IRS-1) fails to block insulin-like growth factor-I (IGF-I) stimulation of brain growth and myelination.* Brain Res Dev Brain Res, 2002. **136**(2): p. 111-21.
230. Pardini, A.W., et al., *Distribution of insulin receptor substrate-2 in brain areas involved in energy homeostasis.* Brain Res, 2006. **1112**(1): p. 169-78.
231. Schubert, M., et al., *Insulin receptor substrate-2 deficiency impairs brain growth and promotes tau phosphorylation.* J Neurosci, 2003. **23**(18): p. 7084-92.
232. Rui, L., et al., *Regulation of insulin/insulin-like growth factor-1 signaling by proteasome-mediated degradation of insulin receptor substrate-2.* J Biol Chem, 2001. **276**(43): p. 40362-7.
233. Dudek, H., et al., *Regulation of neuronal survival by the serine-threonine protein kinase Akt.* Science, 1997. **275**(5300): p. 661-5.
234. Gupte, A.A., et al., *Lipoic acid increases heat shock protein expression and inhibits stress kinase activation to improve insulin signaling in skeletal muscle from high-fat-fed rats.* J Appl Physiol, 2009. **106**(4): p. 1425-34.
235. Craner, M.J., et al., *Preferential expression of IGF-I in small DRG neurons and down-regulation following injury.* Neuroreport, 2002. **13**(13): p. 1649-52.
236. Giovannone, B., et al., *Insulin receptor substrate (IRS) transduction system: distinct and overlapping signaling potential.* Diabetes Metab Res Rev, 2000. **16**(6): p. 434-41.
237. Sullivan, K.A., B. Kim, and E.L. Feldman, *Insulin-like growth factors in the peripheral nervous system.* Endocrinology, 2008. **149**(12): p. 5963-71.
238. Kilpatrick, E.S., A.S. Rigby, and S.L. Atkin, *Insulin resistance, the metabolic syndrome, and complication risk in type 1 diabetes: "double diabetes" in the Diabetes Control and Complications Trial.* Diabetes Care, 2007. **30**(3): p. 707-12.

239. Schauer, I.E., et al., *Insulin resistance, defective insulin-mediated fatty acid suppression, and coronary artery calcification in subjects with and without type 1 diabetes: The CACTI study.* Diabetes, 2011. **60**(1): p. 306-14.
240. DeFronzo, R.A., R. Hendler, and D. Simonson, *Insulin resistance is a prominent feature of insulin-dependent diabetes.* Diabetes, 1982. **31**(9): p. 795-801.
241. Orchard, T.J., et al., *Insulin resistance-related factors, but not glycemia, predict coronary artery disease in type 1 diabetes: 10-year follow-up data from the Pittsburgh Epidemiology of Diabetes Complications Study.* Diabetes Care, 2003. **26**(5): p. 1374-9.
242. Ueno, M., et al., *Regulation of insulin signalling by hyperinsulinaemia: role of IRS-1/2 serine phosphorylation and the mTOR/p70 S6K pathway.* Diabetologia, 2005. **48**(3): p. 506-18.
243. Hirosumi, J., et al., *A central role for JNK in obesity and insulin resistance.* Nature, 2002. **420**(6913): p. 333-6.
244. Zick, Y., *Ser/Thr phosphorylation of IRS proteins: a molecular basis for insulin resistance.* Sci STKE, 2005. **2005**(268): p. pe4.
245. MacAulay, K., et al., *Glycogen synthase kinase 3alpha-specific regulation of murine hepatic glycogen metabolism.* Cell Metab, 2007. **6**(4): p. 329-37.
246. Krebs, M., et al., *The Mammalian target of rapamycin pathway regulates nutrient-sensitive glucose uptake in man.* Diabetes, 2007. **56**(6): p. 1600-7.
247. Jiang, G., et al., *Salicylic acid reverses phorbol 12-myristate-13-acetate (PMA)- and tumor necrosis factor alpha (TNFalpha)-induced insulin receptor substrate 1 (IRS1) serine 307 phosphorylation and insulin resistance in human embryonic kidney 293 (HEK293) cells.* J Biol Chem, 2003. **278**(1): p. 180-6.
248. Herschkovitz, A., et al., *Common inhibitory serine sites phosphorylated by IRS-1 kinases, triggered by insulin and inducers of insulin resistance.* J Biol Chem, 2007. **282**(25): p. 18018-27.
249. Liu, Y.F., et al., *Serine phosphorylation proximal to its phosphotyrosine binding domain inhibits insulin receptor substrate 1 function and promotes insulin resistance.* Mol Cell Biol, 2004. **24**(21): p. 9668-81.
250. Broughton, S. and L. Partridge, *Insulin/IGF-like signalling, the central nervous system and aging.* Biochem J, 2009. **418**(1): p. 1-12.
251. Sima, A.A., *Encephalopathies: the emerging diabetic complications.* Acta Diabetol, 2010. **47**(4): p. 279-93.
252. Morris, J.K., et al., *Neurodegeneration in an animal model of Parkinson's disease is exacerbated by a high-fat diet.* Am J Physiol Regul Integr Comp Physiol, 2010. **299**(4): p. R1082-90.
253. Kim, B. and E.L. Feldman, *Insulin resistance in the nervous system.* Trends Endocrinol Metab, 2012. **23**(3): p. 133-41.
254. Lee, K.O., et al., *Insulin resistance is independently associated with peripheral and autonomic neuropathy in Korean type 2 diabetic patients.* Acta Diabetol, 2010.
255. Ojamaa, K., et al., *Defects in human insulin receptor gene expression.* Mol Endocrinol, 1988. **2**(3): p. 242-7.
256. Knutson, V.P., G.V. Ronnett, and M.D. Lane, *Control of insulin receptor level in 3T3 cells: effect of insulin-induced down-regulation and dexamethasone-induced up-regulation on rate of receptor inactivation.* Proc Natl Acad Sci U S A, 1982. **79**(9): p. 2822-6.
257. Green, A. and J.M. Olefsky, *Evidence for insulin-induced internalization and degradation of insulin receptors in rat adipocytes.* Proc Natl Acad Sci U S A, 1982. **79**(2): p. 427-31.
258. Kenner, K.A., et al., *Protein-tyrosine phosphatase 1B is a negative regulator of insulin- and insulin-like growth factor-I-stimulated signaling.* J Biol Chem, 1996. **271**(33): p. 19810-6.
259. Gum, R.J., et al., *Reduction of protein tyrosine phosphatase 1B increases insulin-dependent signaling in ob/ob mice.* Diabetes, 2003. **52**(1): p. 21-8.

260. Elchebly, M., et al., *Increased insulin sensitivity and obesity resistance in mice lacking the protein tyrosine phosphatase-1B gene.* Science, 1999. **283**(5407): p. 1544-8.
261. Kim, M.K., et al., *PAR-5359, a well-balanced PPARalpha/gamma dual agonist, exhibits equivalent antidiabetic and hypolipidemic activities in vitro and in vivo.* Eur J Pharmacol, 2008. **595**(1-3): p. 119-25.
262. Chaplan, S.R., et al., *Quantitative assessment of tactile allodynia in the rat paw.* J Neurosci Methods, 1994. **53**(1): p. 55-63.
263. Kim, B., et al., *Cortical neurons develop insulin resistance and blunted Akt signaling: a potential mechanism contributing to enhanced ischemic injury in diabetes.* Antioxid Redox Signal, 2011. **14**(10): p. 1829-39.
264. Bitar, M.S. and F. Al-Mulla, *ROS constitute a convergence nexus in the development of IGF1 resistance and impaired wound healing in a rat model of type 2 diabetes.* Dis Model Mech, 2012.
265. Gavin, J.R., 3rd, et al., *Insulin-dependent regulation of insulin receptor concentrations: a direct demonstration in cell culture.* Proc Natl Acad Sci U S A, 1974. **71**(1): p. 84-8.
266. Dicou, E., S. Attoub, and P. Gressens, *Neuroprotective effects of leptin in vivo and in vitro.* Neuroreport, 2001. **12**(18): p. 3947-51.
267. Nguyen, M.T., et al., *JNK and tumor necrosis factor-alpha mediate free fatty acid-induced insulin resistance in 3T3-L1 adipocytes.* J Biol Chem, 2005. **280**(42): p. 35361-71.
268. Langlais, P., et al., *Global IRS-1 phosphorylation analysis in insulin resistance.* Diabetologia, 2011.
269. Gu, H., et al., *Deletion of a DNA polymerase beta gene segment in T cells using cell type-specific gene targeting.* Science, 1994. **265**(5168): p. 103-6.
270. Zhou, X., et al., *Deletion of PIK3C3/Vps34 in sensory neurons causes rapid neurodegeneration by disrupting the endosomal but not the autophagic pathway.* Proc Natl Acad Sci U S A, 2010. **107**(20): p. 9424-9.
271. Abe, N., et al., *Mammalian target of rapamycin (mTOR) activation increases axonal growth capacity of injured peripheral nerves.* J Biol Chem, 2010. **285**(36): p. 28034-43.
272. Zurborg, S., et al., *Generation and characterization of an Advillin-Cre driver mouse line.* Mol Pain, 2011. **7**: p. 66.
273. Minett, M.S., et al., *Distinct Nav1.7-dependent pain sensations require different sets of sensory and sympathetic neurons.* Nat Commun, 2012. **3**: p. 791.
274. Hasegawa, H., et al., *Analyzing somatosensory axon projections with the sensory neuron-specific Advillin gene.* J Neurosci, 2007. **27**(52): p. 14404-14.
275. Rogers, D.C., et al., *SHIRPA, a protocol for behavioral assessment: validation for longitudinal study of neurological dysfunction in mice.* Neurosci Lett, 2001. **306**(1-2): p. 89-92.
276. Fowler, S.C., et al., *A force-plate actometer for quantitating rodent behaviors: illustrative data on locomotion, rotation, spatial patterning, stereotypies, and tremor.* J Neurosci Methods, 2001. **107**(1-2): p. 107-24.
277. Hargreaves, K., et al., *A new and sensitive method for measuring thermal nociception in cutaneous hyperalgesia.* Pain, 1988. **32**(1): p. 77-88.
278. Dixon, W.J., *Efficient analysis of experimental observations.* Annu Rev Pharmacol Toxicol, 1980. **20**: p. 441-62.
279. Lalonde, R., A.N. Bensoula, and M. Filali, *Rotorod sensorimotor learning in cerebellar mutant mice.* Neurosci Res, 1995. **22**(4): p. 423-6.
280. Jack, M.M., J.M. Ryals, and D.E. Wright, *Protection from diabetes-induced peripheral sensory neuropathy--a role for elevated glyoxalase I?* Exp Neurol, 2012. **234**(1): p. 62-9.
281. Nassar, M.A., et al., *Nociceptor-specific gene deletion reveals a major role for Nav1.7 (PN1) in acute and inflammatory pain.* Proc Natl Acad Sci U S A, 2004. **101**(34): p. 12706-11.

282. Fasanella, K.E., et al., *Distribution and neurochemical identification of pancreatic afferents in the mouse.* J Comp Neurol, 2008. **509**(1): p. 42-52.
283. Tsui, H., et al., *'Sensing' autoimmunity in type 1 diabetes.* Trends Mol Med, 2007. **13**(10): p. 405-13.
284. Brissova, M. and A.C. Powers, *Revascularization of transplanted islets: can it be improved?* Diabetes, 2008. **57**(9): p. 2269-71.
285. Ahren, B., *Autonomic regulation of islet hormone secretion--implications for health and disease.* Diabetologia, 2000. **43**(4): p. 393-410.
286. MacGregor, R.R., et al., *Small rat islets are superior to large islets in in vitro function and in transplantation outcomes.* Am J Physiol Endocrinol Metab, 2006. **290**(5): p. E771-9.
287. Chirivella, L., et al., *IRS2 signalling is required for the development of a subset of sensory spinal neurons.* Eur J Neurosci, 2012. **35**(3): p. 341-52.
288. Sathianathan, V., et al., *Insulin induces cobalt uptake in a subpopulation of rat cultured primary sensory neurons.* Eur J Neurosci, 2003. **18**(9): p. 2477-86.
289. Tsui, H., et al., *Islet glia, neurons, and beta cells.* Ann N Y Acad Sci, 2008. **1150**: p. 32-42.
290. Hermansen, K. and B. Ahren, *Dual effects of calcitonin gene-related peptide on insulin secretion in the perfused dog pancreas.* Regul Pept, 1990. **27**(1): p. 149-57.
291. Fu, X.W. and A.M. Sun, *Stimulative effect of substance P on insulin secretion from isolated rat islets under normobaric oxygen incubation.* Zhongguo Yao Li Xue Bao, 1989. **10**(1): p. 69-73.
292. Khachatryan, A., et al., *Targeted expression of the neuropeptide calcitonin gene-related peptide to beta cells prevents diabetes in NOD mice.* J Immunol, 1997. **158**(3): p. 1409-16.
293. Radu, B.M., et al., *TRPV1 Properties in Thoracic Dorsal Root Ganglia Neurons are Modulated by Intraperitoneal Capsaicin Administration in the Late Phase of Type-1 Autoimmune Diabetes.* Cell Mol Neurobiol, 2013. **33**(2): p. 187-96.
294. Gram, D.X., et al., *Capsaicin-sensitive sensory fibers in the islets of Langerhans contribute to defective insulin secretion in Zucker diabetic rat, an animal model for some aspects of human type 2 diabetes.* Eur J Neurosci, 2007. **25**(1): p. 213-23.
295. Gram, D.X., et al., *Sensory nerve desensitization by resiniferatoxin improves glucose tolerance and increases insulin secretion in Zucker Diabetic Fatty rats and is associated with reduced plasma activity of dipeptidyl peptidase IV.* Eur J Pharmacol, 2005. **509**(2-3): p. 211-7.
296. Rosmalen, J.G., et al., *Islet abnormalities associated with an early influx of dendritic cells and macrophages in NOD and NODscid mice.* Lab Invest, 2000. **80**(5): p. 769-77.
297. Tsui, H., et al., *'Sensing' the link between type 1 and type 2 diabetes.* Diabetes Metab Res Rev, 2011. **27**(8): p. 913-8.
298. Suri, A. and A. Szallasi, *The emerging role of TRPV1 in diabetes and obesity.* Trends Pharmacol Sci, 2008. **29**(1): p. 29-36.
299. Motter, A.L. and G.P. Ahern, *TRPV1-null mice are protected from diet-induced obesity.* FEBS Lett, 2008. **582**(15): p. 2257-62.
300. Grabauskas, G., et al., *Electrophysiological identification of glucose-sensing neurons in rat nodose ganglia.* J Physiol, 2010. **588**(Pt 4): p. 617-32.
301. Grabauskas, G., et al., *Essential elements for glucosensing by gastric vagal afferents: immunocytochemistry and electrophysiology studies in the rat.* Endocrinology, 2013. **154**(1): p. 296-307.
302. Schmalbruch, H., *Fiber composition of the rat sciatic nerve.* Anat Rec, 1986. **215**(1): p. 71-81.
303. Giacca, A., et al., *Peritoneal and subcutaneous absorption of insulin in type I diabetic subjects.* J Clin Endocrinol Metab, 1993. **77**(3): p. 738-42.
304. Renard, E., *Insulin delivery route for the artificial pancreas: subcutaneous, intraperitoneal, or intravenous? Pros and cons.* J Diabetes Sci Technol, 2008. **2**(4): p. 735-8.

305. Agardh, C.D., et al., *The influence of plasma insulin concentrations on tissue insulin levels in rodents: a study of the diabetic Chinese hamster and the ob/ob mouse.* Metabolism, 1986. **35**(3): p. 244-9.
306. Schwartz, M.W., et al., *Kinetics and specificity of insulin uptake from plasma into cerebrospinal fluid.* Am J Physiol, 1990. **259**(3 Pt 1): p. E378-83.
307. Radio, N.M., et al., *Assessment of chemical effects on neurite outgrowth in PC12 cells using high content screening.* Toxicol Sci, 2008. **105**(1): p. 106-18.
308. Bottomley, A., et al., *Short-term treatment-related symptoms and quality of life: results from an international randomized phase III study of cisplatin with or without raltitrexed in patients with malignant pleural mesothelioma: an EORTC Lung-Cancer Group and National Cancer Institute, Canada, Intergroup Study.* J Clin Oncol, 2006. **24**(9): p. 1435-42.
309. Devaskar, S.U., et al., *Insulin gene expression and insulin synthesis in mammalian neuronal cells.* J Biol Chem, 1994. **269**(11): p. 8445-54.
310. Clarke, D.W., et al., *Insulin is released from rat brain neuronal cells in culture.* J Neurochem, 1986. **47**(3): p. 831-6.
311. Schechter, R., et al., *Preproinsulin I and II mRNAs and insulin electron microscopic immunoreaction are present within the rat fetal nervous system.* Brain Res, 1996. **736**(1-2): p. 16-27.
312. Schechter, R., M. Abboud, and G. Johnson, *Brain endogenous insulin effects on neurite growth within fetal rat neuron cell cultures.* Brain Res Dev Brain Res, 1999. **116**(2): p. 159-67.
313. Schechter, R. and M. Abboud, *Neuronal synthesized insulin roles on neural differentiation within fetal rat neuron cell cultures.* Brain Res Dev Brain Res, 2001. **127**(1): p. 41-9.
314. Kawano, T., et al., *ATP-sensitive potassium currents in rat primary afferent neurons: biophysical, pharmacological properties, and alterations by painful nerve injury.* Neuroscience, 2009. **162**(2): p. 431-43.
315. Zoga, V., et al., *KATP channel subunits in rat dorsal root ganglia: alterations by painful axotomy.* Mol Pain, 2010. **6**: p. 6.
316. Greenbaum, C.J., *Insulin resistance in type 1 diabetes.* Diabetes Metab Res Rev, 2002. **18**(3): p. 192-200.
317. Said, G., D. Baudoin, and K. Toyooka, *Sensory loss, pains, motor deficit and axonal regeneration in length-dependent diabetic polyneuropathy.* J Neurol, 2008. **255**(11): p. 1693-702.
318. Krishnan, S.T. and G. Rayman, *The LDIflare: a novel test of C-fiber function demonstrates early neuropathy in type 2 diabetes.* Diabetes Care, 2004. **27**(12): p. 2930-5.
319. Lennertz, R.C., et al., *Impaired sensory nerve function and axon morphology in mice with diabetic neuropathy.* J Neurophysiol, 2011. **106**(2): p. 905-14.
320. Pradhan, L., et al., *Inflammation and neuropeptides: the connection in diabetic wound healing.* Expert Rev Mol Med, 2009. **11**: p. e2.
321. Reddy, G.K., L. Stehno-Bittel, and C.S. Enwemeka, *Laser photostimulation accelerates wound healing in diabetic rats.* Wound Repair Regen, 2001. **9**(3): p. 248-55.
322. Sunami, E., et al., *Morphological characteristics of Schwann cells in the islets of Langerhans of the murine pancreas.* Arch Histol Cytol, 2001. **64**(2): p. 191-201.
323. Bierhaus, A., et al., *Methylglyoxal modification of Nav1.8 facilitates nociceptive neuron firing and causes hyperalgesia in diabetic neuropathy.* Nat Med, 2012. **18**(6): p. 926-33.
324. Moriyama, H., et al., *Induction and acceleration of insulitis/diabetes in mice with a viral mimic (polyinosinic-polycytidylic acid) and an insulin self-peptide.* Proc Natl Acad Sci U S A, 2002. **99**(8): p. 5539-44.
325. Cimini, A., et al., *Distinct cellular responses induced by saporin and a transferrin-saporin conjugate in two different human glioblastoma cell lines.* J Cell Physiol, 2012. **227**(3): p. 939-51.

326. Reiter, C.E., et al., *Diabetes reduces basal retinal insulin receptor signaling: reversal with systemic and local insulin.* Diabetes, 2006. **55**(4): p. 1148-56.
327. Gatica, R., et al., *Altered expression and localization of insulin receptor in proximal tubule cells from human and rat diabetic kidney.* J Cell Biochem, 2013. **114**(3): p. 639-49.
328. Ekberg, K. and B.L. Johansson, *Effect of C-peptide on diabetic neuropathy in patients with type 1 diabetes.* Exp Diabetes Res, 2008. **2008**: p. 457912.
329. Hartman, I., *Insulin analogs: impact on treatment success, satisfaction, quality of life, and adherence.* Clin Med Res, 2008. **6**(2): p. 54-67.
330. Searcy, J.L., et al., *Long-term pioglitazone treatment improves learning and attenuates pathological markers in a mouse model of Alzheimer's disease.* J Alzheimers Dis, 2012. **30**(4): p. 943-61.
331. Wiggin, T.D., et al., *Rosiglitazone treatment reduces diabetic neuropathy in streptozotocin-treated DBA/2J mice.* Endocrinology, 2008. **149**(10): p. 4928-37.
332. Winer, S., et al., *Type I diabetes and multiple sclerosis patients target islet plus central nervous system autoantigens; nonimmunized nonobese diabetic mice can develop autoimmune encephalitis.* J Immunol, 2001. **166**(4): p. 2831-41.
333. Nielsen, N.M., et al., *Type 1 diabetes and multiple sclerosis: A Danish population-based cohort study.* Arch Neurol, 2006. **63**(7): p. 1001-4.
334. Marrosu, M.G., et al., *Patients with multiple sclerosis and risk of type 1 diabetes mellitus in Sardinia, Italy: a cohort study.* Lancet, 2002. **359**(9316): p. 1461-5.
335. Carrillo, J., et al., *Islet-infiltrating B-cells in nonobese diabetic mice predominantly target nervous system elements.* Diabetes, 2005. **54**(1): p. 69-77.
336. Al-Mallah, M., et al., *Do angiotensin converting enzyme inhibitors or angiotensin receptor blockers prevent diabetes mellitus? A meta-analysis.* Cardiol J, 2010. **17**(5): p. 448-56.
337. Scholzen, T.E., et al., *Modulation of cutaneous inflammation by angiotensin-converting enzyme.* J Immunol, 2003. **170**(7): p. 3866-73.
338. Freeman, R., E. Durso-Decruz, and B. Emir, *Efficacy, safety, and tolerability of pregabalin treatment for painful diabetic peripheral neuropathy: findings from seven randomized, controlled trials across a range of doses.* Diabetes Care, 2008. **31**(7): p. 1448-54.
339. Greenway, F. and J. Zheng, *Electrical stimulation as treatment for obesity and diabetes.* J Diabetes Sci Technol, 2007. **1**(2): p. 251-9.
340. Rozman, J., M. Bunc, and B. Zorko, *Modulation of hormone secretion by functional electrical stimulation of the intact and incompletely dysfunctional dog pancreas.* Braz J Med Biol Res, 2004. **37**(3): p. 363-70.
341. Perryman, L.T., *Method, system and apparatus for control of pancreatic beta cell function to improve glucose homeostasis and insulin production*, in *google patents*, U.S.P.a.T. Office, Editor 2012, Neural Diabetes Foundation, Inc.: United States.
342. Wolfe, D., M. Mata, and D.J. Fink, *Targeted drug delivery to the peripheral nervous system using gene therapy.* Neurosci Lett, 2012. **527**(2): p. 85-9.
343. Aston-Jones, G. and K. Deisseroth, *Recent advances in optogenetics and pharmacogenetics.* Brain Res, 2013.
344. Gonsorcikova, L., et al., *Autosomal inheritance of diabetes in two families characterized by obesity and a novel H241Q mutation in NEUROD1.* Pediatr Diabetes, 2008. **9**(4 Pt 2): p. 367-72.
345. Persson-Sjogren, S., S. Forsgren, and I.B. Taljedal, *Expression of tyrosine hydroxylase, calcitonin gene-related peptide, substance P and protein gene product 9.5 in mouse islets transplanted under the kidney capsule.* Neuropeptides, 1998. **32**(4): p. 307-18.
346. Kozlova, E.N. and L. Jansson, *In vitro interactions between insulin-producing beta cells and embryonic dorsal root ganglia.* Pancreas, 2005. **31**(4): p. 380-4.

347. Barton, F.B., et al., *Improvement in outcomes of clinical islet transplantation: 1999-2010.* Diabetes Care, 2012. **35**(7): p. 1436-45.
348. Schroeder, I.S., *Potential of pluripotent stem cells for diabetes therapy.* Curr Diab Rep, 2012. **12**(5): p. 490-8.